Chiral Retinoid Derivatives:
Synthesis and Structural Elucidation of a New Vitamin A Metabolite

Von der Fakultät für Lebenswissenschaften
der Technischen Universität Carolo-Wilhelmina
zu Braunschweig
zur Erlangung des Grades einer
Doktorin der Naturwissenschaften
(Dr. rer. nat.)
genehmigte

D i s s e r t a t i o n

von
Madalina Andreea Stefan
aus Ploiesti (Rumänien)

1. Referent : Prof. Dr. Henning Hopf
2. Referentin: Prof. Dr. Monika Mazik
eingereicht am: 08.05.2006
mündliche Prüfung (Disputation) am: 14.07.2006
Druckjahr 2006

Vorveröffentlichungen:

Teilergebnisse aus dieser Arbeit wurden mit Genehmigung der Fakultät für Lebenswissenschaften, vertreten durch den Mentor der Arbeit, in folgenden Beiträgen vorab veröffentlicht:

Tagungsbeiträge:

M. Stefan, H. Hopf, J. P. Schuchardt, G. Eichele, H. Nau: Synthesis and Characterization of a new vitamin A metabolite (Poster), Chemical Society of Japan, Annual Meeting, Frühjahrsymposium, Yokohama, Japan 2005

M. Stefan, H. Hopf, N. Giese, H. Nau, A New Vitamin A Metabolite: Synthesis and Characterization (Poster), ORCHEM, Bad Nauheim 2004

M. Stefan, H. Hopf, N. Giese, H. Nau, Synthesis and Characterization of a New Vitamin A Metabolite (Poster), GDCh Frühjahrsymposium, Heidelberg 2004

M. Stefan, H. Hopf, N. Giese, H. Nau, Total Synthesis of New Vitamin A Metabolite (Poster), GDCh Jahrestagung, München 2003

Die vorliegende Arbeit wurde in der Zeit von August 2002 bis September 2005 am Institut für Organische Chemie der Technischen Universität Braunschweig unter der Leitung von Prof. Dr. H. Hopf angefertigt.

I wish to express my sincere gratitude to Prof. Dr. Henning Hopf for his supervision, support and encouragement throughout this research. Without his advice and endless interest, this study could not have been carried out and completed. Personally and scientifically I have developed myself learning from his advices and experience.

I am very grateful to Prof. Y. Okamoto for the research opportunity he gave me during my visit in Nagoya, Japan. I also wish to thank him for his advice, ideas, valuable discussions and remarks.

I thank Prof. H. Nau and his co-workers J.-P. Schuchardt and N. Giese for their cooperation and valuable discussions during this research project.

I offer my sincere thanks to Ms. P. Holba-Schulz for high resolution and 2D NMR spectra; Ms. K. Kadhim for UV and IR spectra; Dr. U. Papke and Ms. D. Döring for MS spectra, Dr. T. Beuerle for GC/MS analyses; Dr. J. Grunenberg for his supervision on the molecular modeling studies.

I am very grateful to Prof. Dr. L. Ernst for his discussions and support during assignment of the isomers of **11** by NMR spectra**.**

I am thankful to Prof. M. Mazik for agreeing to be the co-referee of my thesis.

I thank Dr. U. Jahn for his advices and to his group and all the group members of Prof. Dr. H. Hopf for the great moments spend together at the Institute of Organic Chemistry. My special thanks is going to Dr. Heino Hinrichs, Emanuela Dinca, Susanne Kritsch, Dr. Jens Reichwagen and Harald Berger. I also thank all the members of the Okamoto group who made my time in Nagoya to be a great experience.

Dedicated to my parents,

my brother and to Heino

Table of Contents

1 Introduction

The importance of vitamin A in health and disease has been recognized relatively late in human history, if we consider that humans have been confronted with night blindness, a typical disease resulting from vitamin A deficiency, for thousands of years. The curative role of the juice of cooked liver extracts in the treatment of night blindness was first recognized and practiced by the Egyptians in ancient times.[1] Just at the beginning of the 20th century, several research groups identified a lipid-soluble component in milk, butter and egg yolk which was therapeutic for this disease.

In 1912, Funk suggested the term “vitamine” to describe the growth factor present in food which was essential for life.[2] It later became clear that there was more than one growth factor, and McCollum divided them into two classes ”fat-soluble A” and “water-soluble B”.[3] Objecting to the chemical implications of the suffix '-ine', Drummond suggested deletion of the final 'e', renamed McCollum's two groups vitamin A and vitamin B, and proposed that further members of this series should be called vitamin C, vitamin D, etc.[4]

In 1934, Wald isolated from animal retina a substance he called retinene.[5] Morton[6] suggested that this compound was the aldehyde of vitamin A, and called it retinaldehyde (rather than retinal).[7] The correct structure of vitamin A was deduced in 1931 by Karrer[8] who proposed the name axerophthol[9] (*Axerophtol* in German), based on its action in preventing the eye disease xerophthalmia. A second vitamin A, isolated by Morton and others, was called vitamin A_2.[10]

Although the first recommendations for the nomenclature of the vitamins were published by IUPAC in 1960,[11] including names for the three parent compounds - retinol, retinal and retinoic acid - as well as for their 3-dehydro analogues, just in 1982 the IUPAC defined the retinoids as “a class of compounds consisting of four isoprenoid units joined in a head-to-tail manner. All retinoids may be formally derived from a monocyclic parent compound containing five carbon-carbon double bonds and a functional group at the terminus of the acyclic portion”.[12] Due to newly synthesized non-polyisoprenoid compounds, more active than retinol in typical assays for retinoid activity, and due to better understanding on the functions of some retinoids not always mediated through retinoid receptors, a new definition considered retinoids as substances that are either structurally related to vitamin A alcohol (retinol) or display vitamin A

activity. According to this definition, non-active compounds are considered retinoids only if they are structurally related to retinol.

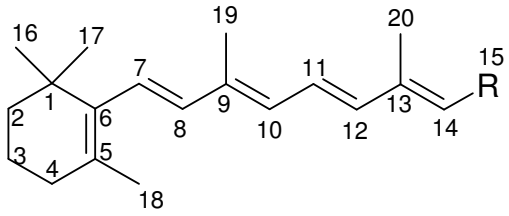

R		
CH_2OH	**1**	retinol
CHO	**2**	retinal
COOH	**3**	retinoic acid

The three retinoids all-*trans*-retinol (**1**), retinal (**2**) and retinoic acid (tretinoin, **3**) are the most characteristic examples of naturally occurring retinoids. Their structure is generally divided into three segments: a hydrophobic β-ionone ring, a conjugated tetraene side chain and a polar terminal group. Replacement of the β-ionone ring by a substituted benzene ring leads to aromatic compounds, some with higher therapeutic activity than naturally occurring retinoids, like etretinate (**4**). A further class of retinoids was obtained by restriction on the flexibility of the conjugated side chain by incorporating of aromatic ring systems in different positions. By incorporation of amide, sulfonamide or other groups, highly active retinoids were obtained (Figure 1).

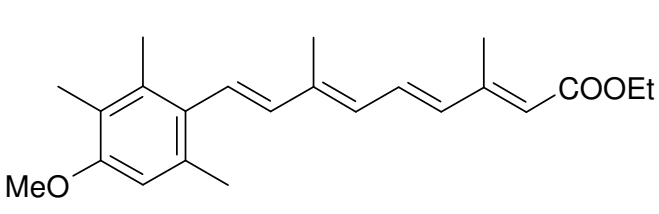

4, etretinate

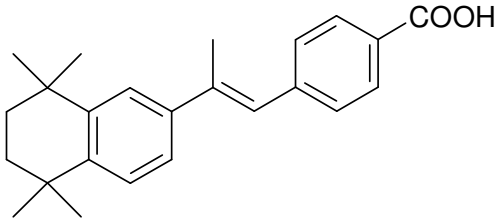

5, TTNPB

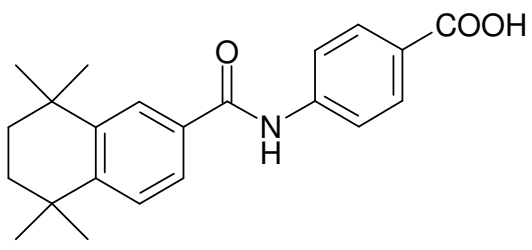

6, Am-580

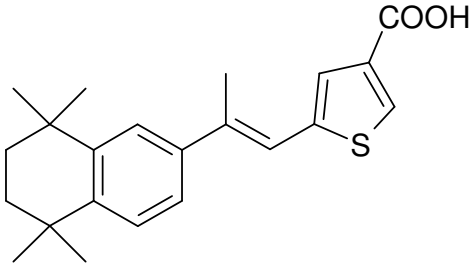

7, AGN191701

Figure 1. Structure of modified retinoids.

Rich sources of vitamin A can be found in food (milk, cheese, butter, eggs, internal organs, fish). Mammals cannot synthesize vitamin A active compounds, therefore the necessary quantities are obtained by ingestion of vitamin A (retinol and retinyl ester) or by consumption of appropriate provitamin A compounds, such as β-carotene (**8**). Carotenoids, red or yellow fat-soluble pigments, are produced exclusively by plants and photosynthetic bacteria.[1] Their basic structure consists of eight isoprenoid units, which is cleaved in the organisms by carotenoid dioxygenase mostly at the central C15-C15' double bond to retinal. Cleavage of other double bonds give β-apo-carotenals, which can be further oxidized to retinal and reduced by retinal reductase to retinol. Although more then 400 natural carotenoids are known, only 50-60 of them have provitamin A activity, which means that they can be converted to vitamin A, β-carotene being the most active. Other carotenoids, like lycopene (**9**), have no vitamin A activity but they are particularly efficient antioxidants.[13] Oxidation of carotenoids to biologically inactive xanthophylls represents an important degradation pathway for these compounds.

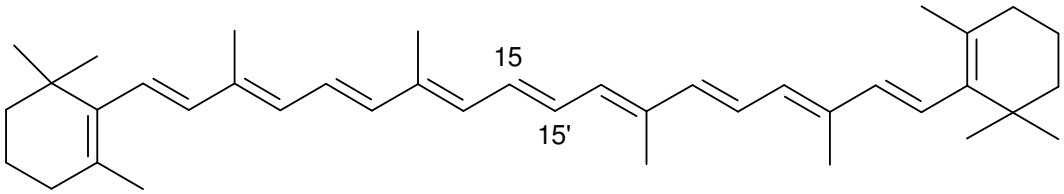

8, *trans*-β-carotene

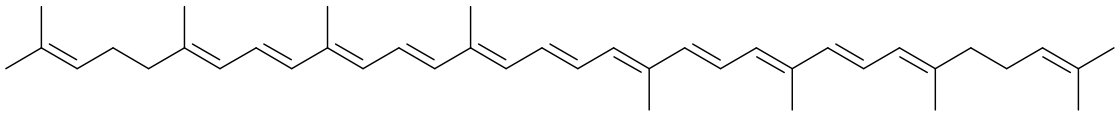

9, *trans*-lycopene

Figure 2. A selection of provitamin A compounds.

1.1 Biological Importance of Vitamin A Derivatives

The biological potency of vitamin A has been known since the second decade of the 20th century. Initial studies had focused on retinol deficiency and its major consequences: night blindness and xerophthalmia. More recently, it became evident that retinoids, natural and synthetic analogues, are essential for both normal embryonic development and maintenance of differentiation in the adult organism,[14] accounting for intense interest in these compounds in biology and medicine.

All-*trans*-retinol (ROH, **1**) is the most abundant retinoid in blood (approximately 95 to 99 % of all retinoids in the circulation), however the retinyl ester is the most abundant storage form.[15] In the body **1** is metabolized into hormonally active metabolites. The major established pathway of retinol activation involves metabolization of retinyl ester, the reversible oxidation of the released retinol to retinal (RAL, **2**) by alcohol dehydrogenase and irreversible conversion of RAL into retinoic acid (RA, **3**) by retinal dehydrogenase (RALDH, Figure 3).

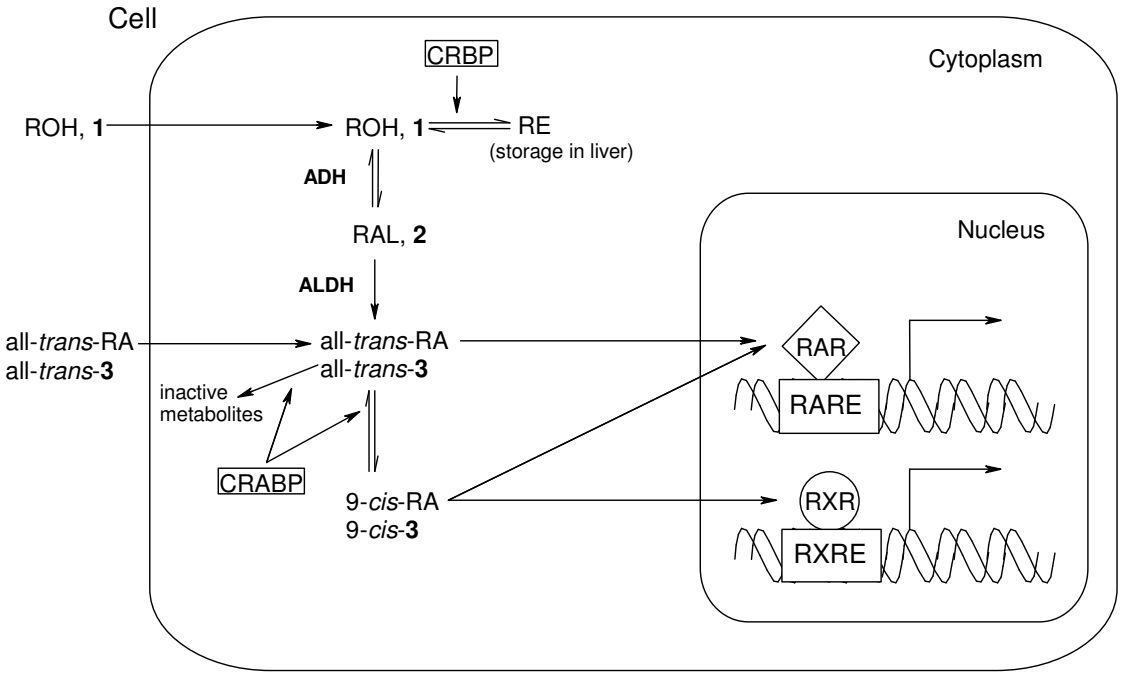

Figure 3. The retinoid signal transduction pathway.[12a]

Metabolites of all-*trans*-RA generated *in vivo* include 13-*cis*-RA, 9-*cis*-RA, retinoyl β-glucuronide, 5,6-epoxy-RA, 4-hydroxy-RA, 4-oxo-RA, 18-hydroxy-RA, 14-hydroxy-4,14-retro-retinol and 3,4-didehydro-RA.[12b] Some of these metabolites are active in mediating RA functions, whereas others are probably catabolic products.

Unlike the water soluble peptide hormones and growth factors, which bind to cell-surface receptors, the retinoids are fat soluble hormones that can pass through the lipid bilayer of the cell membrane, after which they are free to interact with intracellular proteins. This hormone-receptor complex is able to initiate the cellular response. There are several proteins found to bind *in vivo* retinol and retinoic acid. Extracellular retinol is transported from retinoid stores in the liver to target tissues by binding the extracellular retinol binding protein (RBP). The first intracellular protein was discovered by Ong and Chytil in 1978 as cellular retinoic acid binding protein (CRABP), but its absence in the nucleus showed that other receptors are mediating the

retinoid signaling pathway (Figure 3).[12a] Two families of nuclear retinoid receptors have been discovered: the retinoid acid receptor (RAR) and retinoid X receptor (RXR), each consisting of three types α, β and γ. They are members of a superfamily consisting of the nuclear receptors of steroid hormones, thyroid hormone, vitamin D and retinoids, as well as receptors of yet unidentified ligands called orphan receptors. Once all-*trans*-RA and 9-*cis*-RA have been metabolically produced in the cytoplasm, they are transported to the nucleus by a yet unknown mechanism and bind to the corresponding receptor. While RARs have almost equal affinity to all-*trans*-RA and 9-*cis*-RA, RXRs preferentially bind 9-*cis*-RA. Therefore, to understand the function and activation pathway of different isomers of vitamin A metabolites, it is essential to understand their role in the body.

The mechanism of retinoid action can be mediated by interaction with the retinoid receptors, as shown before, or by other mechanisms in which retinoid receptors are not directly involved, like the visual process. In the retinal pigment epithelium an unidentified enzyme carries out the isomerization of all-*trans*-ROH to 11-*cis*-ROH, which can be oxidized to 11-*cis*-RAL, the active metabolite of ROH. Visual pigment generation involves the interaction of 11-*cis*-RAL (or derivatives) with opsin, a protein tailor made to shift the absorption spectrum of the retinoid into the visible range, increase its quantum efficiency of photoisomerization and activate further biochemical response.[12c] The absolute requirement of vitamin A for vision is well known and proven by half a million of new cases of childhood blindness occurring annually, from which approximately 70 % are the result of severe vitamin A deficiency.[12c]

Vitamin A is an essential nutrient for humans. An equilibrated intake of vitamin A is vital in embryo genesis, growth and development, cell proliferation and differentiation, the visual process, immunity, and reproduction. Also its pharmacological use in bone diseases, dermatology, cancer and leukemia prevention and therapy is today of essential importance.

When ingested in large doses, vitamin A can be toxic. The three categories of toxicity are acute, chronic and teratogenic toxicity. Vitamin A is non-toxic until there is no more retinol binding protein (RBP) available to bind it, and ROH circulates freely in the plasma. When unbound retinol is presented to cells and membranes, vitamin A toxicity tends to appear, because ROH is metabolized to RA, which is the toxic species.[12d]

1.2 Aim of this Work

Following investigations on vitamin A metabolism, Shirley reported in 1996 that 9-*cis*-RA can be metabolized in rats by oxidation to 4-hydroxy- and 4-oxo-9-*cis*-RA, as well as by reduction to a new vitamin A metabolite, 9-*cis*-13,14-dihydro-RA (**10**).[16] After administration of an equimolar mixture of labeled and non-labeled 9-*cis*-RA to rats, he observed the formation of a labeled 9-*cis*-13,14-dihydro metabolite, which means that the precursor of the new metabolite was the 9-*cis*-isomer of RA or ROH and not the all-*trans*-isomer. The potential for the new metabolite to retain biological activity was assessed by binding and transactivation studies indicating an activity less than 1 % of the corresponding 9-*cis*-RA. Thus, the minor structural change brought about by reduction may represent an important mechanism for inactivating 9-*cis*-RA *in vivo* by rats.[16]

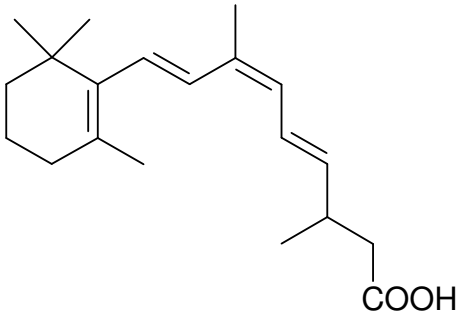

9-*cis*-**10**

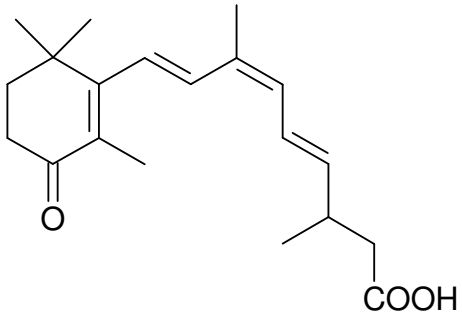

9-*cis*-**11**

In a study on the influence of polychlorodibenzodioxin on the homeostasis of retinoids, Nau and Schmidt reported the discovery and isolation of a second 13,14-dihydro vitamin A metabolite.[17] The new metabolite was detected in liver, kidney and serum of mice and rats, and in one human liver. Spectroscopic analysis (^{1}H NMR, MS and UV) indicated the 9-*cis*-4-oxo-13,14-dihydro-RA (**11**) structure, but insufficient amounts of the isolated substance made a complete characterization and further investigations impossible. Higher dietary levels of vitamin A palmitate in mice result in higher level of the new metabolite accompanied by higher total ROH and lower all-*trans*-RA contents. A reason for this finding may be the acute saturation of the metabolic capacity of the organism in case of higher dosing regimes, in which retinoids may be metabolized via additional pathways. Due to the relatively high hepatic levels, one can assume that **11** is biosynthesized in the liver. There are two possible pathways by which the formation of this metabolite may proceed: it may originate from all-*trans*-RA following isomerization, reduction and oxidation, or it is also possible that the precursor is 9-*cis*- or 9,13-di-*cis*-ROH.[18] Further studies were necessary to clarify whether this new

metabolite has any biological activity or if it is just one inactivated derivative in the catabolism of vitamin A. To confirm the assigned structure of this metabolite, for a better under-standing of its function and formation pathway, and for biological tests, synthetic material was needed.

Subsequently during the course of this work, Palczewski[19a] reported investigations on reduced metabolites of vitamin A and described a novel enzyme (RetSat) that carries out the saturation of the C-13/C-14 bond of all-*trans*-ROH to generate all-*trans*-13,14-dihydro-ROH (all-*trans*-**12**), which was oxidized to all-*trans*-13,14-dihydro-RA (all-*trans*-**10**). Trying to find out more about the 13,14-dihydro-RA metabolites, he performed the synthesis of **11**, respectively **10** in 13 steps, without taking the chirality at C-13 into consideration.[19b] After feeding rats with synthetic **12** the only isolated metabolites were all-*trans*-**10** and all-*trans*-**11**. The 9-*cis*-isomer of this 13,14-dihydro-RA derivatives is evidently not formed. No information about the absolute configuration of the isolated 13,14-dihydro-retinoids is given, and the biological tests were performed with racemic compounds.[19b] Contrary to the previous report of Shirley, the enzyme RetSat could not convert all-*trans*-RA into all-*trans*-13,14-dihydro-RA, which implies that the previously observed 13,14-dihydro metabolites should be downstream products of the oxidation of all-*trans*-13,14-dihydro-ROH. This supposition holds when all three 13,14-dihydro metabolites are products of the same metabolization pathway. It is also known that 9-*cis*-RA can participte in additional metabolization pathways, independent of that for all-*trans*-ROH.[15]

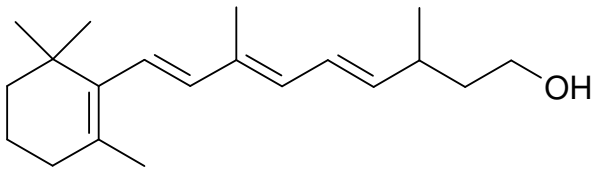

all-*trans*-**12**

As shown before, the major established pathway of ROH activation, involves reversible oxidation to retinal (RAL), and irreversible conversion of the latter into retinoic acid (RA), which can undergo oxidative metabolism to yield 4-hydroxy-RA or 4-oxo-RA. If this observation concerning a possible metabolic pathway is true for 9-*cis*-**11**, it still remains unclear at what stage the C-9/C-10 bond isomerization occurs and the C-13/C-14 double bond is reduced. Information about the biological activity of all new derivatives and their role in the metabolism are vital for a better understanding of the general vitamin A metabolism.

Another important aspect not mentioned in the previous papers is the chirality of these vitamin A analogues. Within the body, the metabolites exist in a chiral environment where their release, absorption, transport, action and degradation involve interactions with enzymes, cell surface and so on. This means that two enantiomeric molecules should be acted on differently by the body and the new chiral vitamin A enantiomers should be investigated separately.

With this in mind, the synthesis of **11** was the first target, to confirm the structure that Nau and co-workers had assigned for their isolated vitamin A metabolite. All geometric isomers should be obtained and investigated. The racemic synthesis offers the advantage that both enantiomers can be compared with the isolated compound, while an enantioselective synthesis can confirm the assigned configuration. Separation of the racemate by chiral high pressure liquid chromatography (HPLC) would make further analysis in biological assays with both enantiomers possible. The developed method for chiral separation should give the possibility for analysis of all diastereomers of the new reported RA metabolites.

After synthesis of 4-oxo-13,14-dihydro-RA (**11**) and complete characterization of the new metabolite, its possible precursor in the metabolization process, 13,14-dihydro-RA (**10**) should also be synthesized and analyzed. Several methods were followed here for the preparation of these new retinoids. Wittig reactions were preferentially used to obtain all geometrical isomers. By controlling the synthesis of the phosphonium salts, an enantioselective or racemic synthesis can be achieved. Using new substitution patterns on the phosphonium salts or on the β-ionone skeleton further modification of the retinoid chain can be performed. Most reactions started from an ionone derivate.

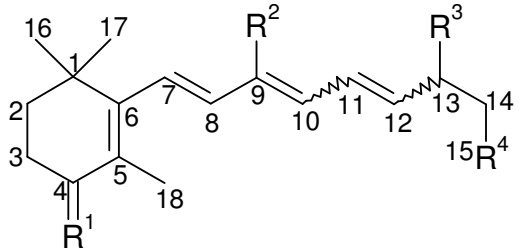

13

Figure 4. Modifications undertaken on the retinoid skeleton.

Modifications on the retinoid skeleton were undertaken at C-4, C-9 and C-13. Mechanism of formation and action, as well as further degradation pathways for the 13,14-dihydro metabolites can be studied with labeled retinoids. For some of the known active retinoids, like ROH and RA synthesis of labeled material has been reported in the

literature.[12e] Because these methods could not be applied here, a similar approach was developed for the 13,14-dihydro-RAs. Deuterium labeling offers the advantage of inexpensive starting materials, stable labeled products and a simple analysis by mass spectrometry. It is known that oxidative decarboxylation and β-oxidative chain shortening are other metabolic processes of all-*trans*-RA.[16] When rats were treated with [14-^{14}C]-ROH or [15-^{14}C]-all-*trans*-RA, radiolabelled $^{14}CO_2$ was lost through respiration. For this reason, the 13,14-dihydro retinoids were labeled at C-9 (R^2), a position that would enable their monitoring by mass spectrometry over several chain degradation steps in the metabolization path.

For further theoretical and practical biological investigations, modification of the retinoid skeleton, at C-13 (R^3) was performed. This position was chosen because retinoid activity can be modified when bulky groups at C-13, near the retinoic acid active center, substitute the native methyl group. The *trans*-isomers are the most active isomers in retinoid metabolism. Which role the 9-*cis*-13,14-dihydro retinoid metabolites are playing is not clear presently. By inserting a sterically demanding substituent at C-13, the 9-*cis*-isomers can be investigated in the retinoid receptor pocket and their interactions with the amino acids could be analyzed. One can try to get additional information about the binding affinity of the different isomers, especially when steric interactions in the retinoid receptor pocket are playing an additional role. This information can help to understand the role and the biological activity of the newly discovered 13,14-dihydro retinoids.

Theoretical calculations of the newly synthesized retinoids can be obtained ahead of the experimental biological tests. Spectroscopic analysis helps to understand the conformation and other possible interaction of different isomers.

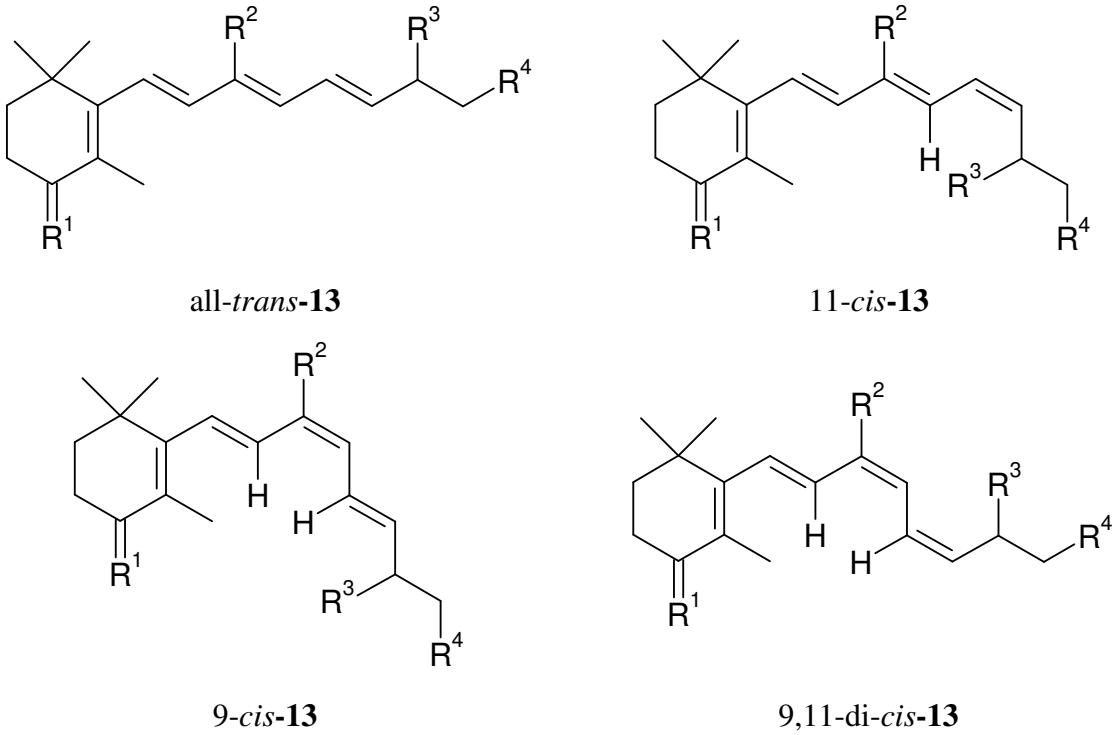

Figure 5. Steric hindrance due to larger substituents at C-13.

In summary, the structure of a new chiral vitamin A metabolite (**11**) has to be confirmed and its absolute configuration to be assigned. The developed synthetic methods should provide other possible isomers of the found metabolite as well, and the biological function of each isomer should be investigated. If the isolated compound is produced as one enantiomer, an enantioselective synthesis should be developed. Furthermore, a chiral separation method should be developed for the analysis and comparison of synthetic samples with biological material.

Differently substituted retinoids have to be synthesized and their properties to be compared. The synthetic approach for the new chiral retinoids, the development of analytical separation by chiral and non-chiral chromatography, the spectroscopic characterization, and theoretical calculations should give information on their biological activity. Further investigations with all newly synthesized retinoids are necessary to understand their biological function and to complete our assumptions on a new endogenous metabolic pathway of vitamin A.

2 Retrosynthesis

A general classification of synthetic routes to the retinoid polyene skeleton distinguishes two processes, double and single bond formation, and labels the building blocks according to the number of carbon atoms contributing to the final diterpene skeleton. Wittig- and Horner-Wadsworth-Emmons (HWE) condensations are among the most often used double bond formation reactions in vitamin A synthesis. Julia olefination is also often used as an alternative.[20] The synthesis of polyenes involving C-C single bond formation usually features metal-catalyzed cross-coupling reactions between alkenyl organometallic reagents and alkenyl electrophiles. This second methodology has been established mostly for constructing biaryl substituted retinoids. Variation of coupling reactions has permitted the synthesis of ring systems bearing functional groups such as ester, amide and nitro groups. This metallorganic chemistry will not be discussed here. Double bond formation through Wittig and HWE reactions of carbonyl compounds with triphenylphosphonium halides, respectively dialkylphosphonates, will be presented and discussed here for the synthesis of the novel retinoids.

In his Nobel lecture "*Von Diylen über Ylide zu meinem Idyll*",[21] Wittig mentioned the importance of the Wittig reaction in vitamin A synthesis that made its industrial production possible. Today there are several technical processes for the synthesis of vitamin A, most of them still using the Wittig reaction.

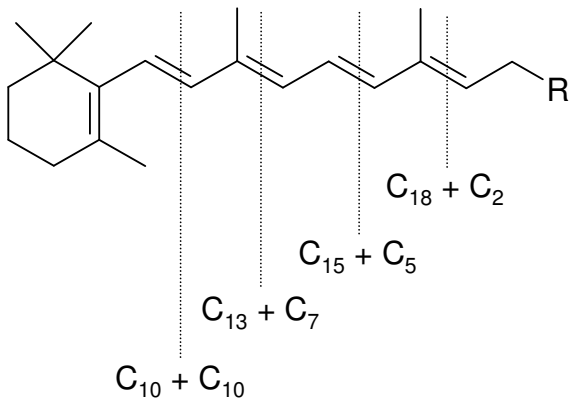

Figure 6. Possible building blocks for retinoids.

The methodology for synthesizing many retinoid analogs is based on established methods because the goals are drug discovery based on structure-activity investigations and the use of previously reported preparative methods rather then development of new synthons. In this study several methods for the synthesis of chiral 13,14-dihydro-retinoic acid derivatives have been developed to enable preparation of a particular

diastereomer selectively or without any selectivity for a one pot synthesis of all diastereomers. The best method was optimized to produce the desired product enantioselectively in a few steps. Retrosynthetically the new metabolites could be synthesized using one of the following pathways:

a) The C_{13}+C_7 pathway using the Horner-Wadsworth-Emmons (HWE) reaction of β-ionone derivative **14** with phosphonate **15** offers a *trans*-selective synthetic method for the retinoid derivatives. By controlling the configuration at the chiral center of the phosphonate, an enantioselective synthesis of the retinoids should be possible.

b) Wittig reaction between the C_{15} phosphonium salt **16** and the C_5 aldehyde **17** can be used for obtaining retinoic acid derivatives as well as retinol derivatives, mostly in *trans*-configuration.

c) Stepwise construction of the conjugated double bonds by Wittig reactions offers the possibility of a better control of the *cis-/trans*-isomer formation. Enantioselective synthesis of phosphonium salt **19** allows the enantioselective synthesis of the vitamin A derivatives. New substituents can be incorporated in the retinoid backbone when phosphonium salt **19** is chemically modified at the desired positions. Using just one of the isomers of aldehyde **18**, a *cis*-, respectively *trans*-selective synthesis can be performed.

   c_1) Several modifications on the retinoid skeleton can be planned when starting from commercially available ionone. The chain length can be increased with additional double bonds by Wittig reactions. The C-4 position can be oxidized to give 4-oxo and 4-hydroxy derivatives. The methyl group at C-9 can be substituted with deuterium to give labeled retinoic acid derivatives.

   c_2) The synthesis of aldehyde **18** was designed to be *cis*-selective by using a metal catalyzed addition to alkyne **21.**

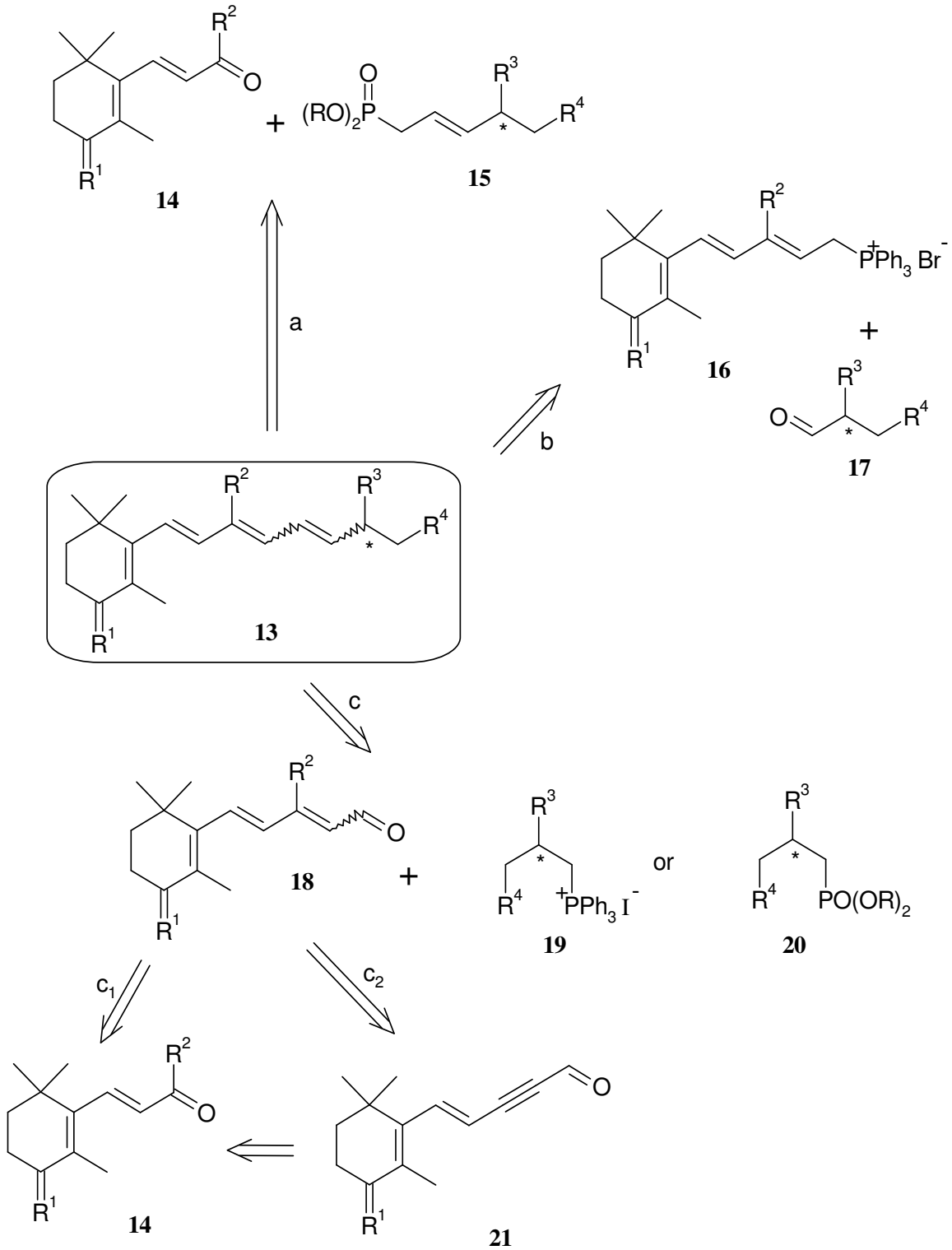

Figure 7. Retrosynthesis of 13,14-dihydro retinoid derivatives **13**.

3 Syntheses

3.1 β-Ionone (22) and 4-Oxo-β-ionone (23) as Starting Materials

Ionone derivatives are one of the most important building blocks in vitamin A and carotenoid synthesis. β-Ionone and α-ionone are commercially available, other derivatives can be easily obtained. 4-Oxo-β-ionone (**23**) can be extracted from *Osmanthus Absolue*[22] or the juice of the yellow *Passion Fruit*[23], and it has been found in the black tea aroma[24] and in tobacco fractions.[25] Synthesis of **23** can start from β- or α-ionone, to 4-hydroxy-β-ionone which can be oxidized to the 4-oxo derivative.[26,27] Better yields are obtained in a one step reaction, by which **22** reacts with pyridiniumchlorochromate (PCC), in DMSO at 100 °C to give 53 % of **23** as yellow crystals.[27] This second approach was used in this work for the synthesis of **23**.

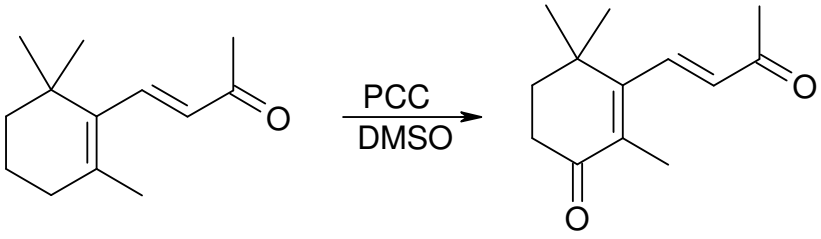

22 **23** (53 %)

Scheme 1. Oxidation of β-ionone (**22**).

To investigate all potential metabolites of RA, the newly discovered 4-oxo-dehydro-RA metabolite[17] but also possible precursors, all new retinoids synthesized in this thesis were based on the β-ionone and the 4-oxo-β-ionone skeleton, respectively.

3.2 Synthetic Approach to 13,14-Dihydro-retinoids by Horner-Wadsworth-Emmons Reaction. Retrosynthetic Path a

Following route **a**, phosphonate **27** was chosen as one of the starting materials for the HWE reaction with **22** to the 13,14-dihydro retinoids. One important advantage of this phosphonate is the possibility to synthesize it in enantiomerically pure form as *S*-**27** and *R*-**27**, which will enable enantioselective syntheses of 13,14-dihydro retinoids. This approach seems to be ideal for a *trans*-enantioselective synthesis of **11**.

1,2-Addition of crotonaldehyde (**25**) to the phosphonate **24** gave allyl alcohol **26** as racemic mixture. By using the Sharpless methodology of kinetic resolution of racemic allylic alcohols, it should be possible to separate this hydroxy phosphonate racemate into its enantiomers.[28] The next reaction step with racemic or enantiomerically pure **26** is a Claisen rearrangement, which proceeds stereospecifically, so no racemisation will affect the enantiomeric purity of **27.**[28] Racemic synthesis was first undertaken. The Claisen rearrangement[29] (Scheme 3) of **26** with triethyl orthoacetate and a catalytic amount of propionic acid, gave the appropriate *trans*-ester phosphonate **27** in 53 % yield (Scheme 2).

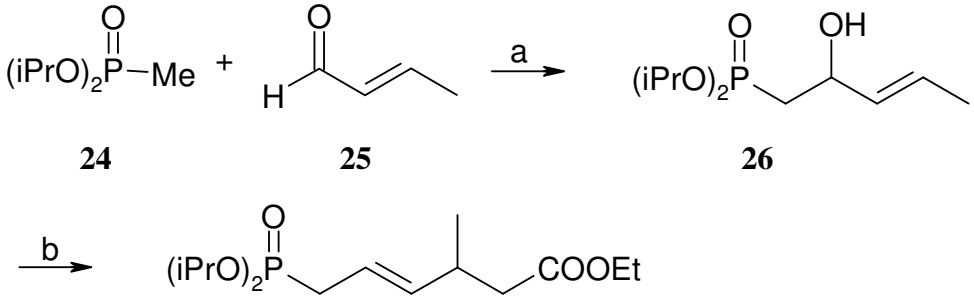

a) *n*BuLi, THF, -78 °C (58 %); b) $MeC(OEt)_3$, EtCOOH, 140 °C (53 %)

Scheme 2. Synthesis of C_7 phosphonate.

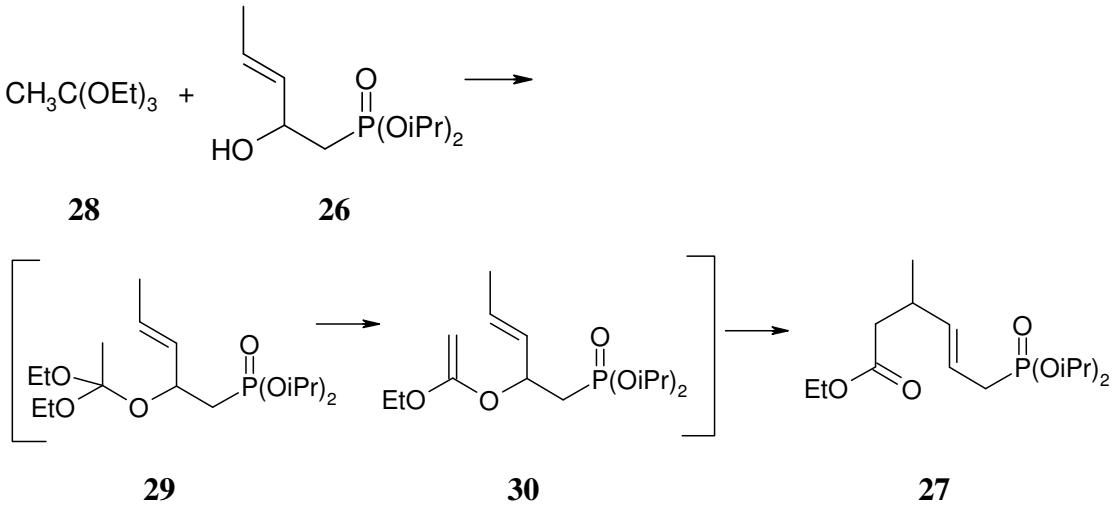

Scheme 3. Mechanism of Claisen rearrangement to **27**.

Under several deprotonation conditions (base: NaH, LDA, NaHMDS, *n*BuLi, KO*t*Bu) **22** was reacted with phosphonate **27**, but the reaction failed to give the desired product.

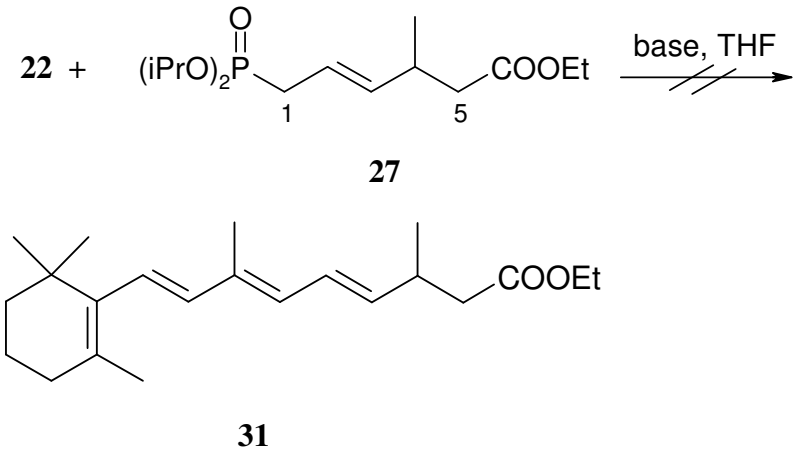

Scheme 4. Attempted Horner-Wadsworth-Emmons reaction of **22** with phosphonate **27**.

To understand the reason for this failure, investigations on the acidity of the protons of **27** were conducted by deprotonation with different bases and quenching the resulting anion with D_2O. When NaH was used, no deprotonation took place. With LDA and NaHMDS deprotonation took place at C-1 and C-5. KO*t*Bu and *n*BuLi gave possible deprotonation of C-1 but several other decomposition products. NaH followed by *n*BuLi gave complete decomposition of the phosphonate. Computational calculation of the proton affinity of the acidic protons at C-1, C-4 and C-5 were performed for a deeper understanding on the reactivity of this phosphonate. These results will be discussed in Chapter 8.

To overcome the competition between the deprotonation reactions of the acidic protons near the ester and the phosphonate group, the carboxylic function was protected as a cyclic ortho ester **34** (Scheme 5). Saponification of the phosphonate ester **27** gave the corresponding acid **32**, which was reesterificated to the oxetane **33** with 3-methyl-3-hydroxymethyloxetane, DMAP and DCC in Et_2O at 25 °C. The oxetane rearranged under acidic conditions to give the new cyclic ortho ester **34**.

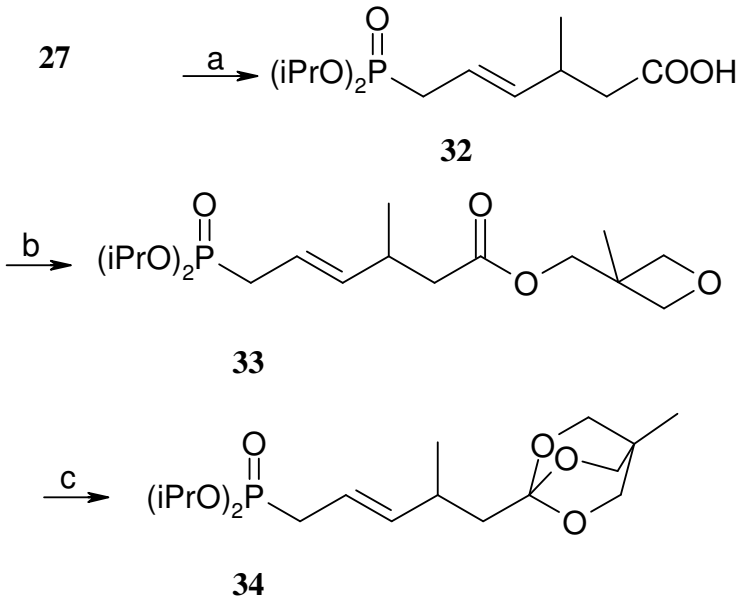

a) KOH, EtOH, H_2O (93 %); b) (3-hydroxymethyl)-3-methyloxetane, DMAP, DCC, Et_2O, 25 °C (87 %);
c) [i] BF_3-Et_2O, CH_2Cl_2, -4 °C; [ii] NEt_3 (74 %)

Scheme 5. Synthesis of ortho ester phosphonate **34**.

The phosphonate **34**, with a protected carboxylic function, was treated again with several bases and quenched with D_2O to gain a first impression of its reactivity in the HWE reaction. The new phosphonate was not stable enough and decomposition took place easily. Due to these results, further investigations on this pathway to the 13,14-dihydro retinoids were not continued.

3.3 Synthesis of Retinoic Acid Derivatives by Wittig Reaction with C_{15}+C_5 Backbones. Retrosynthetic Path b

The retrosynthetic route **b**, was developed as described by Rosenberger and his group using the Wittig reaction.[30] The same methodology has been used previously by Isler for the vitamin A and A_2 synthesis[31] and by researchers at *Hoffmann-La Roche* for the synthesis of carotenoids.[32,27] This method uses the C_{15} + C_5 path for building the retinoid skeleton with C_{15} phosphonium salt and C_5 aldehyde. Retinol can also be obtained by this procedure. Instead of phosphonium salt **37**, the analogous C_{15} sulfonium salt has been used by Rosenberger to obtain RA derivatives.[30b] Building the retinoid backbone by Wittig reactions, as shown in Scheme 4, is one of the methods that found its application in the industrial synthesis of retinoids and carotenoids by the BASF company.[33]

This methodology based on the Wittig reaction can be used successfully for the synthesis of the all-*trans*-isomers. All other isomers are obtained as by-products in very small quantities and can be isomerized to the all-*trans*-product. By this protocol, RA and 4-oxo-RA were obtained as analytical standards and synthetic material for biological investigations.

Grignard reaction of β-ionone (**22**) with vinylmagnesium chloride followed by treatment of formed vinyl-β-ionol **35** with $Ph_3P{\cdot}HBr$ in MeOH gave phosphonium salt **37**. The crude phosphonium salt was used directly in the Wittig reaction, further purification by recrystallisation showed decomposition of the salt and consequently a decrease of the yield. In the same way, the 4-oxo phosphonium salt **38** was synthesized by Grignard reaction of **23** with vinyl magnesium chloride to provide 4-oxo-vinyl-β-ionol (**36**) followed by reaction with $Ph_3P{\cdot}HBr$ (Scheme 6).

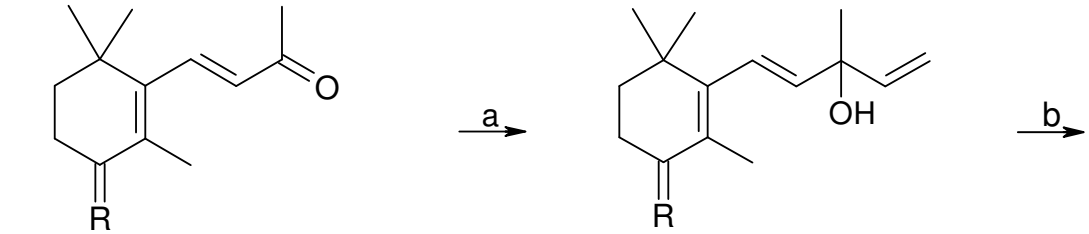

R		
H,H	**22**	
O	**23**	

R		%
H,H	**35**	80
O	**36**	35

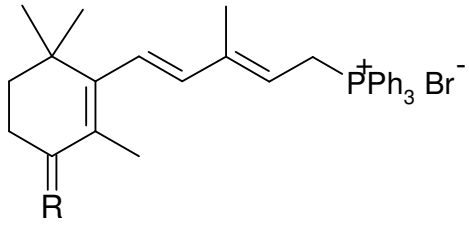

R		%
H,H	**37**	100
O	**38**	100

a) CH_2=CHMgCl, THF, -78°C; b) PPh_3HBr, CH_2Cl_2

Scheme 6. Synthesis of C_{15} phosphonium salts.

Wittig reaction of **37** with aldehyde **39** gave the esters of all-*trans*- and 11-*cis*-RA, which were saponificated with KOH in EtOH/H_2O to the corresponding acids **3** and **42** (Scheme 7). The ratio of the two isomers, all-*trans*-/11-*cis*- = 2:1, was determined by ^1H

NMR spectroscopy and confirmed by HPLC on Puropsher RP-18 endcapped column, 5 μm material, with CH_3CN/H_2O 60:40, isocratic flow of 0.7 mL/min.

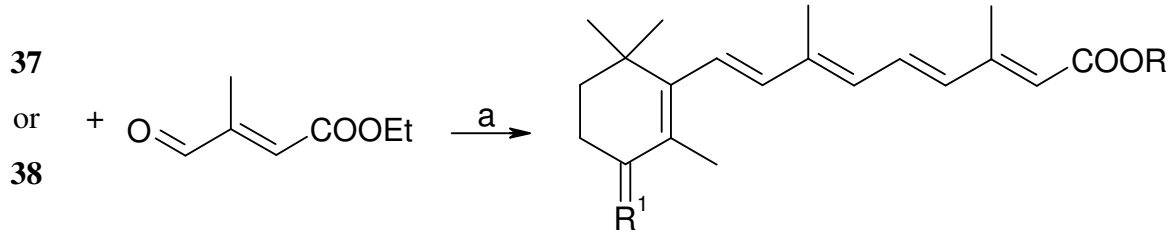

39

R^1	R		%
H,H	Et	**40**	72
H,H	H	**3**	98
O	Et	**41**	73
O	H	**42**	99

a) [i] NaOEt, EtOH, -30 °C to room temp., 2 h; [ii] KOH, $EtOH/H_2O$, 3h reflux

Scheme 7. C_{15}+C_5 Wittig reaction.

The 13,14-dihydro retinoids can be obtained by this pathway when the aldehyde **43** is used in the last Wittig steps. Heterogeneous reduction of **39** on Pd/C and 10 bar H_2 pressure at 30 °C gave **43** in 62 % yield (Scheme 8)

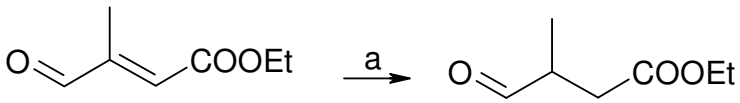

39 **43**

a) H_2, Pd/C, ethylacetate, 10 bar, 30 °C (62 %)

Scheme 8. Hydrogenation of **39**.

Enantioselective reduction of the C-C double bond should be possible when using a chiral reduction catalyst. Investigations on the proper catalyst for a good enantioselective reduction were not undertaken here, because the Wittig reaction of the synthesized aldehyde **43** and **38** yielded mostly the all-*trans*-isomer and not the desired 9-*cis*-isomer of **11** (all-*trans*-, 9-*cis*-, 11-*cis*-, 9,11-di-*cis*-ratio = 8.1:1.6:2.0:1.0).

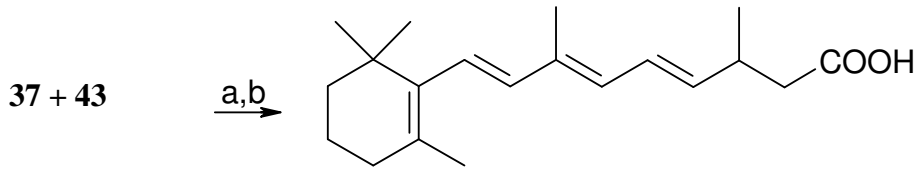

11

a) KO*t*Bu, THF, room temp.; b) KOH, EtOH/H_2O (23 %)

Scheme 9. C_{15}+C_5 Wittig reaction.

Thus, route **b** is a good alternative for the synthesis all-*trans*-RA and all-*trans*-13,14-dihydro-RA derivatives.

3.4 Consecutive Double Bond Formation of the Retinoid Skeleton. Retrosynthetic Path c

3.4.1 Synthesis of β-Ionylidene-acetaldehyde (47) and 4-Oxo-β-ionylidene-acetaldehyde (53)

The consecutive double bond formation pathway was chosen for a better control of the *cis-/trans*-selectivity in the synthesis of the finally required retinoids. Keeping in mind that the supposed configuration of the new metabolite isolated by Nau[18] is *cis* at C-9/C-10 and *trans* at C-11/C-12, the first double bond formation reaction from β-ionone backbone should be *cis*- and the second *trans*-selective.

Although the stereoselectivity of the conversion of aldehydes into olefins can be more than 95 %, that of ketones to olefins is often disappointingly low.[34] This synthetic problem was tried to be solved here, by an alternate carbometallation reaction of the ketones **22** and **23**.

Recently, an aromatic retinoid derivative has been synthesized *cis* selectively by 1,4-addition of dimethyllithiumcuprate (Me_2CuLi) to a propargyl ester derivative to produce tri-substituted alkenes.[35] Bennani reported previously the same *cis* selective 1,4-addition of Me_2CuLi to the acetylenic nitrile analogue of **46**.[36] For our purpose, the alkyne aldehyde **46** seems ideal as the starting material for the reaction with the cuprate, because no further reduction steps of the terminal group would be necessary. For this reason, the Negishi method for conversion of methyl ketones into teminal acetylenes was used.[34] Deprotonation of **22** with LDA, followed by reaction of the enol with

diethyl chlorophosphate gave the enol phosphonate **44**. This was reacted further in an one pot reaction with 2 equivalents of LDA to give in a β-elimination the terminal alkyne **45** (i.e. its metal salt) followed by quenching of the reaction mixture with DMF to yield the aldehyde-alkyne **46**. This compound was subsequently reacted with Me_2CuLi to provide **47** (Scheme 10).

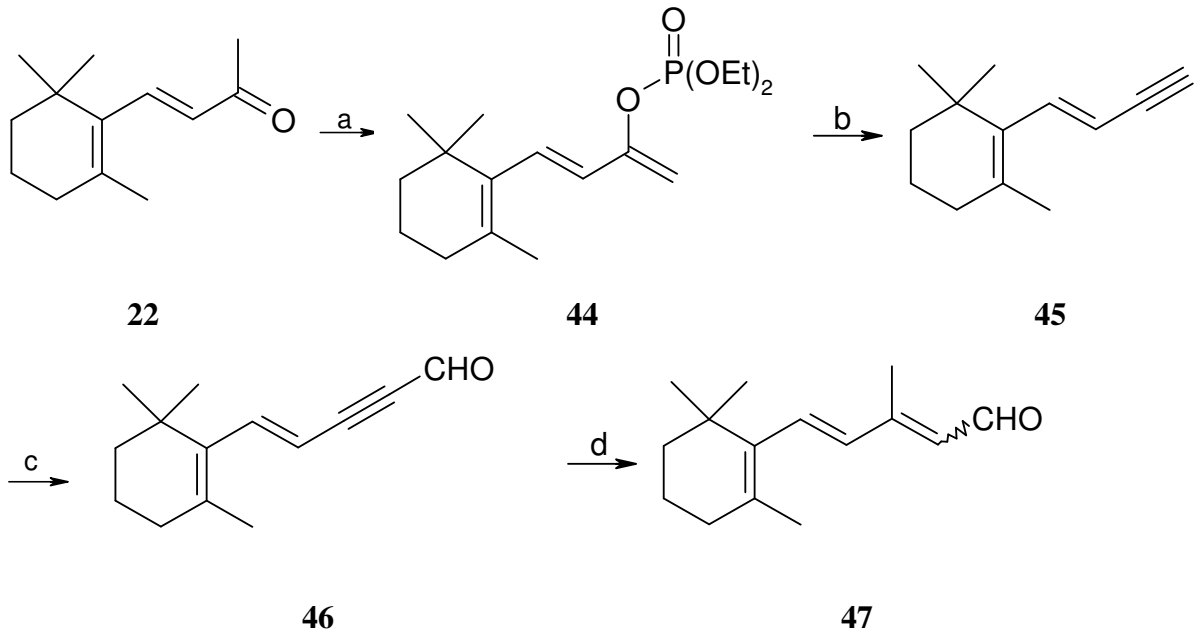

a) LDA, $ClPO(OEt)_2$, THF; b) LDA (2 eq.); c) DMF (68 %);

d) Me_2CuLi, -78 °C, THF (48 %)

Scheme 10. Synthesis of **47** by cuprate addition.

The product obtained in acceptable yield was a *cis-/trans*-mixture of **47** in 1:1 ratio. Although, as mentioned before, the 1,4-addition of organometallic copper compounds R_2CuLi (Gilman's cuprate) to conjugated alkyne-acid ester gives mostly the kinetically controlled product of the *syn* addition,[35] this was not observed for the α,β-unsaturated aldehyde **46**. In this case keto-enol tautomerism of the final products **51/47** was the reason for a unselective stereochemistry. The mechanism of this reaction is shown in Scheme 11. The Gilman cuprate dimer formed from methyllithium and a mixture of CuBr · DMS reacts with the unsaturated system to the Li-enolate **48** in which the Cu forms a π-complex with the alkyne group. After reductive elimination, a new C-C bond is formed between one methyl group from Cu and the β-carbon to give monomeric Me_2CuLi, which by dimerisation will generate the starting reactive Gilman cuprate again, and the Li-enolate **49**, associated with CuMe. In the presence of an electrophile, like aqueous NH_4^+, the formed enolate yields the *cis-/trans*-mixture of aldehyde **46** by tautomerisation.

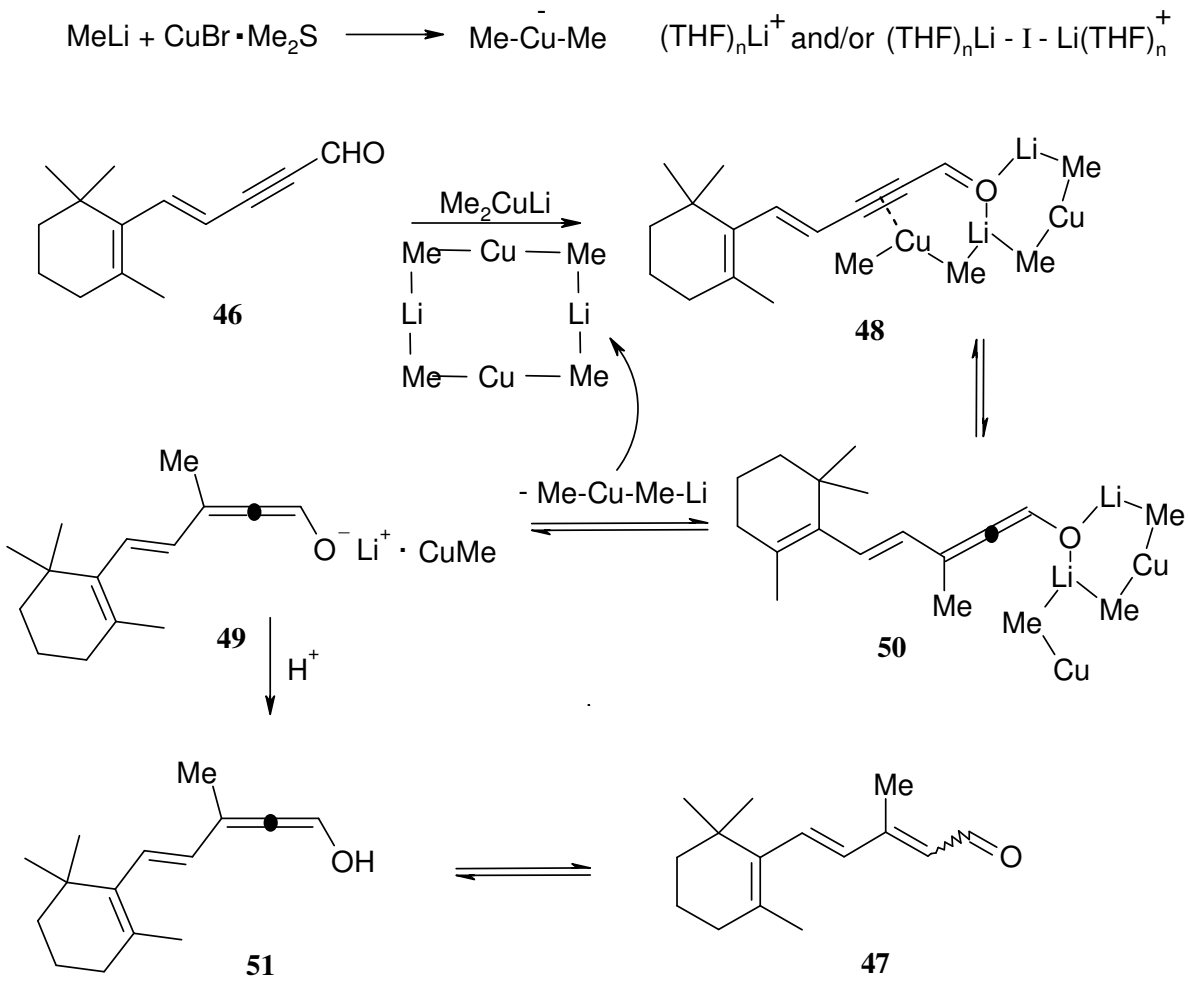

Scheme 11. Mechanism of 1,4-addition of Gilman's cuprate to the α,β-unsaturated aldehyde **46**.

Because this metallation pathway was not *cis* selective, the aldehydes **47** and **53** were synthesized in a one step Wittig reaction starting from **22** and **23** (Scheme 12).

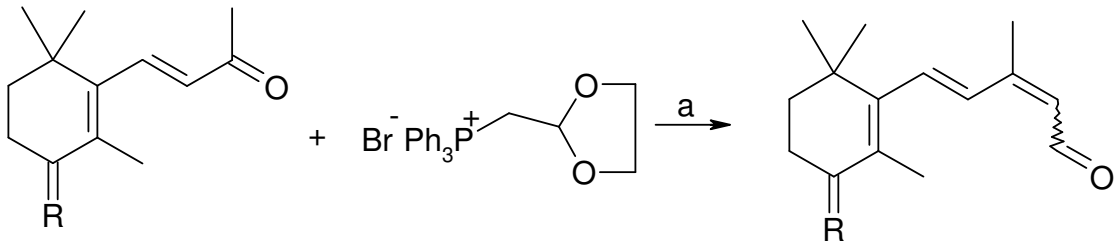

R	
H,H	**22**
O	**23**

52

R		%
H,H	**47**	83
O	**53**	80

a) KO*t*Bu, THF, room temp.

Scheme 12 C-9/C-10 double bound extension by Wittig reaction.

β-Ionone (**22**) was reacted with [(1,3-dioxan-2-yl)-methyl]-triphenylphosphonium bromide (**52**) in the presence of KO*t*Bu as base, followed by dioxolane ring cleavage

with oxalic acid to give the desired **47** in 71 % yield as a mixture of *cis*-/*trans*-isomers in 1:2 ratio. When 4-oxo-β-ionone (**23**) was used, aldehyde **53** was obtained in 80 % yield and 1.0:1.5 *cis*-/*trans*-isomer ratio. The Wittig salt **52** is commercially available but can be easily prepared by reacting one equivalent of 2-(bromomethyl)-1,3-dioxolane with one equivalent of triphenylphosphine for 84 h at 70 °C, and precipitating the product from acetone. The Wittig reaction with **52** offers a one step alternative to the often used method for preparing **47** and analogues by HWE reaction with (diethoxy-phosphoryl) acetic acid ethyl ester or cyanomethylphosphonate followed by reduction of the ester, respectively cyano derivative, to the aldehydes.[37,38,39] The HWE reaction gives preferentially the *trans*-isomer, which was not desired here, on the way to the target vitamin A metabolite. This one step method has the advantage to give the *cis*-isomer in considerable amounts compared to other methods. Variation of the reaction conditions (base: KO*t*Bu, LiHMDS, NaHMDS) did not show any improvement of the *cis*-selectivity of the formed product.

This can be explained by the mechanism of Wittig reaction shown in Scheme 13. The *cis/trans*-ratio can be influenced by several parameters: temperature, solvent, concentration and choice of the aldehyde, type of the ylide and the presence or absence of lithium salts.

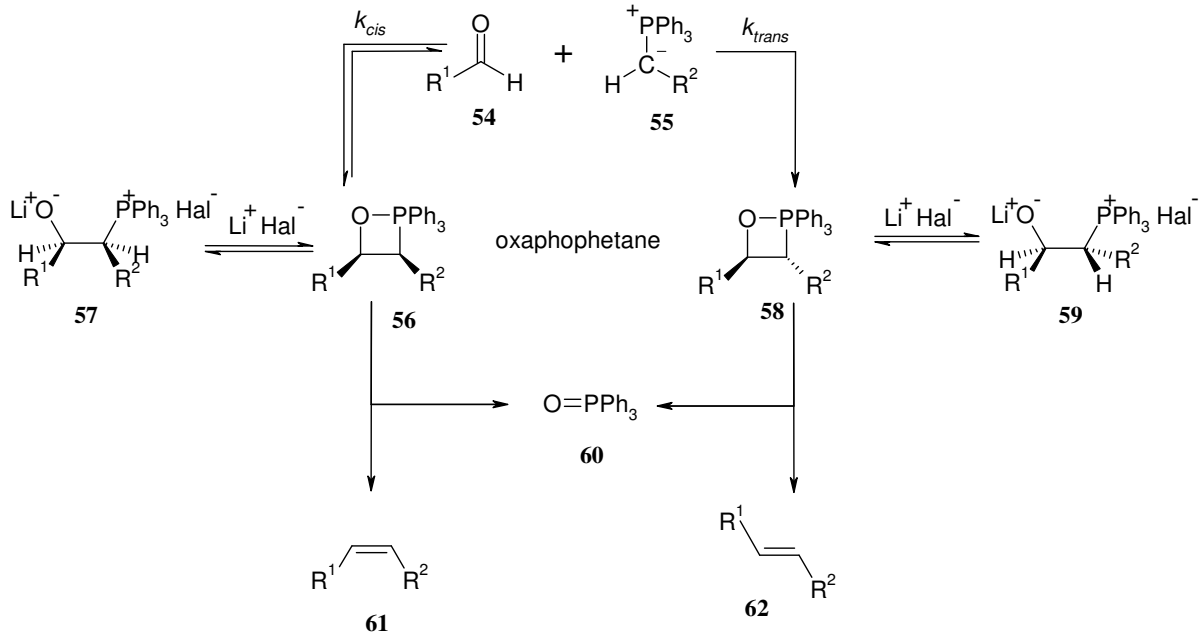

Scheme 13. Mechanism of the Wittig reaction.[40a]

The first step in the Wittig reaction is a [2+2]cycloaddition of the ylid **55** to the aldehyde **54** to form the oxaphosphetanes **56** and **58**.[40a] This heterocyclic intermediate then decomposes further into triphenylphosphine oxide **60** and the alkenes **61** and **62**.

cis-Disubstituted oxaphosphetane **56** decomposes stereospecifically to the *cis*-alkene **61** whereas *trans*-disubstituted **58** decomposes to the *trans*-alkene **62**. Which of the two oxaphosphetanes is formed depends on the ylid used in the reaction. The non-stabilized ylids give the *cis*-oxaphosphetane **56** very rapidly (k_{cis} is the rate constant for the formation of the *cis*-oxaphosphetane) and reversibly. On the other hand, from the same ylid the *trans*-oxaphosphetane **58** is formed very slowly (k_{trans} is the rate constant) but irreversibly. The *cis*-oxaphosphetane can isomerize to the *trans*-diastereomer before decomposing to the alkene, giving rise to a mixture of olefinic isomers. To prevent this isomerization, the Wittig reaction is performed in the absence of Li salts, using bases like $NaNH_2$, NaHMDS, KO*t*Bu. This type of Wittig reaction of non-stabilized ylids under "Li free conditions" is known to give *cis*-olefins stereoselectively. When Li salts are present, the faster formed oxaphosphetane **56** cannot react further to the *cis*-aldehyde **61**, because the cycle is opened to form the zwitterionic intermediate betaine **57**. In this reversible process, isomerization can occur and the *trans*-oxaphosphetane **58** is thermodynamically favored. The reaction of non-stabilized ylids in the presence of Li-salts is called the Schlosser variant of the Wittig reaction.

P-ylids react faster with C=O groups on increasing the electrophilicitiy of this bond. For this reason ketones react more slowly than aldehydes, enabling isomerization processes and yielding product mixtures of the two isomers without selectivity.

This was observed in the case of β-ionone (**22**), and 4-oxo-β-ionone (**23**), respectively, in reaction with phosphonium salt **52.** TLC and GC monitoring after 2 days of reaction saw complete transformation of the starting materials. The two isomers were formed in almost equal amounts.

Separation of the *cis*-/*trans*-isomers of aldehyde **47** and **53** is possible by column chromatography, although several runs are necessary for complete separation of the reaction products. Independently, the separated two isomers have been used further in a second Wittig reaction. As an alternative, the isomeric mixture cam also be used and subsequently all isomers of the final products can then be separated by HPLC.

3.4.2 Racemic and Enantioselective Synthesis of Phosphonium Salt 66 and its Derivatives

For the second Wittig reaction used to build the retinoid backbone, phosphonium salt **66** was synthesized. The synthesis was developed for the racemic phosphonium salt so that

eventually both enantiomers of **11** would be available for comparison with the natural product.

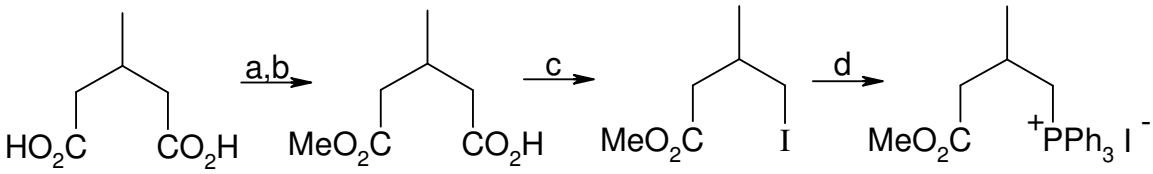

63 **64** **65** **66**

a) Ac_2O, reflux, 16 h (63 %); b) MeOH, reflux, 1h (86 %); c) I_2, $Pb(AcO)_4$, CCl_4 (60 %); d) PPh_3, benzene (61 %)

Scheme 14. Synthesis of *rac*-**66**.

Starting from commercially available 3-methyl-glutaric acid (**63**) the corresponding anhydride was obtained after 16 h reflux in acetic acid anhydride, followed by hydrolysis in methanol to the half acid ester **64**. This was reacted in a Hunsdiecker iodination with I_2 and $Pb(OAc)_4$ in CCl_4 to the iodo derivative **65**. Reaction with triphenylphosphine in benzene gave the desired phosphonium salt **66** as a racemic mixture. The iodo derivative proved to be quite instable so immediate reaction with triphenylphosphine was necessary, first without heating and after 10 h by heating the yellow solution slowly to 70 °C for 2 d. After the solvent had been evaporated the resulting viscous oil was stirred vigorously with diethyl ether to precipitate the white phosphonium salt **66**.

This was reacted with aldehyde **53**, as shown below, and the hydrolyzed product **11** was compared with the isolated vitamin A metabolite. Spectroscopic analysis and molecular modeling calculations indicated the *S* configuration of the natural product. To confirm this assumption an enantioselective synthesis of *S*-**66** was developed, using sections of the synthetic method already presented for *rac*-**66**.

3-Methyl-glutaric acid (**63**) was first esterified with methanol to the diester **67**, which in an enzymatically catalyzed desymmetrization reaction introduced the chiral center on the glutarate molecule enantioselectively.

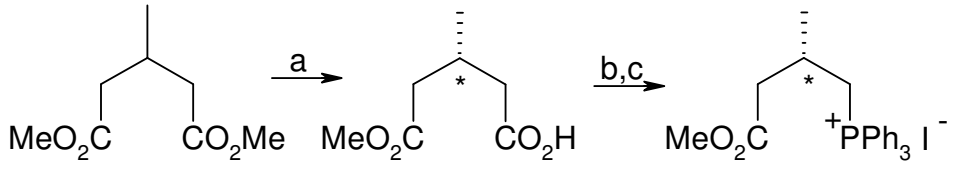

67 *R*-**64** (92%) *S*-**66** (36%)

a) NaOH (1 eq.), PLE (92 %); b) I_2, $Pb(AcO)_4$, CCl_4 (65 %);

c) PPh_3, toluene (55 %)

Scheme 15. Synthesis of *S*-**66**.

The asymmetric enzymatic synthesis of glutarates using pig liver esterase (PLE) has often been used in recent times. PLE is one of the hydrolytic enzymes with considerable asymmetric synthetic potential whose value for the production of useful chiral synthons, like 3-substituted glutarate monoesters has been demonstrated.[28] PLE-catalyzed hydrolysis of **67** was performed at pH 7 by addition of 1M aqueous sodium hydroxide. The reaction was worked up after addition of 1 equivalent of base. The diester **67** gave the *R*-half acid **64** in 70-80 % ee, depending on the reaction temperature and other solvent additives.[28] Mechanistically it has been proposed that the ester group to be hydrolyzed must be located adjacent to the nucleophilic serine function, the catalytic site of PLE.[28] The substituent at C-3 has a significant influence on the rate and stereoselectivity of the hydrolysis. For small substituents the hydrolysis is fastest but it falls progressively as the substituents become larger. Also, the stereoselectivity decreases for the 3-substitueted diester glutarate from methyl to propyl substituents and for larger groups inversion of the configuration was observed.[28]

Following the route given for *rac*-**64**, Hunsdiecker iodination of *R*-**64** gave *S*-**65,** which was reacted with triphenylphosphine to *S*-**66**.

The monoester *R*-**64** is commercially available, but for a significant price. Taking into account that the PLE needed for the synthesis of **64** is also quite expensive, and the product ee is lower than for the commercial compound, it is recommendable to start the synthesis of chiral phosphonium salt **66**, from commercially available *R*-**64**. In this case, 94 % ee of S-**11** was determined by chiral HPLC. The ee of **64**, **65**, and **66** is difficult to determine experimentally without further derivatization, and for this reason the ee of the enantioselective reaction was measured on the final chiral retinoids, by HPLC. The half ester *R*-**64**, has a very small reported $[\alpha]_D$ value of 0.4° in neat form, which makes calculation of the ee difficult. Because of the very low absorption spectra, these compounds were not detectable with the HPLC UV detector. The iodo derivate *S*-**65**

(measured at room temp. $[\alpha]_D$ = -0.53 °, c = 1.7055 g/100 mL in $CHCl_3$) and the phosphonium salt ***S*-66** (measured at room temp $[\alpha]_D$ = +0.98 °, c = 1.4285 g/100 mL in $CHCl_3$) have not been reported in the literature, so the $[\alpha]_D$ could not be compared to published values.

The racemic pathway to phosphonium salt **66** was applied for the synthesis of other new derivatives e.g. **72**, **73**, which were used, as described below, for the synthesis of C-13 modified retinoids.

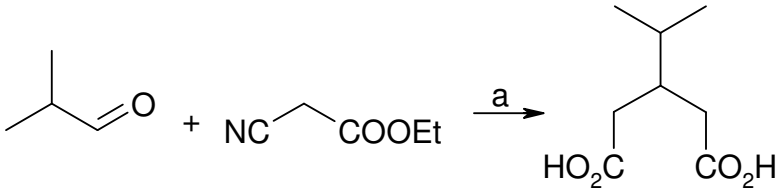

68 **69** **70**

a) [i] piperidine, benzene, reflux 1.5 h; [ii] diethylmalonate, Na, MeOH, reflux 4 h (64 %)

Scheme 16. Synthesis of 3-substituted glutaric acid derivative **70**.

3-Isopropyl-glutaric acid **70** was obtained as described in Scheme 16 by refluxing *sec*-butyraldehyde **68**, ethylcyanoacetate **69** and piperidine in benzene under Dean-Stark conditions until dehydration was complete.[41] The formed 2-cyano-4-methyl-2-penteneoic acid ethyl ester was refluxed with sodium dimethylmalonate in a Michael addition followed by acid catalyzed hydrolysis of the cyano and ester groups and decarboxylation to the diacid **70**. Following the same methodology described for the synthesis of rac-**66**, **70** was reacted to the corresponding phosphonium salt **72** (Scheme 17).

R	
*i*Pr	**70**
Ph	**71**

R	
*i*Pr	**72**
Ph	**73**

a) Ac_2O, reflux, 16 h (*i*Pr: 88 %, Ph: 62 %); b) MeOH, reflux, 1 h (*i*Pr: 62%, Ph: 98 %); c) I_2, $Pb(AcO)_4$, CCl_4 (*i*Pr: 64 %, Ph: 87 %); d) PPh_3, benzene (*i*Pr:10 %, Ph: 74 %)

Scheme 17. Synthesis of substituted phosphonium salts.

Commercially available 3-phenyl-glutaric acid was used for the synthesis of **73**, *via* the anhydride and iodo derivatives.

These modified phosphonium salts **72** and **73** were prepared as racemic mixtures, an enantioselective synthesis was not needed before first biological tests with the C-13 substituted retinoids would show any interesting properties.

3.4.3 Synthesis of 13,14-Dihydro-retinoic Acid (10) and 4-Oxo-13,14-dihydro-retinoic Acid (11)

Using the aldehydes **47**, and **53**, respectively, two methods were developed for the synthesis of the target vitamin A derivatives. Wittig and HWE reactions were used to construct the terminal part of the retinoid chain. For this purpose, the new phosphonium salt **66** and the analog phosphonate **105** were employed. Each of these reactions presented advantages and disadvantages, as will be discussed below.

The Wittig reaction was performed between aldehyde **47** or **53** and the nonstabilized phosphonium salt **66**, which, because of the reasons discussed above, will form the *cis* double bond stereoselectively. But in the target compound **11**, the C-11/C-12 double bond should be *trans* and for this reason, the stereochemical preference was shifted to this isomer by the presence of Li containing bases. Li ions induce the heterolytic cleavage of the O-P bond of the oxaphosphetane, forming the lithiobetaine **57** and **59** (Scheme 13), which influence the stereochemical course of the Wittig reaction because the faster reaction path to the alkene **61** is hindered. Further details of this process remain to be established until today.[40a]

The Wittig reaction between aldehyde **47** and phosphonium salt **66** was carried out in the presence of lithium hexamethyldisilazide (LiHMDS) as a base. When the *trans*-aldehyde **47** was used, all-*trans*- and 11-*cis*-13,14-dh-RA methyl ester (**74**) were obtained in 1.0:1.5 ratio. The *cis*-aldehyde **47** gave 9-*cis*- and 9,11-di-*cis*-**74** in 1:1 ratio. If **47** was used without previous separation of the isomers, all possible four isomers (all-*trans*-, 9-*cis*-, 11-*cis*-, 9,11-di-*cis*-**47**) were obtained in 1.7:1.0:3.0:1.0 ratio.

Most isomer ratios presented in this work were assigned by ^{1}H NMR analysis of the isomer mixtures directly after the reaction. HPLC chromatograms are not always giving reproducible results because isomerization occurs within time or because long retention times needed for a good separation increased the peaks area and gave incorrect integrals.

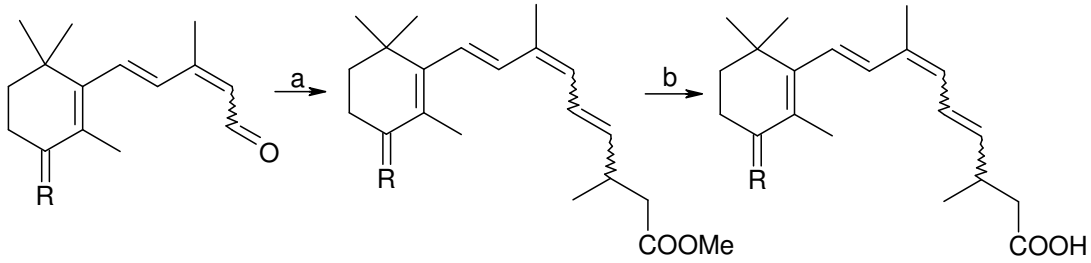

R		R		%	R		%
H,H	**47**	H,H	**74**	78	H,H	**10**	98
O	**53**	O	**75**	62	O	**11**	91

a) **66**, LiHMDS, THF, -78 °C - room temp., 3 h; b) KOH, EtOH/H_2O, reflux, 3 h

Scheme 18. Synthesis of dh-RA derivatives **10** and **11**.

Using the same Wittig reaction conditions, aldehyde **53** gave the four possible isomers all-*trans*-, 9-*cis*, 11-*cis*- and 9,11-di-*cis*-**75** in 2.0:1.0:3.4:1.0 ratio. When the separated isomers of **53** were employed, all-*trans*- and 11-*cis*-**75** were obtained in 1.2:1.0, and 9-*cis*- and 9,11-di-*cis*-**75** were obtained in 1.0:1.2 ratio, respectively. Hydrolysis to the corresponding acids **11** and **10** was performed with KOH in EtOH/H_2O as shown in Scheme 18. All isomer ratios are summarized in Table 1.

Table 1. Isomer ratios for 13,14-dihydro-retinoids determined by ^{1}H NMR spectroscopy.

	all-*trans*	9-*cis*	11-*cis*	9,11-di-*cis*
13,14-dh-RA-methyl ester (**74**)	1.7	1.0	3.0	1.0
	1.0	-	1.5	-
	-	1.0	-	1.0
13,14-dh-RA (**10**)	1.6	1.0	3.0	1.2
	1.0	-	1.7	-
	-	1.0	-	1.1
4-oxo-13,14-dh-RA-methyl ester (**75**)	2.0	1.0	3.4	1.0
	1.0	-	1.5	-
	-	1.0	-	1.3
4-oxo-13,14-dh-RA (**11**)	2.2	1.0	3.1	1.2
	1.2	-	1.0	-
		1.0		1.2

The esters, and the acids of the RA derivatives, respectively, synthesized here were analyzed by reversed phase and normal phase HPLC. Analytical separation methods were developed for some of the new derivatives and complete characterization was performed by the usual spectroscopic techniques (NMR, MS, IR, UV) and CD for the diastereomers separated by chiral HPLC.

3.4.4 Synthesis of Modified 13,14-Dehydro-retinoids

New retinoids incorporating a bulky substituent at the chiral center C-13 were synthesized as described before for the methyl derivative.

When phosphonium salt **73** was reacted with **47** in the presence of LiHMDS as base, 13-phenyl-13,14-dh-RA methyl ester (**78**) was obtained in 85 % yield. Saponification with KOH in EtOH/H_2O gave the corresponding acid **82** in 92 % yield. Wittig reaction of the 4-oxo-aldehyde **53** with **73** and LiHMDS furnished the ester **79** in 82 % yield, which was hydrolyzed to the corresponding acid **83** almost quantitatively. Under the same conditions, the isopropyl substituted phosphonium salt **72** was reacted with aldehyde **47**, and **53** to give the 13-isopropyl substituted retinoid esters **76**, and **77** respectively. During hydrolysis these esters underwent additional reactions, which were not further clarified after the first experiments. Due to insufficient quantity of available starting material **72** the reaction was not repeated.

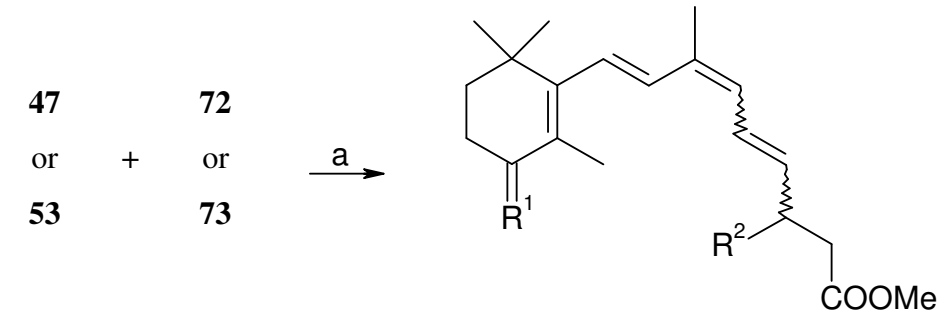

R^1	R^2		%
H,H	*i*Pr	**76**	3
O	*i*Pr	**77**	3
H,H	Ph	**78**	85
O	Ph	**79**	82

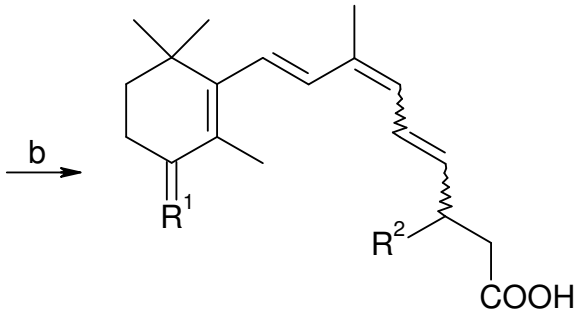

R^1	R^2		%
H,H	*i*Pr	**80**	0
O	*i*Pr	**81**	0
H,H	Ph	**82**	92
O	Ph	**83**	97

a) LiHMDS, THF; b) KOH, EtOH/H_2O

Scheme 19. Synthesis of C-13 substituted 13,14-dh-RA derivatives.

These new C-13 substituted retinoids can be tested for their biological properties using the racemic products. If pure enantiomers are needed, good chiral HPLC separation methods have to be developed. This was achieved for the 4-oxo-13-ph-dh- and 13-ph-dh-retinoids. Alternatively, a new enantioselective synthesis has to be developed. Further details are given in Chapter 4.

3.4.5 Synthesis of Labeled 13,14-Dihydro-retinoic Acids

The developed pathway for the synthesis of 13,14-dh-RA derivatives, offers not only a short and fast synthetic method to the desired new retinoids, but also the possibility to

design new derivatives. Substitution of hydrogen atoms by deuterium can be performed and the labeled retinoids can be used for a deeper understanding of the metabolism of RA. Investigations on the mechanism of retinoid interaction with receptor proteins have been carried out already with labeled vitamin A derivatives.[12e] The methods include labeling with ^{2}H, ^{3}H, ^{14}C, ^{125}I at different positions of the retinoid skeleton.

In this study the most convenient method was to use deuterium labeling, because deuterated retinoids are particularly useful in investigations in which mass spectrometric analysis of HPLC peaks can be used to detect the retinoid metabolites. The deuteration position was chosen in such a way, that, if further metabolization occurs on the chain or on the cyclohexen ring, the retinoid backbone could be traced through all steps. Oxidations, reductions and other degradation processes are known to take place at the terminal functional group of the chain and/or on the cyclohexene ring, and for this reason the C-9 position seems ideal for labeling.

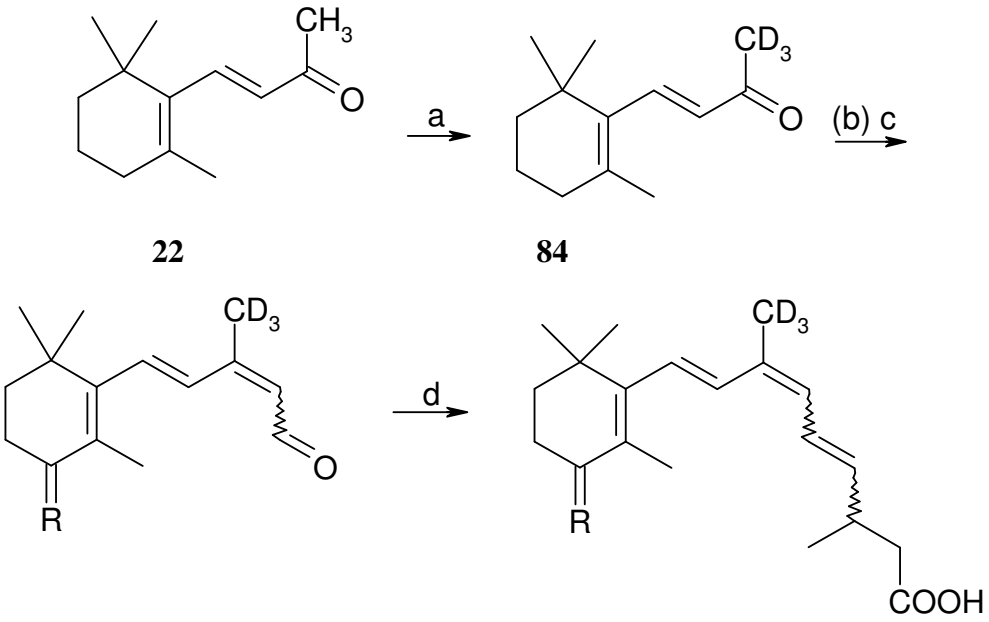

R	
H,H	**85**
O	**86**

R^1	R	
H,H	Me	**87**
H,H	H	**88**
O	Me	**89**
O	H	**90**

a) NaOD, D_2O, pyridine, 1 h, room temp. (100 %); b) for obtaining **86**: PCC, DMSO, 5 h, 105 °C (43 %); c) **52**, KO*t*Bu, THF, $C_2H_2O_4/H_2O$ (75 %, 73 %); d) [i] **66**, LiHMDS, THF; [ii] KOH, EtOH/H_2O (66 %, 74 %)

Scheme 20. Synthesis of D-labeled 13,14-dh-RA derivatives.

β-Ionone (**22**) was first labeled with deuterium, using a procedure developed by Liaaen-Jensen for carotenoids.[42]

Deuterium was introduced by base-catalyzed deuterium exchange of enolizable hydrogen. Reaction of **22** with NaOD, in D_2O/pyridine gave after 1 hour in quantitative chemical yield 80 % CD_3 incorporation, 18 % CD_2H incorporation and 2 % monodeuterated **84**.

Oxidation of **84** at C-4 with PCC gave deuterated 4-oxo-β-ionone (**91**). During acidic work-up of this reaction some of the deuterium was exchanged by hydrogen. The retinoids were further synthesized as described for the unlabeled compounds. In the first Wittig reaction, although some of the deuterium was exchanged again by hydrogen in the acid deprotection steps of the dioxolan ring, the samples were still over 60 % deuterated. In the next steps, no further loss of deuterium was observed, the isotopic pattern in the mass spectra remaining constant.

The deuterium ratio was determined from the MS spectra, and is summarized in Table 2.

Table 2. Deuterium incorporation (%) determined by mass spectrometry.

	CH_3	CH_2D	CHD_2	CD_3
84	0.3	2.2	17.9	78.7
91	21.0	40.7	29.1	8.9
85	12.2	40.2	28.8	15.9
86	38.4	39.9	18.4	3.9
87	16.6	34.9	31.1	14.4
88	16.2	35.1	31.4	14.7
89	43.6	38.0	13.7	4.0
90	45.7	36.6	13.2	3.7

The characteristic pattern of the molecular ion peaks in the mass spectra of the deuterated samples allows using these samples in biological matrices, which after treatment with the labeled retinoids can be extracted and analyzed for the different metabolites by HPLC/MS. For these investigations, very small amounts of sample are needed and the gained information can be vital in understanding unknown steps in retinoid metabolism.

3.4.6 Synthesis of 4-Hydroxy-retinoids

As mentioned above, consecutive built-up of the retinoids by Wittig reactions has several advantages for the preparation of other new derivatives. Starting materials α-

and β-ionone offer several possibilities for chemical modification of the cyclohexene ring, near 4-oxo-dh-RAs shown above, the synthesis of 4-hydroxy-13,14-dh-RA (**98**) was designed.

A first approach to synthesize this derivative started from the 4-oxo ester **75**. Reduction with $NaBH_4$ gave a complex mixture of inseparable compounds and proved to be unsuccessful.

The second approach was to obtain 4-hydroxy-β-ionone (**94**), protect the hydroxy group, perform the Wittig reactions to the target retinoid esters, and in one step deprotect the hydroxy function and hydrolyze the ester to the free acid. For this sequence α-ionone (**92**) was chosen as starting material. The non-conjugated double bond was oxidized with metachloroperbenzoic acid (MCPB) to the epoxide **93** in 96 % yield. By treatment of **93** with $NaOCH_3$ the epoxide ring opens to the free alcohol **94**. Because racemic α-ionone was used in this synthesis, **94** was obtained as a mixture of the two enantiomers. The same reaction sequence could be enantioselectively performed when starting from enantiomerically pure α-ionone, because epoxidation of **92** is *cis*-stereoselective.[26] In this way enantiocontrol at C_4 could be achieved, which could be advantageous for the final chiral separation of **97**, **98** respectively.

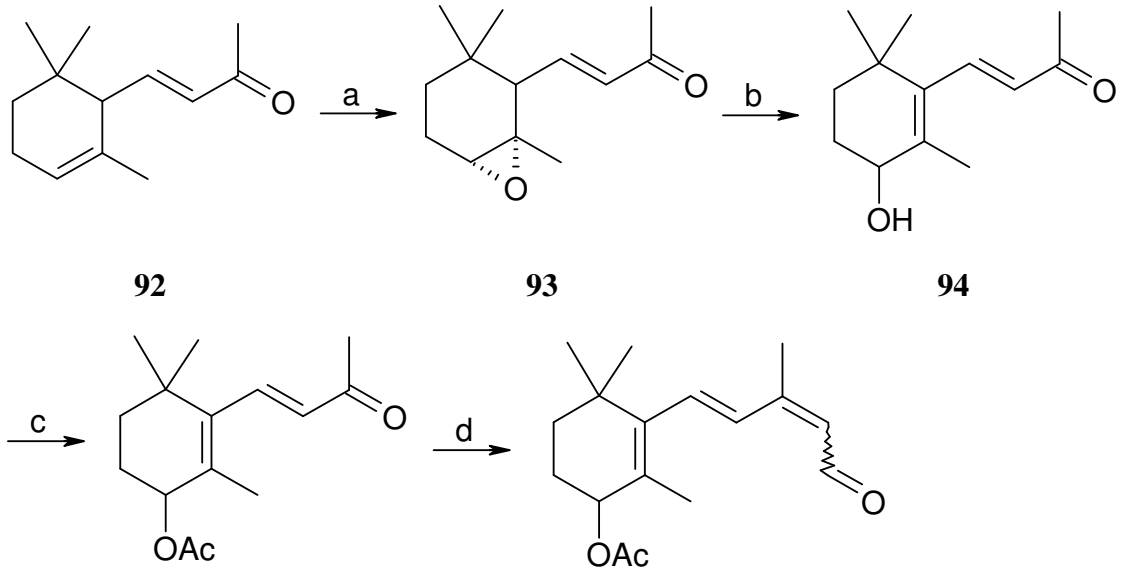

92 **93** **94**

95 **96**

a) MCPB, CH_2Cl_2, room temp., 3 h (96 %); b) NaOMe, MeOH (86 %); c) Ac_2O, pyridine, CH_2Cl_2 (42 %); d) **52**, KO*t*Bu, THF, $C_2H_2O_4/H_2O$ (41 %)

Scheme 21. Synthesis of aldehyde **96**.

Allyl alcohol **94** was protected with triethylsilyl chroride (TESCl) to the corresponding silyl ether, which, similar to β-ionone, was reacted in a first Wittig reaction with

phosphonium salt **52** to the appropriate chain elongated aldehyde. The obtained product was not the expected 4-OTES protected aldehyde but the 4-hydroxy aldehyde. Hydrolysis of the dioxolan ring deprotected also the silyl ether, even when aqueous acetic acid in THF (4:1:1 $CH_3COOH/H_2O/THF$), rather than oxalic acid was used. To avoid this deprotection, the acetyl function was used as protecting group and aldehyde **96** was obtained. Following the same synthetic route as described for **74**, by means of a second Wittig reactions, the ester **97** was obtained as a mixture of four isomers (all-*trans*/9-*cis*/11-*cis*/9,11-di-*cis*) in 1.7:1.0:2.6:1.1 ratio.

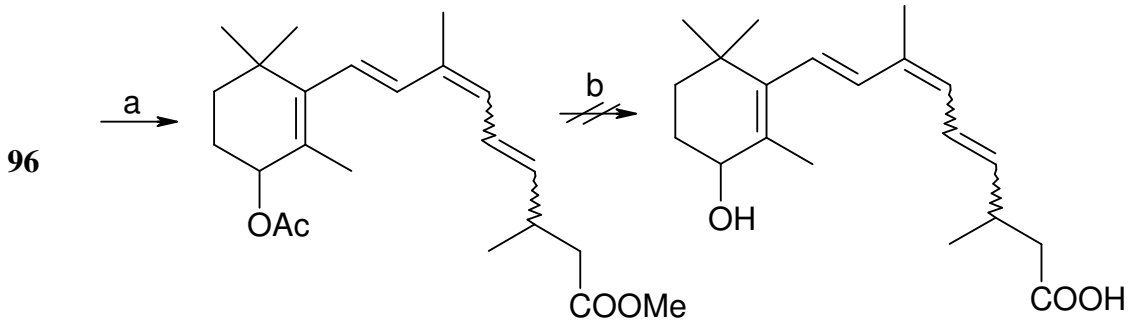

97 **98**

a) **66**, LiHMDS, THF (32 %); b) KOH, $EtOH/H_2O$

Scheme 22. Wittig reaction and saponification to derivative **98**.

Hydrolysis of the two ester groups was performed using KOH in $EtOH/H_2O$. After 2 h at 70 °C, under Ar, the reaction mixture was extracted with ether. The basic aqueous phase was acidified to pH 5-5.5 with diluted acetic acid, so that the free acid group can be protonated and hydroxy-acid **98** can be extracted from water into the organic phase. It seems that during this step, the deprotected hydroxyl function was also protonated in the acidic milieu and undesired reactions took place, which destroyed the product. The 4-OH-13,14-dh-RA **98** could not be isolated.

The instability of this molecule could be also one reason why this metabolite was not detectable so far in retinoid polar fractions of analyzed biological samples.

3.4.7 Horner-Wadsworth-Emmons Approach

The synthesis of the target molecule **11** was achieved as shown above, by two consecutive Wittig reactions. The *cis*-/*trans*-selectivity of these reactions can be controlled only poorly so that almost equal amounts of all four isomers were obtained. This enables biological investigations on all isomers after their separation. However, the most active derivatives should be the all-*trans*- and the 9-*cis*-isomers.

The HWE reaction is known to have a higher *trans*-selectivity than the Wittig reaction. For this reason an alternative HWE two reaction sequence was developed for the all-*trans*-**11** and all-*trans*-**10** retinoids.

Alternatively, after construction of the C-9/C-10 double bond by Wittig reaction (as described above for **47** and **53**) and separation by column chromatography of the formed isomers, each of them can be used separately in a HWE reaction to build the C-11/C-12 double bond *trans*-selectively. In this way, using a combination of Wittig- and HWE-reactions, a stereoselective synthesis of all-*trans*- and 9-*cis*-**11** and -**10** would become available.

In carotenoid and retinoid synthesis there are several examples in which the HWE reaction was used to form the linear polyene chain. Eugster and coworkers used this reaction for the synthesis of various new substituted carotenoids.[38] Using the same procedure, the aldehyde **47** was obtained.

Deprotonation of diethoxyphosphoryl acetic acid ethyl ester (**99**) with NaH and reaction of the formed anion with **22** gave the ester **100** as a *trans*-/*cis*-isomer mixture in 8:1 ratio. This ester was reduced with DIBAL to the corresponding alcohol **101**, which was reoxidized with MnO_2 to the aldehyde **47**. The *trans*-selectivity of the C-9/C-10 bond is obviously improved by this pathway. However, this route cannot be used for the 4-oxo derivative **53**, without an additional protection step of the 4-oxo ketone group, because reduction of the ester function with DIBAL or other reducing reagents will also reduce this function.

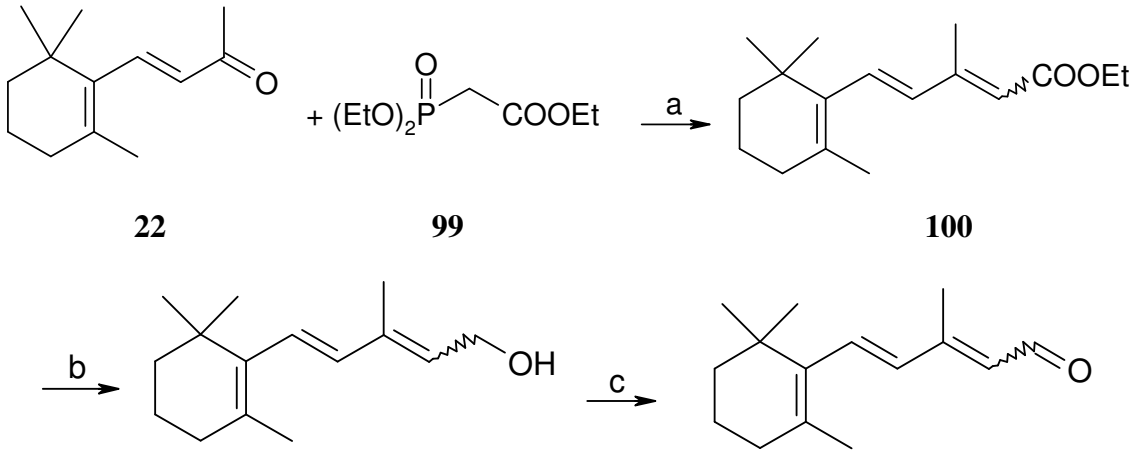

a) NaH, THF (31 %); b) DIBAL, Et_2O (100 %); c) MnO_2, ethyl acetate (72 %)

Scheme 23. Synthesis of aldehyde **47** by HWE reaction followed by oxidation.

For constructing the next double bond, C-11/C-12 of the final retinoids, the phosphonate corresponding to the phosphonium salt **66** was synthesized.

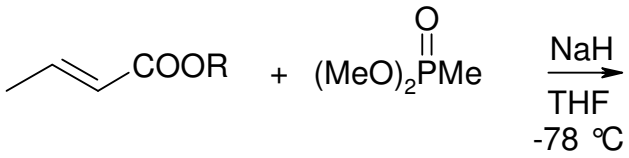

R	
Et	**102**
*t*Bu	**103**

104

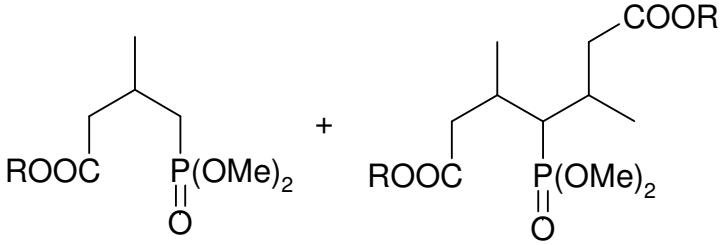

R	
Et	**105**
*t*Bu	**106**

107 (R = Et)

Scheme 24. Michael addition to the phosphonates **105** and **106**.

Michael addition of ethyl crotonate **102** to the phosphoric acid derivative **104** gave the 1,4-addition product **105** as well as di-addition product **107** in approximately 1:5 ratio (obtained by GC analysis). To avoid this undesired product, *t*-butyl crotonate **103** was used. In this case only the 1,4-addition product **106** was observed.

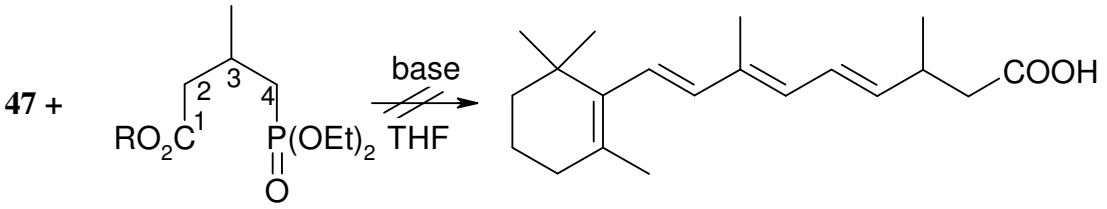

R	
Et	**105**
^{t}Bu	**106**

10

Scheme 25. Attempted synthesis of **10** by HWE reaction.

HWE reaction of **106** and aldehyde **47** was performed using NaH as base. Since GC control showed that no reaction took place, a stronger base was employed for deprotonation. Using *n*BuLi, a complex mixture of products was observed by GC

analysis. Since *n*BuLi is not only a strong base but also a good nucleophile, side reactions can take place on the carbonyl or on the phosphonate groups.

Deprotonation experiments with one equivalent of *n*BuLi followed by quenching the anion with D_2O showed deuterium incorporation at C-2. By using 2 equiv. of *n*BuLi and quenching again with D_2O, the same methylene group was deuterated and the ester function was attacked by the *n*-butyl rest.

The acidity difference between the methylenic groups C-2 and C-4 of phosphonate **105** was calculated by computational methods. These calculations measure thermodynamic acidity. The energy of the starting phosphonate was compared with the energy of the deprotonated species and ΔG was calculated. Under equilibrium conditions, the thermodynamically most stable product will be the predominant or even exclusive product.[40b] Calculations of the kinetic acidity (which reaction path has the lower activation barrier and which product is formed faster) were not undertaken here.

The energy difference between deprotonation of the two methylene groups C-2 (ΔG_1), and C-4 (ΔG_2) is relatively small (ΔG_1-ΔG_2 = 4.8 kcal/mol). Comparable energy differences in the proton affinity of the CH_2 groups in the vicinity of an ester and of a phosphonate function were also noted in case of phosphonate **27** (see Chapter 3.2 and Chapter 8). For phosphonium salt **66** this energy difference is much higher ($\Delta\Delta G$ = 26.2 kcal/mol), enabling selective deprotonation. Details about these theoretical proton affinity calculations will be discussed in Chapter 8.

These facts made the stereoselective synthesis of all-*trans*-, respectively 9-*cis*-retinoids unattainable at present.

Thus, the best method for the synthesis of 13,14-dihydro-retinoids is the consecutive Wittig reaction protocol, followed by HPLC-purification (see next chapter). Even if selective reactions would have been available, small amounts of the undesired isomers are always formed, which for biological investigations should be removed.

4 Analysis of Retinoids by High Performance Liquid Chromatography

4.1 Separation of Retinoids by Reversed Phase HPLC

High performance liquid chromatography (HPLC) is the method of choice for separating and quantifying naturally occurring and synthetic retinoids. Most retinoids analyses are performed under reversed phase conditions, using a hydrophobic stationary phase (typically RP C_2, C_8, C_{18}) and a more polar mobile phase (methanol, acetonitrile with small amounts of water).[43] The polar components interact less with the unpolar alkyl chains bound to silica and are eluted faster than the nonpolar samples. Partition chromatography (reversed phase) has the advantage to give a better separation for different classes of retinoids, which is the case in biological samples where ROH, RAL, RA and retinyl esters have to be first separated from each other. Adsorption chromatography (normal-phase) sometimes gives better results in separating the isomers of retinoids. In adsorption chromatography the sample is adsorbed onto the polar stationary phase and is displaced from its adsorption sites by the mobile phase, typically hexane. In this mode, less polar samples are eluted before the more polar. Normal phase columns were used especially in early carotenoid analysis as open-columns, later on HPLC.[44] There are no standard methods for separation of retinoids, most researchers develop their own methods with different eluents and additives of the mobile phase.

For the analysis and separation of the synthetic retinoids reported here, both types of HPLC columns were used and compared. Adsorption chromatography was performed on chiral columns also as will be discussed later.

Reversed phase chromatography combined with gradient or isocratic HPLC was used to separate **11** and **10**. Several columns, respectively stationary phase materials were used and compared: Hibar RT 250-10 filled with Lichrosorb RP-18 (7 μm) material, LiChroCART 250-4 filled with Purospher RP-18 endcapped (5 μm) material, and Nucleosil 250-10, C_{18} (7 μm) material. The retinoids were detected by measuring the absorbance of ultraviolet light with a diode array detector (DAD) or UV detector. Octadecylsilane (ODS, C_{18}) stationary phase was used by Nau and co-workers for analysis of liver extracts and for comparison of isolated metabolites with synthetic products.

The characteristics of different packings are determined by the mode of preparation of the silica particles, the mode of covalent attachment of the hydrocarbon chains to the silica, the density of hydrocarbon coverage (carbon load) of the column, and the presence or absence of unreacted silanol groups. Unreacted silanol groups on the silica particles can interact by hydrogen bonding with some functional groups of the analytes. Some commercial column packing are endcapped (those silanol groups remaining after covalent addition of the octadecyl chains are subsequently reacted with trimethylsilyl groups) to reduce these silanol-sample interactions.[44]

Unfortunately, only a small number of isocratic separation methods have been developed, mostly because the isomers are not baseline separated and long retention times are required for a good separation. Of course, an isocratic method would be easier to use and also more economical than the gradient method because no stabilization of the column is necessary after each run.

Purospher RP-18 material, which consists of tightly packed 5 μm spherical silica particles was expected to show high efficiency in the separation of the isomers. Smaller particles packed into columns with higher density allow less diffusion of the sample between particles causing narrower, sharper peaks. On this material, shorter analysis times are noted, and an isocratic method could become suitable.

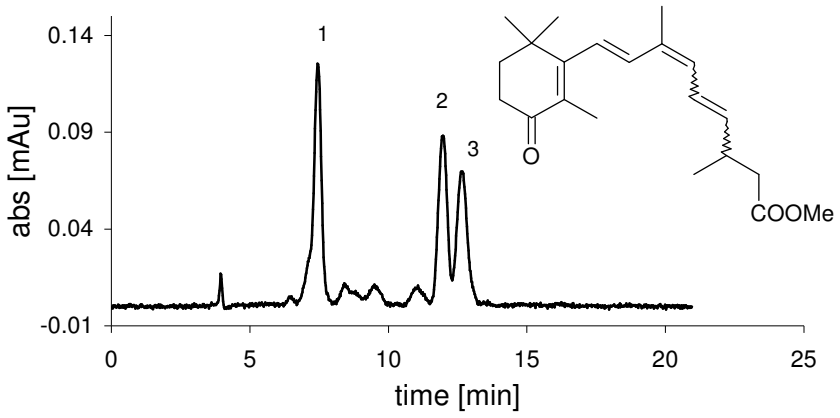

Figure 8. HPLC separation of **75** on Purospher RP-18, 5 μm, CH_3CN/H_2O 60:40, 1 mL/min.
Fraction 1: 9-*cis*- and 9,11-di-*cis*-**75**; fraction 2: 11-*cis*-**75**; fraction 3: all-*trans*-**75**.

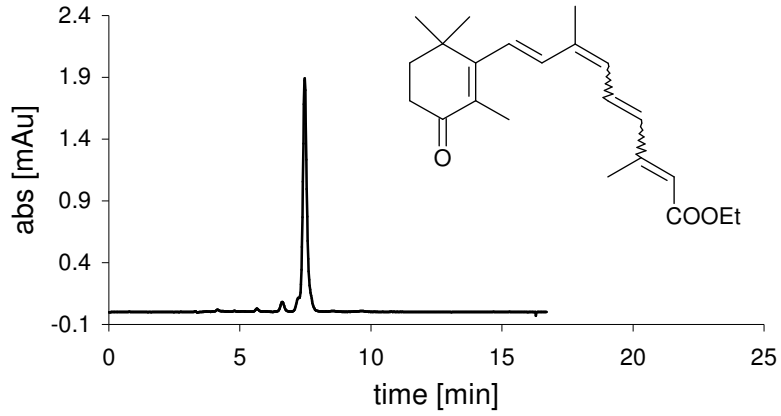

Figure 9. HPLC separation of **41** on Purospher RP-18, 5 µm, CH_3CN/H_2O 60:40, 1 mL/min (all-*trans*- and 11-*cis*-isomers eluted together).

The synthesized 13,14-dihydro retinoids **11, 75, 10, 74** were analyzed on a Purospher endcapped column and compared with the known retinoids RA ester and 4-oxo-RA ester. On this column, different isocratic methods methanol/water and acetonitrile/water in several proportions were tried.

The isomers of the 4-oxo-13,14-dh-RA ester (**75**) were not completely resolved on this column. The retention time of all-*trans*-**41** is shorter than that of all-*trans*-**75** and almost identical with that of the 9-*cis*- and 9,11-di-*cis*-isomers of **75**, which were eluted together.

The acids **11** and **10** are eluting too fast on this column. The reason could be their high polarity and the lack of any additional interactions of the acid group with free hydroxyl groups on the endcapped material of the column.

When the all-*trans*- and 11-*cis*-**74** products of the selective synthesis were injected, the two isomers were separated (Figure 11), while 9-*cis*- and 9,11-di-*cis*-**74** eluted together (Figure 10), as the 4-oxo ester **75**. All-*trans*-**40** eluted later than the same isomer of the 13,14-dihydro compound.

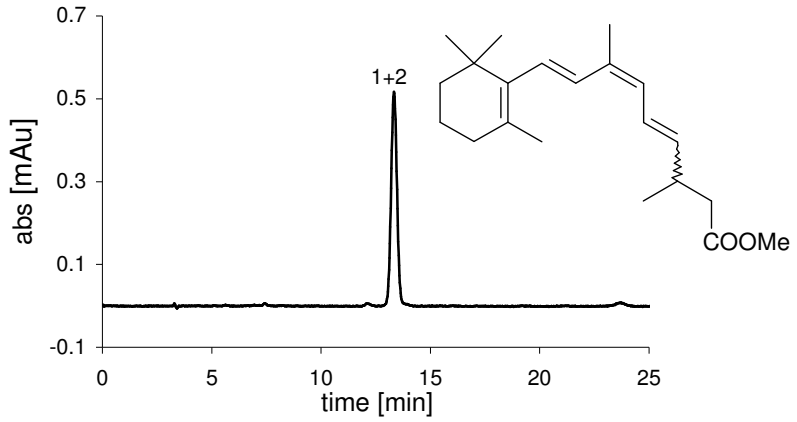

Figure 10. HPLC analysis of 9-*cis*- and 9,11,-di-*cis*-**74** on Purospher RP-18-endcapped, 5 µm, CH_3CN/H_2O 60:40, 1mL/min.

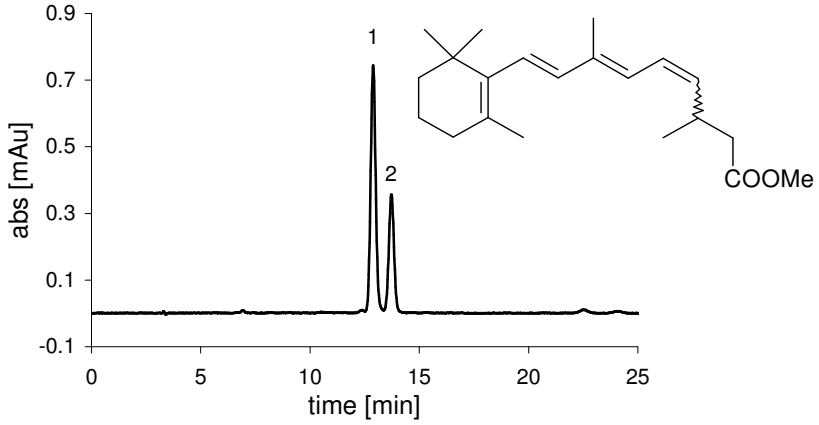

Figure 11. HPLC separation of **74** on Purospher RP-18-endcapped, 5 µm, CH_3CN/H_2O 60:40, 1mL/min. Fraction 1: all-*trans*-**74**; fraction 2: 11-*cis*-**74**.

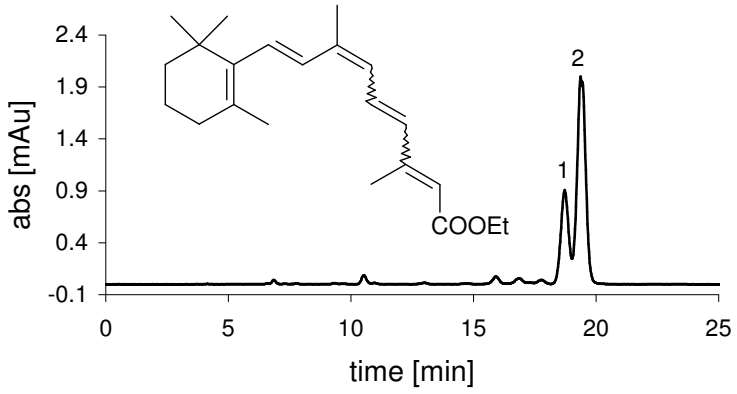

Figure 12. HPLC separation of **40** on Purospher RP-18-endcapped, 5 µm, CH_3CN/H_2O 60:40, 1mL/min. Fraction 1: 11-*cis*-; fraction 2: all-*trans*-**40**.

On a Lichrosorb RP-18 column, particle size 7 µm, an isocratic method for separating the isomers of **11** also proved unsuccessful. Although under the same isocratic

conditions, the retention time was longer than on the Purospher column, complete separation of all isomers was not achieved.

For retinoid analysis, an isocratic program that can separate the isomers in a short time and with no buffer eluents was desirable. Because this was not achieved on the Purospher and Lichrosorb columns, other columns and gradient methods were tested.

On Nucleosil C_{18}, particle size 7 μm, separation of all four isomers was possible only with a very long gradient program. The solvents used were A: water, B: methanol, C: acetonitrile at a constant flow of 2 mL/min in the following program:

time (min)	B (%)	C (%)
0	10	10
60	10	10
61	20	10
64	20	10
65	30	10
80	30	10
90	30	20
100	10	10

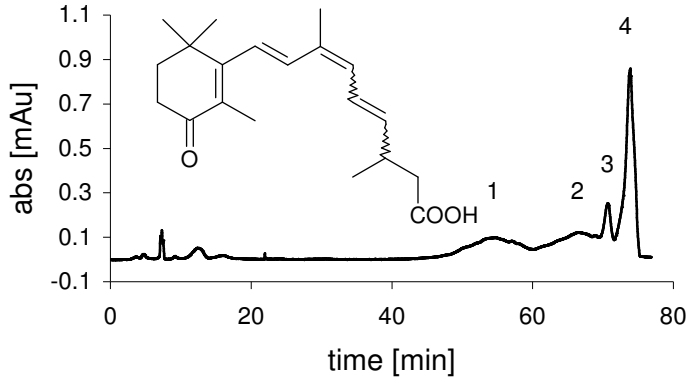

Figure 13. HPLC analysis of **11** on Nucleosil C_{18}, 7 μm with a gradient program. Fraction 1: 9,11-di-*cis*-; fraction 2: all-*trans*-; fraction 3: 9-*cis*-; fraction 4: 11-*cis*-**11**.

Because of the long retention time, the peaks became broad so the solvent polarity had to be increased. The chromatogram with the new method is shown in Figure 14. The program was run with the same solvents and flow and the new gradient was:

time (min)	B (%)	C (%)
0	10	10
40	10	10
42	20	10
60	20	10
80	30	10
85	30	20
100	10	10

Using this method, 9-*cis*-**11** is not separated anymore from the 11-*cis*-isomer. Several modifications on the solvent mixture and the gradient program did not improve the separation.

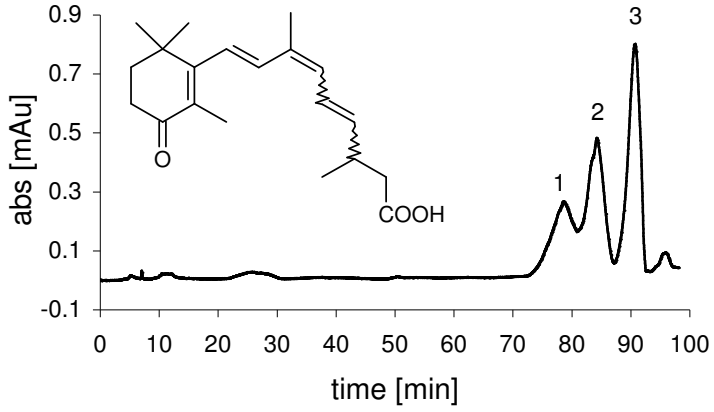

Figure 14. HPLC analysis of **11** on Nucleosil C_{18}, 7 µm, gradient program and buffer additive.
Fraction 1: 9,11-di-*cis*-; fraction 2:all-*trans*-; fraction 3: 9-*cis*- and 11-*cis*-**11**.

An improvement was achieved by using a buffer in the mobile phase.

A binary gradient of solvent A: 1:1 methanol/water with ammonium acetate, 60 mM, and B: methanol was used. The gradient composition was: 1) 0 min 1 % B, 2) 20 min 1 % B, 3) 22 min 10 % B, 4) 45 min 10 % B, 5) 49 min 1 % B, 6) 60 min 1 % B, at a constant flow rate of 3 mL/min (Figure 15). The method was adapted after the analytic separation method developed by C. Schmidt for the analysis of polar retinoids in biological samples.[17]

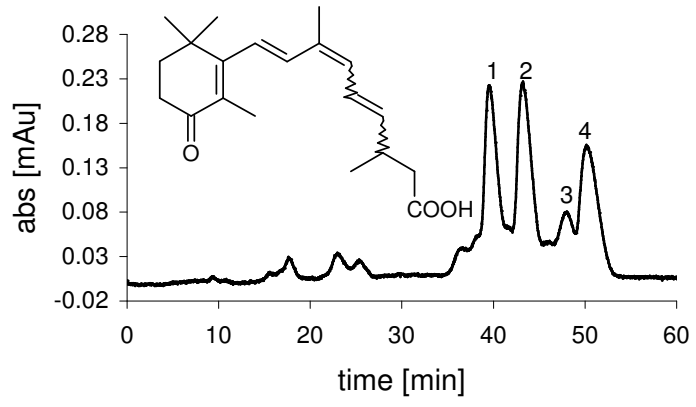

Figure 15. HPLC separation of **11** on Nucleosil C_{18}, 7µm, 250 x 10 mm with a gradient program.
Fraction 1: 9,11-di-*cis*-; fraction 2: all-*trans*-; fraction 3: 9-*cis*-; fraction 4: 11-*cis*-**11**.

In conclusion, the differently modified RAs are easily separated by using isocratic methods on RP-18 HPLC columns, as shown on a Purospher 5 µm column, but to find a proper method for the complete separation of all geometric isomers of the 13,14-

dihydro retinoids proved to be time consuming. For this reason normal phase HPLC was tested.

4.2 Enantioselective Separation

Resolution of racemates is one of the most important methods to obtain optically active compounds. Since Pasteur succeeded in the first resolution of a racemic compound,[45] sodium ammonium salt of (±)-tartaric acid in 1848, numerous methods of resolution have been developed. The first method was crystallization (ex: manual sorting of conglomerates, preferential crystallization, resolution as diastereomer, inclusion in a optically active host compound). Other methods include kinetic resolution by enzymes or chromatographic separations.

Chiral separation by HPLC using a chiral stationary phase (CSP) is today one of the most efficient methods to separate enantiomers, not only on the analytical but also on the preparative scale.

There are basically two types of CSPs: one consist of a chiral selector, like a chiral small molecule that is usually bound to an achiral support, such a silica gel; the second is based on a chiral polymer which can be used as a porous gel or can be bound on silica. The first stationary phase belonging to the first group, prepared by Pirkle,[46,47] was based on dinitrobenzoyl derivatives of amino acids, particularly phenylglycine and leucine, coated onto silica materials. These ionic phases showed excellent efficiency but were limited to low-polarity solvents, which initiated the development of covalently bound phases[46] like β-naphthoyl derivatives of alanine. The second group of chiral phases includes polyacryamides, one-handed helical polymethacrylates, polyamides, proteins and polysaccharide derivatives. Polysaccharides such as cellulose, amylose and chitin are the most accessible optically active polymers on earth. These polysaccharides themselves show rather low chiral recognition, but their derivatives, such as triacetate, tribenzoate, and triphenylcarbamates, exhibit high chiral recognition ability and can resolve a broad range of racemates. The first CSP derived from cellulose was prepared by Hesse and Hagel in 1973.[48,49]

These results provided a breakthrough in the area of chiral stationary phases based on derivatized polysaccharides. Among the cellulose esters, cellulose carbamates and amylose carbamates show characteristic high resolving abilities as CSP when coated on silica gel.[50] Chiral recognition greatly depends on the substituents on the aromatic ring, but also on the coating conditions, particularly the additives added to the solvent used

for coating.[51] Another important step in improving the properties of the chiral phase was achieved by Okamoto[52] with the development of chiral immobilized phases by radical copolymerization with styrene or 2,3-dimethylbutadiene. The immobilization of polysaccharides on a matrix has been considered as an evolutionary approach to implement universal solvent compatibility on the CSPs. Table 3 lists some of the polysaccharide derivatives that have already been commercialized as CSPs for HPLC. From them, Chiracel OJ, OD, AD, AS and Chiralpak IA, IB were tested for the separation of **11, 75, 10, 74, 79, 83, 78, 82**. The best efficiency was achieved on Chiracel OD and OJ columns (analytical column 0.46 x 25 cm, and preparative column 2 x 25 cm), using normal or reversed phase conditions. Althrough several eluents were tested and their composition was varied, Chiracel AD, AS, IA, IB columns were tested without satisfactory results. Some explanations and conclusions for the success of a specific separation will be discussed.

Table 3. Structure of polysaccharides derivatives with a high chiral resolving power.[53]

Polysaccharide derivatives	R	Commercial names
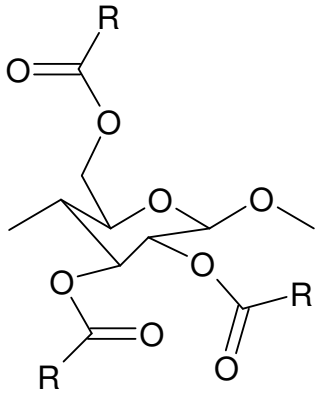 Cellulose ester	-CH_3	Chiracel CTA (micro-crystalline), Chiracel OA (coated type)
	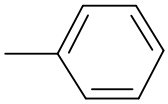	Chiracel OB
	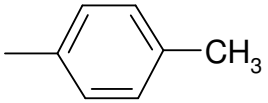	Chiracel OJ
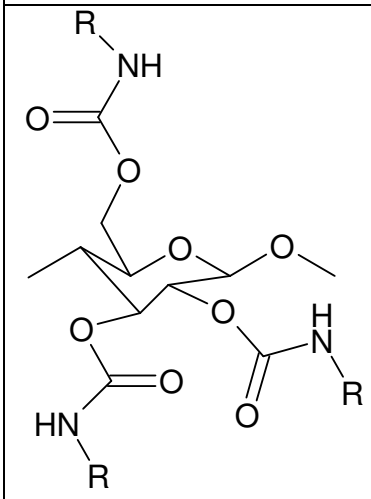 Cellulose carbamates	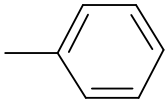	Chiracel OC
	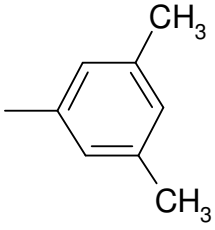	Chiracel OD Chiralpak IB (immobilized type)
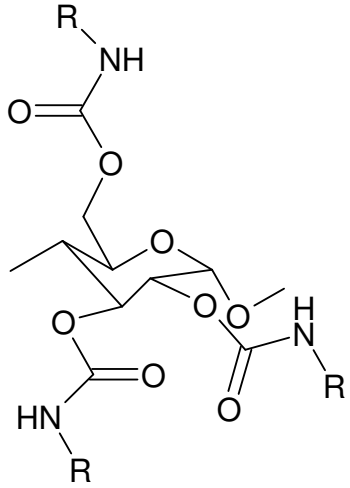 Amylose carbamates	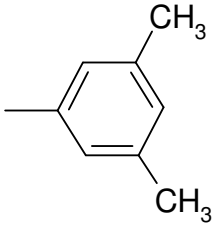	Chiracel AD Chiralpak IA (immobilized type)

The known metabolites of vitamin A are usually achiral, so most separations of the *cis-/trans*-isomers, were performed on non-chiral columns. There are just very few

examples of isolated chiral retinoids and even less methods for their enantioseparation. Lately a chiral retinal dimer formed in the visual process was characterized by chiral HPLC on a Chiracel OD column.[54] The chirality of the 13,14-dihydro retinoid metabolites reported to date, the 9-*cis*-4-oxo-13,14-dh-RA (by Nau), 9-*cis*-13,14-dh-RA (by Shirley), all-*trans*-13,14-dh-ROH and all-*trans*-13,14-dh-RA (by Palczewski) was not investigated by the original authors.

4.3 Chiral Separation of 4-Oxo-13,14-dihydro-retinoic acid (11) and its Ester

Using an isocratic method with hex/*i*PrOH/TFA 95:5:0.1 and a flow rate of 0.5 mL/min from 0 to 40 min then 1 mL/min to the end, all diastereomers of **11** were separated on a Chiracel OJ column, 0.46 x 25 cm, 10 µm particle size.

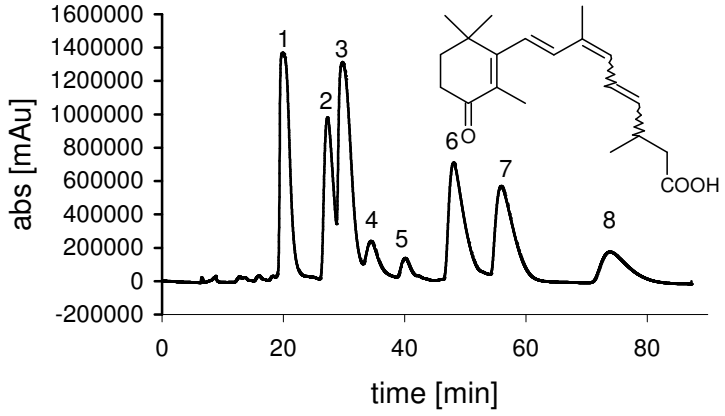

Figure 16. Chiral separation of racemic 4-oxo-13,14-dh-RA (**11**) on Chiracel OJ, hex/*i*PrOH/TFA 95:5:0.1. (Fraction 1: *R*-11-*cis*-; fraction 2: *S*-9,11-di-*cis*-; fraction 3: *S*-all-*trans*-; fraction 4: *S*-9-*cis*-; fraction 5: *R*-9-*cis*-; fraction 6: *S*-11-*cis*-; fraction 7: *R*-all-*trans*-; fraction 8: *R*-9,11-di-*cis*-**11**).

When a Chiracel OJ-H, 5 µm particle size column was used, the resolution became better because the separation surface of the column material increased. This time the flow rate was 0.9 mL/min from start 0 min to 30 min, increased to 1.2 mL/min till 35 min, and kept constant until the end of the separation. These additional improvements resulted in a reduction of the retention time and sharper peaks.

A very good separation of all diastereomers of **11** was important because these will be used further for biological investigations. If the esters are first separated and subsequently saponificated there is a high possibility of isomerization during workup, and purification has to be repeated again. This supposition was verified by preparing the ester **75** from the separated isomers of aldehyde **53** followed by saponification to **11**. In this case just four diastereomers were obtained (Figure 17). HPLC peak ratios and ^{1}H

NMR spectra show that no isomerization occurred during the saponification and the workup of **75** to **11.** However, isomerization of the acid takes place in time. 11-*cis*-**11** isomerizes to all-*trans*-**11** and the 9,11-di-*cis*-derivative to the 9-*cis*-isomer quite rapidly (hours to days), while 9-*cis*-**11** isomerizes to all-*trans*-**11** only slowly (days to weeks). The possibility of isomerization during HPLC separation due to the use of TFA additive in the eluent mixture was also investigated. Immediately after the fractions were separately collected and the solvent removed, their purity was established by HPLC. All chromatograms showed just one peak. This crucial observation is important also for the analysis of the isolated vitamin A metabolite on the Chiracel OJ column with the same separation method.

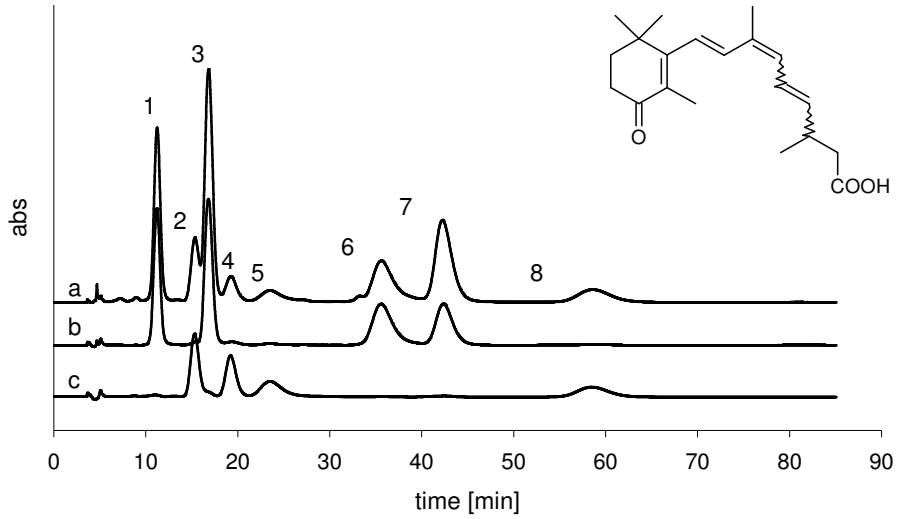

Figure 17. Chiral separation of **11** on Chiracel OJ-H, 5 µm, hex/*i*PrOH/TFA 95:5:0.1 (curve a: racemix mixture, fraction 1: *R*-11-*cis*-; fraction 2: *S*-9,11-di-*cis*-; fraction 3: *S*-all-*trans*-; fraction 4: *S*-9-*cis*-; fraction 5: *R*-9-*cis*-; fraction 6: *S*-11-*cis*-; fraction 7: *R*-all-*trans*-; fraction 8: *R*-9,11-di-*cis*-**11**, curve b: 11-*cis*- and all-*trans*-**11**, curve c: 9,11-di-*cis*- and 9-*cis*-**11**).

Because the spectroscopic data were not sufficient for a clear identification of chirality for each separated fraction, an enantioselective synthesis of **11** was carried out (see previous chapter). The chiral analysis of *rac*-**11** compared with the isolated metabolite, CD spectroscopy, and molecular modeling studies supported a target enantioselective synthesis for the *S* enantiomer. Comparison of the two chromatograms of *rac*-**11** and *S*-**11** allowed the assignment of all synthetic enantiomers (Figure 18) and of the absolute configuration of the natural vitamin A metabolite as *S* (see Chapter 9).

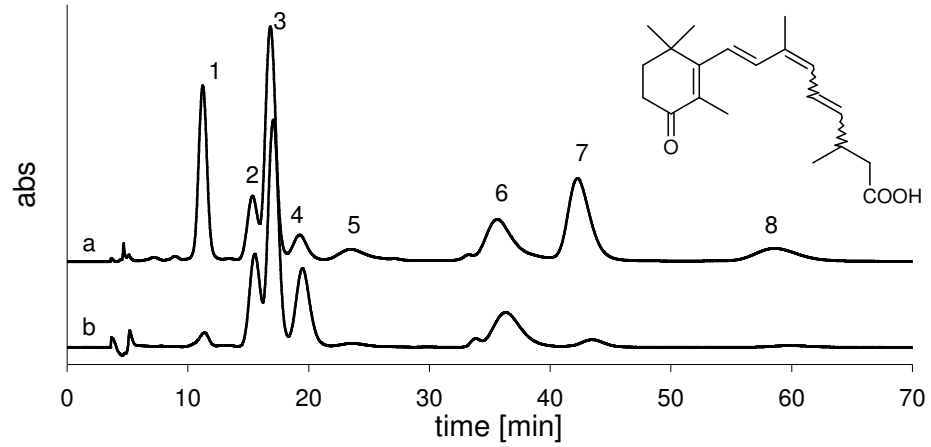

Figure 18. Chiral HPLC of **11** on Chiracel OJ-H, hex/*i*PrOH/TFA 95:5:0.1 (curve a: product of racemic synthesis, curve b: product of enantioselective synthesis). Fraction 1: *R*-11-*cis*-; fraction 2: *S*-9,11-di-*cis*-; fraction 3: *S*-all-*trans*-; fraction 4: *S*-9-*cis*-; fraction 5: *R*-9-*cis*-; fraction 6: *S*-11-*cis*-; fraction 7: *R*-all-*trans*-; fraction 8: *R*-9,11-di-*cis*-**11**.

The developed separation method allows a good preparative chiral separation on a Chiracel OJ 10 μm, 2 x 25 cm column, with a flow rate of 10 mL/min. All diastereomers were characterized by CD and by the usual spectroscopic techniques (NMR, MS, IR and UV analysis). This separation method was also used for purification and analysis of the samples used for the biological tests.

The ester **75** was separated on a Chiracel OJ column with hex/*i*PrOH 93:7 and 0.5 mL/min flow rate. A perfect resolution of all diastereomers was not achieved, but was also not the goal as long as the acids had been completely resolved. The fractions were paired by CD spectroscopy to the corresponding enantiomer pairs. From the NMR spectra of the reaction mixture, the ratio between the isomers was known and comparing the elution order on the same chiral material between the diastereomers of the acid **11** and its ester **75**, each fraction was assigned to the corresponding diastereomer. Also from the peak ratio, fraction 1 and 4 were postulated to be the enantiomers of 9-*cis*- or 9,11-di-*cis*-isomer. However, a definite assignment was not possible without preparative separation and investigation of each fraction by NMR analysis. For fraction 2 and 3 the 11-*cis*-configuration was assigned, while fraction 5 and 6 are the enantiomers of all-*trans*-**75**. This isomer assignment was confirmed by molecular modeling calculations of the CD spectra in comparison with the experimental results as will be shown in detail in Chapter 6.

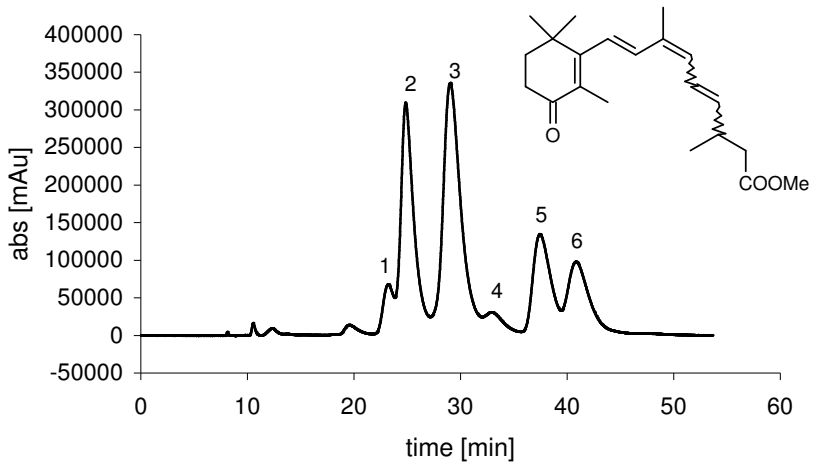

Figure 19. Chiral separation of **75** on Chiracel OJ, hex/*i*PrOH 97:3, 0.5 mL/min.
Fraction 1, fraction 4: 9,11-di-*cis*-, 9-*cis*-; fraction 2: *R*-11-*cis*-; fraction 3: *S*-11-*cis*-; fraction 5: *S*-all-*trans*-; fraction 6: *R*-all-*trans*-**75**.

4.4 Chiral Separation of 13,14-Dihydro-retinoic acid (10) and its Ester

Several columns were tested for the chiral resolution of **10** and the ester **74**. Chiracel OD, OJ, AD, AS and Chiralpak IA and IB columns under a variety of normal phase solvent conditions could not resolve these retinoids. The solvents used for the Chiracel columns were hexane and *i*PrOH in different proportions, for the acid derivative additional TFA was used. Chiral separation on the Chiralpak columns was tried with different mixtures of hexane and chloroform. All these columns show no adsorption of the 13,14-dihydro retinoids on the chiral stationary phase. Retention time was always between 5 and 10 min. Reversed phase conditions were tested on a Chiracel OD column, again with unsatisfactory results. The absence of the 4-oxo group in the molecule changes the adsorption affinity on the CSP, so that **10** and **74** were eluted without any adsorption on the CSP. The mechanism of the chiral separation will be discussed later and possible solutions for the resolution of the 13,14-dihydro retinoids are proposed based on this mechanism.

4.5 Chiral Separation of 4-Oxo-13,14-dihydro-13-phenyl-retinoic acid (83) and its Ester

The 4-oxo-moiety in **83** and **79** proved again to play a decisive role in the separation. These derivatives have been successfully separated by isocratic methods on an analytical Chiracel OD column, 10 µm. The acid **83** was separated with hex/*i*PrOH/TFA

96:4:0.1 and a constant flow rate of 0.5 mL/min while the corresponding esters **79** show the best resolution with hex/*i*PrOH 90:10 at the same flow rate.

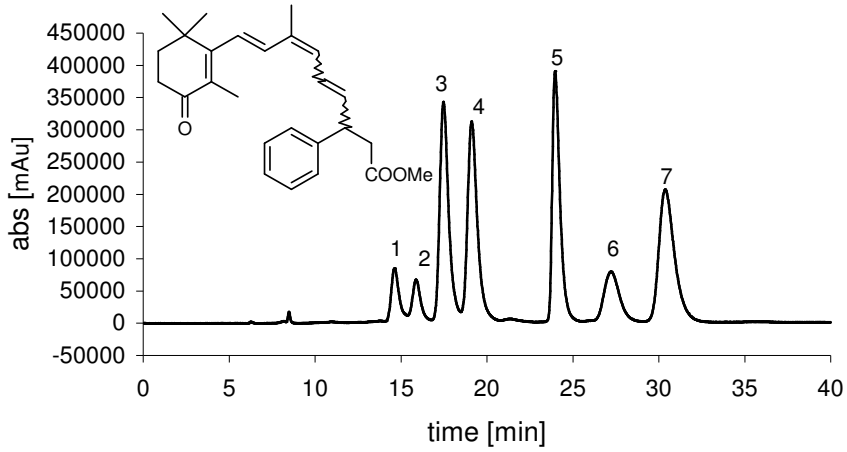

Figure 20. Chiral separation of **79** on Chiracel OD, 10 µm, hex/*i*PrOH 90:10.
Fraction 1: *S*-9,11-di-*cis*-; fraction 2: *S*-9-*cis*-; fraction 3: *S*-11-*cis*-; fraction 4: *S*-all-*trans*-; fraction 5: *R*-all-*trans*-; fraction 6: *R*-9,11-di-*cis*-; fraction 7: *R*-11-*cis*-**79**.

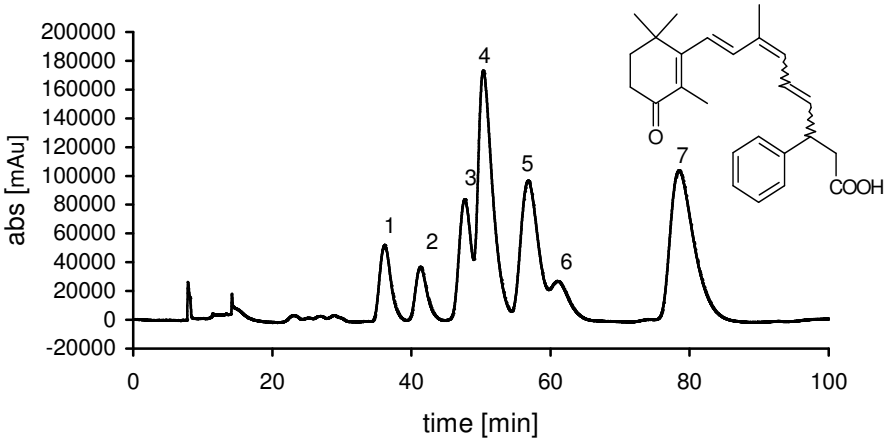

Figure 21. Chiral separation of **83** on Chiracel OD, 10 µm, hex/*i*PrOH/TFA 96:4:0.1.
Fraction 1: *S*-9,11-di-*cis*-; fraction 2: *S*-9-*cis*-; fraction 3: *S*-11-*cis*-; fraction 4: *S*-all-*trans*-; fraction 5: *R*-all-*trans*-; fraction 6: *R*-9,11-di-*cis*-; fraction 7: *R*-11-*cis*-**83**.

The enantiomers were paired by their CD spectra and the isomers were assigned by ^{1}H NMR spectroscopy and comparison of the NMR and HPLC isomer ratio of the reaction product. The HPLC separation of **79** is shown in Figure 20, where the peaks 1 and 6 are assigned to the *S* and *R* enantiomers of the 9,11-di-*cis*-isomer, peak 2 is the *S*-9-*cis*-isomer, the 3rd and the 7th peaks belong to the *S*- and *R*-11-*cis*-isomer, and the peaks 4 and 5 are the two *S* and *R* enantiomers of the all-*trans*-isomer, respectively. The second enantiomer of the 9-*cis*-isomer is co-eluting with another diastereomer. The

corresponding acids **83** show a similar resolution on the chiral stationary phase, all diastereomers display the same elution order. The assignment of the absolute configuration for each isomer of **79** and **83** was performed by CD spectroscopy and molecular modeling calculations and will be discussed in detail in Chapter 6.

4.6 Chiral Separation of 13,14-dihydro-13-phenyl-retinoic acid (82) and its Ester

As expected, the separation of the 13-phenyl substituted retinoids without the keto functionality at C-4 was not trivial. The Chiracel OD, OJ, AD, AS and Chiralpak IA and IB were again tested under normal phase conditions. Several methods were developed; none of them gave a satisfactory separation. When reversed phase conditions were tried on a Chiracel OD column, the esters **78** show an improvement of the retention time, indicating adsorption on the CSP. After method optimization, with the eluent mixture MeOH/H_2O 90:10 and a constant flow rate 0.5 mL/min., a partial separation was finally possible (Figure 22).

The isomer ratio known from ^{1}H NMR analysis was used for configuration assignment: peaks 1, 3, 6 should belong to 9-*cis*- and 9,11-di-*cis*-**78**, while peaks 2, 4, 5 should belong to all-*trans*- and 11-*cis*-**78**. Two diastereomers are eluted under these peaks as well. From their CD spectra, peaks 1 and 3, 2 and 4 were paired. Again, experimental CD spectra were compared with the calculated spectra for enantiomer assignment. All this information leads to the following assignment: peak 1: *S*-9,11-di-*cis*-, peak 2: *S*-all-*trans*-, peak 3: *R*-9,11-di-*cis*-, peak 4: *R*-all-*trans*-**78**. The other diastereomers were not assigned.

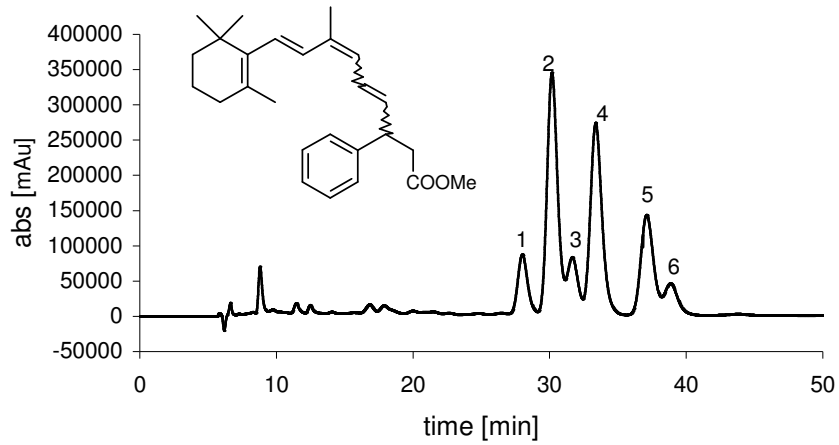

Figure 22. Chiral separation of **78** on Chiracel OD, MeOH/H_2O 90:10, 0.5mL/min.
Fraction 1: *S*-9,11-di-*cis*-; fraction 2: *S*-all-*trans*-; fraction 3: *R*-9,11-di-*cis*-; fraction 4: *R*-all-*trans*-**78**; fraction 5 and fraction 6 not assigned.

When comparing the two esters **78** and **74** the only difference between these molecules is the substituent at C-13, the phenyl ring, and the methyl group, respectively. This means that the phenyl ring interacts with the CSP so that adsorption becomes possible on the column, which is evidently not the case for **74**.

The different adsorption mechanism of the four molecules, **11**, **10**, **83** and **82**, tested here for separation on the different CSP was analyzed and is discussed further.

4.7 Chiral Separation Mechanism

To understand the retention mechanism is of essential importance when a stationary phase is chosen for separation. To elucidate the chiral recognition mechanism, experiments using chromatography, NMR spectroscopy, X-ray crystallography and computational methods have been used.[55] These results show that chiral polymers have a number of different binding sites with different affinities for enantiomers. The cellulose polymer chains are held together by intramolecular and intermolecular hydrogen bonds that result in the formation of sheets. Chiral cavities are created between sheets, further imparting chiral character. The chiral recognition mechanism for derivatized cellulose involves attractive interactions followed by the steric fit of the molecules into the chiral surface.

This means that the analyte-CSP complexes are first formed by attractive interactions and chiral discrimination takes place due to the steric fit of the analyte into the chiral cavity. The attractive interactions make use of hydrogen bonding, dipole-dipole, and π-

π interactions. Different mechanistic aspects were found to play a stronger role in the cellulose esters compared to the celullose carbamates CSP.[55]

On Chiracel OD, with phenylcarbamate derivatized cellulose as CSP, the chiral recognition mechanism most likely involves the formation of diastereomeric analyte-CSP complexes by hydrogen bonding and interactions between the polar carbamate moieties, NH and C=O groups with the functional groups of the analyte. Stabilization of these complexes is due to insertion of the aromatic ring of the analyte, **79**, **83**, **78**, into the chiral cavities of the CSP, and by dipole-dipole interactions between the analyte and CSP. The phenyl carbamate ring on the CSP is 3,5-disubstituted with electron donating groups and methyl groups, which increase the electron density at the carbonyl oxygen atom of the carbamates and therefore enhanced hydrogen bonding is induced.

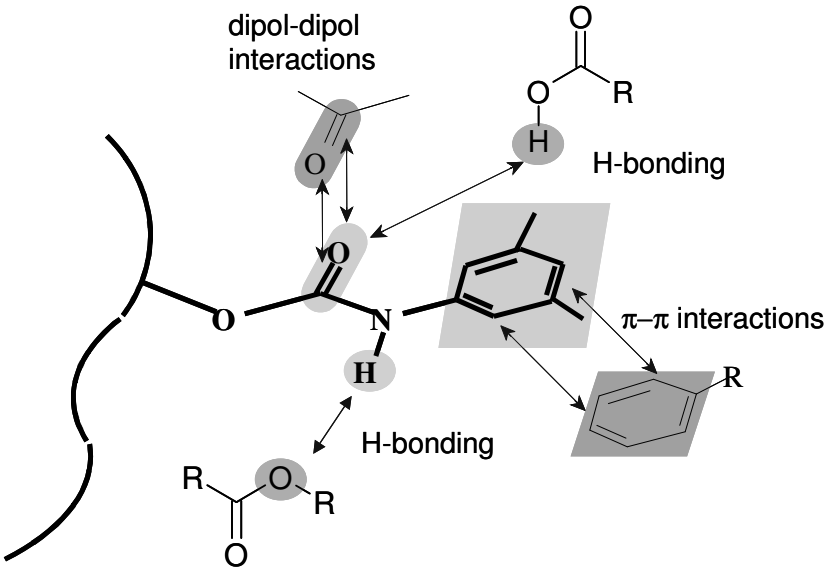

Figure 23. Chiral separation mechanism on carbamate CSP (Chiracel OD).

The chiral recognition mechanism on a Chiracel OJ column, with cellulose ester as CSP, takes place by an inclusion of the enantiomers in the chiral cavities.[55]

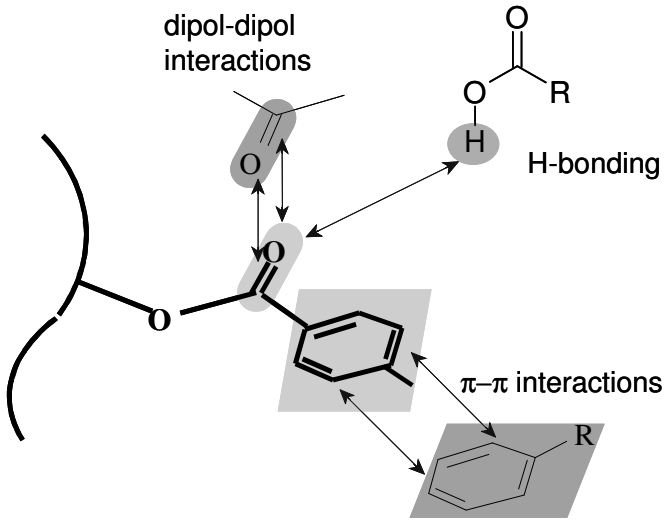

Figure 24. Chiral resolution on the cellulose ester CSP (Chiracel OJ).

The main chiral adsorption sites of the cellulose tribenzoate phase are considered to be the polar carbonyl group of esters, which can interact with the racemate of **11** or **75** by way of hydrogen bonds and dipol-dipol interactions. The inclusion of the molecules in the cavity is due to attractive interactions through functional groups rather than the shape of the analyte. This agrees with the observations previously presented here where the 4-oxo-13,14-dh-RAs were resolved best on the cellulose tribenzoate ester. Here a strong interaction can take place between the 4-oxo group and the ester function on the CSP. The 13,14-dh-RAs on the other hand do not possess have enough interaction sites for absorption on the CSP.

On the cellulose ester CSP, consisting of cellulose triacetate (CTA), the chiral resolution was postulated to function in an opposite way as for the cellulose tribenzoate (CTB).[55] The inclusion of the molecules in the cavity is not governed by attractive interactions between functional groups but mainly by the shape of the molecules. On such a column it should be possible to resolve the RA derivatives **10** and **74**. In this project, a cellulose triacetate column was not available for testing.

In conclusion, the 4-oxo-13,14-dh-retinoids can be resolved on Chiracel OD or Chiracel OJ columns, while the 13,14-dh-retinoids are not suited for separation on these columns, as long as additional functional groups capable to interact with the CSP are present in the retinoid backbone.

5 Spectroscopic Analysis

5.1 Infrared Spectroscopy

Infrared spectroscopy (IR) was used for the characterization of the new retinoids, especially for the identification of the functional groups, which give a characteristic IR absorption signal and indicate intra- and/or intermolecular hydrogen bonds of the acid and other polar functions.

The absorption due to the C-H stretch of methyl and methylene groups is for all retinoids in the range 2965-2820 cm^{-1}. The H-C-H bending mode can be observed at 1456-1437 cm^{-1} for the asymmetric and 1380-1350 cm^{-1} for the symmetric vibrations. The H-C=C-H stretching of the different isomers can be assigned from the lower wavelength range of the IR spectra. *trans*-Isomers give a band of medium intensity around 970-960 cm^{-1} and the *cis*-isomers between 760-700 cm^{-1}. The C=C stretching vibration produces a medium to weak band around 1605-1580 cm^{-1}. For the RA derivatives a broad band at 3400 cm^{-1} due to the acidic OH group is observed. A characteristic differentiation between the different RA derivatives based on this group was not possible because of the width of the signal. This indicates that no intramolecular hydrogen bonds are formed, which would cause sharper signals; but intermolecular H-bonds are present because the absorption band is extending to almost 2600 cm^{-1}. Strong sharp bands between 1720 and 1600 cm^{-1} are attributed to the stretching mode of the carbonyl groups. For **11** and **75** (Figure 25), two bands are observed, one for the carbonyl of the acid function at 1781-1690 cm^{-1} and the second one for the 4-oxo carbonyl function almost at constant wavelength 1660-1658 cm^{-1}. For **10** and **74** (Figure 26) only the first band can be observed. The carbonyl absorption band of the ester function is visible at higher wavelengths (1781-1712 cm^{-1}) compared to the same group in the acid functions (1736-1690 cm^{-1}). Retinoids incorporating the phenyl ring at C-13 (Figure 27) show weak signals for this group at 3070-3000 cm^{-1}. The IR spectra of the labeled compounds do not differ very much from those of their unlabeled analogs; the stretching vibrations are very slightly shifted to smaller frequencies as expected. The exact values for all newly synthesized RA derivatives are summarized in Table 4. Because there is almost no literature on the IR spectra of retinoids, some of the spectra of the newly synthesized RA derivatives are shown here.

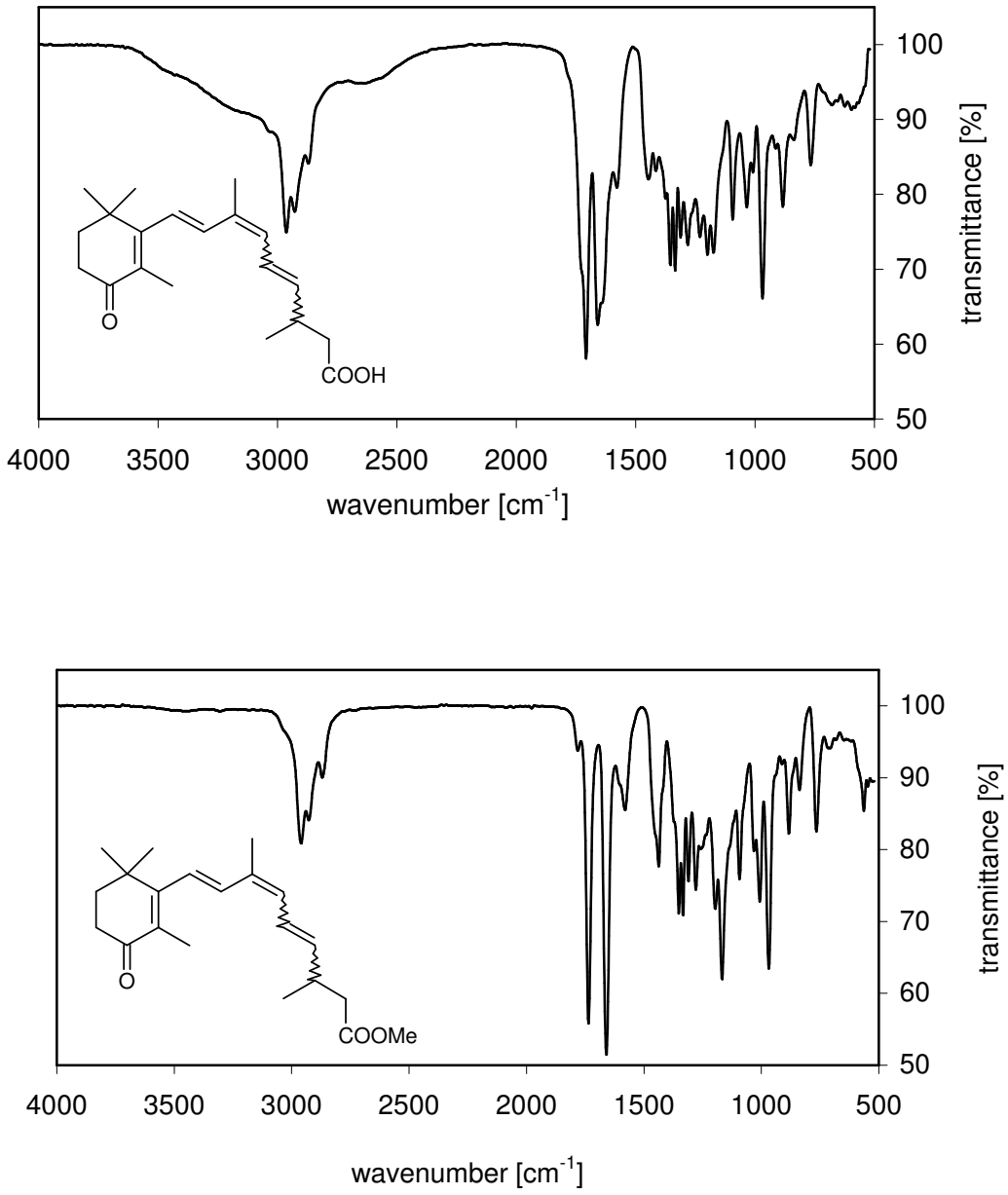

Figure 25. IR spectrum of **11** and **75**.

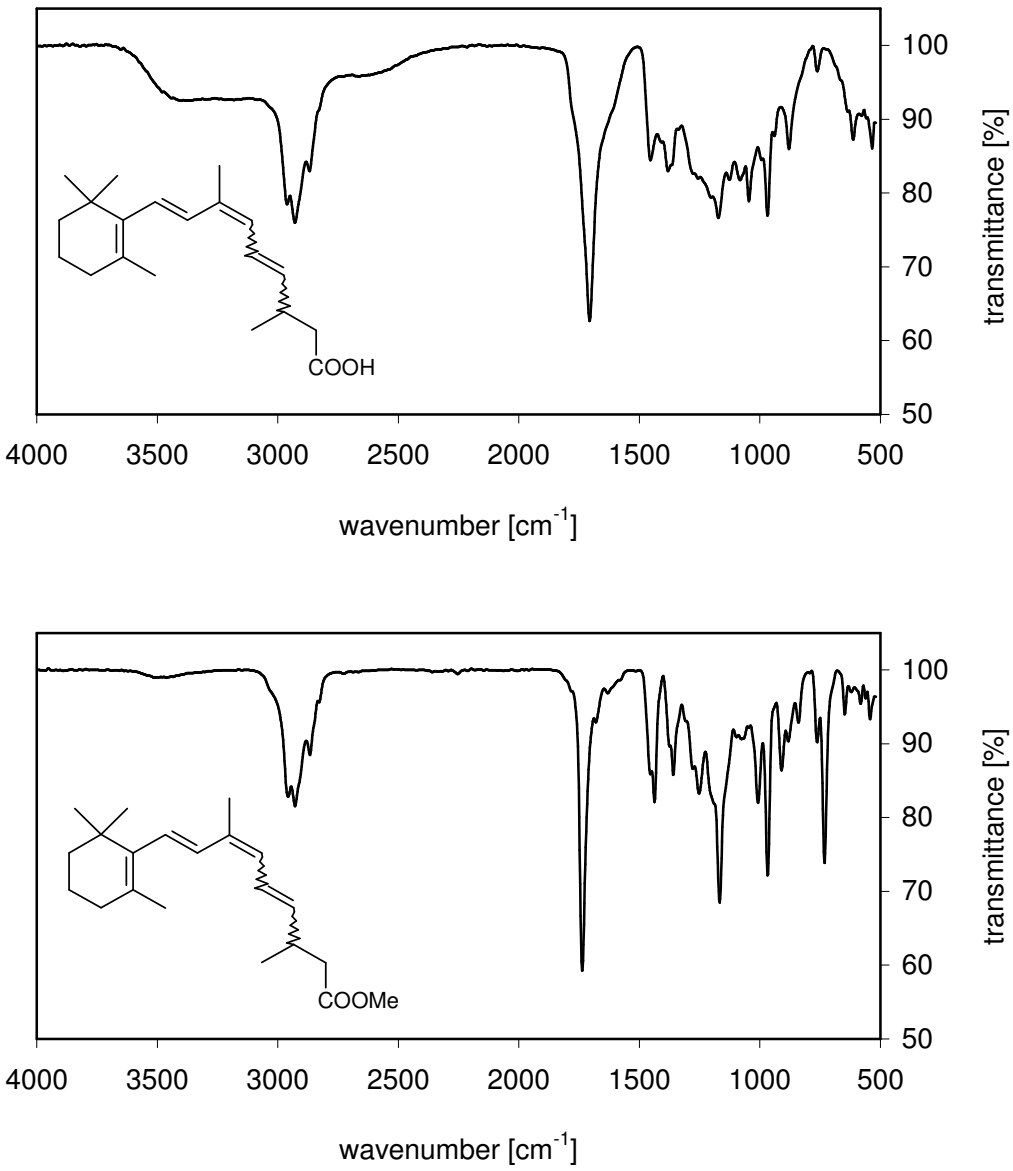

Figure 26. IR spectra of **10** and **74**.

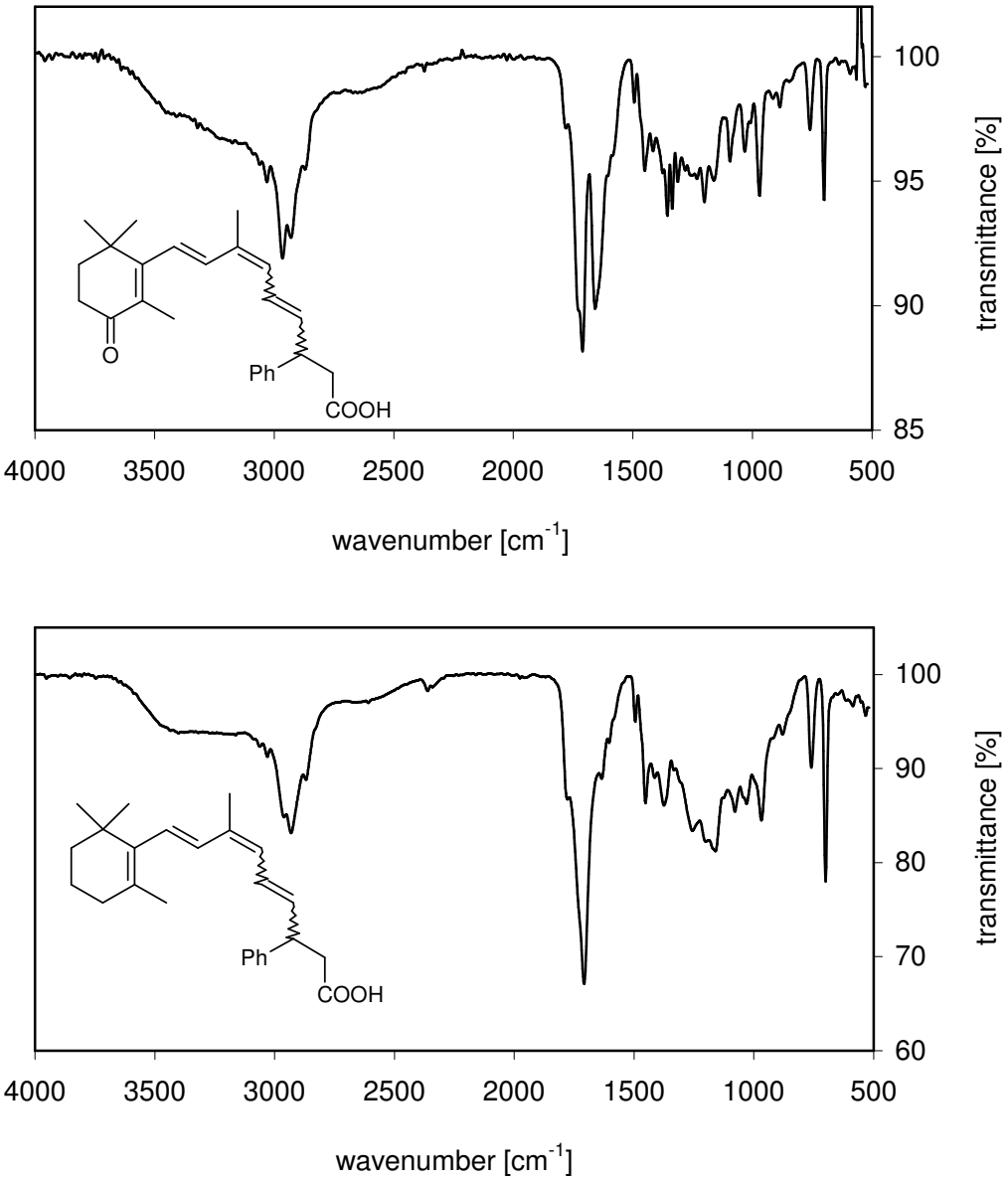

Figure 27. IR spectra of phenyl substituted derivatives **83** and **82**.

Table 4. IR absorption of selected retinoids.

	RA's	CO**OH**	C-H stretch	**CO**OH	CO	C=C stretch	H-C-H (non-sym)	H-C-H (sym)	Fingerprint region (1300-1100 cm^{-1})
1	**40**[57]		2950-2860	1712(s)		1609(w),1583(m),1570(w)			
2	**3**[57]		2930-2820	1690(m)		1605(s),1578(s),1565(m)	1445(w)	1350(m)	1260(s), 1255(s), 1190(s), 1160(m)
3	**42**[57]	3400	2940	1735(w)	1660(s)	1605(m),1560(s),1555(s)			
4	**74**		2957-2867(m)	1781(s)		1682(w)	1454(m)	1360(m)	1252(m), 1167(m)
5	**10**	3402	2961-2868(m)	1706(s)			1454(m)	1381(m)	1172(m), 1126(m), 1083(m)
6	**75**		2958-2869(m)	1736(s)	1659(s)	1582(w),	1437(m)	1351(m)	1279(m), 1197(s)
7	**11**	3431	2965-2873(m)	1731(s)	1661(s)		1456(w)	1375(m)	1333(m), 1199(m), 1144(m), 1089(m)
8	**78**		2953-2827(m)	1740(s)		1494(m)	1451(m), 1437(m)	1359(w)	1253(m), 1204(m), 1161(m)
9	**82**	3401	2961-2869(m)	1708(s)		1635(m), 1495(w)	1452(m)	1375(m)	1256(m), 1201(s), 1161(s), 1079(m)
10	**79**		2957-2925(m)	1736(s)	1658(s)	1582(m), 1494(w)	1437(m)	1352(m)	1310(m), 1279(m), 1197(m), 1092(m)
11	**83**	3400	2965-2870(m)	1711(s)	1658(s)	1494(m)		1356(m),	1201(m), 1094(m)
12	**23**		2956-2870(m)		1660(s)				
13	**91**		2957-2870		1660(s)	1601(w),	1450(m)	1350(m)	1296(m), 1252(m), 1206(m), 1143(m)
14	**53**		2962-2858(m)		1667(s)	1616(m), 1595(m),	1447(m)	1351(m)	1203(m), 1148(m), 1092(m)
15	**86**		2961-2738(m)		1657(s)	1614(m)	1445(w)	1351(m)	1199(m), 1146(m), 1117(m), 1091(m)
16	**85**		2957-2744(m)		1650(s)	1606(m)	1450(s)	1378(s)	1300(s), 1198(m), 1147(m), 1103(m)

Although from the IR spectra it is often difficult to assign a structure unambiguously, there is a lot of information that can be derived from these spectra, like the existence of hydrogen bonding, if the retinoid is a RA, RAL or ROH derivative, containment of further carboxyl or carbonyl functions etc. Furthermore, one can determine the absolute configuration of chiral retinoids by using vibration circular dichroism (VCD). Chirality can be studied using the vibration optical activity (VOA) of a molecule, and the IR form of VOA is the VCD.[56] This technique can be very useful for the analysis of biological samples, because the nature of the retinoid metabolites and, if existent their chirality, can be analyzed directly by an IR or VCD detector coupled to a HPLC instrument without further separation and purification steps. Another important aspect concerns the possibility to calculate, by molecular modeling, the IR and the VCD spectrum of a molecule and compare them with the experimental spectra. For this reason, IR spectroscopy is a powerful method in retinoid and biological sample analysis.

5.2 UV/Vis-Spectroscopy

Electronic absorption spectroscopy is one of the most useful spectroscopic methods for the analysis of retinoids because of their characteristic absorption spectra due to the conjugated double bond system. The absorption of each isomer can be investigated particularly easily when the UV detector is coupled to HPLC.

Under standard conditions the shape of the spectrum is determined by the number of double bonds, the substituents, *cis-/trans*-isomerism and by the solvent and its pH.

The UV spectra were measured in different eluent mixtures, in hex/*i*PrOH with or without TFA as buffer, the fractions from normal phase HPLC, in acetonitrile/water (CH_3CN/H_2O) or methanol/water ($MeOH/H_2O$) the fractions from reversed phase HPLC and in ethanol (EtOH) the pure substances, directly after reaction, without separation of the isomers by HPLC.

Table. 5. UV absorption maximum of selected RAs in different solvents.

	λ_{max1} (nm)	λ_{max2}(nm)	solvent
40	243	355	EtOH
	247	353	CH_3CN/H_2O
41	233/288	355	EtOH
	235/288	362	CH_3CN/H_2O
74	227	290	EtOH
	-	279	CH_3CN/ H_2O
10	233	289	EtOH
	-	298	CH_3CN/H_2O
75	250	314	EtOH
	252	318	CH_3CN/H_2O
	252	320	hex/*i*PrOH
11	256	332	EtOH
	255	320	CH_3CN/H_2O
	257	339	CH_3OH/H_2O
	250	320	hex/*i*PrOH/TFA

The wavelength shift noted in most retinoids is caused by the polarity of the solvents (solvatochromism). In the presence of hydroxylic solvents, the lone pairs on the carbonyl function act as an electron donor to the hydrogen of the solvent to form a hydrogen bond. The shift of the long-wavelength maximum (assigned to be produced by the n-π* transition) to lower wavelengths when changing to more polar solvents is a measure of the strength of the hydrogen bond in the solvent.[58] This effect can be seen in the UV spectra taken in EtOH (Table 5). In aqueous solution, the acidic species to be measured can dissociate and the measured spectrum is that of the ion. For this reason the acidity of the sample, as well of the eluents contribute to the UV absorption.

The shorter wavelength band is known to be produced by the π–π* transitions.[58] This absorption band is shifted bathochromically, in the opposite direction of the n-π* transition band, when going from hexane to ethanol and water. Another bathochromic shift is seen for both absorption maxima when additional double bonds are conjugated, as in the case of the 4-oxo retinoids (Table 5).

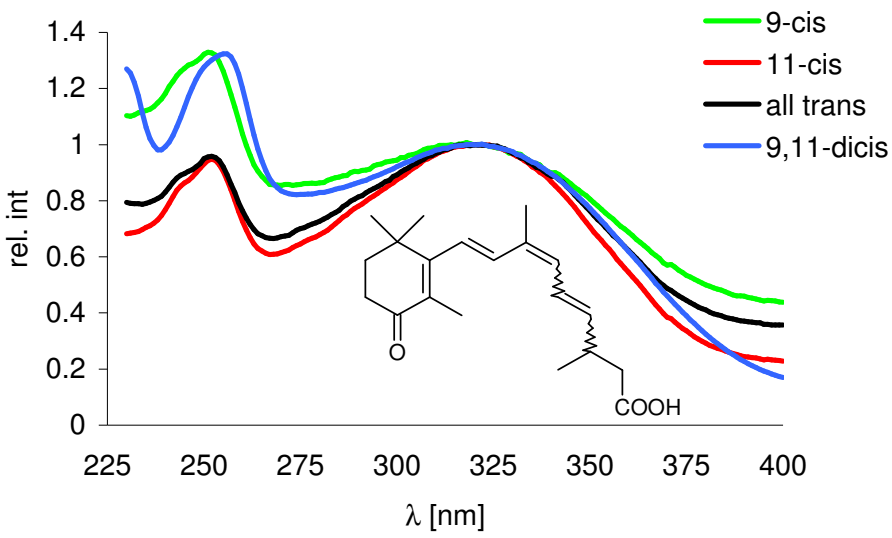

Figure 28. UV spectrum of **11** in hex/*i*PrOH/TFA (95:5:0.5).

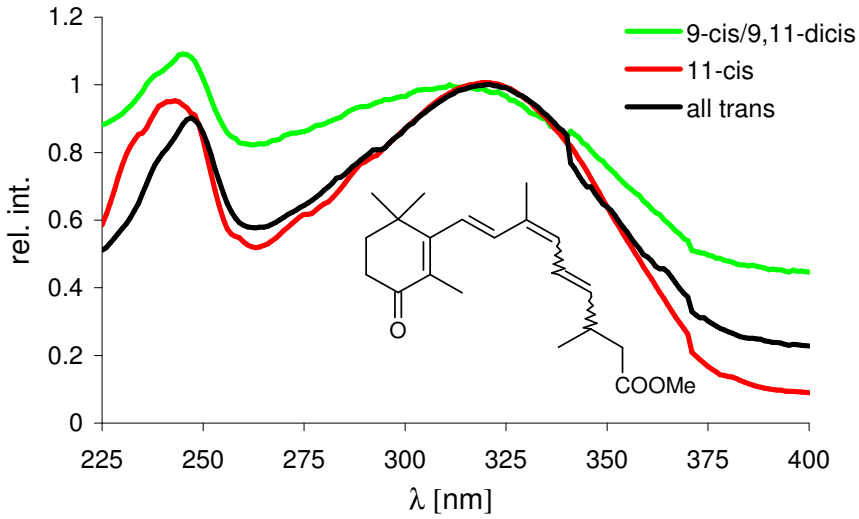

Figure 29. UV spectrum of **75** in hex/*i*PrOH (97:3).

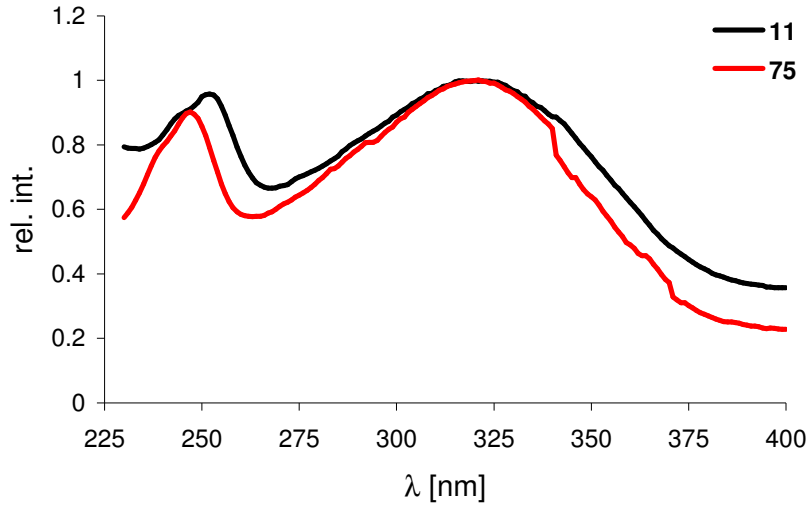

Figure 30. Comparison between the UV spectra of all-*trans*-**11** and the corresponding ester all-*trans*-**75**.

The UV spectrum of **11** shows two maxima at 250 and 320 nm in hex/*i*PrOH/TFA (95:5:0.5), while the corresponding ester **75** in hex/*i*PrOH (97:3) show almost the same absorption pattern, with a very small hypsochromic shift (Figure 30). The change from linear all-*trans*-configuration to an angular *cis*-isomer results in the increase of the intensity of the short-wavelength band, as seen especially in the case of the 9-*cis*- and the 9,11-di-*cis*-isomers.

As expected, the acid **10** and its ester **74**, show the absorption maximum at shorter wavelength (all-*trans*-**10** at 298 nm and all-*trans*-**74** at 278 nm) in CH_3CN/H_2O 60:40. A similar UV absorption spectrum was recorded for the 4-acetoxy dehydro-retinoid **97**, with two maxima in EtOH at 229 and 289 nm, because the conjugated system in **97** is the same as in **74**.

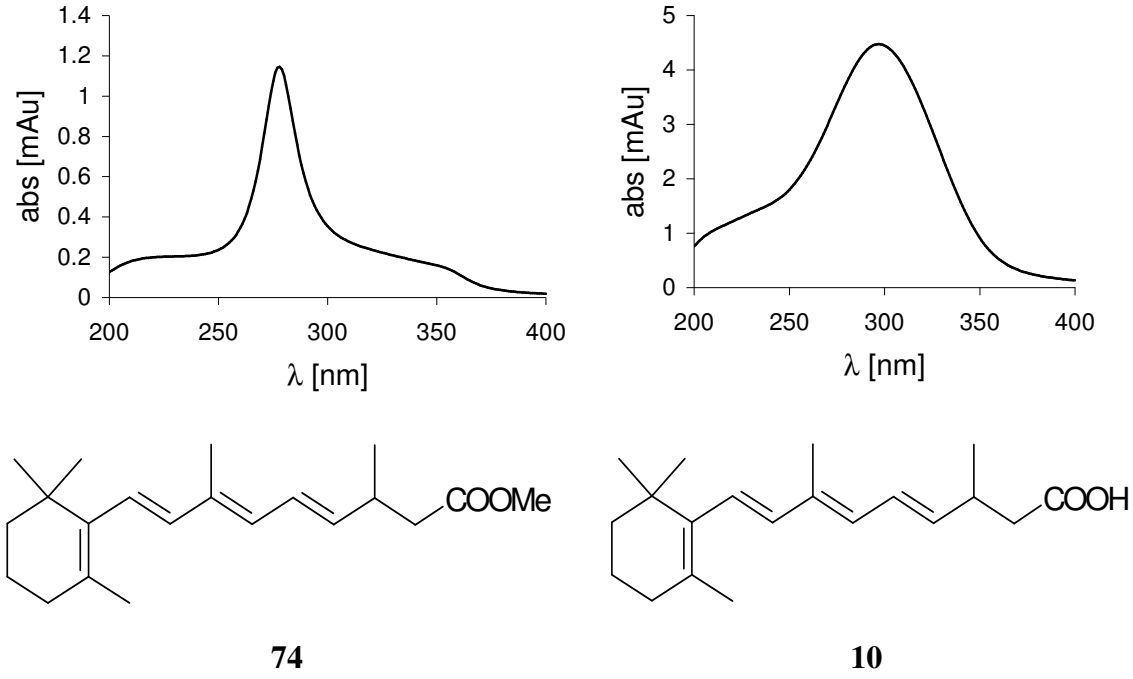

Figure 31. UV spectra of all-*trans*-**74** and all-*trans*-**10** in CH_3CN/H_2O (60:40).

Comparison of the dh-RAs (**74, 75**) with the RAs (**40, 41**) demonstrates convincingly that the conjugation between the polyene chain and the terminal group is broken. The hypsochromic shift of **74** to **40** amounts to 80 nm, while **75** is shifted by 25 nm to a lower wavelength compared to **41**. Characteristic for the 4-oxo retinoids is the presence of two absorption maxima, while the retinoids non-oxidized at C-4 give one absorption maximum.

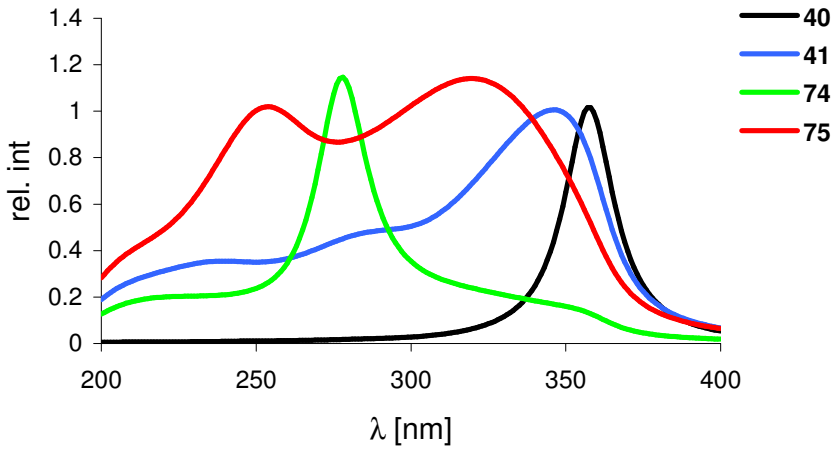

Figure 32. UV spectra of **74, 75, 40, 41** in CH_3CN/H_2O (60:40).

When a phenyl group, as in **79** and **83**, replaces the methyl substituent at C-13 the UV spectrum does not change significantly because the conjugated system is hardly changed. The isolated phenyl substituent does not contribute significantly to the UV

spectrum; the expected absorption band at 260 nm is covered by the more intensive absorption of the polyenes.

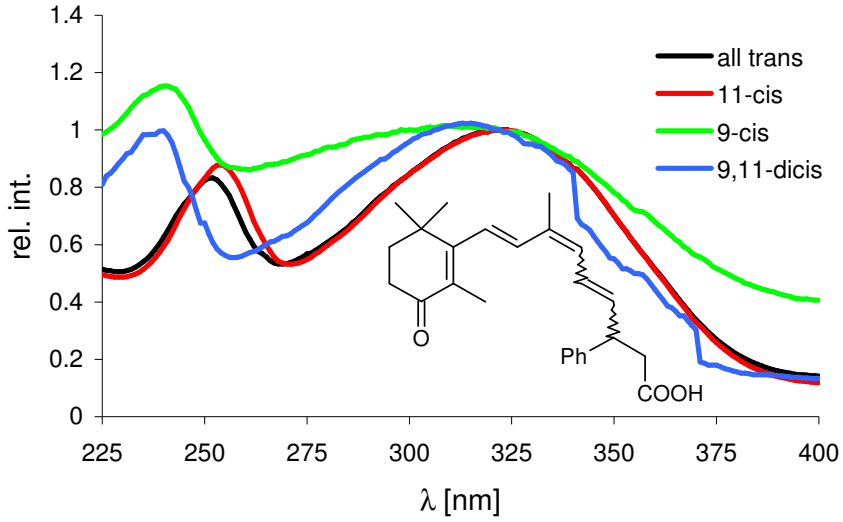

Figure 33. UV spectrum of **83** in hex/*i*PrOH/TFA (96:4:0.1).

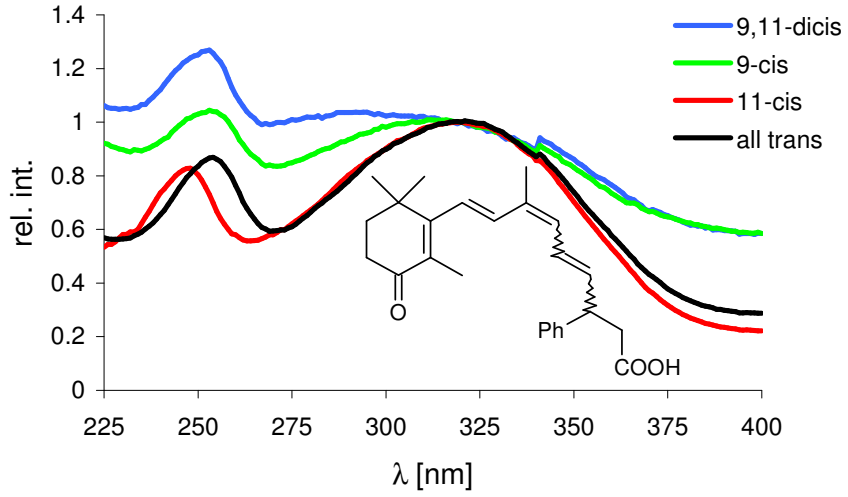

Figure 34. UV spectrum of **83** in hex/*i*PrOH (90:10).

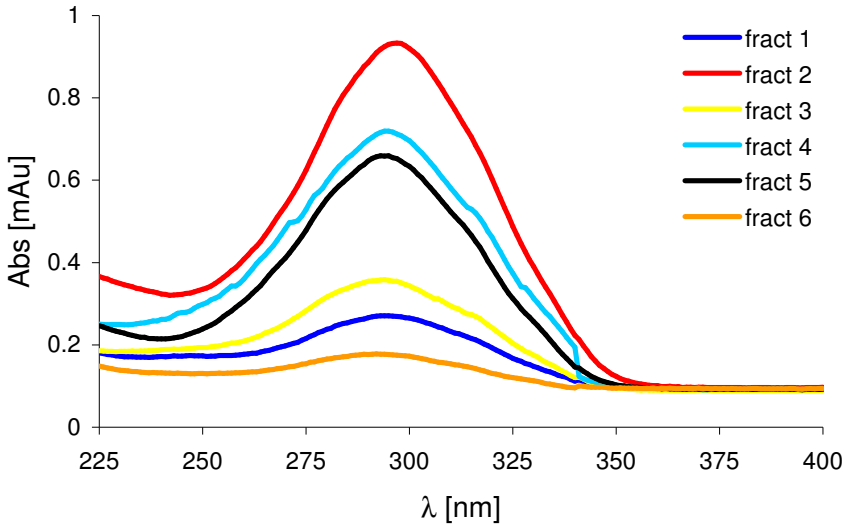

Figure 35. UV spectrum of HPLC fractions of **78** (in MeOH/H_2O 90:10).

The absorption spectrum of the phenyl substituted derivative **78** is similar to the methyl derivative **74**, because no additional conjugation due to the phenyl group is possible in the molecule. The maximum at 295 nm was measured in CH_3OH/H_2O for each fraction eluted from the Chiracel OD column. Because the double bond configuration was not clearly identified for all HPLC fractions, these are shown together in Figure 35.

5.3 Mass Spectrometry

Mass spectrometry was used for the characterization of the synthesized RA derivatives and to determine the deuterium content of labeled retinoids. It is not possible to distinguish between the isomers by mass spectrometry. The electron ionization method (EI) at high and low resolution proved the structure of all newly synthesized retinoids. The fragmentation pattern caused by the electron impact of the retinoids and by their thermal decomposition products were analyzed together.

Most peaks in the low mass region arise from complicated multiple fragmentation reactions. Apart from uncharacteristic, though abundant, ions of low mass caused by the cleavage of the polyene chain, a number of common peaks were detected in all new retinoids. Some of the mass spectra are shown below. The characteristic pattern of the deuterated samples was compared with those of the non-deuterated ones.

The fragmentation pattern of 4-oxo-dh-RAs and the dh-RAs are very similar especially in the low mass region, because of the fragmentation of the polyene chain. Some of the ions can be seen in almost all derivatives, e.g. *m/z* = 55, 69, 77, 91/95, 105, 119/123,

133, 145/149, 159, 173/177. In the high mass region, the differences are clearly related to the molecular structure.

Some of the possible ions formed from **11** are shown in Figure 36. The isoprenoid chain can split alternatively at the C-C single or double bonds.

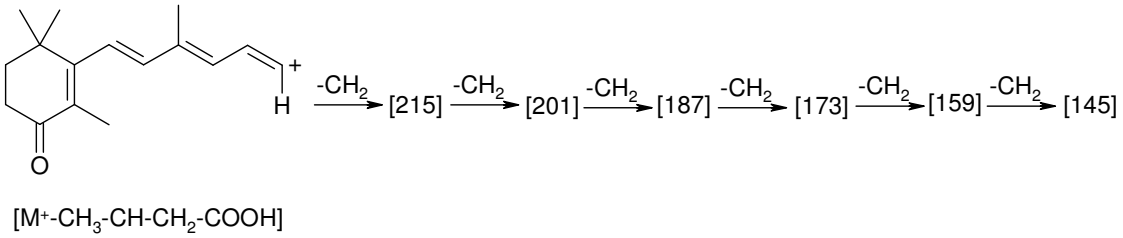

Figure 36. Isoprene chain splitting in **108**.

From investigations of the mass spectra of carotenoids, it was demonstrated that the double bond system can undergo a 8 e^- or 12 e^- cyclization to form toluene, xylene or even naphthalene derivatives.[59] When this mechanism was applied to the retinoid chain, as exemplified in Figure 37 and Figure 40 for the model compound **108**, several aromatic ions were identified in the mass spectra. *cis*-/*trans*-isomerizations, known to occur in polyenes by thermal activation, has to precede before this mechanism can occur. The exact configuration and conformation of the chain preceding the cyclization is unknown, so the arrangement of the chain drawn in Figure 37 is arbitrary.

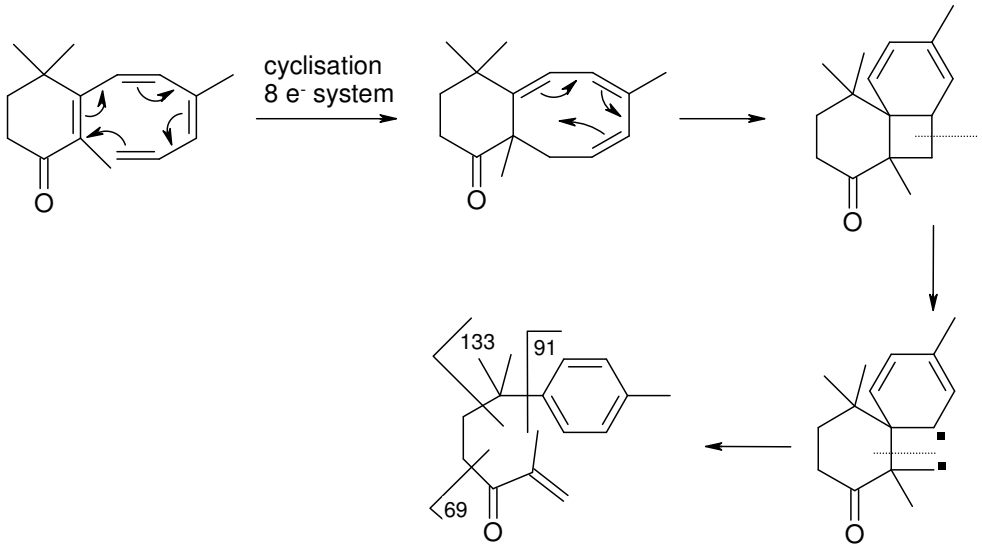

Figure 37. Mechanism of an 8 e^- cyclization of a model compound (**108**).

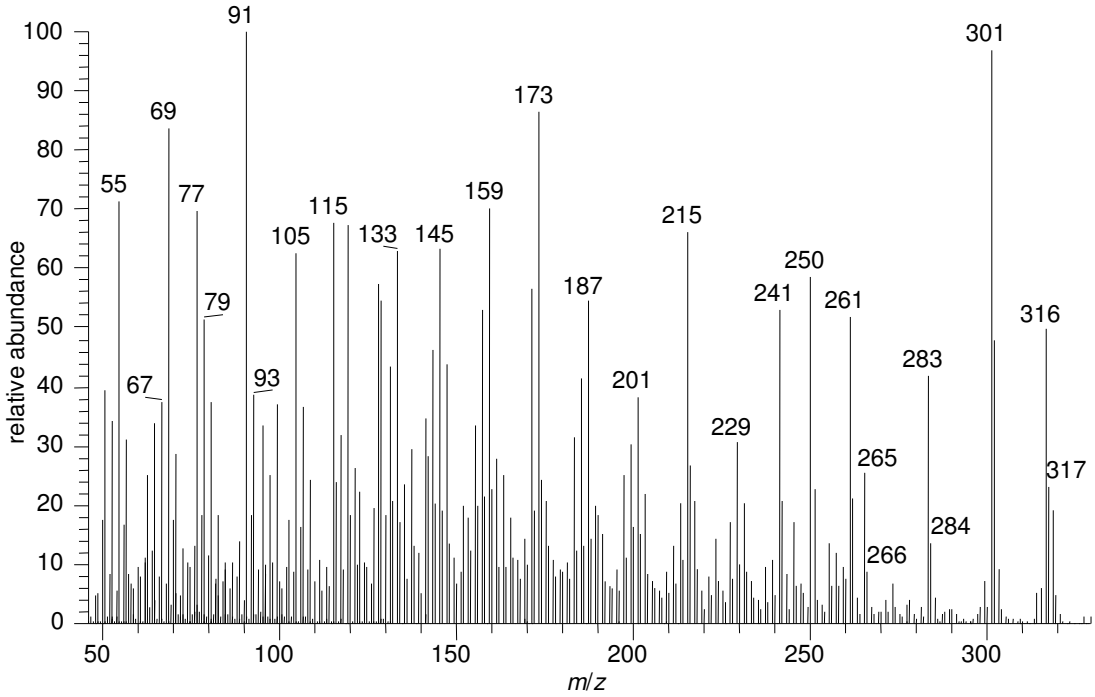

Figure 38. MS [EI] spectrum of the 4-oxo-13,14-dh-RAs (**11**).

The ester **75** (Figure 39) shows a similar ionization pattern in the low mass region, only very few of the signals differ from those of the acid analog. Cleavage of the terminal part of the polyene chain containing the ester group caused modifications of the MS pattern. Splitting of a methyl group from the molecular ion (*m/z* = 330) gives *m/z* = 315, from which methanol can be eliminated to give *m/z* =283. Further cleavage of a molecule of water gives *m/z* =265.

Cleavage of the methoxy group (*m/z* = 31) from the molecular ion gives the ion 299.

Splitting at C-12/C-13 gives the ion with *m/z* = 229, $[M^+\text{-}CH_3CHCH_2COOCH_3]$ which was also observed in the mass spectrum of the acid **11**. Further fragmentation of this ion is shown in Figure 36. The ion with *m/z* = 163 is a very intensive peak; it was attributed to the cyclohexene substituted molecule resulting from the rupture of the C-8/C-9 bond.

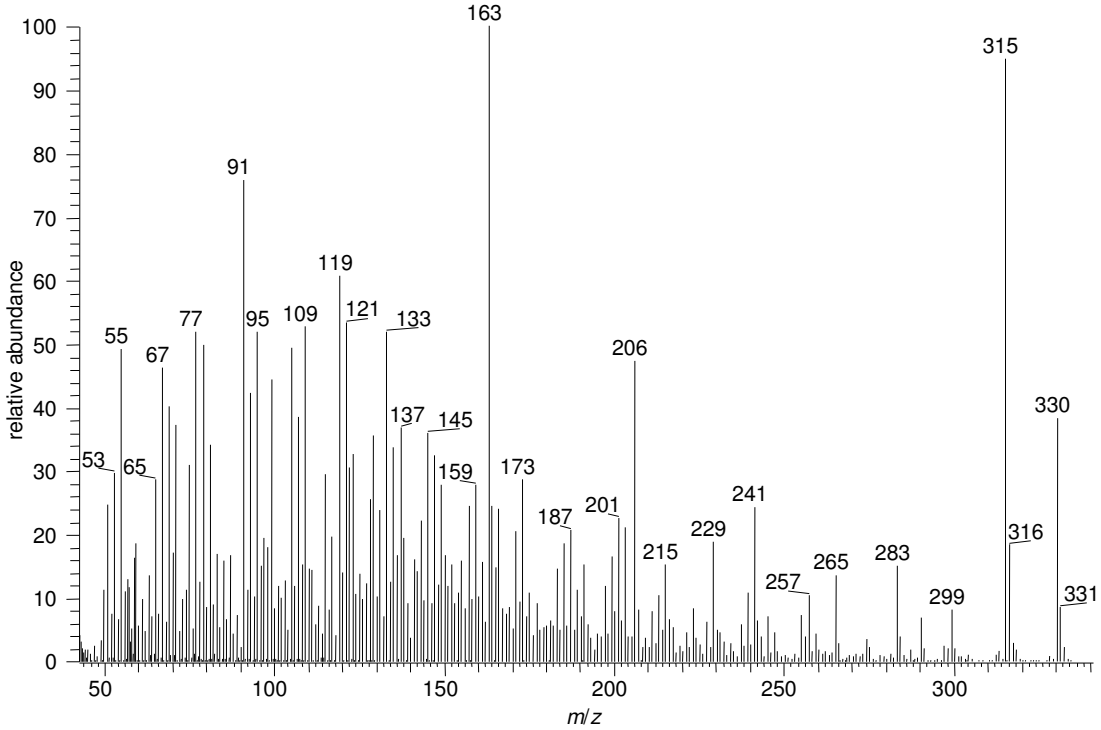

Figure 39. MS [EI] spectrum of the 4-oxo-13,14-dh-RA ester **75**.

The cyclohexene ring can undergo a retro-Diels-Alder reaction in the mass spectrometer and lose ethene (*m/z* = 28) as exemplified in Figure 40 for **10**. The signal at *m/z* = 215 can be explained by formation of the fragment [M^+-CH_3-CO_2-C_2H_4]. The dienophile of the retro-Diels-Alder reaction can also undergo a 8 electron cyclization. The formed aromatic product isopropenylbenzene with *m/z* = 119, was identified in the mass spectrum. The formation of other aromatic ions in the mass spectrometer, like $C_6H_5^+$ (*m/z* = 77), $C_7H_7^+$ (*m/z* = 91) were also identified. The molecular ion (*m/z* = 302) is first loosing one methyl group to give the ion with *m/z* = 287, followed by CO_2 elimination, or McLafferty rearrangement of the acid group with one proton from C-20 to *m/z* = 243.

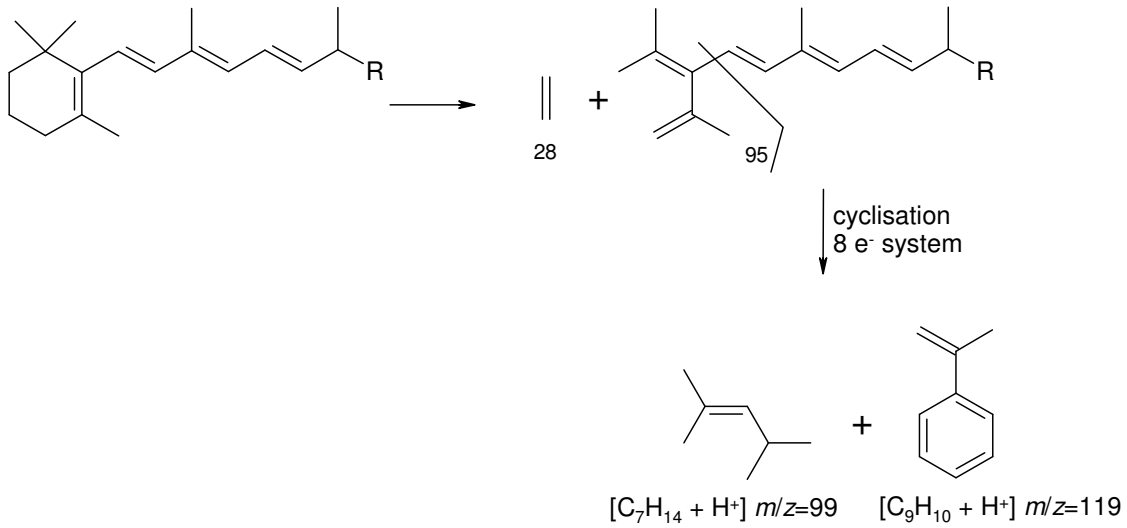

Figure 40. Retro-Diels-Alder followed by 8 e^- cyclization of **10** (R = COOH).

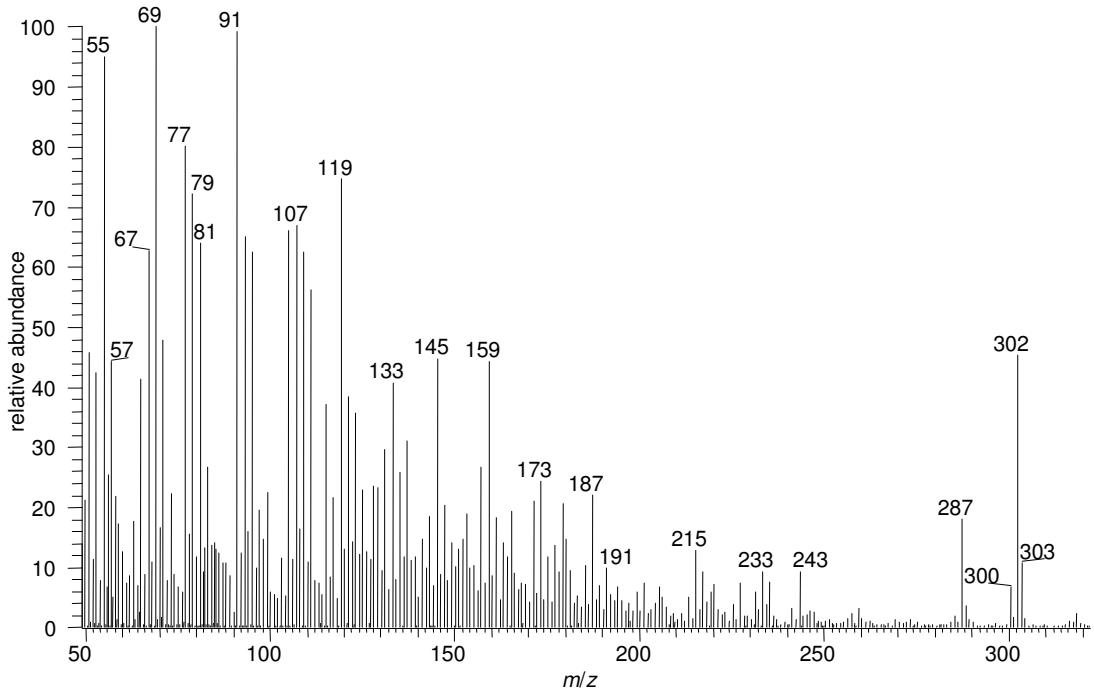

Figure 41. MS [EI] spectrum of 13,14-dh-RA **10**.

The loss of one methyl group [M^+-15] is characteristic for all retinoids.

The dihydro retinoids **11** and **75** were labeled with deuterium for biological studies. MS analysis of deuterated samples makes the tracing of further metabolization products easier and allows analysis in biological matrices with very small amounts of compounds. A higher degree of labeling should be achieved by using DCl in the workup instead of other H-containing acids.

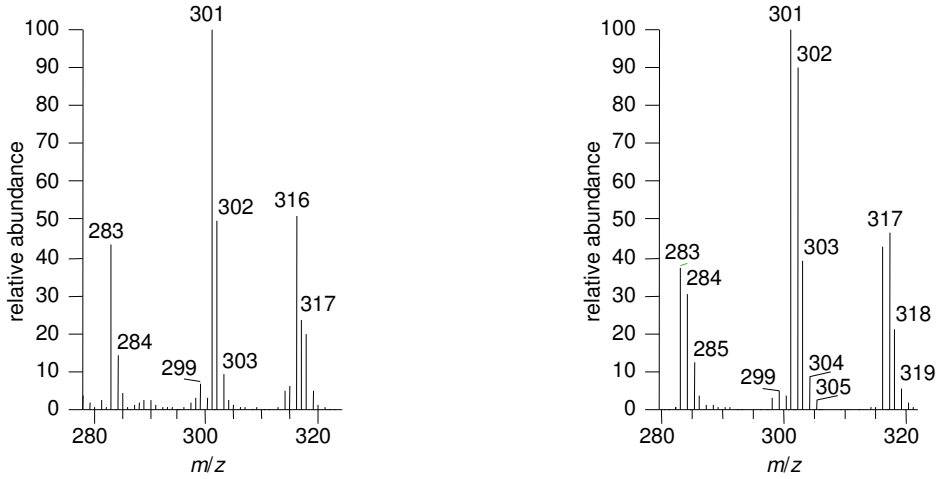

Figure 42. MS pattern of 4-oxo-13,14-dh-RA (**11**) and its labeled derivative **90**.

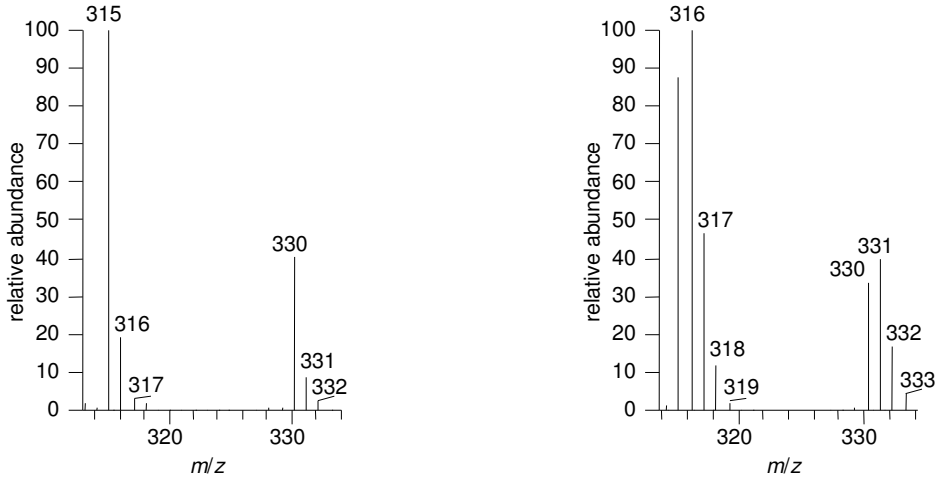

Figure 43. MS pattern of ester **75** and deuterated ester **89**.

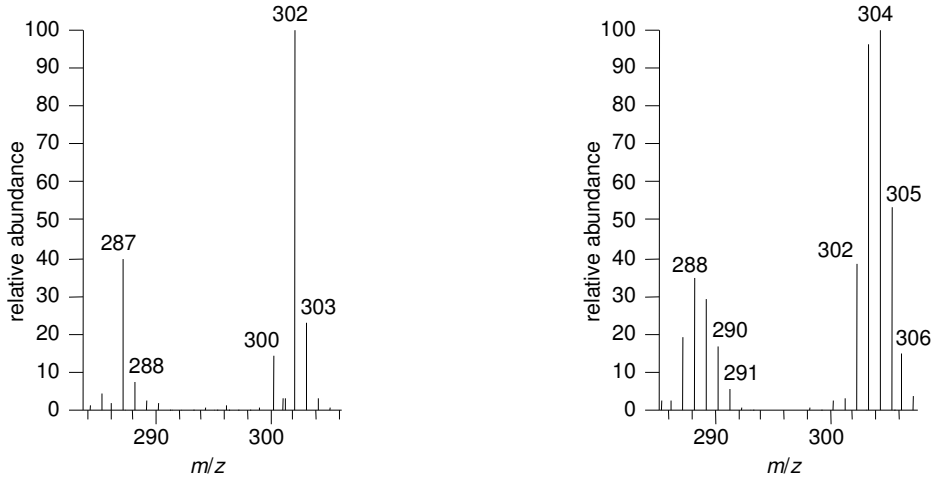

Figure 44. MS pattern of 13,14-dh-RA (**10**) and its labeled derivative **88**.

The phenyl substituted retinoids are giving ions characteristic for the cleavage of the polyene chain, in the lower mass region and aromatically substituted ions in the higher region. It also seems that after initial fragmentations, the large phenyl group was cleaved off together with the terminal acid or ester group.

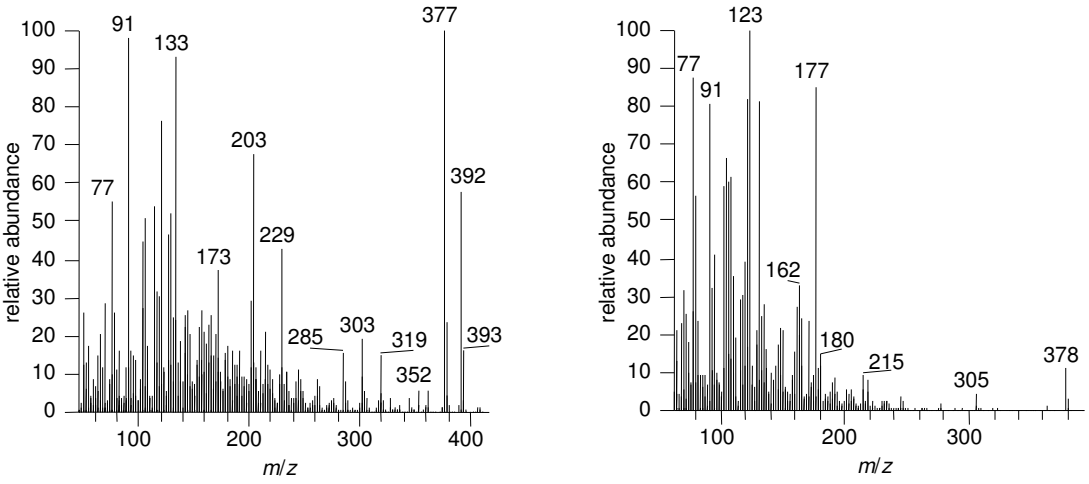

Figure 45. MS [EI] spectra of **79** and **78**.

Other modified retinoids, synthesized here, also showed the peak characteristic for a polyene as discussed before. All details are given in the experimental data.

5.4 NMR Spectroscopy

Nuclear magnetic resonance (NMR), particularly ^{1}H NMR spectroscopy, plays a major role in identifying and elucidating molecular structures in retinoid chemistry. Besides MS, UV and IR spectroscopy, NMR analysis was used to confirm the structure of the new vitamin A metabolite and of the newly synthesized retinoids. The structure and spatial arrangement of the retinoid isomers was established by ^{1}H and 2D NMR spectroscopy, as will be discussed below. All spectra were referenced to TMS or d_4-MeOH. The two main retinoid structures, **11** and **10**, both possible intermediates in the metabolism of vitamin A, will be discussed in detail. All other retinoid derivatives show almost the same signal pattern, with very small displacement of the protons or carbon atoms near the newly introduced groups in comparison with the core structures.

5.4.1 4-Oxo-13,14-dh-RA (11)

The separated fractions of **11** were analyzed immediately after elution from the HPLC column and solvent evaporation. The olefinic regions of the ^{1}H NMR spectra are shown

in Figures 46-49. Although basis line separation was achieved and all isomers should have been pure, for two of them, 11-*cis*- and 9,11-di-*cis*-**11**, the ^{1}H NMR spectrum show small signals belonging to other isomers. Small fractions of 11-*cis*-**11** isomerized into all-*trans*-**11** and 9,11-di-*cis*-**11** into 9-*cis*-**11**. All fractions were kept in the dark, under nitrogen and stored in the refrigerator (0-4 °C). ^{1}H NMR spectra of 11-*cis*-**11** and 9,11-di-*cis*-**11** taken after two days show that no further isomerization took place under these conditions. However, the clean ^{1}H NMR spectrum of 9-*cis*-**11** showed after several days partial isomerization into all-*trans*-**11**. This process also revealed itself in changes of the peak ratios of the HPLC chromatograms when samples were stored for longer time.

Steric repulsion between the methyl group C-16/C-17 and the hydrogen atoms at C-7 and between the methyl C-18 and the hydrogen 8-H are present in the molecule and fix the conformation of the C-6/C-7 bond. This has been demonstrated for several carotenoids incorporating a cycloxene ring.[59] These steric interactions were shown to produce a downfield shift of the protons for which the internuclear distances are smaller than the sum of their van der Waals radii.[59] However, the steric repulsion is partly relieved by a bending of the planar zigzag chain with the methyl groups pointing towards the convex side of the molecule. This effect will be discussed below.

A comparison of the chemical shift data of the *trans*-/*cis*-isomers indicate that shift changes occur only for the protons attached or in close geometrical proximity to the corresponding *cis* bond. The terminal group on the chain does not play a significant role as seen by the comparison between the chemical shifts of the acid **11** and its corresponding methyl ester **75** (Table 6 and 7).

Table 6. Chemical shifts for the polyene chain of **11** and **75**.

11	7-H	8-H	10-H	11-H	12-H	13-H	14-H
all-*trans*	6.27	6.34	6.15	6.49	5.78	2.77-2.75	2.33
9-*cis*	6.24	6.82	6.09	6.52	5.68	2.72-2.71	2.30
11-*cis*	6.32	6.41	6.52	6.37	5.42	3.23-3.18	2.32
9,11-di-*cis*	6.32	6.86	6.57	6.37	5.35	3.12-3.11	2.14
75							
all-*trans*	6.23	6.31	6.10	6.44	5.74	2.86-2.76	2.36-2.32
9-*cis*	6.25	6.79	6.04	6.47	5.66	2.82-2.72	2.32-2.25
11-*cis*	6.27	6.35	6.43	6.33	5.38	3.27-3.16	2.33-2.25
9,11-di-*cis*	6.21	6.82	6.38	6.37	5.30	3.28-3.16	2.36-2.25

Table 7. Chemical shifts of methyl and methylene protons of **11**.

11	2-H	3-H	16-H/17-H	18-H	19-H	20-H
all-*trans*	1.86	2.49	1.20	1.81	1.94	1.1
9-*cis*	1.88	2.51	1.21	1.85	1.95	1.14
11-*cis*	1.87	2.50	1.21	1.82	1.94	1.14
9,11-di-*cis*	1.89	2.41	1.21	1.84	2.01	1.03

The different isomers were distinguished from each other by the shift changes of the protons close or part of the *cis* double bonds. For instance, a significant shift of the proton 8-H is only observed in the isomers where 9-H/10-H are in *cis*-configuration, as for 9-*cis*-**11** and 9,11-di-*cis*-**11**, respectively. The shift difference to all-*trans*-**11** is +0.48 ppm for the 9-*cis*-isomer and +0.52 ppm for the 9,11-di-*cis*-isomer. The signal of 10-H is shifted considerably downfield only in the isomers for which the protons 11-H/12-H are *cis*-configurated. For the 11-*cis*-isomer this shift is +0.37 ppm and for the 9,11-di-*cis*-isomer +0.42 ppm compared to the all-*trans*-isomer. Although the configuration at C-5 is identical in all isomers, the methyl groups at this position show a small downfield shift of +0.04 ppm and +0.03 ppm in the 9-*cis*- and 9,11-di-*cis*-isomers, because of the steric interactions with the proton 11-H. Another indicator for steric hindrance due to a *cis* double bond in its proximity is the proton 13-H. As seen in Figure 50, this proton is oriented to the center of the cavity formed by the polyene chain. This configuration is geometrically favored to avoid higher interactions when the methyl group will be oriented to the cavity center. This is the reason for the downfield shift of 13-H by +0.46 ppm in the 11-*cis*- and 9,11-di-*cis*-isomers. These characteristic shifts agree with the geometrical configuration determined by the 2D NMR spectra, mostly the NOESY spectra (see below).

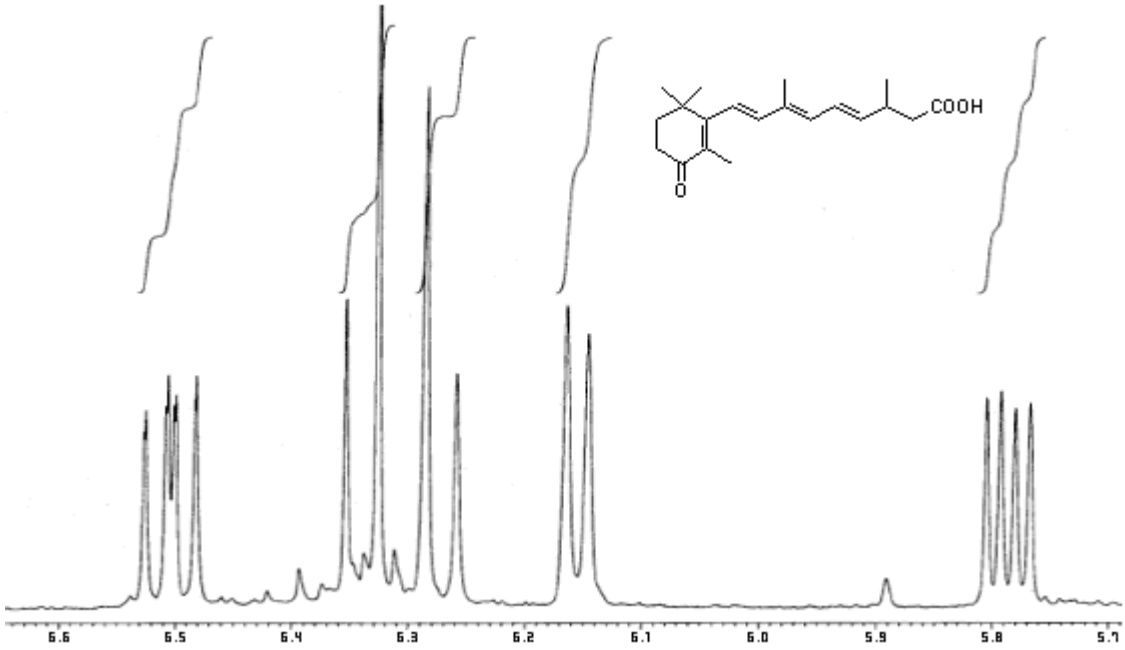

Figure 46. ^{1}H NMR spectrum of all-*trans*-**11**.

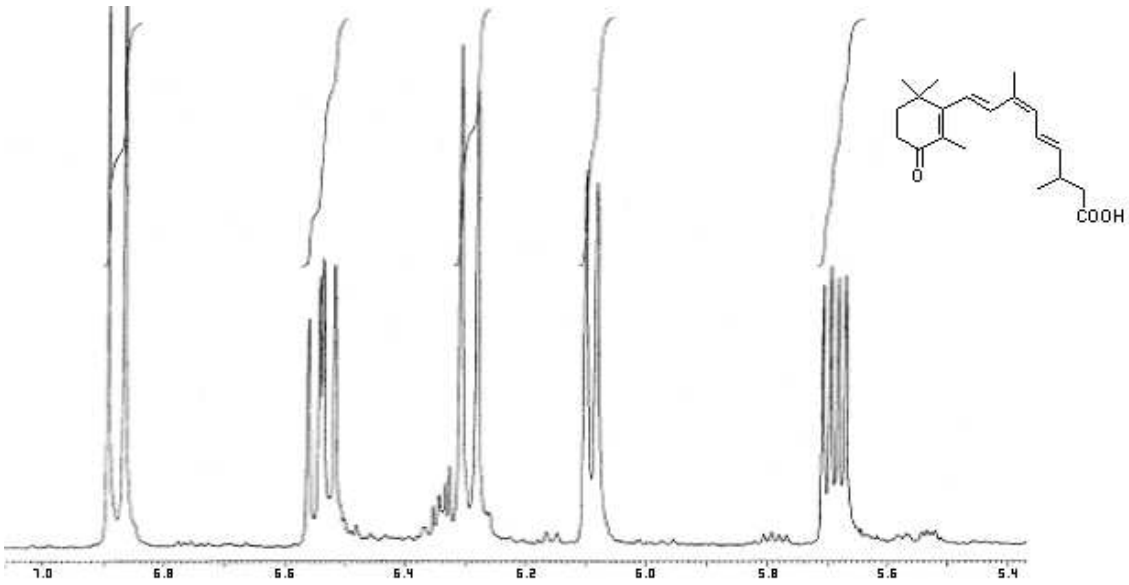

Figure 47. ^{1}H NMR spectrum of 9-*cis*-**11**.

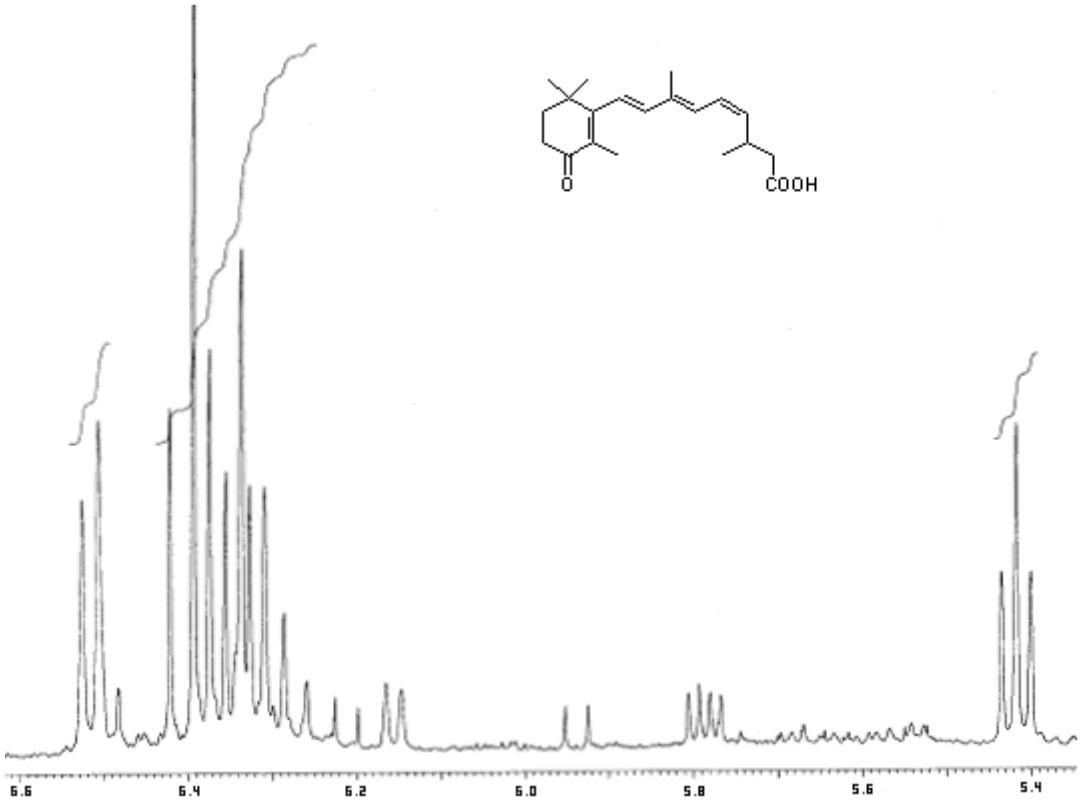

Figure 48. ^{1}H NMR spectrum of 11-*cis*-**11**.

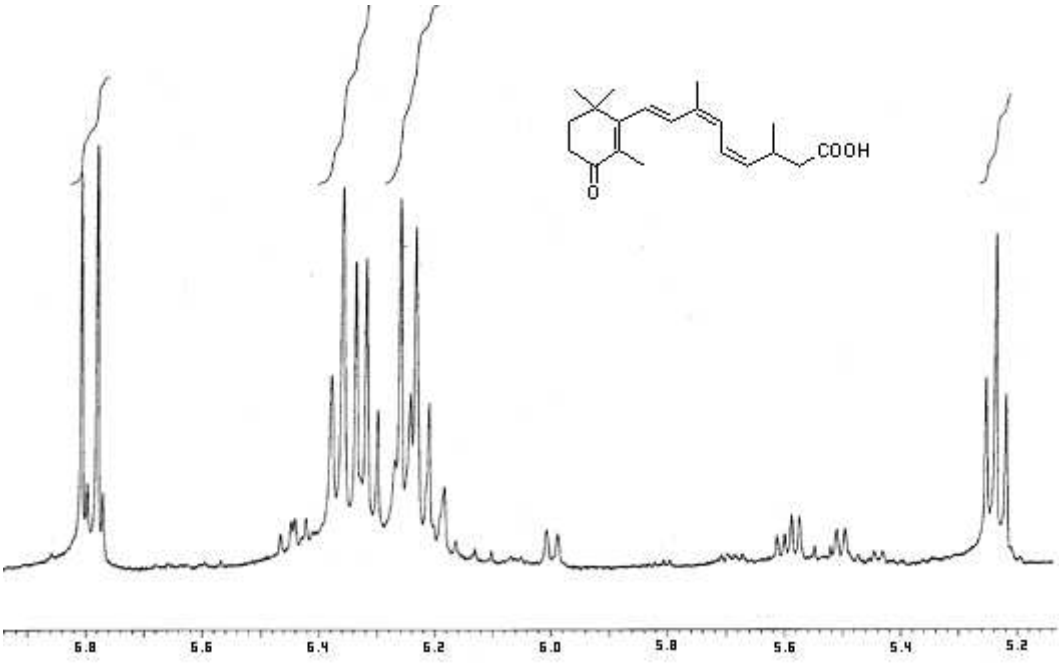

Figure 49. ^{1}H NMR spectrum of 9,11-di-*cis*-**11**.

The structures of the different isomers can also be assigned from the coupling constant of the proton signals.

The coupling constant between 7-H/8-H shows a characteristic *trans*-coupling of 16.2 Hz for all isomers, whereas for all other protons this constant depends on the

geometrical orientation of the rest of the conjugated double bonds. With values between 10.9 and 11.4 Hz the coupling between 10-H and 11-H is very similar for all isomers, because 10-H is always *trans* to 11-H to avoid steric hindrances with the neighboring protons. Furthermore, the isomer differentiation at C-11/C-12 can be derived from 11-H/12-H and 12-H/13-H as shown in Table 8. A characteristic *cis* coupling of 11 Hz between 11-H/12-H is seen in 11-*cis*-**11** and 9,11-di-*cis*-**11**, while a bigger coupling constant of ca. 15 Hz is seen when this bond is in *trans*-configuration. The proton 12-H gives a double doublet for the all-*trans*- and 9-*cis*-isomers, with a small downfield shift ($\Delta\delta$ = +0.1 ppm) for the proton in all-*trans*-**11** compared to 9-*cis*-**11**, whereas the 11-*cis*- and 9,11-di-*cis*-isomers give a triplet, with 12-H in 11-*cis*-**11** downfield shifted by $\Delta\delta$ = +0.17 ppm compared to the 9,11-di-*cis*-isomer.

Table 8 Coupling constants (in Hz) for the olefinic protons in **11**.

11	all-*trans*	9-*cis*	11-*cis*	9,11-di-*cis*
7-H, 8-H	16.2	16.2	16.2	16.2
10-H, 11-H	11.0	11.2	11.4	10.9
11-H, 12-H	15.0	14.9	11.5	11.5
12-H, 13-H	7.7	7.6	10.5	10.1

The final evidence for the configuration of the isomers was obtained from the H,H-NOESY experiments. A summary of these spectra is shown in Figure 50.

NOESY signal between the protons 10-H/12-H, 11-H/19-H and 11-H/20-H indicate a linear configuration, which was assigned to the all-*trans*-isomer. When 19-H is showing a cross peak with the neighbor proton 10-H, the substituents on C-9/C-10 must be in *cis* configuration, while a cross peak between 19-H and 11-H indicates a *trans*-configuration of this double bond. On the other hand, NOESY signal between 8-H and 10-H is the sign for the *trans*-configuration of the substituents at C-9/C-10, while a cross peak between 8-H and 11-H is showing the *cis* configuration of this double bond. With this information, the configuration of the C-9/C-10 double bond can easily be assigned. When 10-H and 12-H are giving a cross peak in the NOESY spectrum, they are on the same side of the chain and the two conjugated double bonds at which 10-H and 12-H are attached have the same geometry. A cross peak between 11-H and 12-H is possible when these two protons are in *cis* orientation, while 10-H and 12-H give a NOESY signal, when 11-H and 12-H are in *trans*-orientation.

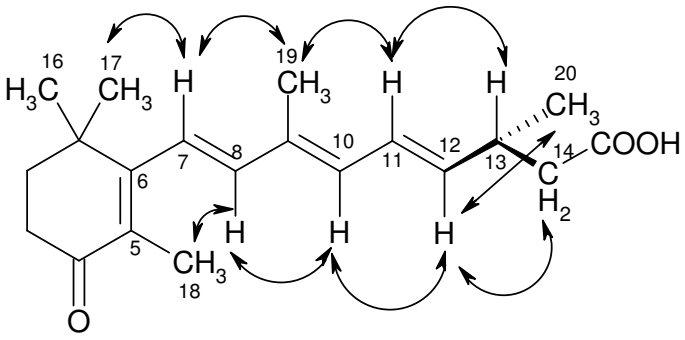

all-*trans*-**11**

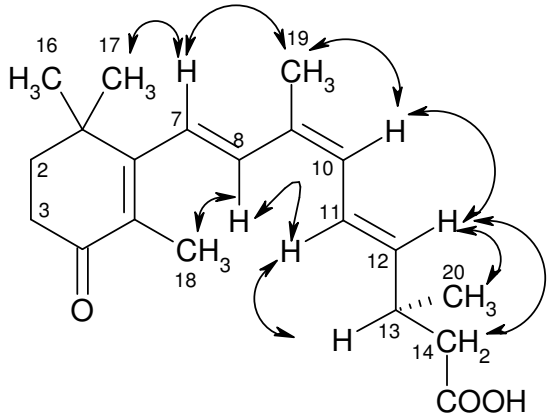

9-*cis*-**11**

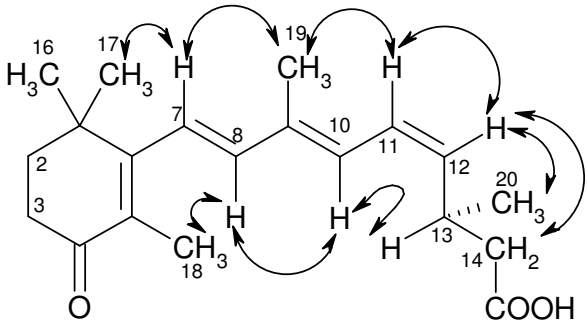

11-*cis*-**11**

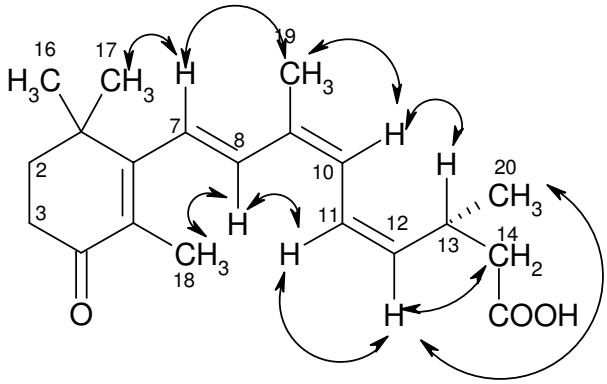

9,11-di-*cis*-**11**

Figure 50. NOESY determined coupling mechanisms in **11**.

Taking all these observations into consideration, the configuration of the isomers can be assigned. In all isomers NOESY signals were observed between 7-H/17-H, 7-H/19-H and 8-H/18-H because of the *trans*-configuration at C-7/C-8 double bond. Additional cross peaks between 12-H/14-H and 12-H/20-H are noted in all spectra. This means that in all isomers, the most stable configuration in solution is that one for which the methyl group C-20 is pointing away from the cavity formed by the polyene chain, while the proton at C-13 is oriented towards the center of this cavity, to overcome steric interactions with the other alkene protons. The all-*trans*-configuration was assigned for the spectra where the following additional cross peaks were present: 8-H/10-H, 10-H/12-H, 11-H/19-H and 11-H/13-H. The 9-*cis*-isomer shows cross signals for 10-H/19-H and 8-H/11-H indicating the *cis* configuration at C-9/C-10 double bond whereas cross peaks between 11-H/13-H and 10-H/12-H indicate a C-11/C-12 *trans* double bond. Cross peaks between 8-H/10-H and 11-H/19-H show a *trans* C-9/C-10 double bond, while coupling between 10-H/13-H and 11-H/12-H is a sign of a *cis* configuration of the C-11/C-12 double bond, all together proving the 11-*cis*-isomer. The 9,11-di-*cis*-isomer gave cross peaks in the NOESY spectrum between 8-H/11-H and 10-H/19-H for the *cis* C-9/C-10 double bond and 10-H/13-H, 11-H/12-H for the *cis* C-11/C-12 double bond.

5.4.2 13,14-Dihydro-RA (10)

The 13,14-dh-RA (**10**) and its ester **74** were analyzed by NMR spectroscopy as described for the 4-oxo derivative **11**. The conjugated double bond system contains one double bond less than **11**, the 4-oxo keto group. The absence of this function is responsible for the upfield shift of all signals in **10**, as seen in Table 9.

Table 9. Chemical shifts of the polyene chain protons of **10** and **74**.

10	7-H	8-H	10-H	11-H	12-H	13-H	14-H
all-*trans*	6.05	6.02	5.96	6.45	5.64	2.79-2.66	2.25-2.37
9-*cis*	6.20	6.60	5.89	6.51	5.58	2.76-2.65	3.31-2.24
11-*cis*	6.15	6.13	6.31	6.32	5.29	3.26-3.10	2.33-2.20
9,11-di-*cis*	6.14	6.58	6.25	6.38	5.22	3.29-3.12	2.31-2.24
74							
all-*trans*	6.09	6.04	5.98	6.42	5.62	2.80-2.75	2.41-2.36
9-*cis*	6.13	6.57	5.88	6.50	5.55	2.80-2.72	2.40-2.26
11-*cis*	6.14	6.14	6.30	6.31	5.26	3.24-3.16	2.36-2.28
9,11-di-*cis*	6.17	6.60	6.21	6.41	5.19	3.25-3.17	2.40-2.26

Table 10. Chemical shifts of the different methyl and methylene protons of **10**.

10	2-H	3-H	4-H	16-H/17-H	18-H	19-H	20-H
all-*trans*	1.53-1.40	1.72-1.55	2.01	1.01	1.67	1.87	1.10
9-*cis*	1.51-1.47	1.68-1.61	2.04	1.03	1.72	1.95	1.07
11-*cis*	1.53-1.40	1.72-1.55	2.01	1.01	1.69	1.88	1.05
9,11-di-*cis*	1.51-1.47	1.68-1.61	2.04	1.02	1.70	1.89	1.05

The methylene and methyl chemical shift differences between the isomers of **10** are minimal. The protons 4-H are shifted downfield by $\Delta\delta$ = +0.03 ppm in 9-*cis*- and 9,11-di-*cis*-**10** compared to the all-*trans*-isomer, because of steric repulsion. For the same reason, 18-H is shifted downfield by $\Delta\delta$ = +0.05 ppm in the 9-*cis*-, by $\Delta\delta$ = +0.03 ppm in the 9,11-di-*cis*- and only by $\Delta\delta$ = +0.02 ppm in the 11-*cis*-isomer. The proton 19-H in 9-*cis*-**10** is shifted downfield by $\Delta\delta$ = +0.08 ppm compared to the same proton in the all-*trans*-isomer, while for the 11-*cis*- and 9,11-di-*cis*-isomers just minimal shifts of +0.01 ppm and +0.02 ppm are registered.

The proton attachment to the double bonds resulted in the same multiplicity pattern as in **11**, however shifted to higher fields. In comparison with the all-*trans*-isomer, 8-H of 9-*cis*- and 9,11-di-*cis*-**10** was strongly shifted downfield, while 10-H was shifted downfield in the 11-*cis*- and 9,11-di-*cis*-isomers. The same characteristic signal pattern as described for **11**, was seen for 12-H of **10** (double doublet with coupling constants of 7.6 Hz and 15 Hz for the all-*trans*- and 9-*cis*-isomers, and a triplet with a 10.5 Hz coupling constant for the 11-*cis*- and 9,11-di-*cis*-isomers).

Although not all new retinoid derivatives prepared in this thesis were preparatively separated on HPLC (HPLC separation was undertaken in analytical amounts for biological assays), their configuration was assigned from the ^{1}H and 2D spectra of the isomeric mixture. When Wittig reaction was performed with the separated isomers of aldehyde precursor **47**, the product **10** contained only two diastereomers, all-*trans*-/11-*cis*-**10** or 9-*cis*-/9,11-di-*cis*-**10,** for which the chemical shift was easily assigned.

As described in detail for **11**, the configuration of the isomers of all other retinoids synthesized here, was assigned by chemical shifts, vicinal coupling constants and the NOESY experiments.

In conclusion, NMR spectroscopy is the best method for configuration assignment of new retinoids.

6 Circular Dichroism

6.1 Introduction

When linearly polarized light interacts with a molecule, this experiences an oscillating electric and magnetic field.[60] The positive nucleus and the negative electrons start to oscillate, but when the light wavelength λ is smaller than 1000 nm, the frequencies become to large and the heavy nucleus cannot oscillate significantly. The electron cloud is polarized along the direction of the oscillating electric field vector $\vec{E}$. As any oscillating charge, part of the energy used for polarization of the electron cloud is emitted again. If the light energy is large enough, no energy is emitted again, and the molecule will be promoted to a higher excited state. The absorbed energy $h\nu$ equals the energy difference between the ground S_0 and the excited state S_i ($\nu = E_i - E_0)/h$). This equation gives the position of an absorption line in the spectrum. A chiral compound is rotating the plane of linearly polarized light, or the oscillating direction of the electric field vector $\vec{E}$.[60]

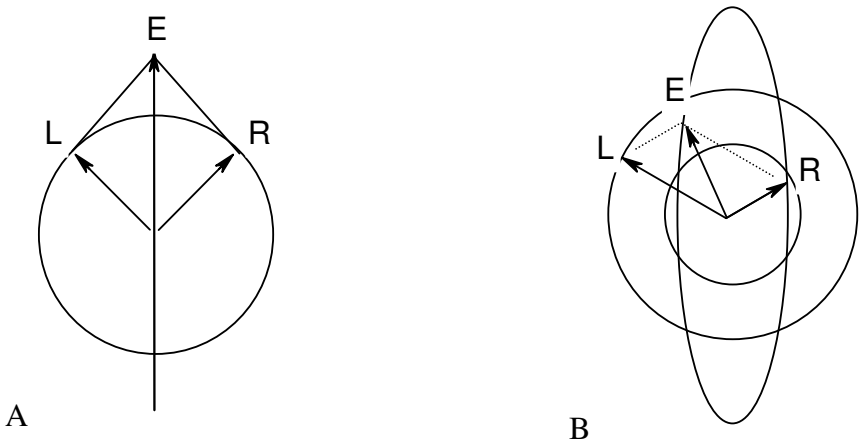

Figure 51. A) Plane polarized light resolved into two circularly polarized components R and L, with the same intensity and phase, the resultant will lie in the plane. **B)** Right circularly polarized light is less intense (more absorbed) than left circularly polarized light, the resultant electric vector follows an ellipse, and the corresponding light is elliptically polarized.[60]

When light passes through an absorbing optically active substance, the left and right circularly polarized rays travel at different speeds ($c_L \neq c_R$) which leads to different wavelength ($\lambda_L \neq \lambda_R$) and the rays are absorbed to a different extent, i.e. with different absorption coefficients ($\varepsilon_L \neq \varepsilon_R$). The difference $\Delta\varepsilon = \varepsilon_L - \varepsilon_R$ is called circular dichroism (CD) and can be measured by a CD spectrometer as differential absorption of left and

right hand circularly polarized components of light when plane polarized light is transformed into elliptically polarized light.[60]

The Beer-Lambert-Bouguer law can be used for the description of the circular dichroism as follows:

$$\Delta A = A_L - A_R = \log\left(\frac{I_0}{I_L}\right) - \log\left(\frac{I_0}{I_R}\right) = \log\left(\frac{I_R}{I_L}\right)$$

and

$$\Delta\varepsilon = \frac{\Delta A}{c \cdot l}$$

where A is the absorbancy, c the sample concentration, l the path length, I_0 the intensity of the incoming light, and I_L and I_R the intensities of the left, respectively right circularly polarized light leaving the cell. If c is given in mol·L^{-1} and l in cm then ε is called the molar absorption coefficient or molar absorptivity.[60]

When the incoming light interacts with a chiral substance, the exiting light has different intensities $I_L \neq I_R$. If the right hand circularly polarized component is less intense, i.e. is absorbed more, than the left circularly polarized component, the electric vector of the light follows an elliptical path, corresponding to the elliptically polarized light (Figure 51). The shape of the ellipse is mathematically determined by the angle $\psi = \arctan(b/a)$ (a is maximum diameter and b is the minimum diameter of the ellipse), which is called ellipticity.[60] Measurements have shown that:

$$\psi = 33\ \Delta A$$

Another method for quantitative characterization of chiroptical properties measures the rotation of the plane of linearly polarized light traveling through a substance. This method is the least reliable for structure elucidation, although it is often used as a criterion for enantiomeric purity. The measured rotation α depends on the sample concentration c (or density) and the length of the tube l. The specific rotation in solution can be calculated as:

$$[\alpha] = \frac{100 \cdot \alpha}{c \cdot l}$$

Biot noticed that this value depends on the temperature and very characteristically on the wavelength λ. When proceeding from long to short wavelengths, α increases with A/λ which he called normal optical rotatory dispersion (ORD).[60] Biot noticed also that the value of α rises more slowly with shorter wavelengths, an effect termed anomalous optical rotatory dispersion.

The three effects described here: CD, ellipticity and anomalous ORD are called Cotton effect (CE).

Using the sign of the CE, information about the conformation of a molecule can be derived, i.e. the sign of the torsion angle around a bond, but not about the absolute configuration.[62] The Cotton effect is a property of the chromophoric system, which is determined either by its own absolute configuration or by the sum of interactions with many chirally arranged atoms or bonds.

There are several theoretical rules to assign the absolute configuration of a molecule.[66b] In the case of dh-RA derivatives obtained in this synthetic work, the chromophores themselves are achiral. The CD spectrum can be the result of interactions of the chromophores, or, when the energy difference between the chromophores is too large, they cannot interact anymore and only of the chiral arrangement of the substituents at the chiral center is producing the CD spectrum. In the first case, one can use the exciton coupling method to assign of the absolute configuration of a molecule; in the second case it is hard to define an exact theoretical methodology.

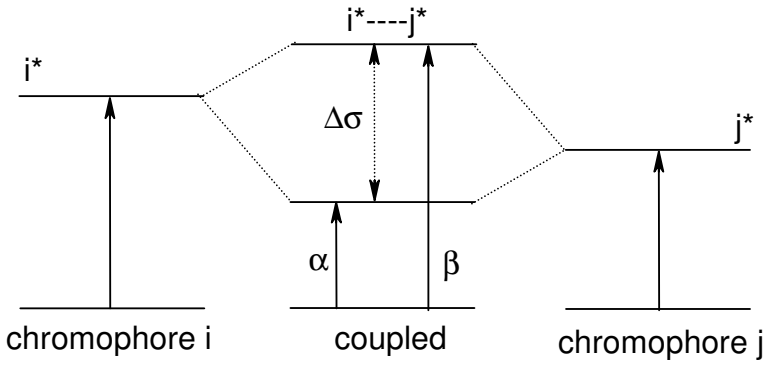

Figure 52. Exciton coupling of two chromophores.[60]

When the exciton chirality method is employed, the determination of the absolute configuration is equivalent to the determination of the absolute sense of chirality between the chromophores. In this case, the geometry of the molecule (relative orientation of the chromophores) plays a decisive role in determining the sign of the CD. If the transition moments between the two chromophores are arranged in a clockwise fashion, defined as positive, the CD is bisignate with a first positive CE and a second negative CE, which means also a CD with a positive sign and positive chirality, and vice versa. The distance between the peak and trough of a split CD curve is defined as amplitude (A) and either a positive or a negative sign is assigned to it depending on whether the first CE is positive or negative.[60]

When the difference between the absorption maxima of the chromophores is large, the amplitude of the CD spectra is very small. The amplitude decreases with increasing energy difference between the chromophores. This was calculated and verified experimentally for several molecules with different chromophores.[60] On the other hand, if the energy gap is too big, the chromophores do not interact anymore, and the exciton chirality method for prediction of the CD sign cannot be used.

Although the difference between the absorption maximum of the chromophores attached to the chiral center of 13,14-dihydro-retinoids synthesized in this work can be theoretically calculated, it was still not clear if the exciton chirality method can be used, because the value of $\Delta\lambda$ value is quite large (60 nm). To have a safer and more reliable prediction method of the CD spectra, molecular modeling calculations were performed.

6.2 Experimental Determination of Circular Dichroism

The synthetic mixture of 4-oxo-13,14-dh-RA (**11**), was first characterized by MS, IR, UV and NMR spectroscopy. After chiral separation on a Chiracel OJ column (see Chapter 4, Figure 16) and *cis-/trans*-configuration assignment for each HPLC fraction by NMR spectroscopy (see Chapter 5), the fractions were analyzed by CD spectroscopy. All diastereomers of **11** show a bisignate CD spectrum. Fractions 1, 2, 3 and 5 gave a first positive CE and the first CE for the other fractions was negative (see Figure 53).

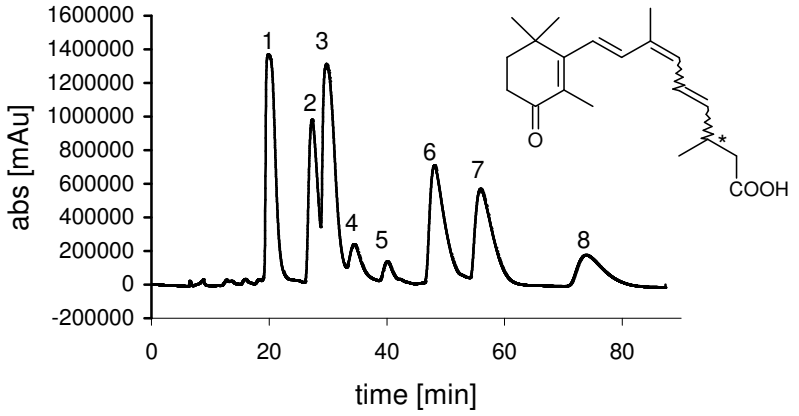

Figure 16. Chiral separation of racemic 4-oxo-13,14-dh-RA (**11**) on Chiracel OJ, hex/*i*PrOH/TFA 95:5:0.1. Fraction 1: *R*-11-*cis*-; fraction 2: *S*-9,11-di-*cis*-; fraction 3: *S*-all-*trans*-; fraction 4: *S*-9-*cis*-; fraction 5: *R*-9-*cis*-; fraction 6: *S*-11-*cis*-; fraction 7: *R*-all-*trans*-; fraction 8: *R*-9,11-di-*cis*-**11**.

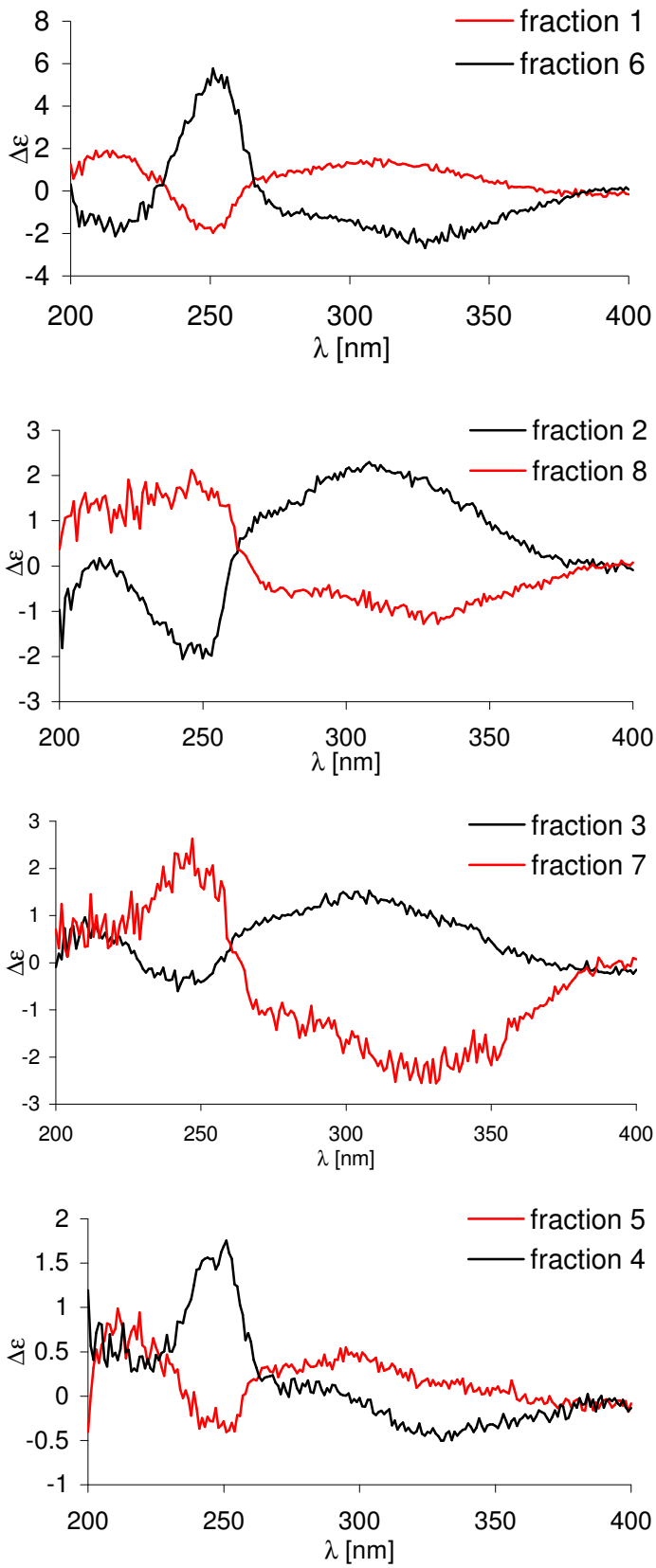

Figure 53. Experimental CD spectra of different HPLC fraction of **11**. Fraction 1: *R*-11-*cis*-; fraction 2: *S*-9,11-di-*cis*-; fraction 3: *S*-all-*trans*-; fraction 4: *S*-9-*cis*-; fraction 5: *R*-9-*cis*-; fraction 6: *S*-11-*cis*-; fraction 7: *R*-all-*trans*-; fraction 8: *R*-9,11-di-*cis*-**11**.

Chiral HPLC comparison with the product of the (*S*)-enantioselective synthesis of **11** (Figure 17, Chapter 4.3) shows that the peaks 2, 3, 4 and 6 are the *S*-enantiomers. Combining the information of these two analyses, one can see that although fraction 1, 2, 3, 5 gave a first positive CE, different enantiomers are assigned for each of them: fraction 1 and 5 are the *R*-enantiomers while 2, 3 are the *S*-enantiomers, indicating that the chromophore orientation in each enantiomers of **11** is different.

Table 11. Assignment of chiral HPLC of **11**.

fraction	1	2	3	4	5	6	7	8
enantiomer	*R*	*S*	*S*	*S*	*R*	*S*	*R*	*R*
first CE	+	+	+	-	+	-	-	-

These experimental results provide the most important information on the absolute configuration of the molecules investigated. To gain additional information about the spatial-arrangement and conformation of all diastereomers of **11,** detailed conformational analysis were performed by computational modeling.

6.3 Theoretical Calculations of Circular Dichroism Spectra

The theoretical elucidation of absolute configuration by quantum chemical calculations consists first of a conformational analysis of the molecule under consideration. The second step is the calculations of the electronic circular dichroism spectra.

The geometry of each isomer of **11** was first optimized to the lowest energy conformation by DFT calculations using Becke's three parameter hybrid Hartree-Fock DFT method (B3) in combination with the Lee-Yang-Parr correlation functional (LYP) and the 6-31G(d) basis set (B3LYP/6-31G(d)).[56] A pre-optimization step was performed using the PM3 method,[56] which proves to give quite similar results as B3LYP. Electronic excitation energies and rotational strengths were calculated by DFT TD using the same method and basis set as for geometry optimization, calculations being performed for 20 excited states. For all these calculations the GAUSSIAN 03 program was used. The velocity form of R_V (rotatory strength) and the wavelengths of the corresponding electronic transitions were used for the simulation of the CD spectra.

The theoretical definition of rotatory strength is given by a product of the electric and the magnetic transition moment vectors[60]

$$R = \mu \cdot m \cdot \cos(\mu, m)$$

where μ and m are the magnitudes of the electric and magnetic dipole transition moments, respectively, and the cosine of the angle between these vectors. The determination of μ and m will not be discussed here. These parameters are unsigned so the CD sign is given by the cosine of the angle between them. If the angle is pointed (or even 0 for parallel vectors) then the cosine and the CD is positive. For an obtuse angle (maximum antiparallel vectors) the CD is negative because R_V is negative.

The experimental rotational strength is the λ -weighted, integrated CD multiplied by a factor f.[61]

$$R_V = \frac{3 \cdot h \cdot c \cdot 10^3 \cdot \ln 10}{32 \cdot \pi^3 N_L} \cdot \int_{\lambda_1}^{\lambda_2} \frac{\Delta\varepsilon(\lambda)}{\lambda} \mathrm{d}\lambda = 0.229 \times 10^{-38} \cdot \int_{\lambda_1}^{\lambda_2} \frac{\Delta\varepsilon(\lambda)}{\lambda} \mathrm{d}\lambda$$

For the optimized configurations of *S*-**11**, rotational strengths were calculated using the methods and the program mentioned; the results are summarized in Table 12.

Table 12. Calculated absorption maxima (λ), oscillator strengths (*f*), and rotational strengths (R_v velocity in cgs (10^{-40} erg-esu-cm/Gauss)) by the B3LYP method, basis set 6-31G(d).

	f	R_v		*f*	R_v
S-4-oxo-all-*trans*-13,14-dh-RA (**11**)			*S*-4-oxo-11-*cis*-13,14-dh-RA (**11**)		
393	0.0001	0.1258	393	0.0001	2.1163
362	1.3799	59.8105	361	1.2637	96.8946
294	0.0967	7.9377	294	0.0920	13.5793
254	0.0110	-34.5073	255	0.0113	-38.9707
246	0.1264	-7.315	246	0.0867	-58.3732
243	0.0119	-0.0209	245	0.0243	-17.5179
237	0.0018	-5.5108	239	0.0036	2.7951
231	0.0018	-0.1832	232	0.0039	-0.5907
226	0.0034	4.9066	227	0.0043	1.7843
212	0.0009	2.6285	212	0.0132	17.2557
212	0.0018	4.579	212	0.0034	2.1139
211	0.1661	-14.2487	211	0.1510	-7.1954
203	0.0010	-5.2925	204	0.0045	-12.1002
201	0.0000	0.0396	203	0.0002	-2.5772
S-4-oxo-9-*cis*-13,14-dh-RA (**11**)			*S*-4-oxo-9,11-di-*cis*-13,14-dh-RA (**11**)		
393	0.0001	-1.255	392	0.0002	3.2031
364	1.0701	-86.0883	368	1.0714	39.7879
294	0.1547	-18.5397	296	0.1696	10.9178
252	0.0179	55.0903	253	0.0077	-3.3452
248	0.0993	59.6329	252	0.0149	-48.6742
243	0.0023	1.227	249	0.0502	-12.6714
237	0.0022	1.1779	243	0.0005	-0.5348
233	0.0073	-4.0644	236	0.0098	2.7419
228	0.0031	-2.0693	229	0.0038	0.54
214	0.1530	-23.0284	216	0.1388	7.0725
212	0.0016	4.7428	213	0.0018	-14.8302
212	0.0403	23.2884	212	0.0262	-6.1459
205	0.0537	11.5501	208	0.0022	-7.5779
201	0.0000	-0.1763	206	0.0265	-4.1724

The wavelength shift in the simulated CD spectra, compared with the measured ones, could be due to solvent effects, which were neglected in our calculations.

The simulated and experimental CD spectra were compared and, surprisingly, for two isomers, all-*trans*- and 11-*cis*-**11**, the calculated CD spectra show the reverse sign.

For a rigid molecule, the typical procedure to calculate the CD spectra consists first in finding the conformation with least energy. Because of the molecular flexibility and the probability that the molecules can adopt several geometries, several conformations were analyzed separately by adjusting the dihedral angles between the bonds at the chiral center and by inverting the cyclohexene ring.

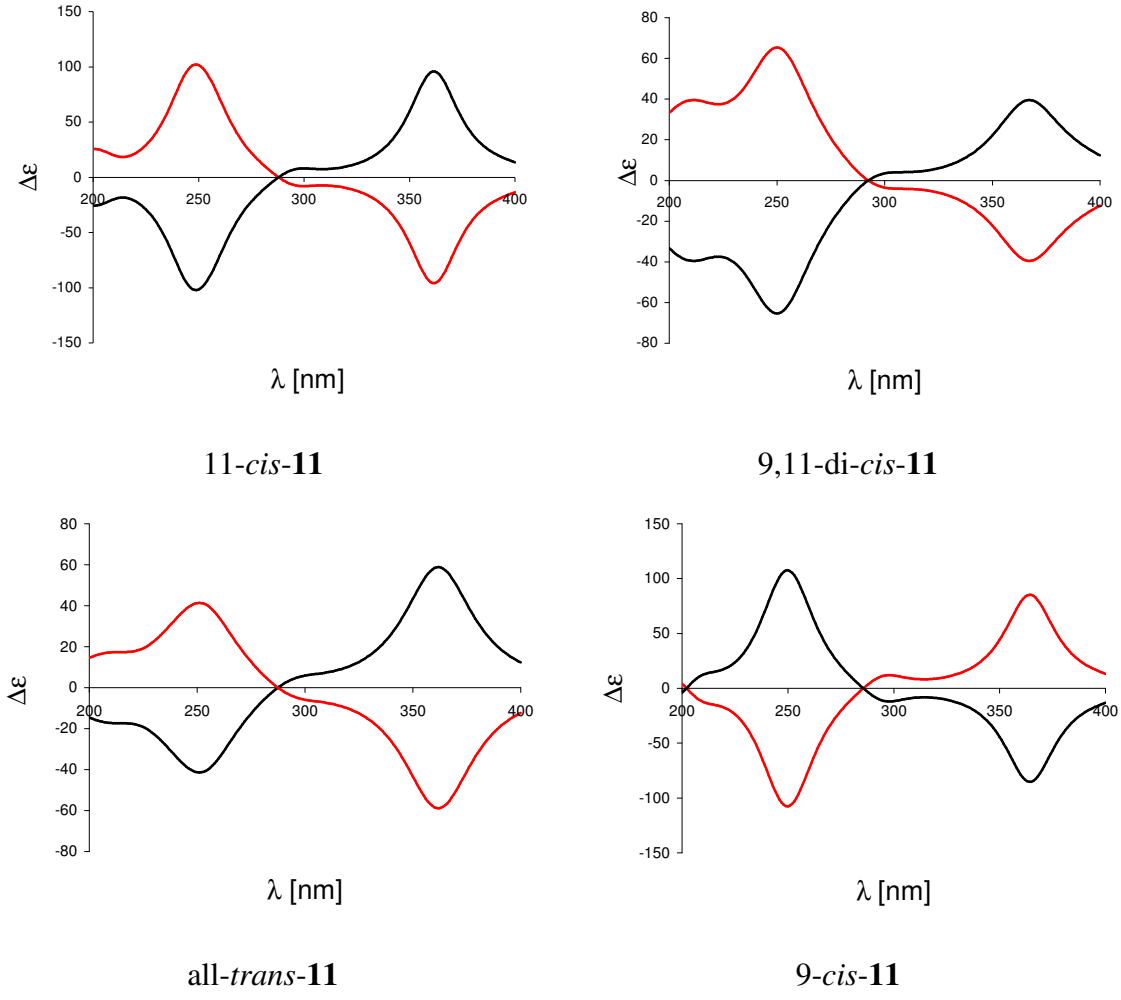

Figure 54. Calculated CD spectra for all diastereomers of **11** (red line: *R* enantiomer, black line: *S* enantiomer).

The initial calculations showed that the first energy minimum for *all-trans*-**11** was just a local and not the global minimum. For the new conformation found for the all-*trans*-isomer, the CD spectrum was again calculated and this time was in accordance with the experimental CD spectrum (Figure 53 and 54). This example demonstrates convincingly that, especially for flexible molecules, one should calculate more than one

conformation, to be sure that the found conformation has the lowest energy. For this reason for all other isomers of **11** at least two alternative conformations with different energies were investigated.

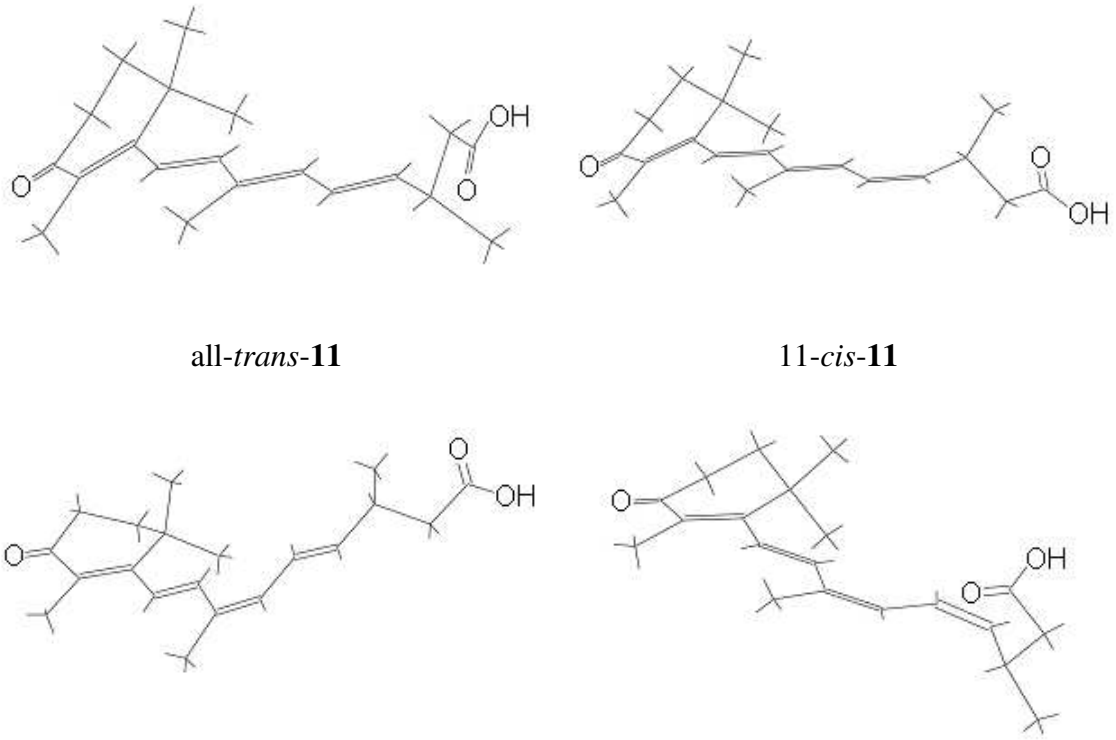

all-*trans*-**11** 11-*cis*-**11**

9-*cis*-**11** 9,11-di-*cis*-**11**

Figure 55. Envelope conformation of the cycloxene ring and different orientation of substituents at C-13 for the calculated global minimum conformation of **11**.

The calculated structures revealed some close through-space H-H interactions. The calculated distance between the protons 10-H and 13-H in the 11-*cis*-isomer is 2.07 Å and in the 9,11-di-*cis*-isomer 2.13 Å, while in the all-*trans*- and 9-*cis*-isomers 13-H does not show any important H-H interactions with other protons. The carboxyl group points away from the ellipse formed by the alkene chain in all isomers except in the 9,11-di-*cis* case where it is oriented towards the inside. This "closed" geometry can influence also the biological properties of this isomer because the carboxyl group can not interact anymore so easily with the amino acids of the receptor pocket; access to the pocket could be also hindered.

The differences between the global minimum and the first found local minimum are 0.7 kcal/mol for 9-*cis***-11**, 0.9 kcal/mol for 11-*cis***-11**, 1.6 kcal/mol for all-*trans*-**11** and 5.2 kcal/mol for 9,11-di-*cis*-**11**. Also between the isomers, the energy differences are not significantly larger, especially between the most stable isomers. As expected, for the all-*trans*- and the 9-*cis*-isomer, the difference is only small (0.9 kcal/mol). This means that

the stability of the 9-*cis*-isomer is not very high and it can isomerize easily. The 11-*cis*-isomer with an energy difference of 1.6 kcal/mol follows next, and with 2.6 kcal/mol the 9,11-di-*cis*-compound displays the highest energy difference compared to the all-*trans*-isomer. These energies refer to the most stable conformations (compared to global minimum energy) found for each isomer.

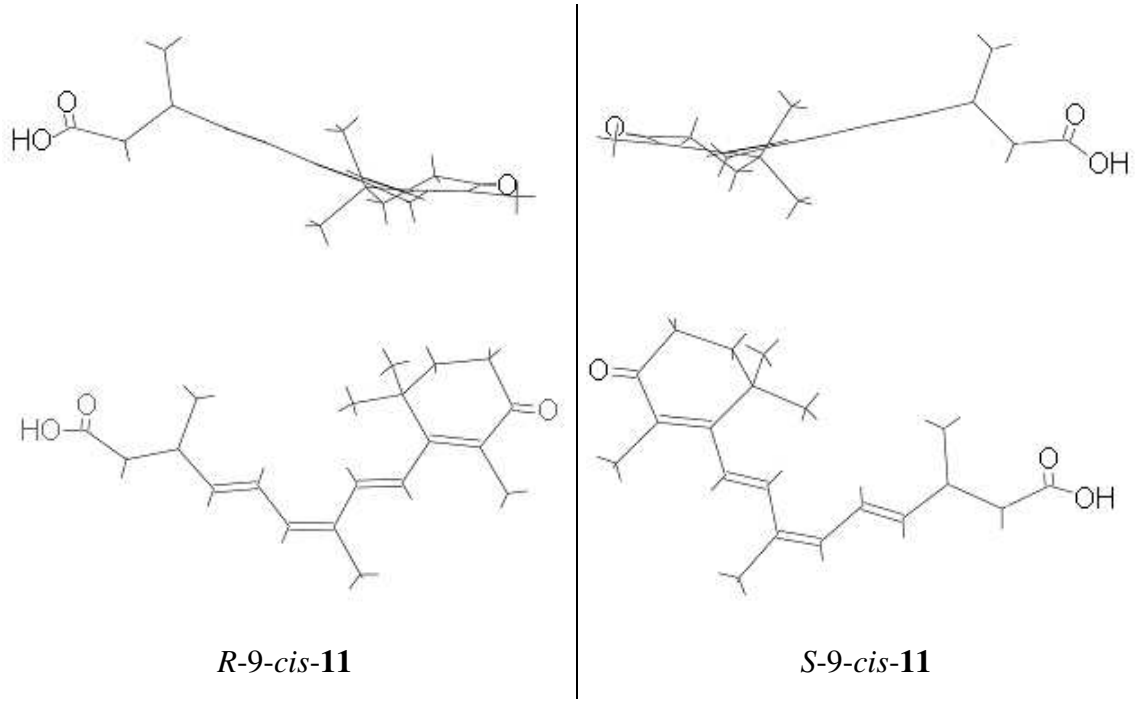

R-9-*cis*-**11** *S*-9-*cis*-**11**

Figure 56. Calculated conformations for the enantiomers of 9-*cis*-**11** top: global minimum, bottom: first local minimum. In both molecules the chiral center at C-13 was fixed and the molecule looked at from the same point of view.

Comparing all calculated conformations leads to the following generalizations: the cyclohexenone ring can exist in two conformations, C-2 pointing up or down. The conjugated chain prefers an elliptical form and the geometry at C-13 is also changing due to free rotation around the single bonds. As one can see in Figure 55, none of the four isomers is adopting the same conformation at their minimum energy level.

As assumed, the differences of the spatial arrangement at the chiral center in each isomer causes the circularly polarized light to be absorbed with different intensity giving different Cotton effects for each isomer. In Figure 56 these observations are exemplified for two calculated conformations (global minimum and first local minimum) of 9-*cis*-**11**. The sign of the CD spectra for these two conformations is reversed. C-13 was fixed and the view on the molecule was kept constant for all conformations, so that 13-H is oriented in the direction of the view. A 90° rotation of the alkene chain around C-12/C-13 results in different conformations, corresponding to different energy levels, of the same isomer. From the theoretical formula for R_V follows:

when the angle between the electric- and magnetic dipole moment (m and μ) is increasing to 90°, the cosine is changing the sign and the CE sign is also reversing. These observations are valid for the other isomers of **11** as well.

The double bond chain is also playing a significant role in the sign of the CD spectra. In Figure 57 are shown two adopted conformations for all-*trans*-, 9,11-di-*cis*- and 9-*cis*-**11**, for which the calculated CD spectra have inverse sign. The CD spectra for the conformations with the global energy level of all four isomers of **11** are shown in Figure 54.

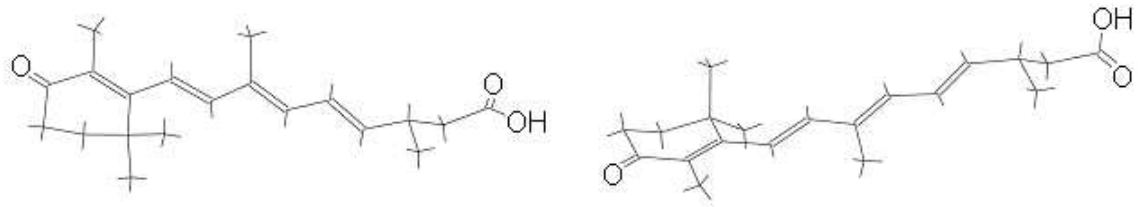

all-*trans*-**11**

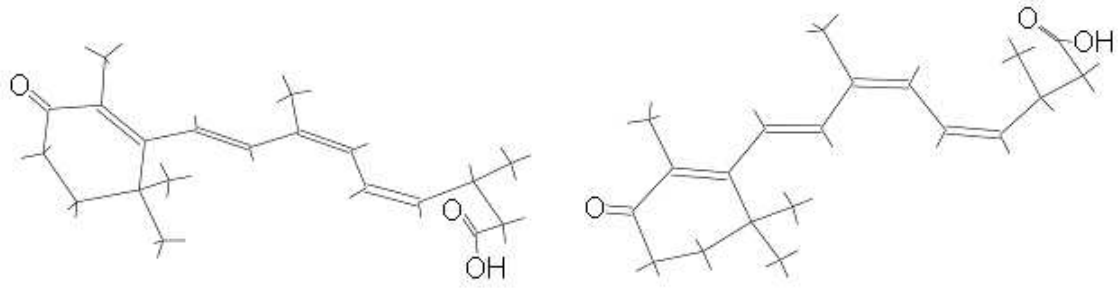

9,11-di-*cis*-**11**

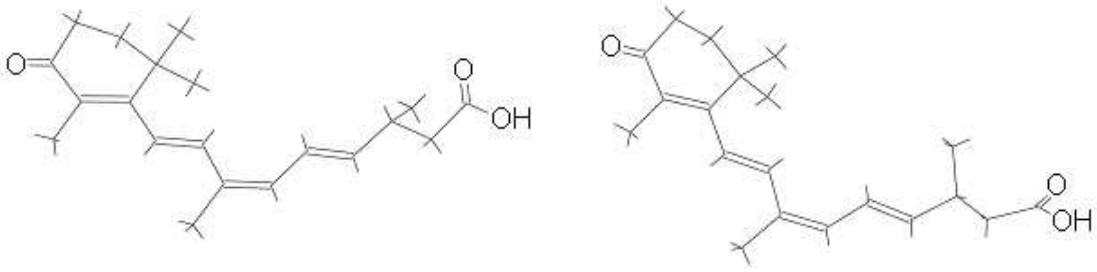

9-*cis*-**11**

Figure 57. Calculated conformations for **11**. Left: global minimum, right: local minimum.

After several optimization steps on the modeled geometries of **11**, different conformations were found with energy differences between 5.1 and 0.7 kcal/mol. All these conformers contribute in different proportions to the final CD spectrum. Since the CD spectrum of a compound depends on the molecular geometry, the experimental CD

spectrum should be considered as the average overall CD behavior of all relevant conformations. Obviously, for a flexible molecule the number of different spatial orientations is high. To obtain an exact theoretical spectrum, the CD average spectra of all conformers that are populated was calculated using the Boltzmann weighted average.[62] Taking into account the calculated minimum energies one can calculate the equilibrium constant between the two conformations **A** and **B** by the standard expression:

$$\mathbf{A} \overset{K}{\rightleftharpoons} \mathbf{B}$$

$$\Delta G = -RT \ln K = \Delta H - T\Delta S$$

For all-*trans*-**11**, ΔG is 1.6 kcal/mol giving a 94 % population of the conformation with the lowest energy, for 9,11-di-*cis*-**11** the energy difference is even larger, 5.1 kcal/mol, which gives the most stable conformer in more than 99.9 %, while ΔG for the 9-*cis*-isomer (0.65 kcal/mol) corresponds to 75 % population of the lowest energy level. Taking these distributions for the two conformers in the gas phase at 25 °C for each isomer into account the most populated energy levels gave the structure for which the CD spectra was also measured. After the optimizations steps, the calculated CD spectra of the conformations with the global minimum energy were in accordance with the experiment, except for the 11-*cis*-isomer. This isomer was further investigated.

More than 10 conformations were calculated to gather more information about other possible energy levels, which can contribute to the final conformer distribution. From all calculated conformations, 5 minima (see Figure 58) were found with energy differences between 0.7-4.0 kcal/mol. The CD spectra of these conformers show different signs.

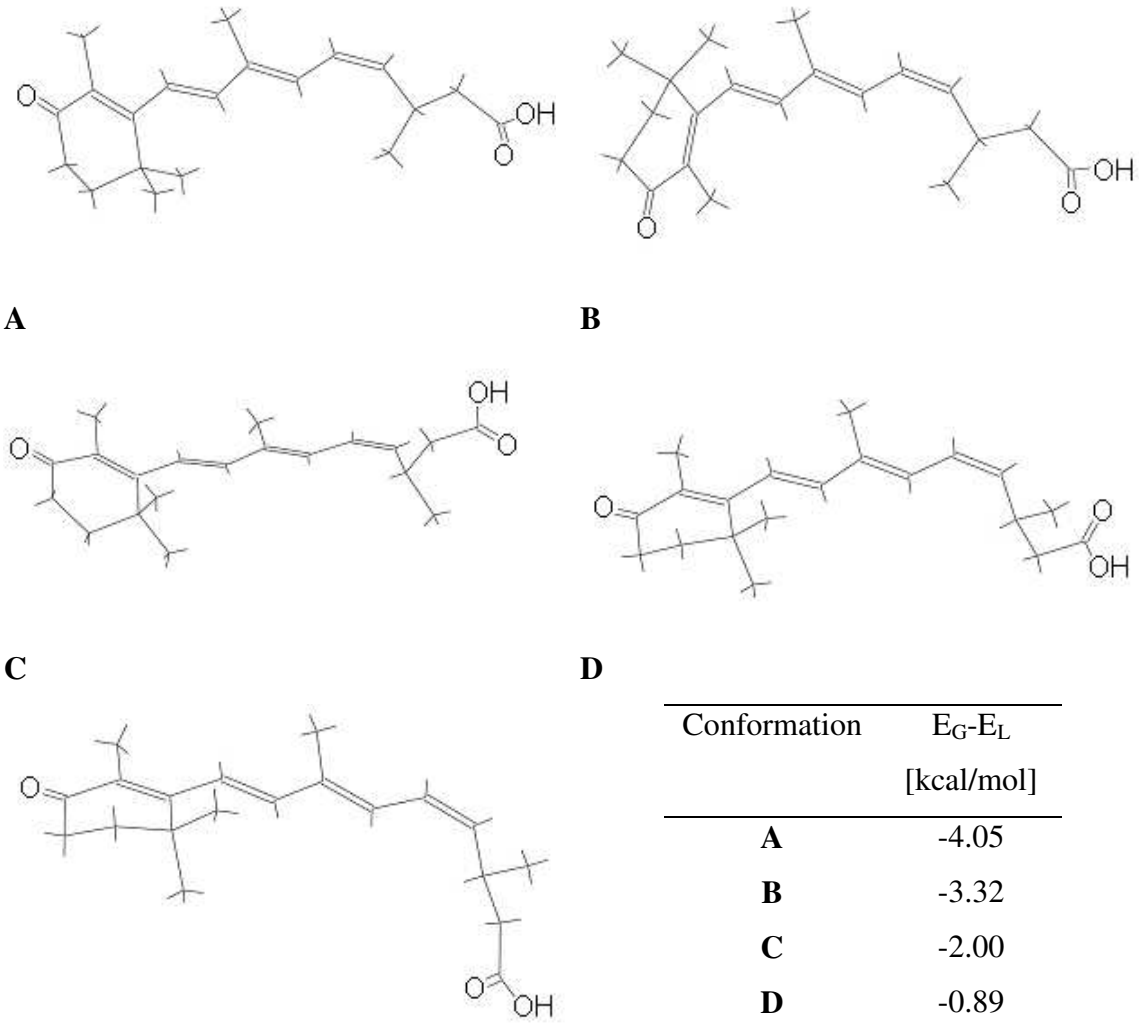

Conformation	E_G-E_L [kcal/mol]
A	-4.05
B	-3.32
C	-2.00
D	-0.89
E	0.00

Figure 58. Calculated conformations of the 5 minima found for *S*-11-*cis*-**11** in order of decreasing energy (**A**, **B**, **C**, **D** correspond to local minima E_L, **E** corresponds to the global minimum E_G).

In conformation **A** and **B**, although the chain keeps the same geometry and just the ring orientation is changed because of the free rotation around the C-6/C-7 bond, the CD spectra show a first positive CE in **B** and a first negative CE in the **A** conformation, respectively. This proves definitely that the geometry of the ring also plays a role in the CD and not only the geometry of the substituents directly bonded to the chiral center C-13. Because of the conjugation, all double bonds from the alkene chain, including the ring, form the chromophore, contributing to the CD. In the next conformations **C**, **D** and **E** the alkene chromophore has the same geometry, this time rotation around the single bond C-13/C-14 and C-14/C-15 gave rise to different conformations with different

energies. For these conformations the calculated CD spectra are the same, with a positive first CE, in agreement with the first CE seen in the measured CD spectra.

The overall CD of 11-*cis*-**11** is determined by the weighted contribution of each individual conformation at a given temperature and by the intensity of its Cotton effect. The intensity of the CE of each conformation has to be considered in a quantitative way because the difference in the CE intensities between conformations can be large and outweigh population factors.[63] The overall CD spectrum was calculated by Boltzmann-weighted averaging of all calculated conformations. For this the factor B, the population distribution, can be calculated by the Boltzmann equation:

$$B = e^{-\frac{Ei - E\min}{k \cdot N_L \cdot T}}$$

where E_i is the energy of local minima for the i conformation, E_{min} is the global minimum, k the Boltzmann constant, N_L the Avogadro constant, and T the temperature. The rotatory strength of each of the 5 confomations of 11-*cis*-**11** was multiplied by the corresponding B factor and averaged to the final R_V. This was considered for the calculation of the averaged CD spectra, which still had the opposite sign of the experimental one. This means that theoretically the conformation of the 11-*cis*-isomer for which the lowest energy level was calculated in the gas phase is not the same as the conformation of the isomer in solution, where other factors are playing an additional role. That this isomer has different properties than the other three can be also seen from the chiral HPLC separation. For all-*trans*, 9,11-di-*cis*- and 9-*cis*-**11** the *S* enantiomers are adsorbed less on the column and eluted first, whereas for the 11-*cis*-isomer, a different geometry and other interactions could be responsible for the retention time of the *S* enantiomer being longer than for its *R* enantiomer, which is also the first of the isomers to leave the column.

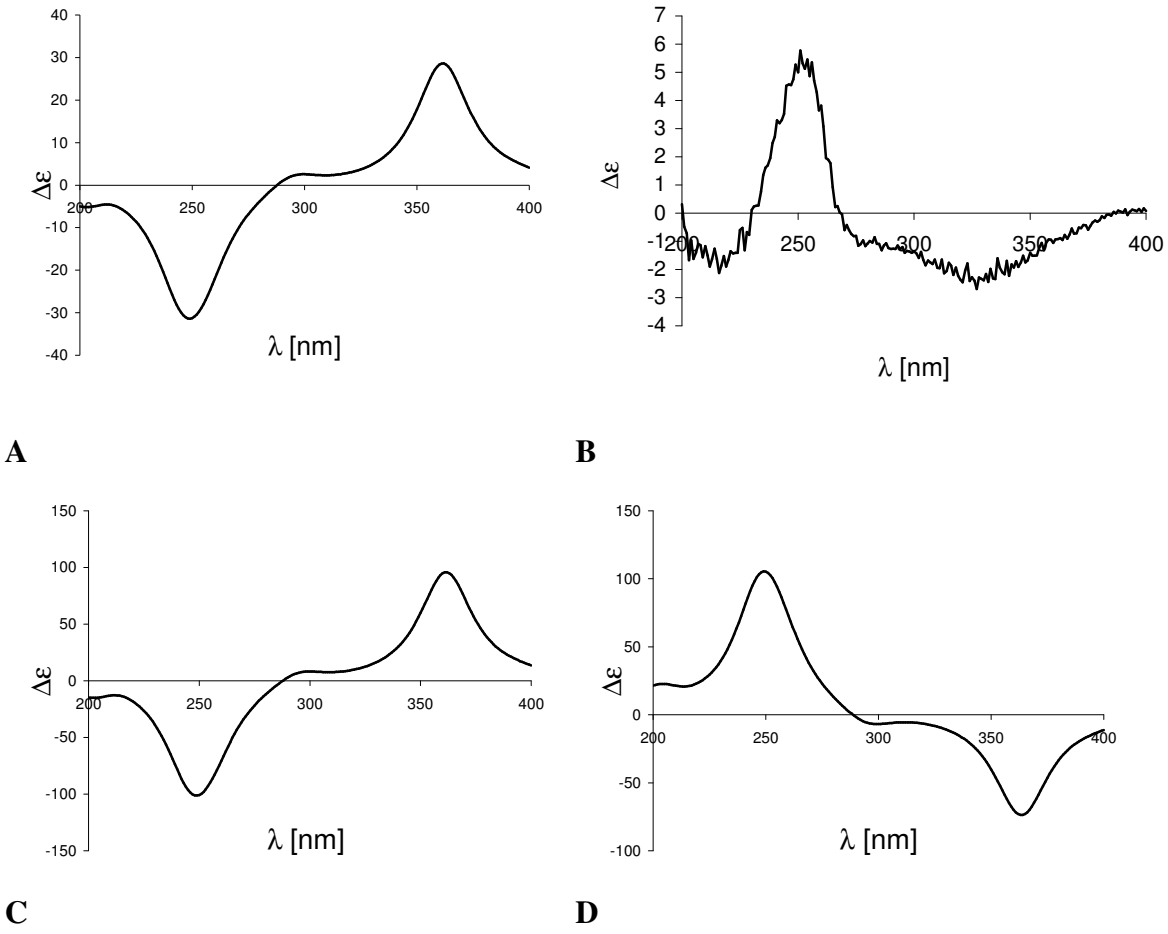

Figure 59. CD spectra of (*S*)-11-*cis*-**11** (**A**: Boltzmann averaged CD spectra, **B**: experimental spectra, **C**: calculated CD for the global minimum conformation, **D**: calculated CD spectrum of the conformation with first local minimum).

Additional effects that can influence the sign of the CD spectrum and even invert it are known from the literature.[60] Computer programs for the calculation of CD spectra offer a simple alternative for these calculations but cannot estimate all effects influencing the CE intensities. It is known that hydrogen bonds to the carbonyl groups stabilize a conformer which would otherwise be unfavored and change the CD spectra significantly.[63] Another fact known in the literature to drastically influence the CD spectra and even invert their signs, is the pH.[67] This additional influence was also not taken in account in the above calculations, although the CD spectrum were measured directly in the HPLC solvent which contained added TFA as buffer. It has also been shown that excitation of a molecule from a solvated ground state must not lead to the energetically most stable solvated conformation of the excited state, but to a conformation geometrically identical to the solvated ground state and necessarily having an energy higher than the equilibrium conformation of the solvated excited

state.[64] A number of factors are involved in the solvation of the ground and excited states, some of them occur in all systems, others only in some.

As shown for 9-*cis*-**11**, the alkene chain can adopt two geometries relative to the chiral center. In one of the conformations, Figure 58 (**E**) and Figure 60 (**E**), the chain is parallel to the hydrogen atom at C-13 and in conformation **A** (Figure 58 and 60) the chain is perpendicular to it. From the retinoid literature[33] it is known that the 11-*cis*-isomer belongs to the geometrically hindered isomers, because of the interactions between 10-H and the C-13 methyl group. This is also seen in the two conformations **A** and **E** (Figure 61). A more stable conformation, also the global minimum, is favored by rotation around C-12/C-13 so that the methyl group is pointing away from the helix formed by the side chain, whereas in conformation **A**, where the methyl group at C-13 is pointing to the center of the helix, interaction with 10-H is possible and the energy is higher. However, when additional effects, like hydrogen bonding due to solvent a effect, favor the conformation where 10-H and the methyl group at C-13 are closer, conformation **A** will be present in solution, rather than the most stable conformation in the gas phase. Because all these results are derived from calculations in vacuum, it is of course possible that in hex./*i*PrOH/TFA, in which the CD spectra were measured, the isopropanol could form additional hydrogen bonds with the RA derivatives.

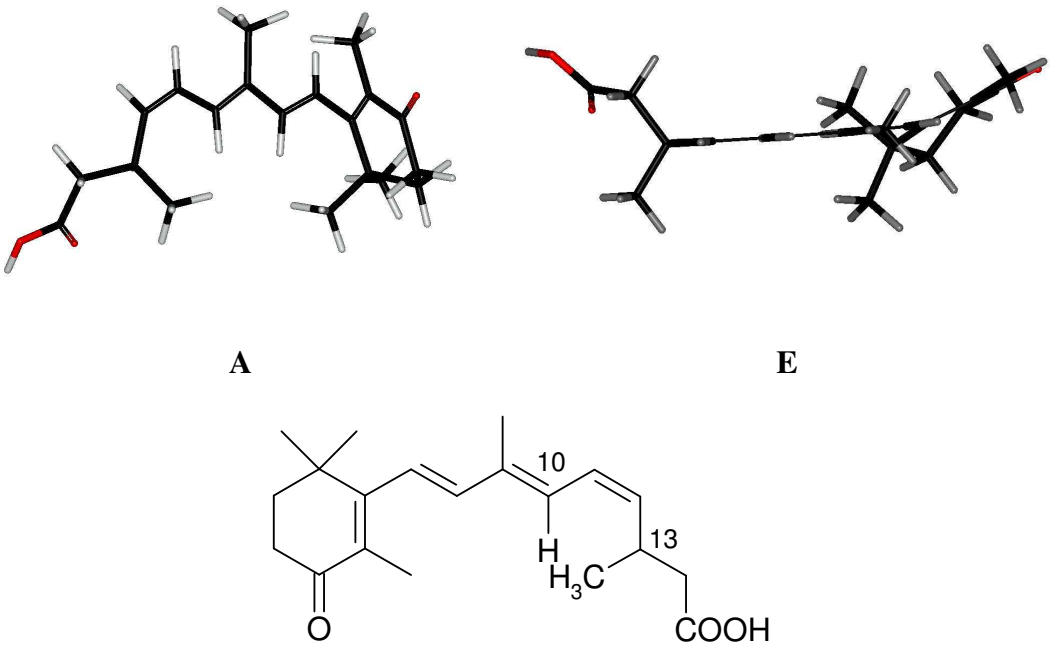

Figure 60. Calculated conformations of 11-*cis*-**11**. CD for conformation **A** (local energy minimum) shows the same CD as the experiment, for conformation **E** (global minimum) the sign reverses.

While calculating and interpreting the obtained results, the question arose, which part of the molecule is really influencing and determining the CD spectrum. The circularly polarized light can be absorbed by two chromophores present in the molecule at the chiral atom C-13. When the energy gap between these chromophores is too large, they will not interact with each other so that the energy of the exited state of the strongest chromophor is determining the sign of the CD spectrum. It was mentioned above for 11-*cis*-**11** that the arrangement of the carboxyl chromophore has no influence on the CD spectrum, and just when the alkene chain is rotating around a C-C bond the CD sign changes. To confirm the assumption, that the chirality is determined only by the double bond system, the molecule without the acid group was modeled, and for the optimized structure the CD spectrum was calculated. Additionally, **11** was truncated at each double bond and the obtained structures were also geometrically optimized and their CD spectra were calculated. The results of all these calculations clearly show that the spatial arrangement of the conjugated double bond system exclusively determines the sign of the CE and the CD spectrum. The CD spectrum of **109** looks almost the same as that of all-*trans*-**11** shown above (Figure 53).

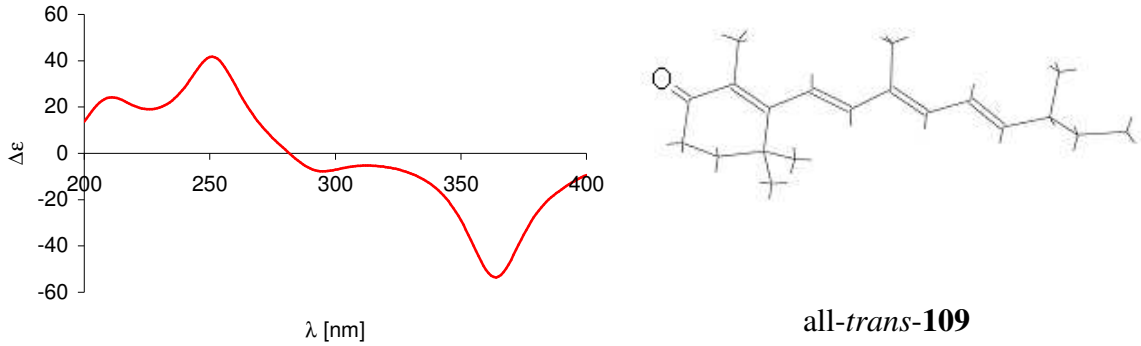

all-*trans*-**109**

Figure 61. Calculated CD spectrum and conformation of all-*trans*-**109**.

For the theoretical prediction of the CD spectra, the program uses implemented empirical rules. These rules allow prediction of the CD sign of a molecule based on certain geometric characteristics. If other practical factors contribute to a measured CD spectrum, the theoretical calculations differ from the experimental ones, and the limits or exceptions of the implemented rules are reached.

In conclusion, these calculations show that the geometry of the cyclohexenone ring in combination with the double bond chain determines the sign of the theoretical CD spectra, while additional experimental factors contribute to the finally measured CD.

6.4 Circular Dichroism of Substituted Retinoids

6.4.1 CD Spectra of 75

CD spectroscopy was used to characterize **75** after its separation on the Chiracel OJ column. The isomers were assigned to the corresponding fractions taking in consideration their peak ratio, known from the ^{1}H NMR analysis, their UV spectra and the enantiomer pairs shown by the CD spectra. The absolute configuration was assigned by comparison of the CD sign between the corresponding isomers of ester **75** and its acid **11**. It is known from the literature, that the configuration of similar molecules can be assigned by comparison of the CD spectra.[66] Furthermore, modeling of the CD spectra was also carried out to confirm the assignment.

The sign of the first CE of each isomer of **75** and the corresponding isomer of **11** were compared. For the 11-*cis*- (fraction 2 and 3) and the all-*trans*- (fraction 5 and 6) isomers, a good separation of the enantiomers was possible. The 9-*cis*- and 9,11-di-*cis*-isomers are eluting as fraction 1 and 4 and possibly coelute with the 11-*cis*-isomer. For this reason these last isomers cannot be characterized by CD spectroscopy. The first CE of *S*-all-*trans*-**11** is positive, meaning that all-*trans*-**75** with a positive first CE is also *S*-configurated; this was the case for fraction 5. Fraction 6 corresponds to *R*-all-*trans*-**75**. For the 11-*cis*-isomer, the first CE is positive in fraction 2, which is also the case in the first CE of *R*-11-*cis*-**11**. For this reason fraction 2 was assigned the *R*- and fraction 3 the *S*-11-*cis*-**75** structure, respectively.

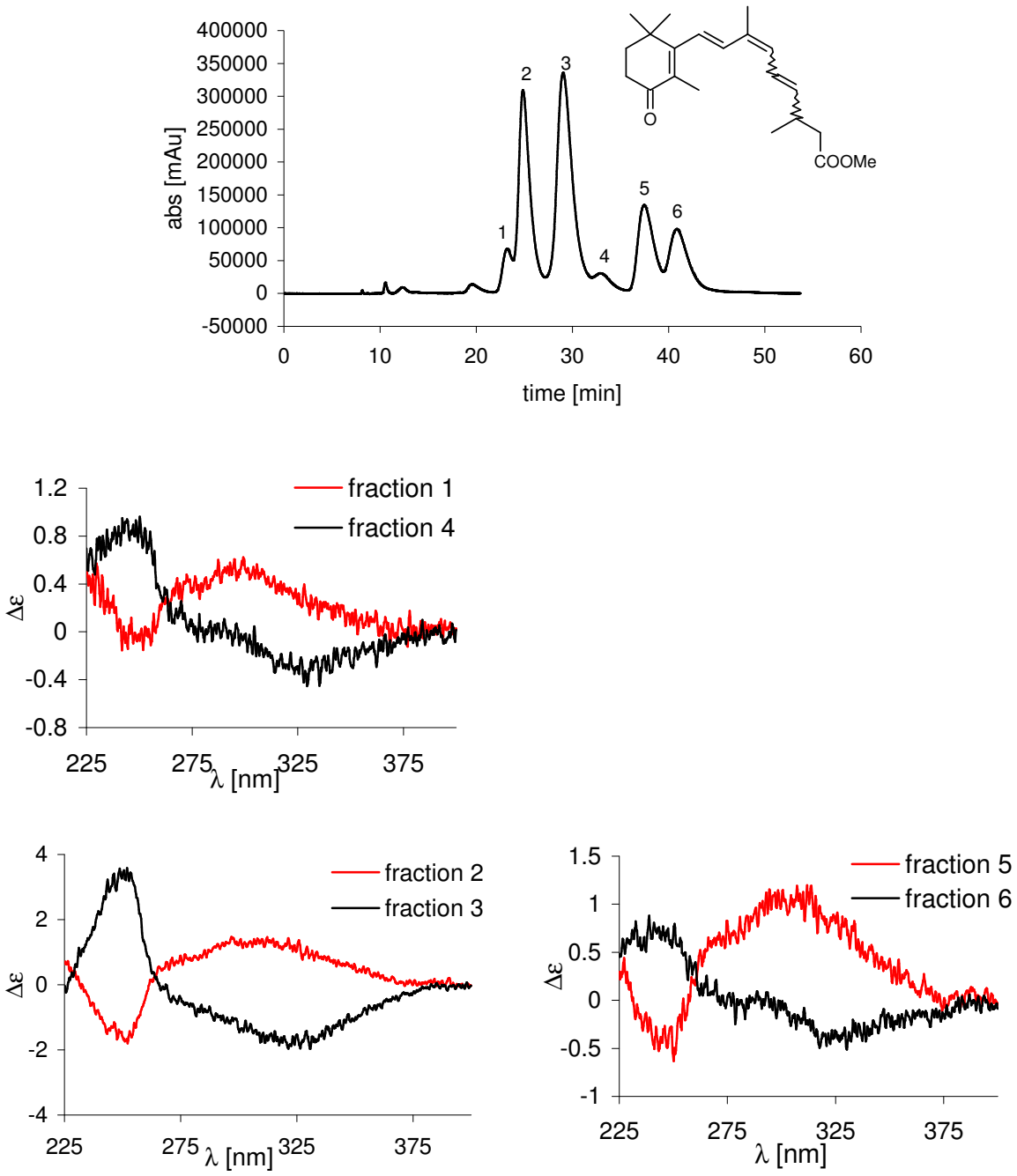

Figure 62. Chiral HPLC and experimental CD of the separated fractions of **75**.

Molecular modeling geometry optimization of the isomers of **75** and calculation of their CD spectra show that the first CE of the acid and its ester, for the same isomer, have the same sign, and the CD spectra all agreed. The calculated CD of ***R*-75** gave a negative first CE for the all-*trans*-, 11-*cis*- and 9,11-di-*cis*-isomers, while the 9-*cis*-isomer shows a positive first CE, in accordance with the first CE seen for **11**.

6.4.2 CD Spectra of Phenyl-substituted Retinoids

Chirality assignment of the HPLC separated fractions of the phenyl substituted retinoids was performed by comparison of their experimental and calculated CD spectra. Each isomer was first geometry optimized by molecular modeling and the CD spectra were then calculated for the most stable conformation. The CD spectra of **11** were also considered during this assignment, because of the structural similarities between these molecules. The experimental spectra of **79** are shown in Figure 63.

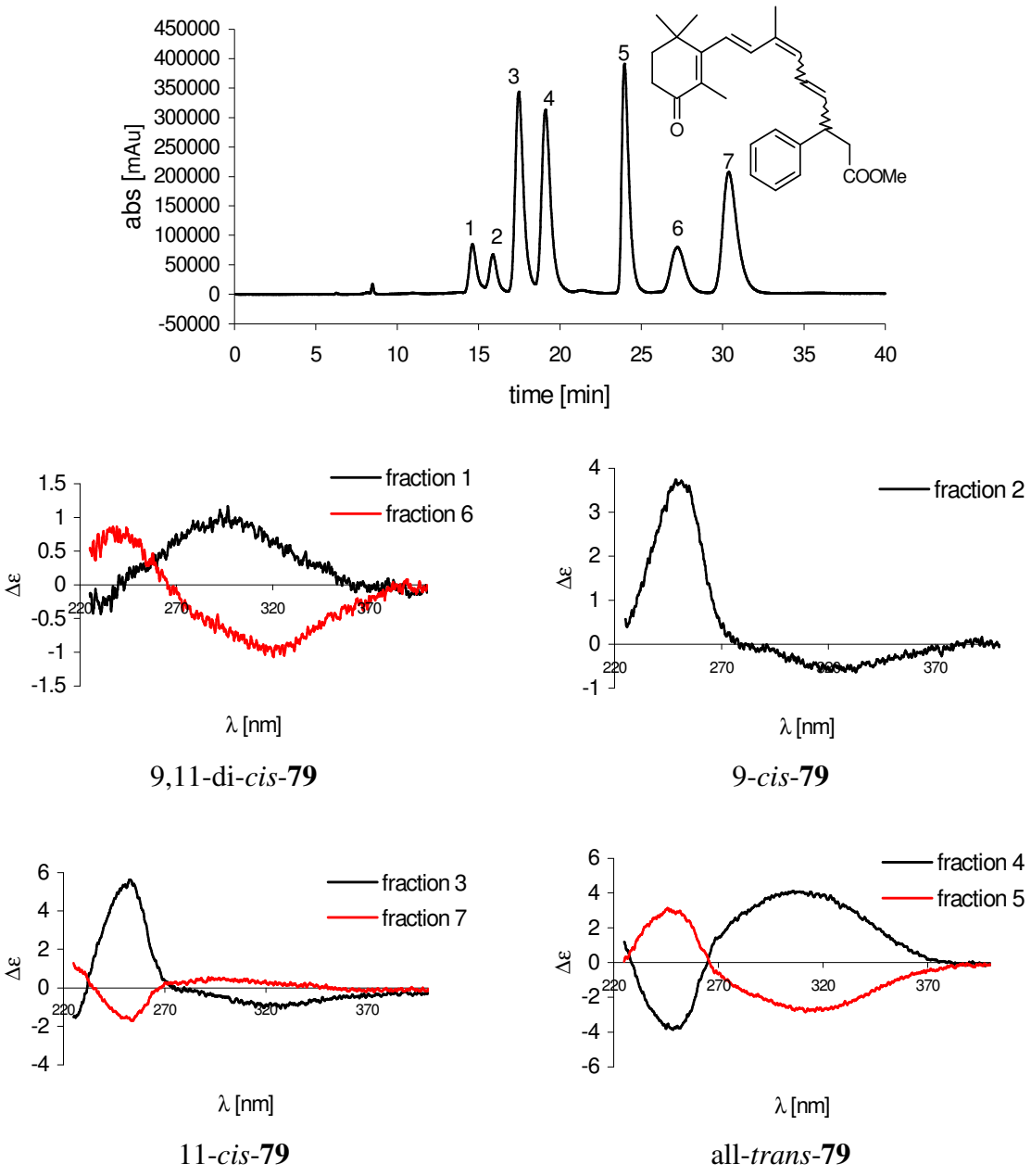

Figure 63. Experimental CD spectra of **79** red curve is assigned for *R* enantiomer, black for the *S* enantiomer.

A positive first CE was observed for the *R* enantiomer of the all-*trans*-, 11-*cis*- and 9,11-di-*cis*-isomers, as assigned by comparison with the computed CD spectra. The experimentally determined enantiomer of 9-*cis*-**79** gave a negative first CE, which by comparison with the calculated spectra is assigned to the *S* configuration. The CD sign of the same isomers was in accordance with the CD of **11**. This indicates that the phenyl group at C-13 does not influence the sign of the CD, in comparison with the methyl substituted derivative. This was also seen for the modeled conformation for which the spatial arrangement was almost identical.

Enantiomer assignment of **78** was also derived form the experimental and calculated CD spectra, respectively.

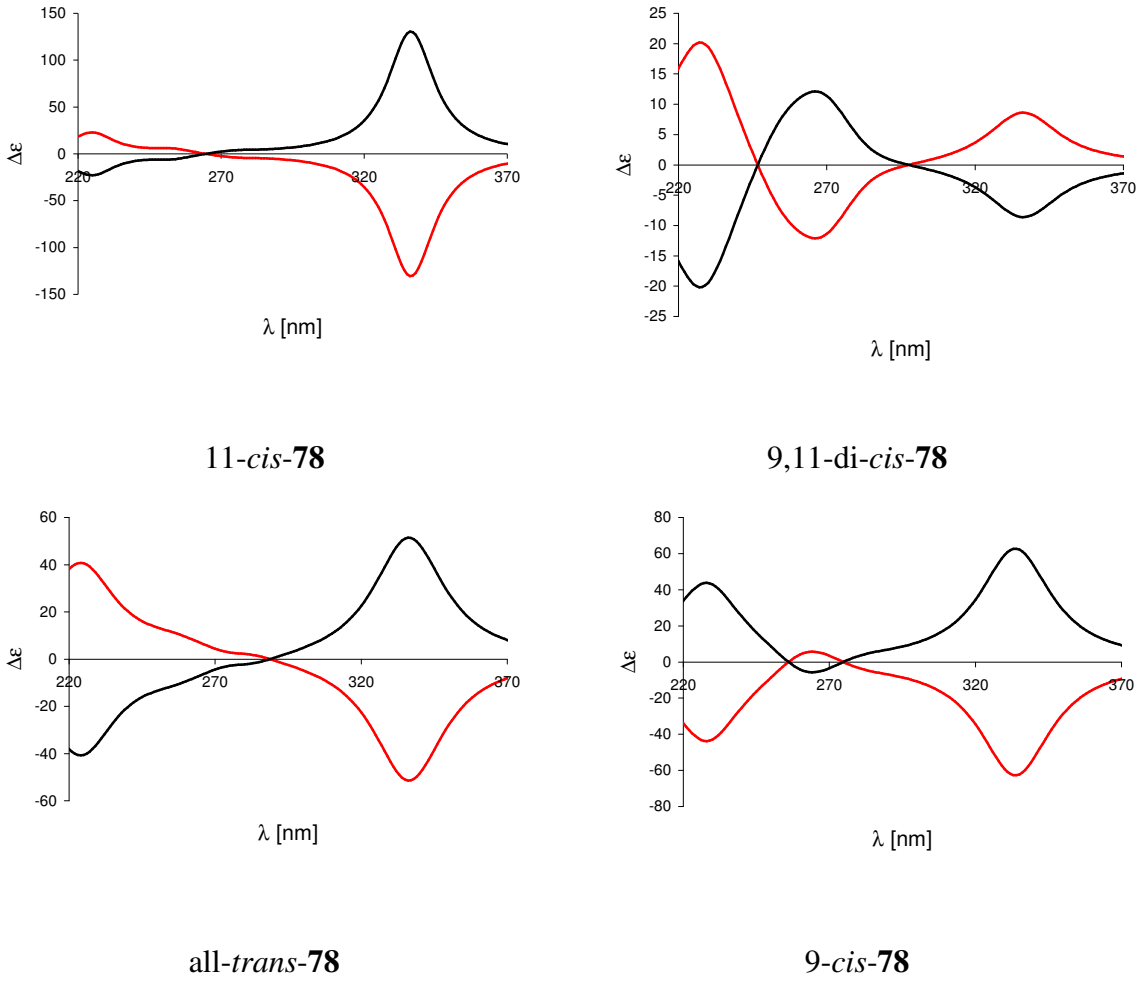

Figure 64. Calculated CD spectra of **78** (red curve: *R* enantiomer, black curve: *S* enantiomer).

The calculated spectra show for the *R* enantiomer of all-*trans*-, 11-*cis*- and 9-*cis*-**78** a negative first CE, while the 9,11-di-*cis*-isomer displays a positive first CE for the *R* enantiomer. This molecule shows a modified absorption spectrum, compared to all other dihydro retinoids, the intensity of the absorption maximum proved to be characteristic for each isomer. Three absorption maxima can be seen in all spectra. This can be

explained by the additional absorption of the phenyl group around 260 nm, which is not hidden anymore under another maximum as seen in the CD spectra of **79**. In two of the isomers, 11-*cis*- and all-*trans*-**79**, the middle absorption maximum is present as a shoulder of the second CE, while in the other two isomers three alternating maxima can be detected. The 11-*cis*-isomer shows a very strong first CE, while the second CE is less intensive. The all-*trans*- and 9-*cis*-isomers absorb almost with the same intensity, a small increase can be observed for their first CE. For the 9,11-di-*cis*-isomer three well separated maxima were noted, the absorbed light intensity increasing from the first to the last CE.

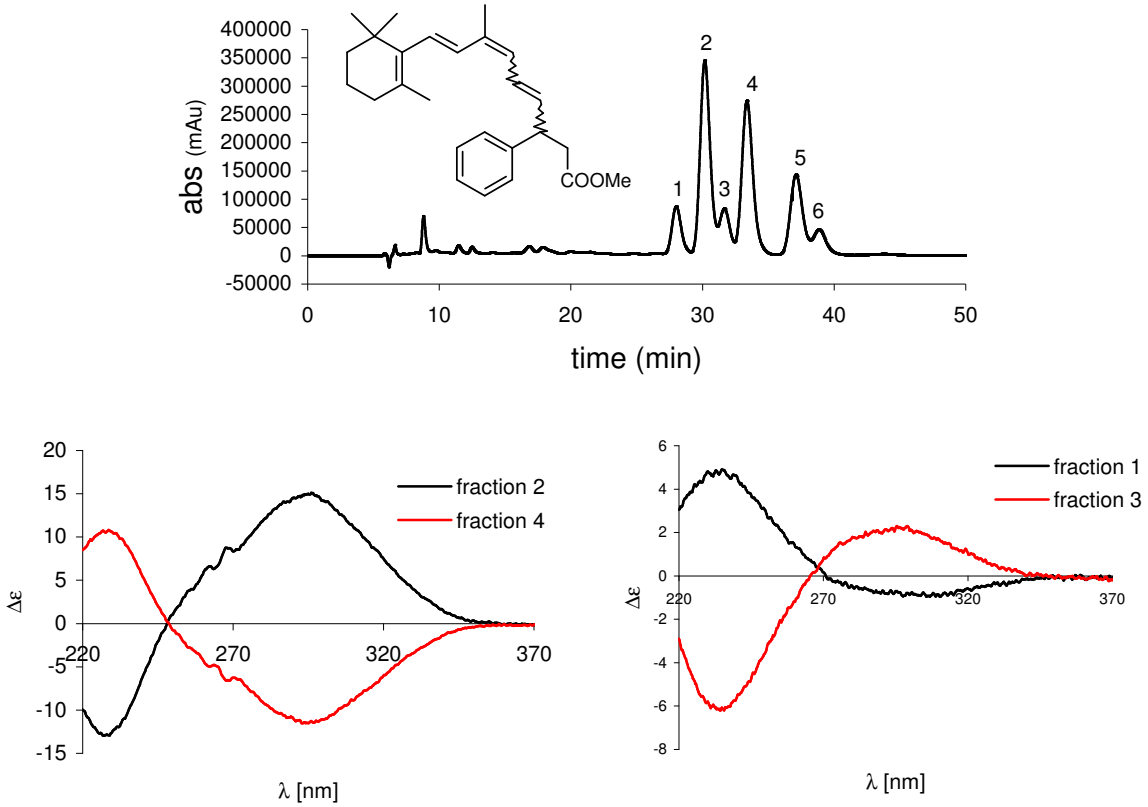

Figure 65. Experimental CD spectra of **78**.

Taking into account the differences discussed above for each isomer, and keeping in mind the isomer ratio determined by NMR spectroscopy, the absolute configuration for the separated diastereomers of **78** was assigned as follows. The first fraction (HPLC chromatogram in Figure 65) was assigned to the *S*-9,11-di-*cis*-isomer and fraction 3, with a positive first CE, to the *R*-9,11-di-*cis*-isomer. Fraction 2 is postulated to be the *S*-all-*trans*-diastereomer, while fraction 4, with a negative first CE, was assigned to the *R* enantiomer of the same isomer, in agreement with the calculated spectra. Comparing the calculated and measured CD spectra of all diastereomers, it is evident that in solution

the configuration of the molecule differs slightly from the calculated spatial arrangement.

All enantiomers of **78** cannot be unambiguously assigned, because the diastereomers were not completely resolved on the chiral HPLC column and joint elution of several diastereomers is possible. This means that the measured CD spectra are produced by more than one diastereomer, the one in higher concentration determining the sign of the observed CD.

7 Receptor-Ligand Interactions of Vitamin A Metabolites

7.1 Possible Metabolization Pathway of ROH to the New Vitamin A Metabolite

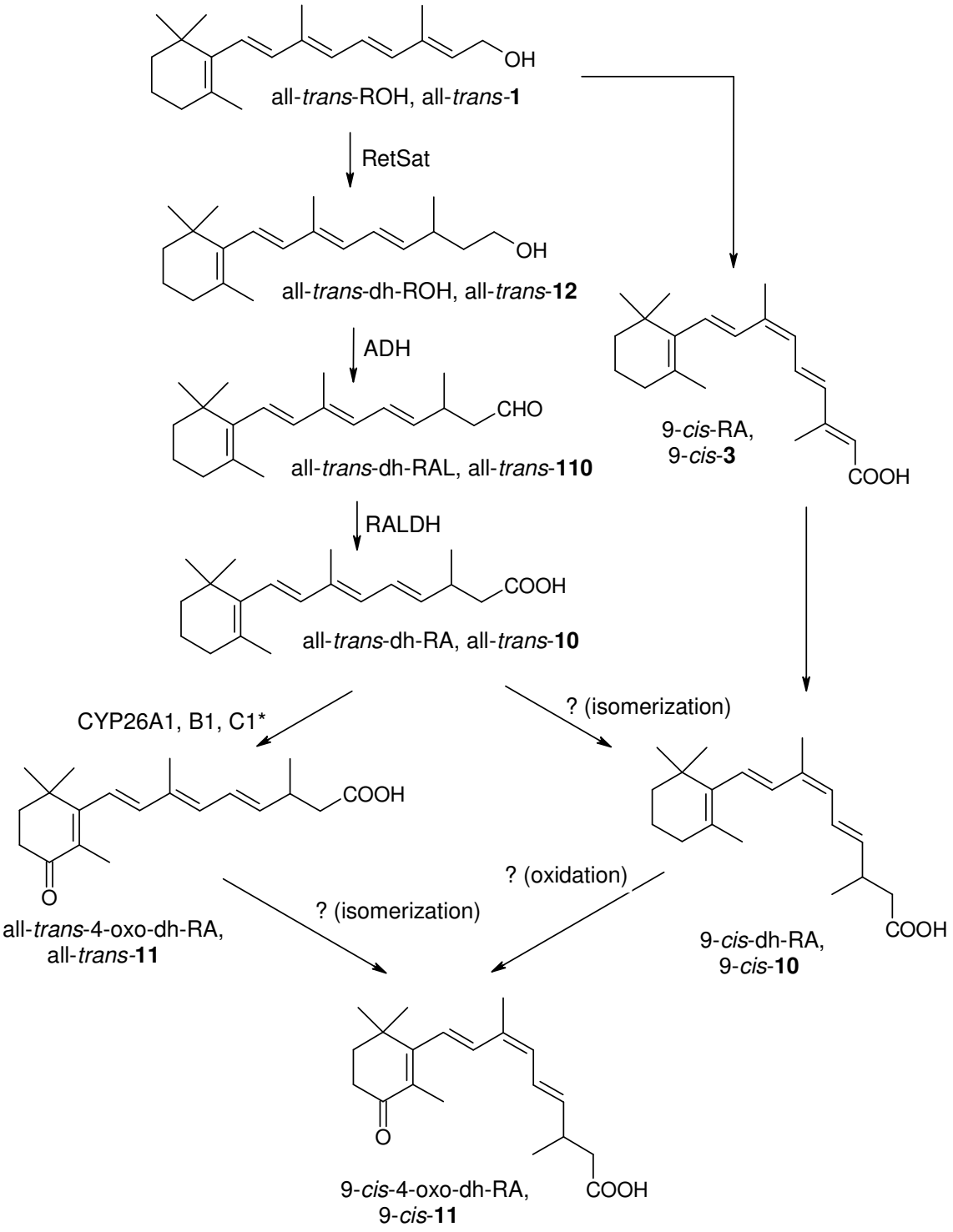

Scheme 26. Possible metabolization pathways of retinol (ROH, **1**) to 9-*cis*-4-oxo-dh-RA (9-*cis*-**11**).

A short overview of retinol metabolism was already mentioned in the introduction of this thesis. The possible pathway to the newly discovered retinoic acid metabolite *S*-9-*cis*-**11** can be derived from the metabolism known so far. When this project began no enzyme was known to reduce the chain double bonds. In the meantime Palczewski[19] described the Retinol Saturase enzyme (RetSat), which performs reduction of the C-13/C-14 double bond in all-*trans*-ROH (**1**), but not in all-*trans*-RA (**3**). It is possible that this enzyme is participating in the metabolization pathway of the new RA metabolite (9-*cis*-**11**) characterized here. Still, doubts remain because of the results published by Shirley,[16] showing that *in vivo* 9-*cis*-RA (9-*cis*-**3**) is metabolized into 9-*cis*-13,14-dh-RA (9-*cis*-**11**). Furthermore, oxidation of **1** to **3** could occur by mechanisms already known,[64] but oxidation at C-4 is not completely understood. Cytochrome P450 is active in metabolizing all-*trans*-**3**, whereas for 9-*cis*-**3** there is no further information about possible metabolization ways.[64] It could be that the oxidation at C-4 occurs first and is followed by isomerization to the final 9-*cis*-4-oxo-**11** metabolite. About the isomerization from the all-*trans*- to the 9-*cis*-isomers, presently only limited information is available. A nonenzymatic process was described for the formation of 9-*cis*-**3** from all-*trans*-**3** by low molecular weight compounds (L-cysteine methyl ester, glutathione) or proteins (apoferritin) containing free sulfhydryl groups.[64] On the other hand, 9-*cis*-**1** was shown to be present in rat kidneys and can undergo oxidation to 9-*cis*-**3** by an enzymatic process.[64] It is possible that 9-*cis*-**3** is formed from all-*trans*-**3** but also that another pathway, independent of all-*trans*-**3** formation, exists at least within some cells and tissues. Further biological studies are necessary for a complete understanding of these pathways and on the new vitamin A metabolite characterized here.

7.2 Ligand-Protein Interactions in Retinoid Receptors

Many important effects of retinoids are mediated by two families of nuclear receptors: retinoic acid receptor (RAR) and retinoid X receptor (RXR), each consisting of three types (α, β and γ). Several natural retinoids are known to act as retinoid receptor ligands. They can be classified as ligands that activate only RARs: all-*trans*-RA (all-*trans*-**3**), all-*trans*-3,4-didehydro-RA, all-*trans*-4-oxo-RA (all-*trans*-**42**), all-*trans*-4-oxo-RAL, all-*trans*-4-oxo-ROH. And ligands that activate both RARs and RXRs such as 9-*cis*-**3** and 9-*cis*-**42**.[64] From their binding affinities it is obvious that these two classes of receptors are quite distinct from each other. While all nuclear receptors

contain the typical domains including a DNA and a ligand-binding domain (LBD), they appear to have low amino acid homologies in their LBD.[64]

The binding mechanism of retinoids to the LBD of the nuclear receptors RAR and RXR has been studied by Moras et al using molecular dynamic simulations.[65]

Several LBD crystal structures of different nuclear receptors, including also RAR and RXR, have been solved.[65a] All structures confirm the existence of a helical sandwich fold for LBDs and that the ligands induce major structural changes upon binding. The existence of a conformational change between an open *apo* form and a compact closed *holo* form has been shown by comparison of the X-ray structures of *apo*-RXRα and *holo*-RXRα bound to 9-*cis*-**3**.[65a] Since the effects of active retinoids are transduced by their nuclear receptors for which they bind, computational calculations can offer information about the nature of ligand-receptor binding of new retinoids.

A corresponding study was performed here to illustrate and to analyze the difference in binding affinity, previous to cell culture binding assays of retinoid nuclear receptors with the retinoids synthesized in this work.

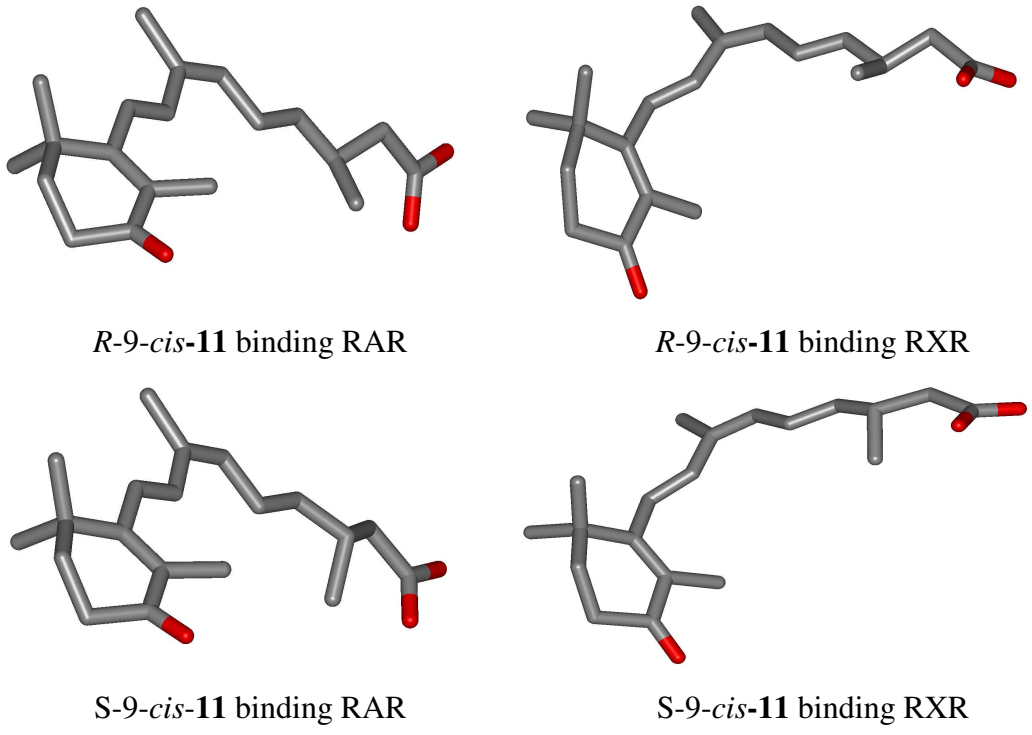

R-9-*cis*-**11** binding RAR | *R*-9-*cis*-**11** binding RXR

S-9-*cis*-**11** binding RAR | S-9-*cis*-**11** binding RXR

Figure 66. Calculated geometry of 9-*cis*-**11** docked in RAR and RXR.

In cooperation with Dr. Jean-Marie Wurtz from the Institute of Genetic and Molecular and Cellular Biology, Strassbourg, France, exploratory studies on ligand-protein interactions were undertaken, using the crystal structure of the nuclear receptors. The optimized structure of 9-*cis*-**11** (the optimization being performed with the

Quanta/Charmm Molecular Simulation Inc software) was docked into the receptor pocket, by modifying the skeleton in order to minimize interactions and the conformer energy. The geometry of the enantiomers of 9-*cis*-**11** after docking in the RAR and RXR receptors is shown in Figure 66. It seems that the 4-oxo-moiety hampers the binding more in RAR than in RXR receptors. While a more compact geometry is adopted in the RAR receptor, the LBD of RXR receptor seems to allow a more open geometry. From the molecular modeling calculations, no significant differences between the enantiomers can be derived, both fitting in the LBD of the retinoid receptors. Selectivity for one of the enantiomers has to be proven by receptor bindings assays in cell cultures.

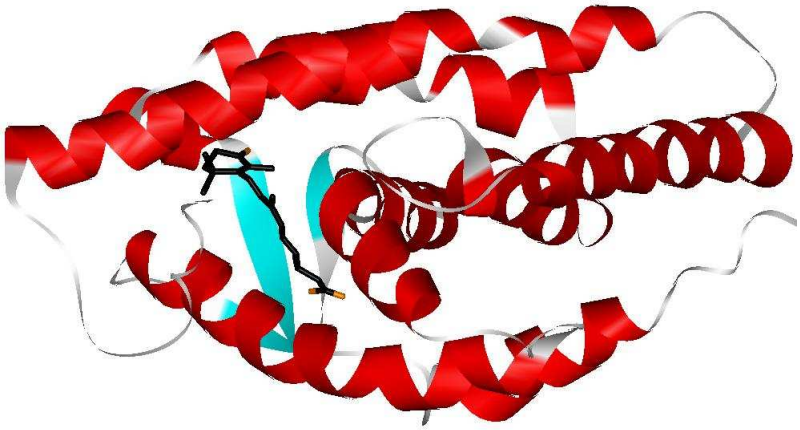

Figure 67. The new RA metabolite 9-*cis*-**11** as a ligand in RXR.

A schematic drawing of the interactions between 9-*cis*-**11** and the amino acids in RXR is shown in Figure 68.

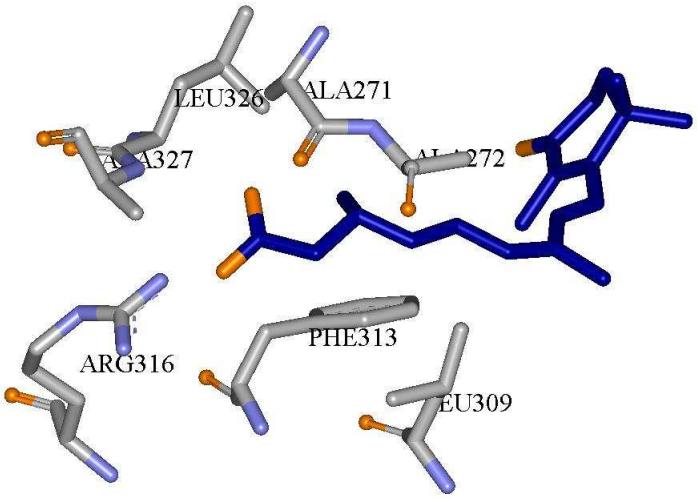

A

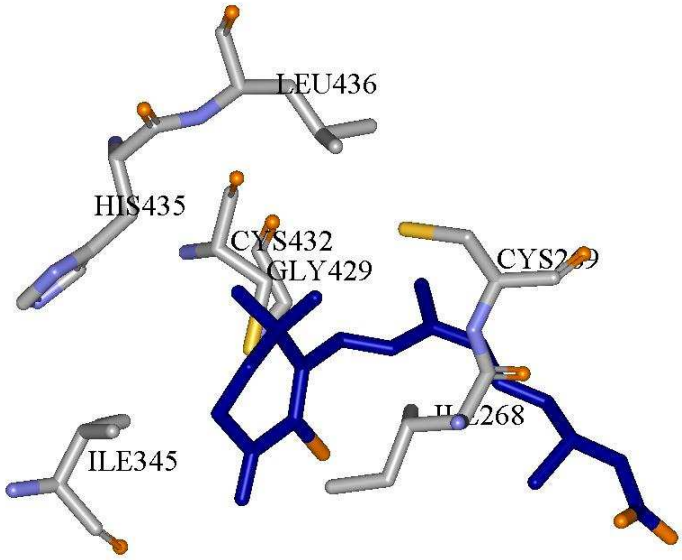

B

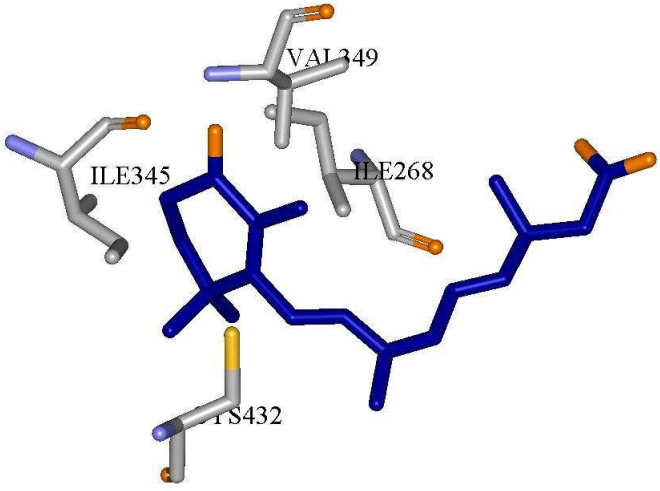

C

Figure 68. Ligand-receptor interactions in RXR. (A, B, C: different views of 9-*cis*-**11** in the retinoid ligand pocket)

The carboxylate group is sandwiched between the phenyl ring of Phe313 on one side, and the Ala271, Ala272 on the other. Phe313 shows interactions with the isoprenic C-11/C-13, with the methyl group C-20 and the carboxyl function. Amino acids Ala271 and Ala272 are near the retinoid chain C-12/C-15. Possible interactions can be seen between the methyl group C-20 and the carboxylic group from Ala271. The carboxyl group of the RA metabolite forms two hydrogen bonds, one with the terminal amino group of Arg316 and the second with one of the amino groups of the Ala327- Leu 326 chain. On the other side of the LBD pocket, more free space can be seen around the β-ionone ring. Again, amino acid interactions are observed from two sides. Ile268 and Cys269 are close to the cyclohexenone ring, the terminal thio group of Cys269 from one side and Cys432 from the other, point to the C-16 and C-17 methyl groups. In the vicinity of the β-ionone ring are the amino acids Ile345, Gly429,Cys432, His 435 and Leu 436, Val349. The thio group of Cys432 is pointing towards C-6 of the β-ionone ring and the imidazol ring of His435 is covering the β-ionone ring. The carbonyl group of Ile345 and the amino function of Val349 are pointing towards the 4-oxo function from the front side while the ethyl rest from Ile268 can interact with the keto function from the back side.

The accessible volume of the cavity in the RXRa LBD is 489 $Å^3$, and it has been shown that the 9-*cis*-RA occupies only 59 % of this cavity with its 291 $Å^3$ volume.[65b] The free space in the ligand pocket could accommodate larger side groups of synthetic analogues of 9-*cis*-RA, offering interesting possibilities for the design of new specific ligands. This is one of the reasons why RA derivatives incorporating larger substituents at C-13 were synthesized in this study. To get a first impression whether these modified RAs could fit into the receptor pocket their volumes were calculated and compared with the available space in the ligand pocket.

Table 13 shows the calculated volume for all RA isomers synthesized in this investigation. Calculations were performed using the GAUSSIAN03 program and the B3LYP/6-31G(d) method,[56] as described in Chapter 6, after geometry optimization of the isomers.

Table 13. Calculated molecular volumes of selected retinoids.

4-oxo-RA (**42**)	Å^3
all-*trans*-	459
9-*cis*-	422
4-oxo-dh-RA (**11**)	Å^3
all-*trans*-	442
11-*cis*-	409
9-*cis*-	489
9,11-di-*cis*-	466
4-oxo-dh-13-ph-RA (**83**)	Å^3
all-*trans*-	423
11-*cis*-	519
9-*cis*-	515
9,11-di-*cis*-	592
4-oxo-dh-13-*i*Pr-RA (**81**)	Å^3
all-*trans*-	492
11-*cis*-	467
9-*cis*-	410
9,11-di-*cis*-	480

RA (**3**)	Å^3
all-*trans*-	385
9-*cis*-	436
dh-RA (**10**)	Å^3
all-*trans*-	426
11-*cis*-	353
9-*cis*-	451
9,11-di-*cis*-	463
dh-13-ph-RA (**82**)	Å^3
all-*trans*-	509
11-*cis*-	420
9-*cis*-	456
9,11-di-*cis*-	514
dh-13-*i*Pr-RA (**80**)	Å^3
all-*trans*-	470
11-*cis*-	466
9-*cis*-	474
9,11-di-*cis*-	412

The calculated volume is the result of surface density approximations and for this reason is different from the volume measured by X-ray diffraction, as can be seen for 9-*cis*-RA. To have a reference for all derivatives, the volume for 9-*cis*-RA, which is known to fit into the RAR and RXR, was also calculated and compared with all others. From these calculations it is not possible to make a general affirmation on the volume order in the isomer series. Depending on the substituents at C-13 and on the 4-oxo function the isomer volume changed, so that no correlation can be made between the isomers, the substituent and the 4-oxo derivatives. For **11** and **80**, the 9-*cis*-isomer has the biggest volume, for **10**, **83** and **82** the 9,11-di-*cis*-isomer is the largest isomer, while for **81** the all-*trans*-isomer occupies most space. All other isomers have volumes between 592 Å^3 (9,11-di-*cis*-**83**) and 353 Å^3 (11-*cis*-**10**).

The known retinoids all-*trans*-RA and 9-*cis*-RA were also calculated. It is an important aspect of these calculations that the volume is not correlated with receptor-ligand binding. Although the 9-*cis*-isomer proved to have a bigger calculated volume than all-*trans*-RA, the former is not binding the RXR. It has been noticed that 9-*cis*-RA adopts different conformations in RAR and RXR; in the last receptor the isomer exhibits a pronounced bent compared with the open conformation in RAR.[65c] The receptor pocket of RXR selects 9-*cis*-RA but excludes all-*trans*-RA due to its flexibility limit.[65c] The calculated volumes in the gas phase do not apply in the receptor pocket anymore. Before docking in the LBD the retinoid skeleton can adopt different geometries and

adjust to the amino acid pocket. Which interaction favors or disfavors the binding ability and the adopted geometry requires a deeper conformational analysis subsequent to the X-ray analysis of the ligands in the receptor's cavity. The most reliable information on the binding abilities of the new retinoids is still experimental data. Cell culture experiments with the new RA derivatives and the retinoid receptors are hence under investigation.

8 Molecular Modeling - Proton Affinity Calculations

In this research project several phosphonates and phosphonium salts were synthesized for the Horner-Wadsworth-Emmons and Wittig reaction, respectively. During these experiments the phosphonium salts proved to be more suitable for deprotonation than the phosphonates, comparing the reactive positions present in the molecule. To gain more information about the deprotonation differences between phosphonates and phosphonium salts, DFT calculations of these molecules were performed. All computations were carried out with the GAUSSIAN 03 program, all structures were studied using the 6-31G(d) basis set and the B3LYP level of theory.[56] Geometry optimizations were performed without restrictions.

For each optimized structure, the proton affinity was then calculated on the basis of the energy difference between the protonated and unprotonated species, means, the thermodynamic acidity was measured. Under equilibrium conditions, the thermodynamically most stable product will be the predominant or even exclusive product.[40b] Calculations on the kinetic acidity (which reaction path has the lower activation barrier and which product is formed faster) were not undertaken here.

$$R \rightleftharpoons H^+ + R^-$$

$$E[R] = E[H^+] + E[R^-] \text{ or} \qquad (1)$$

$$E[H^+] = E[R] - E[R^-]$$

The gas-phase proton affinity for each molecule is shown in Table 14. The energy needed for a proton to be extracted from the molecule corresponds to the affinity of this proton to the molecule and is calculated as the energy difference between the neutral molecule and the corresponding anion. For example, deprotonation of phosphonium salt **66** at C-1 requires 291.2 kcal/mol while deprotonation at C-3 would need 317.5 kcal/mol to proceed. This means that, under basic conditions, deprotonation at C-1 is favored by 26.2 kcal/mol compared to the proton at C-3. In phosphonate **105**, this energy difference between C-4 and C-2 is only 4.8 kcal/mol, while in the phosphonate **27**, where three positions can be deprotonated, the energy deference between C-6 and C-2 is 11.1 kcal/mol and 9.8 kcal/mol between C-6 and C-3, respectively.

Table 14. Proton affinity for acidic CH-positions of selected derivatives.

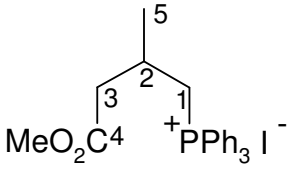

66

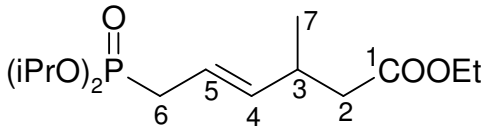

27

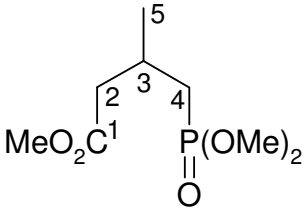

105

Energy [kcal/mol]	**66**	**27**	**105**
$E_1[H^+]$	-291.24	-374.82	-393.86
$E_2[H^+]$	-317.48	-385.96	-389.03
$E_3[H^+]$		-384.66	

The energy needed for deprotonation at a specific site was calculated using formula (1) as follows:

for **66**

E_1 $[H^+]$ = E [**66** (CH_2)]- E [**66** (CH^-)] at C-1

E_2 $[H^+]$ = E [**66** (CH_2)]- E [**66** (CH^-)] at C-3

for **27**

E_1 $[H^+]$ = E [**27** (CH_2)]- E [**27** (CH^-)] at C-6

E_2 $[H^+]$ = E [**27** (CH_2)]- E [**27** (CH^-)] at C-2

E_3 $[H^+]$ = E [**27** (CH_2)]- E [**27** (CH^-)] at C-3

for **105**

E_1 $[H^+]$ = E [**105**(CH_2)]- E [**105**(CH^-)] at C-2

E_2 $[H^+]$ = E [**105**(CH_2)]- E [**105**(CH^-)] at C-4

The energy needed to remove a proton from a phosphonate is higher in comparison with that for the phosphonium salt, which implies that a stronger base has to be used in the Wittig-Horner reaction, which makes also more difficult to distinguish which position will be deprotonate.

Table 15 Proton affinity calculations.

Energy [kcal/mol]	**66**	**27**	**105**
$E_1[H^+]$-$E_2[H^+]$	26.2	11.1	4.8
$E_1[H^+]$-$E_3[H^+]$		9.8	
$E_2[H^+]$-$E_3[H^+]$		1.3	

These calculations show that the difference between the proton affinities for the two acidic methylenic groups of phosphonium salt **66** is higher than that in the phosphonates

implying that a competing deprotonation reaction occurs more readily in **27** and **105**, than in **66**. Additionally in the phosphonate **27** the protons at C-2 and C-3 have almost identical affinity. The deprotonation energy difference is only 1.3 kcal/mol.

Thus, theoretical calculations of thermodynamic acidity prove to be very useful for the prediction of the relative acidity of methylenic groups in the vicinity of various functional groups, allowing a rational selection of the base to be employed and better design of the reagents used in Wittig, HWE reaction respectively.

9 The New Vitamin A Metabolite: Structure and Conformation Assignment

The target molecule to be synthesized and characterized in this thesis was a new vitamin A metabolite, for which the structure of 9-*cis*-4-oxo-13,14-dihydro-RA (**11**) had been proposed.[18] This molecule was first identified in mouse liver as a major endogenous vitamin A metabolite. Mice, fed with different amounts of retinyl palmitate, showed a dose dependent decrease in the all-*trans*-RA level in serum, kidney and brain, whereas the levels of 9-*cis*-4-oxo-13,14-dh-RA, ROH and retinyl esters were dose dependently elevated in serum, kidney and liver. This indicates that the new metabolite could play an important role in vitamin A metabolism and that under special conditions, like excess RA concentration, new metabolization pathways are possible.

To gain sufficient material for further investigations and structure assignment of **11** the synthesis summarized in Scheme 27 was developed in this thesis.

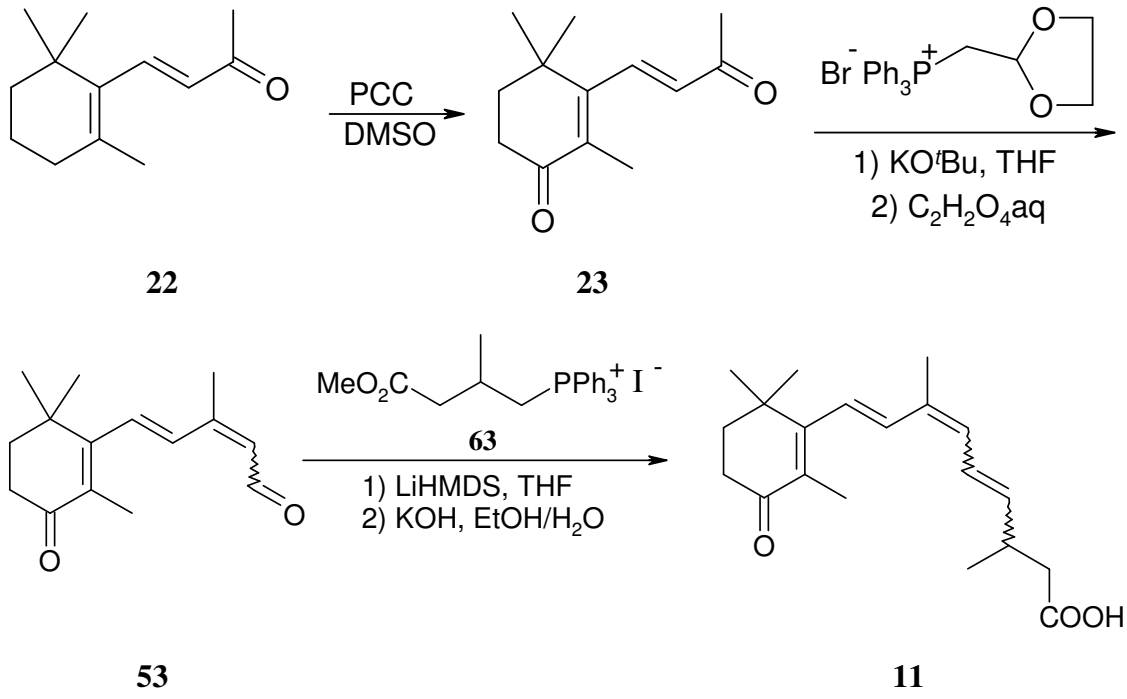

Scheme 27. Synthetic approach to the new vitamin A metabolite.

Oxidation of β-ionone (**22**) to 4-oxo-β-ionone (**23**) followed by Wittig reaction with **49** gave the two isomers of aldehyde **53.** This was used further in a second Wittig reaction with racemic phosphonium salt **63** to obtain *rac*-**11**. Enantioselective synthesis of *S*-**11** was possible with phosphonium salt *S*-**63** (reaction details are given in Chapter 3). The

diastereomers of **11** were completely resolved on a Chiracel OJ-H column and all fractions were analyzed by NMR, CD, UV and IR spectroscopy and MS spectrometry.

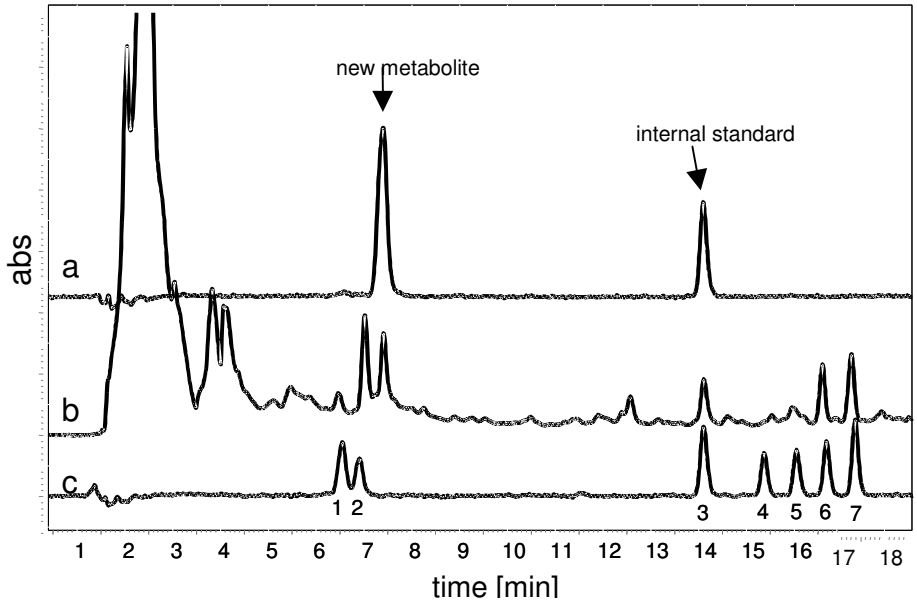

Figure 69. HPLC Spheroclone ODS 3µm, 150 x 2 mm, H_2O/MeOH, pH = 5.5 (curve a: synthetic 4-oxo-9-*cis*-13,14-dihydro-RA with internal standard (IS RO101670), curve b: polar fraction of liver extracts from NMRI mice, curve c: known retinoids; fraction 1: 4-oxo-13-*cis*-RA , 2: 4-oxo-*all-trans*-RA, 3: IS RO101670, 4: 3,4-dehydro-RA, 5: 13-*cis*-RA, 6: 9-*cis*-RA, 7: *all-trans*-RA).

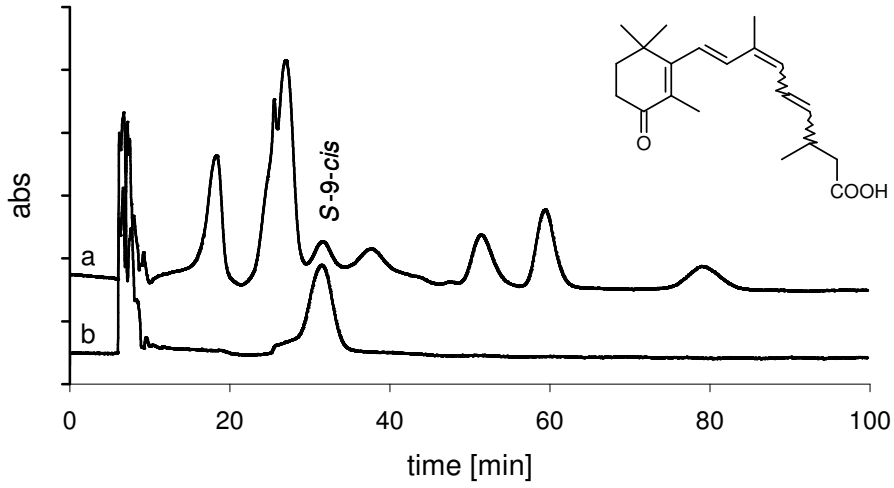

Figure 70. Chiral HPLC separation of **11** on Chiracel OJ 10 µm, 0.46 x 25 cm, hex/*i*PrOH/TFA 95:5: 0.1 (curve a: isolated vitamin A metabolite, curve b: product of racemic synthesis).

The retention time of authentic and synthetic 9-*cis*-**11** on different HPLC columns, reversed and normal phase conditions, was also identical. HPLC chromatograms of synthetic 9-*cis*-**11,** polar fraction of a liver extract containing the new retinoid metabolite and a mixture of known polar retinoids are shown in Figure 69. Chiral

separation of the racemic product **11** and the purified isolated metabolite is shown in Figure 70.

The isomers of **11** were assigned from the 2D-NMR spectra (for a detailed discussion see Chapter 5). ^{1}H NMR, MS and UV spectra of the isolated new RA metabolite were in accordance with the spectra of synthetic 9-*cis*-**11**. The olefinic region of the ^{1}H NMR spectrum of the isolated and synthetic 9-*cis*-**11** is shown in Figure 71.

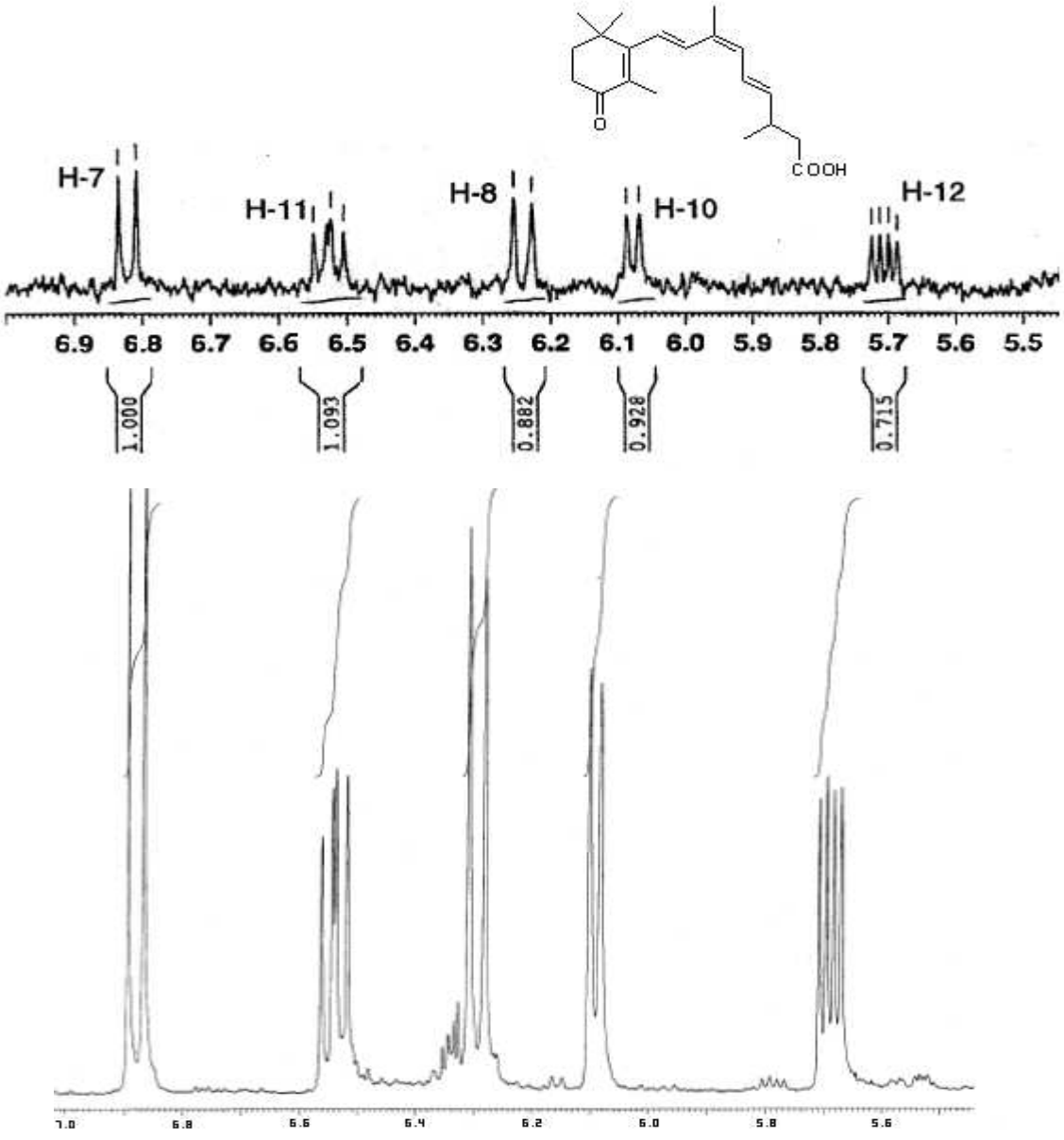

Figure 71. Olefinic region of the ^{1}H NMR spectra of authentic[18] and synthetic vitamin A derivative **11**.

CD measurements of the isolated new vitamin A metabolite did not give relevant information about its absolute configuration because of limited amount of sample available for this experiment. The absolute configuration assigned by comparison of calculated and experimental CD spectra of synthetic *S*-9-*cis*-**11** (Figure 72) was proven

by comparison of the retention time in HPLC separation of the synthetic *S*-**11** and isolated metabolite (Figure 70).

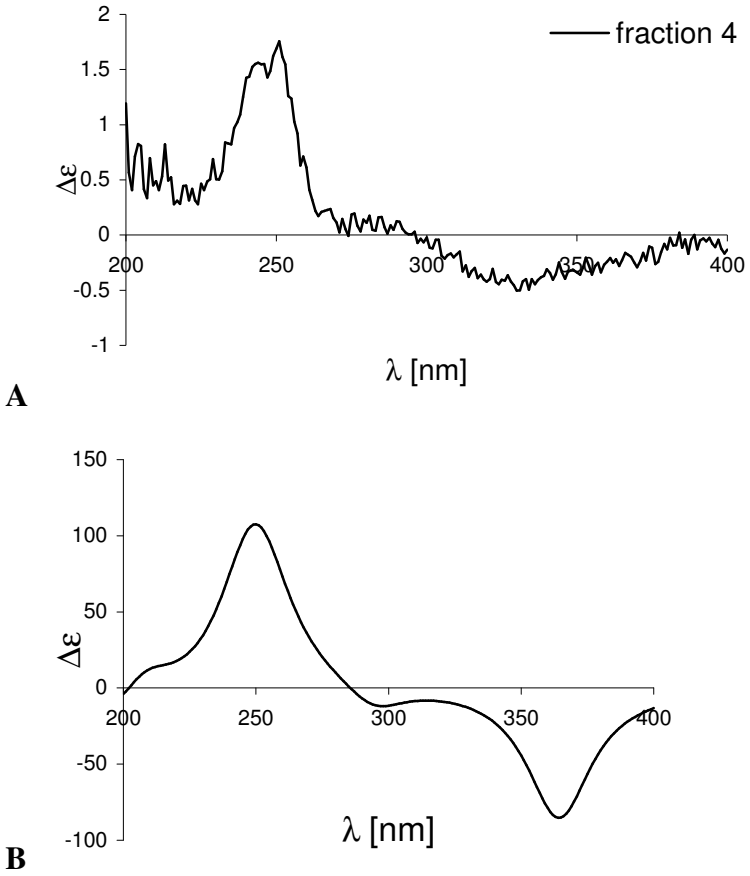

Figure 72. Experimental (**A**) and calculated (**B**) CD spectrum of *S*-9-*cis*-**11**.

The proposed structure 9-*cis*-13,14-dihydro-retinoic acid for the new vitamin A metabolite isolated by Nau and coworkers[18] was confirmed by synthetic and analytic methods. Enantioselective synthesis together with molecular modeling calculations of the CD spectra were used to determine the absolute configuration.

10 Summary and Conclusion

The aim of this work was the full characterization of a new isolated vitamin A metabolite **11** (**13**: R^1 = O, R^2, R^3 = CH_3, R^4 = COOH). This was achieved in a interdisciplinary project, where synthesis, chromatographic and spectroscopic analysis, molecular modeling and first biological investigations were performed.

For the proposed structure of the new vitamin A metabolite, several synthetic methods were investigated. All isomers of *rac*- and *S*-**11** were obtained for comparison with isolated retinoid metabolite. Wittig reaction beginning with **14** proved to give the best results. The isomer ratio attended by this synthesis was 1.1:1.1:1.9:1.0 for all-*trans*-/9-*cis*-/11-*cis*-/9,11-di-*cis*-**11** (HPLC of *S*-enantioselective synthesis).

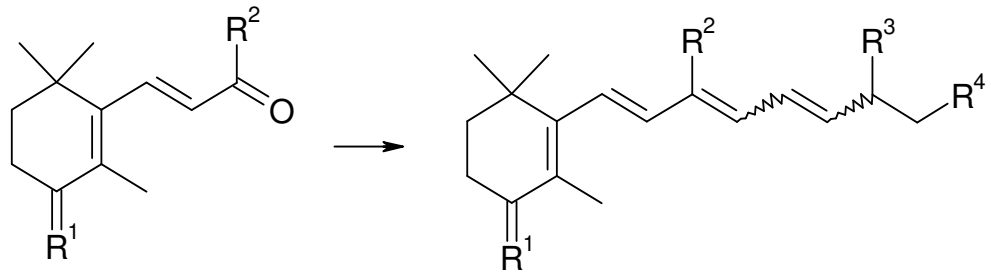

14 **13**

Scheme 28. Synthesis of new 13,14-dihydro retinoids.

This methodology was used further for the synthesis of other possible metabolic precursors of **11**, e.g. acid **10** (**13**: R^1 = H,H, R^2, R^3 = CH_3, R^4 = COOH). Both derivatives **11** and **10** were labeled with deuterium at C-9 (R^2). These retinoids were needed for biological investigations and follow up of their metabolization by LC/MS. Another possible metabolite 4-hydroxy-13,14-dh-RA (**98**, Scheme 28 **13**: R^1 = OH, H, R^2, R^3 = CH_3, R^4 = COOH) was prepared starting from 4-OAc protected ionone (**14**: R^1 = OAc, H, R^2 = CH_3). The synthesis stopped at the ester precursor **97** because of the instability of the corresponding allylic hydroxyl derivate **98**.

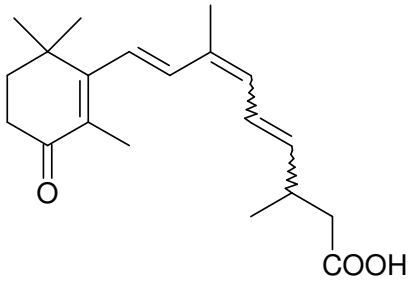

11

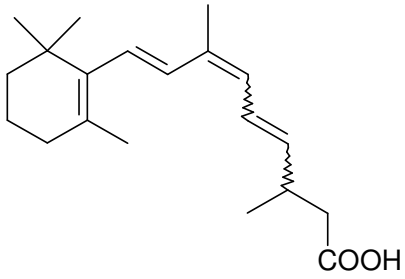

10

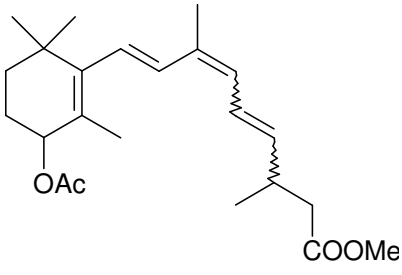

97

Besides the new phosphonium salt **66**, further phosphonium salts, e.g. **72** and **73** were synthesized here.

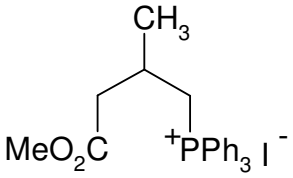

66

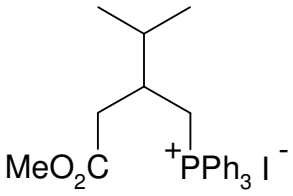

72

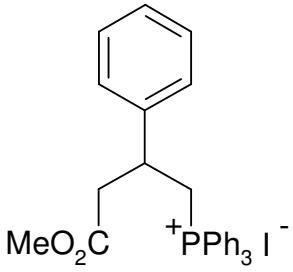

73

These were used in Wittig reaction with aldehydes **47** and **53**, respectively, for the synthesis of modified 13,14-dihydro retinoids like **76**, **77**, **78**, **79**.

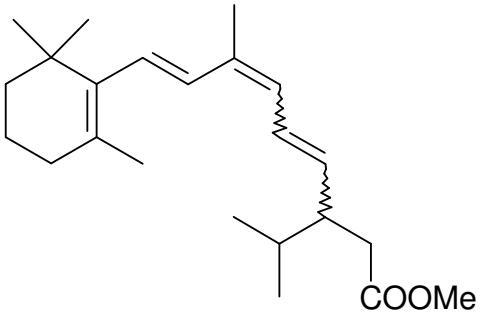

76

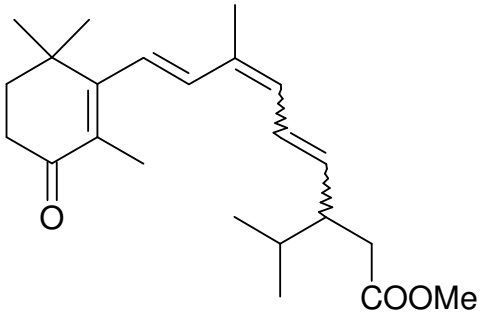

77

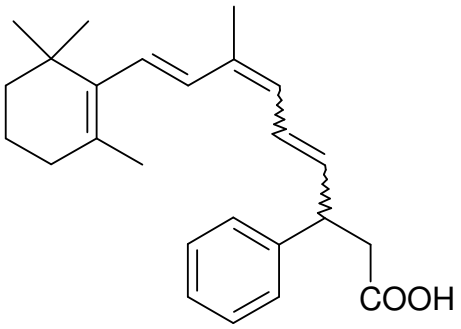

82

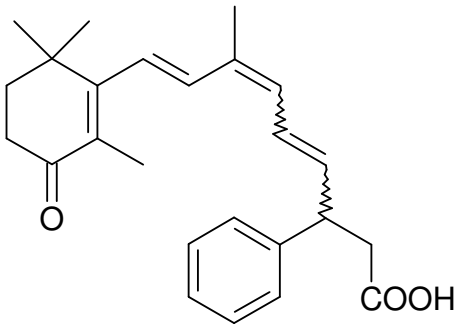

83

Biological properties of the newly obtained 13,14-dihydro retinoids will be analyzed and compared with those of the known retinoids in the group of Prof. Nau. First molecular modeling calculations were performed with all isomers of **13** to gain information about the possible adopted geometries in the retinoid receptor pocket, the occupied volume and the possible interactions with the amino acids of the retinoid receptor.

Because all retinoids synthesized here were obtained as isomeric mixtures, chromatographic separation (reversed and normal phase HPLC) was used for their separation. Acids **11**, **82** and **83** and their corresponding esters were resolved on chiral HPLC.

For characterization of the isomers or isomeric mixtures, NMR, IR, UV/Vis and CD spectroscopy and MS spectrometry were used. The isomers were assigned by 1D and 2D-NMR spectroscopy.

Assignment of the absolute configuration of each HPLC fraction of **11, 82** and **83** was accomplished by CD spectroscopy; the experimental CD spectra were compared with the calculated ones. Molecular modeling calculations of the CD spectra were helpful to predict the absolute configuration of **11,** which enabled the design of a target enantioselective synthesis of the *S*-enantiomer.

11 Experimental Section

11.1 Instrumentation and general experimental considerations

Thin Layer Chromatography: Macherey-Nagel & Co (Düren) "Polygram Sil G/UV_{254}" silica gel plates were used for analytical thin layer chromatography.

Column chromatography was performed on Merck (Darmstadt) silica gel 60 (70-230 mesh) or aluminum oxide activated with 8 % w/w water.

Melting points were determined on a Meltemp II apparatus from Laboratory Devices. The melting points are uncorrected.

NMR Spectroscopy: ^{1}H NMR and ^{13}C NMR were recorded using a Bruker AC-200 (^{1}H NMR 200.1 MHz, ^{13}C NMR 50.3 MHz), Bruker DRX-400 or Varian (^{1}H NMR 400.1 MHz, ^{13}C NMR 100.6 MHz) spectrometer. Chemical shifts are reported in ppm downfield from internal tetramethylsilane. Spin multiplicities are indicated by the following symbols (s = singlet, d = doublet, t = triplet, q = quartet, m = multiplet). For ^{13}C NMR spectroscopy, solvent signals $CDCl_3$ (δ = 77.0 ppm), MeOH-d_4 (δ = 49.3 ppm), or acetone-d_6 (δ = 29.3 ppm) were used as internal standards.

IR spectra were recorded on a Nicolet DX320 FT-IR spectrometer as KBr pellets or on a Bruker Tensor 27 using the diamond ATR technique.

UV/Vis spectra were obtained using a Hewlett-Packard 8452 A diode array, a Varian Cary 100 Bio or a Jasco V-570 spectrometer.

HPLC: Chiral HPLC was performed on Chiracel OD, OJ, AS, AD and Chiralpak IA, IB columns (analytical columns 0.46 x 25 cm, preparative on a Chiracel OJ 4.6 x 250 cm column) from Daicel Chemical Industries LTD, using a Jasco PU-1580 pump and Jasco CO-1560 Column Thermostat. Detection was performed using a Jasco MD-190 Multiwavelenght and a Jasco CD –1595YS detector.

HPLC was also performed on Lichrosorb RP-18 (7 µm) and Purospher RP-18 endcapped (5 µm) 0.46 x 25 cm columns and semi-preparative (2.3 x 25 cm) on Nucleosil 100-7 C18 (7 µm) column using a Hitachi L-6200 Intelligent Pump and Hitachi L-3000 Photo Diode Array Detector or Hitachi L-4200 UV/Vis Detector. All solvents were HPLC grade solvent, except for the preparative separation. Retinoic acid metabolites and the corresponding synthetic samples were analyzed by HPLC equipped with two LC-10AD Pumps and a SPD-$10AV^{VP}$ UV/Vis Detector from Shimadzu, Duisburg. The analytical column was a Spherisorb ODS2, 2.1 x 150 mm, 3 µm particle

size, protected with a security guard from Phenomenex, C18 ODS cartridge, 4 mm x 2 mm.

Mass spectra were recorded on a Finnigan MAT95 mass spectrometer using electron ionization (EI, 70 eV), GC/MS spectra were recorded on a Jeol GCMate spectrometer.

Elemental analyses were carried out at the Institut für Pharmazeutische Chemie and the Institut für Anorganische und Analytische Chemie, TU Braunschweig.

Circular dichroism spectra were measured on a JASCO J-720L spectrometer.

Whenever necessary, experiments with the different retinoids and their precursors were carried out under argon using yellow light. All other experiments were carried out under N_2 or air.

11.2 General experimental procedures

General procedure 1:

To a stirred suspension of phosphonium salt **52** (2 equiv.) in anhydrous THF was added KO*t*Bu (2 equiv.) under argon. An immediate color change from white to yellow-orange was observed. After 30 min at room temp., a solution of the ketone in anhydrous THF was added dropwise and stirring was continued for 24 h. Aqueous oxalic acid solution (7 equiv.) was added. After 1 h, the two phases were separated and the aqueous phase was extracted several times with ether. The organic phase was washed with $NaHCO_3$ solution and dried with Na_2SO_4. After solvent removal, the dark red, oily product was purified by column chromatography.

General procedure 2:

LiHMDS was prepared from HMDS (1 equiv.) and *n*BuLi (1 equiv.) in anhydrous THF at –78 °C, under argon. After 20 min stirring, phosphonium salt (1 equiv.) was added. After additional 20 min at –78 °C, the cooling bath was removed and the yellow slurry was stirred for further 10 min. To the formed clear orange solution the aldehyde (0.8 equiv.) in anhydrous THF was added dropwise. The reaction mixture became dark red. When no starting material was detected by TLC or GC analysis anymore, water was added and the aqueous phase extracted several times with diethyl ether. The organic phase was washed with brine solution, dried with Na_2SO_4 and the solvent removed. The residue was purified by column chromatography on aluminum oxide.

General procedure 3:

To a solution of retinoic acid ester (1 equiv.) in ethanol was added 2.5 M KOH (10 equiv.) solution in ethanol/water. The mixture was heated to 70 °C for 3 h. After cooling to room temp., the red solution was extracted twice with diethyl ether. The aqueous phase was acidified carefully to pH 4-5 with diluted acetic acid or 2 M HCl and extracted with diethyl ether. This organic phase was washed with water and brine solution, dried with Na_2SO_4, and the solvent evaporated. The retinoic acid derivatives were obtained as yellow oils. Further separation of the isomers was performed by HPLC.

General procedure 4:

The 3-substituted glutaric acid (1 equiv.) in acetic acid anhydride (4 equiv.) was heated to reflux for 12 h. After cooling to room temp., the reaction mixture was brought to a basic pH by adding 2 M aqueous NaOH solution. Extraction of the aqueous phase with diethyl ether, and drying the organic phase with Na_2SO_4, followed by solvent evaporation gave the 3-substituted glutaric acid anhydride.

General procedure 5:

A solution of 3-substituted glutaric acid anhydride in methanol was heated to reflux for 3 h. The solvent was evaporated to yield the half acid ester. In most cases, this material was directly used without further purification. In cases where NMR analysis showed impurities, an additional work-up step followed. To the product was added 1 M NaOH solution and diethyl ether. Extraction and separation of the aqueous phase, followed by acidification with 2 M HCl to pH 2 and extraction with ether, drying of the organic phase with Na_2SO_4 and evaporation of the solvent gave pure half acid ester.

General procedure 6:

A mixture of the mono glutarate (1 equiv.) and dry lead tetra-acetate (1.12 equiv.) in dry CCl_4 was heated to reflux under nitrogen. The mixture was irradiated with two 150 W lamps for 10 min and irradiation was continued while iodine (1.45 equiv.) was added in portions during 45 min. The mixture was filtered and the filtrate was washed with aqueous $Na_2S_2O_8$ solution, aqueous Na_2CO_3 solution and water. The organic phase was dried with Na_2SO_4 and the solvent evaporated. The oily iodo-ester was used

immediately without further purification. Within time, the colorless product decomposes and becomes dark, for this reason, the product should be directly used in the next reaction.

General procedure 7:

To a solution of iodo-ester in benzene was added a solution of triphenylphosphine in benzene. After stirring the yellow solution overnight at room temp., the mixture was heated slowly to 70-80 °C for 2 d. The solvent was evaporated and diethyl ether was added to precipitate the phosphonium salt. Recrystallization from acetone/diethyl ether gave the pure white or light yellow phosphonium salt.

11.3 Experimental procedures

(*R*)-3-methyl monomethyl glutarate (**64**):

To dimethyl-3-methyl glutarate (21.97 g, 125.44 mmol) suspended in an aqueous solution of phosphate buffer (pH 8, 147 mL), was added pig liver esterase (PLE, 1342 units, 8.6 mg, 152 units/mg) under vigorous stirring. The pH was kept constant by adding 1 N NaOH (5.02 g, 0.125 mmol in 125 mL water). After consumption of 1 equivalent of base overnight, the pH was adjusted to 9 and the aqueous phase was extracted with ether. The water phase was acidified to pH 2 and extracted again with ether. This ether phase was dried and the solvent evaporated to give the half acid-ester **64** (18.58 g, 116.85 mmol, 92 %, lit.[70] yield: 86 %) as a colorless oil.

***rac*-3-methyl monomethyl glutarate** (**64**):

General procedure 4 with glutaric acid (6.5 g, 44.5 mmol) in acetic anhydride (18.2 g, 178.1 mmol, 16.8 mL) to yield 3-methyl glutaric anhydride (3.58 g, 28 mmol, 63 %). This was further reacted with methanol (10 mL) as described in general procedure 5 to give the half acid-ester **64** (3.9 g, 24.4 mmol, 87 %).

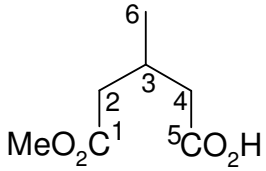

64

The spectroscopic data agree with those given in the literature.[38,69,68]

4-Iodo-3-methyl methyl butarate (**65**):

General procedure 6 with **64** (13.96 g, 87.5 mmol), I_2 (32 g, 126 mmol), $Pb(OAc)_4$ (43.4 g, 98 mmol) and CCl_4 (500 mL) gave **65** (12.81 g, 53.2 mmol, 61 %, lit.[70] yield: 92 %). The enantioselective synthesis of *S*-**65** ($[\alpha]_D$ = -0.53 ° in $CHCl_3$, c = 1.706 mg/mL) was performed using *R*-**64** (bought from Fluka or prepared as described above) .

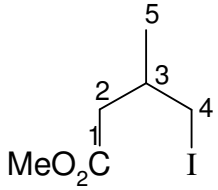

65

^{1}H NMR ($CDCl_3$): δ = 3.69 (s, 3H, COOC**H$_3$**), 3.31-3.23 (m, 2H, 4-H), 2.45 (dd, $^2J_{2,2}$ = 15.8, $^3J_{2,3}$ = 6.6 Hz, 1H, 2-H), 2.25 (dd, $^2J_{2,2}$ = 15.8 Hz, $^3J_{2,3}$ = 7.2 Hz, 1 H, 2-H), 2.05-1.98 (m, 1H, 3-H), 1.05 (d, $^3J_{5,3}$ = 6.6 Hz, 3H, 5-H).

^{13}C NMR ($CDCl_3$): δ = 172.4 (s, C-1), 51.6 (q, COO**C**H$_3$), 40.8 (d, C-3), 31.7 (t, C-2), 20.6 (q, C-5), 15.8 (t, C-4).

MS [EI, 70 eV]: *m/z* (%) = 242 (5) [M^+], 210 (15) [M^+-CH_3O], 169 (10) [M^+-CH_2COOCH_3], 115 (100) [M^+-I], 83 (15), 73 (70), 59 (30), 55 (45).

IR (ATR): $\tilde{\nu}$ = 2956-2844 cm^{-1} (w), 1732 (s, C=O), 1467 (m), 1435 (m), 1356 (m), 1288 (m), 1254 (m), 1196 (s, $COOCH_3$), 1136 (s, $COOCH_3$), 1003 (m).

UV ($CHCl_3$): λ_{max} (lg ε) = 252 nm (2.74).

(3-Methoxycarbonyl-2-methyl-propyl)-triphenylphosphonium iodide (**66**):

General procedure 7 with **65** (11.81 g, 48.76 mmol), triphenylphosphine (12.8 g, 49 mmol) in benzene (80 mL) gave **66** (18.1 g, 36 mmol, 74 %) as a colorless solid. (m.p. 134 °C). When the chiral precursor *S*-**65** was used, *S*-**66** was enantioselectively obtained $[\alpha]_D$ = +0.98 ° in $CHCl_3$, c = 1.43 mg/mL.

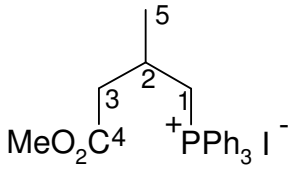

66

^{1}H NMR ($CDCl_3$): δ = 7.95-7.65 (m, Ar-H), 4.09 (ddd, $^{2}J_{1,1}$ = 15.8, $^{2}J_{1,P}$ = 12.5, $^{3}J_{1,2}$ = 8.5 Hz, 1H, 1-H), 3.85 (ddd, $^{2}J_{1,1}$ = 15.8, $^{2}J_{1,P}$ = 14.3, $^{3}J_{1,2}$ = 4.2 Hz, 1H, 1-H), 3.61 (s, 3H, COOC**H$_3$**), 2.78 (dd, $^{2}J_{3,3}$ = 17.0, $^{3}J_{3,2}$ = 6.7 Hz, 1H, 3-H), 2.56 (ddd, $^{2}J_{3,3}$ = 17.0, $^{3}J_{3,2}$ = 6.4, $^{4}J_{3,P}$ = 2.8 Hz, 1H, 3-H), 2.50-2.40 (m, 1H, 2-H), 1.03 (d, $^{3}J_{5,2}$ = 6.7 Hz, 3H, 5-H).

^{13}C NMR ($CDCl_3$): δ = 172.6 (s, C-4), 135.0, 133.7, 133.3, 130.5, 130.4 (d, Ar), 118.5 (s, Ar), 51.6 (q, COO**C**H$_3$), 41.3 (t, $J_{C,P}$ = 12.9 Hz, C-3), 28.2 (t, $J_{C,P}$ = 50 Hz, C-1), 26.0 (d, $J_{C,P}$ = 3.4 Hz, C-2), 21.0 (q, $J_{C,P}$ = 4.8 Hz, C-5).

MS [ESI]: *m/z* (%) = 377 (100) [M^+-I], 277 (40).

UV ($CHCl_3$): λ_{max} (lg ε) = 276 nm (3.69), 294 (3.50), 364 (3.19).

IR (ATR): $\tilde{\nu}$ = 3078-2792 cm^{-1} (w), 1721 (s, C=O), 1585 (w), 1483 (w), 1434 (s, P-phenyl), 1363 (m), 1311 (m), 1257 (m), 1216 (s), 1154 (s), 1107 (s), 1054 (m), 997 (s), 882 (w), 814 (m), 786 (s, C_6H_5), 786 (s, C_6H_5), 714 (s, C_6H_5), 687 (s, C_6H_5).

Elemental analysis: $C_{24}H_{26}O_2PI$ (504.35) calcd. C 57.19, H 5.20; found C 57.20, H 5.15.

***rac*-3-Phenyl monomethyl glutarate** (**111**):

General procedure 4 with 3-phenyl glutaric acid (10 g, 48 mmol), acetic anhydride (19.6 g, 192 mmol, 18 mL) gave 3-phenyl glutaric anhydride which was reacted as described in general procedure 5 to give **111** (6.86 g, 36.1 mmol, 75 %) as a colorless solid (m.p. 99-100 °C).

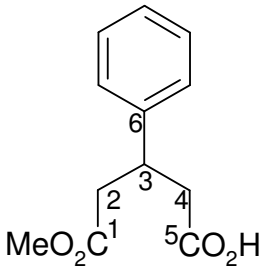

111

Spectroscopic data correspond to the literature.[71]

4-Iodo-3-phenyl methyl butarate (**112**):

General procedure 6 with **111** (7.92 g, 35.67 mmol)**,** $Pb(OAc)_4$ (17.72 g, 40 mmol), CCl_4 (230 mL), I_2 (13.18 g, 51.9 mmol) gave the oily iodo-ester **112** (9.43 g, 31.02 mmol, 87 %) which was used immediately without further purification in the next reaction.

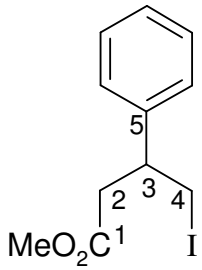

112

^{1}H NMR ($CDCl_3$): δ = 7.31-7.17 (m, 5H, Ar), 3.56 (s, 3H, COO**C**$\mathbf{H_3}$), 3.45-3.35 (m, 3H, 3-H, 4-H), 2.93 (dd, $^2J_{2,2}$ = 16.1, $^3J_{2,3}$ = 5.5 Hz, 1H, 2-H), 2.68 (dd, $^2J_{2,2}$ = 16.1, $^3J_{2,3}$ = 7.6 Hz, 1H, 2-H).

^{13}C NMR ($CDCl_3$): δ = 171.2 (s, C-1), 141.0 (s, C-5), 128.2 (d, Ar), 126.9 (d, Ar), 126.7 (d, Ar), 51.2 (q, O**C**H_3), 43.4 (d, C-3), 39.7 (t, C-2), 11.8 (t, C-4).

MS [EI, 70 eV]: *m/z* (%) = 273 (10) [M^+-CH_3O], 231 (10) [M^+-CH_3COOCH_2], 177 (100) [M^+-I], 145 (20), 135 (40), 117 (100), 104 (40), 91 (20), 77 (10), 59 (15), 51 (10).

UV ($CHCl_3$): λ_{max} (lg ε) = 258 nm (3.00).

IR (ATR): $\tilde{\nu}$ = 3058-2840 cm^{-1} (w), 1729 (s, C=O), 1496 (w), 1453 (m), 1431 (s), 1351 (s), 1277 (s), 1227 (s), 1188 (w), 1163 (s), 1123 (s), 1044 (w), 978 (m), 956 (m), 881 (m), 788 (w), 757 (s), 743 (s), 697 (s), 541 (s).

(3-Methoxycarbonyl-2-phenyl-propyl)-triphenylphosphonium iodide (**73**):

General procedure 7 with **112** (9.43 g, 31 mmol) and triphenylphosphine (23.58 g, 93 mmol) in benzene (80 mL) gave phosphonium salt **73** (13 g, 23 mmol, 74 %) as a pale yellow solid (m.p. 145 °C).

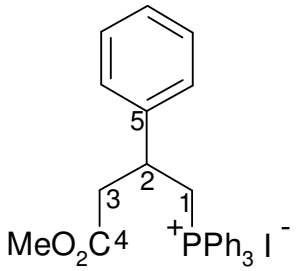

73

^{1}H NMR ($CDCl_3$): δ = 7.77-7.55 (m, 15H, Ar-P), 7.18-7.05 (m, 5H, Ar), 4.69 (ddd, $^2J_{1,1}$ = 16.0, $^2J_{1,P}$ = 11.9, $^3J_{1,2}$ = 11.0 Hz, 1H, 1-H), 4.24 (ddd, $^2J_{1,1}$ = 16.0, $^2J_{1,P}$ = 14.4, $^3J_{1,2}$ = 2.7 Hz, 1H, 1-H), 3.59 (s, 3H, OC**H**$_3$), 3.58-3.53 (m, 1H, 2-H), 3.45 (dd, $^2J_{3,3}$ = 17.4, $^3J_{3,2}$ = 8.7 Hz, 1H, 3-H), 2.82 (dt, $^2J_{3,3}$ = 17.4, $^3J_{3,2}$ = $^4J_{3,P}$ = 4.7 Hz, 1H, 3-H).

^{13}C NMR ($CDCl_3$): δ =172.4 (s, C-4), 140.1 (s, $J_{C,P}$ = 2 Hz, C-5), 134.6 (d, $J_{C,P}$ = 3 Hz, Ar-P), 133.8 (d, $J_{C,P}$ = 10.2 Hz, Ar-P), 130.1 (d, $J_{C,P}$ = 12.7 Hz, Ar-P), 129.0 (d, Ar), 128.1 (d, Ar), 127.7 (d, Ar), 118.3 (s, $J_{C,P}$ = 86 Hz, Ar-P), 51.8 (q, COO**C**$\mathbf{H_3}$), 42.5 (t, $J_{C,P}$ = 15.6 Hz, C-3), 37.4 (d, $J_{C,P}$ = 3 Hz, C-2), 28.8 (t, $J_{C,P}$ = 50 Hz, C-1).

MS [ESI]: *m/z* (%) = 439 (100) [M^+-I].

UV ($CHCl_3$): λ_{max} (lg ε) = 275 nm (3.70), 294 (3.55), 361 (3.26).

IR (ATR): $\tilde{\nu}$ = 3050-2856 cm^{-1} (w), 1744 (s, C=O), 1586 (w), 1487 (w), 1436 (s), 1415 (m), 1361 (m), 1311 (w), 1216 (s), 1190 (m), 1151 (s), 1022 (w), 995 (m), 962 (m), 862 (w), 745 (s), 721 (s), 689 (s).

Elemental analysis: $C_{29}H_{28}O_2PI$ (566.42) calcd. C 61.48, H 4.97; found C 61.21, H 5.04.

***rac*-3-Isopropyl monomethyl glutarate** (**113**):

General procedure 4 with **70**[41] (13.55 g, 77.87 mmol) in acetic anhydride (45 mL) yielded 3-isopropyl-glutaric acid anhydride (10.7 g, 68.52 mmol, 88 %) which was

reacted with methanol (145 mL) as described in general procedure 5 to yield the half acid-ester **113** (16.19 g, 86.12 mmol, 62 %).

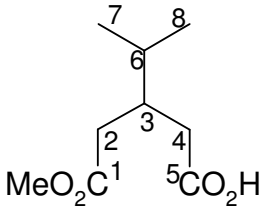

113

The spectroscopic data agree with the literature.[28]

4-Iodo-3-isopropyl methyl butarate (**114**):

General procedure 6 with **113** (16.19 g, 90 mmol), I_2 (35.56 g, 140 mmol), $Pb(OAc)_4$ (44.3 g, 100 mmol) and CCl_4 (360 mL) gave **65** (15.5 g, 57.6 mmol, 64 %).

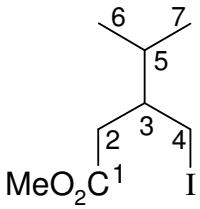

114

^{1}H NMR (400 MHz, $CDCl_3$): δ = 3.68 (s, 3H, COOC**H$_3$**), 3.35 (dd, $^2J_{4,4}$ = 10.1, $^3J_{4,3}$ = 4.7 Hz, 1H, 4-H), 3.29 (dd, $^2J_{4,4}$ = 10.1, $^3J_{4,3}$ = 5.7 Hz, 1H, 4-H), 2.46 (dd, $^2J_{2,3}$ = 16.2, $^3J_{2,3}$ = 5.3 Hz, 1H, 2-H), 2.35 (dd, $^2J_{2,2}$ = 16.2, $^3J_{2,3}$ = 7.7 Hz, 1H, 2-H), 1.80-1.70 (m, 1H, 5-H), 1.70-1.65 (m, 1H, 3-H), 0.92 (d, $^3J_{7,5}$ = $^3J_{6,5}$ = 6.6 Hz, 6H, 6-H, 7-H).

^{13}C NMR (100 MHz, $CDCl_3$): δ = 173.1 (s, C-1), 51.6 (q, COO**C**H$_3$), 42.4 (d, C-3), 36.4 (t, C-2), 30.7 (d, C-5), 19.6, 19.1 (q, C-6, C-7), 12.6 (t, C-4).

IR (ATR): $\tilde{\nu}$ = 2960-2875 cm^{-1} (w), 1778 (m), 1734 (s, C=O), 1463 (m), 1435 (m), 1370 (m), 1336 (m), 1254 (s), 1235 (s), 1195 (s, $COOCH_3$), 1169 (s, $COOCH_3$), 1140 (s), 1014 (m), 890 (w).

UV ($CHCl_3$): λ_{max} (lg ε) = 252 nm (2.92).

(3-Methoxycarbonyl-2-isopropyl-propyl)-triphenylphosphonium iodide (**72**):

General procedure 7 with iodo-ester **114** (15.5 g, 57.6 mmol), triphenylphosphine (22.64 g, 86.4 mmol) in benzene (80 mL) gave **72** (4.93 g, 9.26 mmol, 16 %) as a colorless solid (m.p. 134 °C).

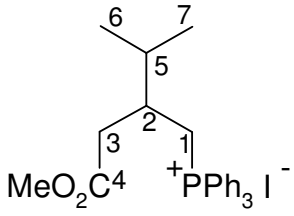

72

^{1}H NMR (400 MHz, $CDCl_3$): δ =7.96-7.45 (m, Ar-H), 3.83-3.70 (m, 1H, 1-H), 3.53 (s, 3H, COOC**H$_3$**), 2.55-2.17 (m, 3H, 2-H, 3-H), 1.65-1.55 (m, 1H, 5-H), 0.93, 0.88 (d, $^{3}J_{6,5}$ = $^{3}J_{7,5}$ = 6.7 Hz, 6H, 6-H, 7-H).

^{13}C NMR (100 MHz, $CDCl_3$): δ =173.1 (s, **C**OOCH$_3$), 135.1, 133.8, 133.3, 131.3, 130.5 (d, Ar), 118.5 (s, Ar), 51.8 (q, COO**C**H$_3$), 35.5 (d, C-2), 34.9 (t, C-1, C-3), 31.7 (d, C-5), 19.6, 18.1 (q, C-6, C-7).

MS [ESI]: *m/z* (%) = 405 (100) [M^+-I], 277 (20).

UV ($CHCl_3$): λ_{max} (lg ε) = 240 nm (4.21).

IR (ATR): $\tilde{\nu}$ = 3050-2871 cm^{-1} (w), 1726 (s, C=O), 1586 (w), 1483 (w), 1435 (s, P-phenyl), 1337 (w), 1183 (w), 1158 (m), 1110 (s), 994 (m), 904 (w), 789 (s, C_6H_5), 745 (s, C_6H_5), 719 (s, C_6H_5), 540 (s, C_6H_5).

HRMS: $C_{26}H_{30}O_2P$ (405.50) calcd. 405.198344; found 405.19889 ± 0.84 ppm.

***E*-(2-Hydroxy-pent-3-enyl)-phosphonic acid diisopropyl ester** (**26**):

To a solution of diisopropyl methyl phosphonate (16.5 g, 91.66 mmol) - prepared by Arbuzov reaction of triisopropyl phosphonate (16.9 g, 81 mmol) with freshly distilled methyl iodide (12.06 g, 85 mmol) - in 90 mL anhydrous THF was added dropwise *n*BuLi (6.35 g, 100.83 mmol, 63 mL, 1.6 M in hexane) at –78 °C under nitrogen. After 30 min stirring, freshly distilled croton aldehyde (6.42 g, 91.66 mmol, 7.6 mL) was added. The mixture was stirred for 40 min and quenched by addition of aqueous NH_4Cl solution. Extraction with diethyl ether, washing with brine solution, drying of the ether

phase with Na_2SO_4, and solvent evaporation gave **26** (16.89 g, 67.6 mmol, 74 %, lit.[72] yield: 64 %). The spectroscopic data correspond to the literature.[72]

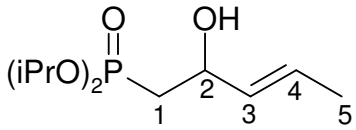

26

***E*-6-(Diisopropoxy-phosphoryl)-3-methyl-hex-4-enoic acid ethyl ester** (**27**):
A mixture of **26** (16.89 g, 67.6 mmol), ethyl orthoacetate (76.6 g, 472 mmol, 86 mL) and propionic acid (0.3 g, 4.05 mmol, 0.3 mL) was heated at 140 °C for 3 h, the formed ethanol being removed by destillation. Unreacted ethylorthoacetate and propionic acid were distilled at 145-150 °C. Purified by bulb to bulb distillation at 103 °C/0.4 torr yielded **27** (11.4 g, 35.6 mmol, 53 %, lit.[72] yield: 76 %) as a colorless oil.

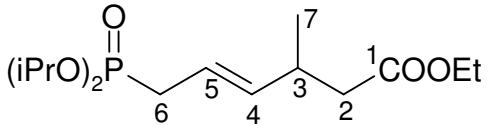

27

^{1}H NMR ($CDCl_3$): δ = 5.51-5.32 (m, 2H, 4-H, 5-H), 4.64-4.56 (m, 2H, C**H**$(CH_3)_2$), 4.05 (q, ^3J = 7.1 Hz, COOC**H$_2$**CH_3), 2.64-2.61 (m, 1H, 3-H), 2.42 (dd, $^2J_{6,P}$ = 21.6, $^3J_{6,5}$ = 7.2 Hz, 2H, 6-H), 2.26 (dd, $^2J_{2,2}$ = 14.9, $^3J_{2,3}$ = 7.0 Hz, 1H, 2-H), 2.17 (dd, $^2J_{2,2}$ = 14.9, $^3J_{2,3}$ = 7.0 Hz, 1H, 2-H), 1.25-1.11 (m, 15H, CH(C**H$_3$**$)_2$ $COOCH_2C$**H$_3$**), 0.98 (d, $^3J_{7,3}$ = 6.8 Hz, 3H, 7-H).

^{13}C NMR ($CDCl_3$): δ =172.1 (s, C-1), 139.0 (d, C-4), 118.3 (d, C-5), 70.0 (d, **C**H$(CH_3)_2$), 60.0 (t, COO**C**H_2CH_3), 41.3 (t, C-2), 33.4 (d, C-3), 31.3 (t, C-6), 23.8 (q, CH(**C**$H_3)_2$), 19.7 (q, C-7), 14.1 (q, $COOCH_2$**C**H_3).

MS [GC-MS]: *m/z* (%) = 320 (15) [M^+], 305 (5), 278 (15), 263 (15), 236 (60), 190 (100), 162 (30), 149 (25), 123 (15), 109 (35), 80 (20), 67 (15), 43 (30).

IR (ATR): $\tilde{\nu}$ = 2978-2873 cm^{-1} (w), 1732 (m), 1456 (w), 1385 (m), 1373 (m), 1245 (m), 1178 (m), 1141 (m), 1106 (m), 973 (s), 887 (m), 777 (m).

UV ($CHCl_3$): λ_{max} (lg ε) = 242 nm (2.31).

***E*-6-(Diisopropoxy-phosphoryl)-3-methyl-hex-4-enoic-acid-3'-methyl-oxetan-3'-ylmethyl ester** (**33**):

To a solution of **27** (3 g, 9.37 mmol) in ethanol (50 mL) was added a solution of KOH (1 g, 17.8 mmol) in water (20 mL), and the mixture was heated to reflux for 3 h. After extraction with diethyl ether and water, the aqueous phase was acidified to pH 2, and extracted with diethyl ether. This organic phase was dried with Na_2SO_4; solvent evaporation gave acid **32** (2.49 g, 8.53 mmol, 91 %) as a colorless oil.

To **32** (1.37 g, 4.68 mmol) in dry diethyl ether (30 mL) was added 3-(hydroxymethyl)-3-methyloxetan (0.52 g, 5.1 mmol), DMAP (0.06 g, 0.47 mmol) and dicyclohexylcarbodiimide (DCC, 1.51 g, 5.1 mmol). The mixture was stirred at 25 °C for 1 h on a water bath. Filtration and evaporation of the solvent gave a viscous oil which was purified by bulb to bulb distillation (60-65 °C/0.06 torr), to yield **33** (1.3 g, 3.45 mmol, 74 %).

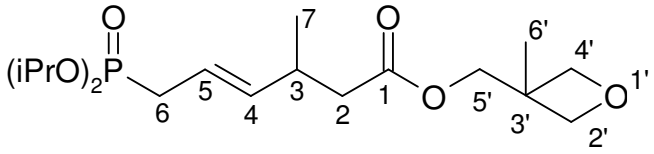

33

^{1}H NMR ($CDCl_3$): δ = 5.58-5.38 (m, 2H, 4-H, 5-H), 4.71-4.65 (m, 2H, C**H**$(CH_3)_2$), 4.51 (d, $^4J_{2',4'} = {}^4J_{4',2'}$ = 6.0 Hz, 2H, 2'-H, 4'-H), 4.38 (d, $^4J_{2',4'} = {}^4J_{4',2'}$ = 6.0 Hz, 2H, 2'-H, 4'-H), 4.16 (s, 2H, 5'-H), 2.72-2.70 (m, 1H, 3-H), 2.49 (dd, $^2J_{6,P}$ = 21.7, $^3J_{6,5}$ = 7.0 Hz, 2H, 6-H), 2.40 (dd, $^2J_{2,2}$ = 14.9, $^3J_{2,3}$ = 7.0 Hz, 1H, 2-H) 2.31 (dd, $^2J_{2,2}$ = 14.9, $^3J_{2,3}$ = 7.6 Hz, 1H, 2-H), 1.33 (d, ^3J = 6.7 Hz, 12H, CH(C**H$_3$**)$_2$), 1.30 (s, 3H, 6'-H), 1.07 (d, $^3J_{7,3}$ = 6.8 Hz, 3H, 7-H).

^{13}C NMR ($CDCl_3$): δ =172.3 (s, C-1), 139.0 (d, C-4), 118.7 (d, C-5), 79.5 (t, C-2', C-4'), 70.1 (d, **C**H$(CH_3)_2$), 68.5 (t, C-5'), 41.3 (t, C-2), 39.0 (s, C-3'), 34.7 (d, C-3), 31.5 (t, C-6), 24.0 (q, CH(**C**H$_3)_2$), 21.2 (q, C-7), 19.9 (q, C-6').

MS [GC-MS]: *m/z* (%) = 376 (30) [M^+], 361 (10), 334 (20), 304 (7), 275 (30), 262 (10), 233 (10), 211 (45), 191 (75), 162 (50), 144 (100), 109 (35), 85 (23), 67 (30), 43 (43).

IR (ATR): $\tilde{\nu}$ = 2978-2871 cm^{-1} (w), 2119 (m), 1736 (m), 1700 (m), 1656 (m), 1533 (w), 1453 (m), 1377 (m), 1239 (m), 1177 (m), 1142 (m), 1107 (m), 976 (s), 890 (m).

UV ($CHCl_3$): λ_{max} (lg ε) = 240 nm (2.55), 257 (2.48).

HRMS: $C_{18}H_{33}O_6P$ (376.43) calcd. 376.201477; found 376.20003 ± 0.61 ppm.

[4-Methyl-5-(4'-methyl-2',6',7'-trioxa-bicyclo[2.2.2]-oct-1'-yl)-pent-2-enyl]-phosphonic acid diisopropyl ester (**34**):

To a solution of oxetane ester **33** (2.2 g, 5.83 mmol) in dry dichloromethane (15 mL) was added $BF_3{\cdot}Et_2O$ (0.2 g, 1.45 mmol, 0.18 mL,) at -15 °C. After stirring for 8 h at -15 °C, the reaction was quenched with triethylamine (0.6 g, 5.83 mmol, 0.8 mL). The solvent was removed under high vacuum and the crude product was purified by column chromatography on basic alumina with dichloromethane to give **34** (1.5 g, 4 mmol, 69 %) as a colorless oil. The product decomposed during analysis and test reactions.

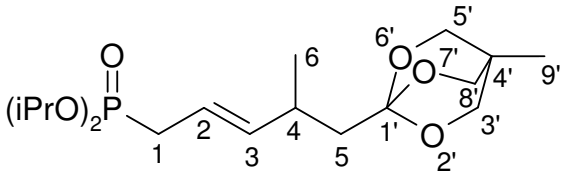

34

^{1}H NMR (acetone-d_6): δ = 5.63-5.56 (m, 1H, 3-H), 5.35-5.26 (m, 1H, 2-H), 4.64-4.55 (m, 2H, C**H**$(CH_3)_2$), 3.85 (s, 3'-H, 5'-H, 8'-H), 2.52-2.48 (m, 1H, 4-H), 2.43 (dd, $^2J_{1,P}$ = 21.7, $^3J_{1,2}$ = 7.0 Hz, 2H, 1-H), 1.68 (dd, $^2J_{5,5}$ = 14.1, $^3J_{5,4}$ = 5.3 Hz, 1H, 5-H), 1.51 (dd, $^2J_{5,5}$ = 14.1, $^3J_{5,4}$ = 8.0 Hz, 1H, 5-H), 1.27 (d, ^3J = 4.8 Hz, 6H, CH(C**H$_3$**)$_2$), 1.26 (d, ^3J = 4.8 Hz, 6H, CH(C**H$_3$**)$_2$), 1.02 (d, $^3J_{6,4}$ = 6.8 Hz, 3H, 6-H), 0.79 (s, 3H, 9'-H).

^{13}C NMR (acetone-d_6): δ =142.0 (d, C-3), 117.8 (d, C-2), 109.4 (s, C-1'), 72.8 (t, C-3', C-5', C-8'), 70.1 (d, **C**H$(CH_3)_2$), 44.0 (t, C-5), 32.5 (t, C-1), 31.8 (d, C-4), 30.2 (s, C-4'), 24.3 (q, CH(**C**$H_3)_2$), 20.7 (q, C-6), 14.4 (q, C-9').

MS [GC-MS]: *m/z* (%) = 376 (40) [M^+], 361 (10), 346 (14), 333 (25), 319 (7), 304 (8), 293 (20), 275 (30), 262 (10), 248 (10), 233 (7), 211 (57), 191 (100), 184 (14), 173 (16), 164 (35), 144 (70), 123 (10), 109 (40), 81 (50), 67 (30), 55 (38), 43 (50).

IR (ATR): $\tilde{\nu}$ = 2977-2876 cm^{-1} (w), 1459 (w), 1398 (w), 1246 (m), 1206 (m), 1178 (m), 1053 (m), 972 (s), 889 (m).

UV (CH_3CN): λ_{max} (lg ε) = 272 nm (2.48).

4-(Dimethoxy-phosphoryl)-3-methyl *tert*-butyl butarate (**106**):

To a solution of dimethyl methyl phosphonate (1.75 g, 14.08 mmol, 1.52 mL) in anhydrous THF (15 mL) was added *n*BuLi (8.8 mL of 1.6 M solution in hexane, 14.08 mmol) at -78 °C. After 30 min, *tert*-butyl crotonate (1 g, 7.04 mmol) was added dropwise, and the reaction was stirred at -78 °C for additional 2 h. The mixture was extracted with diethyl ether. The organic phase was washed with aqueous NH_4Cl and dried with Na_2SO_4. After evaporation of the solvent, the oily product was distilled at 103-107 °C/0.06 torr to give **106** (0.87 g, 7.04 mmol, 47 %, lit.[73] yield: 70 %).

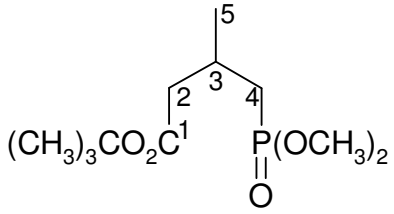

106

^{1}H NMR ($CDCl_3$): δ = 3.74 (dd, $^3J_{H,P}$ = 10.8, $^5J_{H,4}$ = 1.5 Hz, 6H, PO(OC**H$_3$**)$_2$), 2.42-2.35 (m, 1H, 3-H), 2.22-2.15 (m, 2H, 2-H), 1.95-1.85 (m, 1H, 4-H), 1.74-1.64 (m, 1H, 4-H), 1.45 (d, $^5J_{H,2}$ = 1.5 Hz, 9H, COOC(C**H$_3$**)$_3$), 1.11 (d, $^3J_{5,3}$ = 6.2 Hz, 5-H).

^{13}C NMR ($CDCl_3$): δ =170.9 (s, C-1), 79.7 (s, COO**C**(CH$_3$)$_3$), 51.6 (q, PO(O**C**H$_3$)$_2$), 42.7 (t, $J_{C,P}$ = 13 Hz, C-2), 30.4 (t, $J_{C,P}$ = 140 Hz, C-4), 27.5 (q, COOC(**C**H$_3$)$_3$), 25.2 (d, $J_{C,P}$ = 3.8 Hz, C-3), 20.4 (q, $J_{C,P}$ = 8 Hz, C-5).

MS [GC-MS]: *m/z* (%) = 210 (20) [M$^+$-*t*Bu], 193 (100), 151 (60), 124 (80), 57 (40).

IR (ATR): $\tilde{\nu}$ = 2975-2852 cm^{-1} (w), 1723 (s, CO), 1459 (w), 1367 (m), 1308 (m), 1247 (m), 1144 (s), 1059 (s), 1024 (s), 838 (s), 809 (s).

UV ($CHCl_3$): λ_{max} (lg ε) = 241 nm (1.83).

4-[1-(2,6,6-Trimethylcyclohexen-1-yl)]but-3-en-1-ynal (**46**):

To a solution of LDA [prepared from diisopropylamine (2.16 mL, 15 mmol) and *n*BuLi (9.5 mL of 1.6 M solution in hexane, 15 mmol)] in anhydrous THF (40 mL) at –78 °C under argon, stirred for 30 min was added dropwise **22** (2.88 g, 15 mmol, mL) in anhydrous THF (15 mL). After 1 h stirring at –78 °C, diethyl chlorophosphate (2.12 mL, 15 mmol) was added and the cooling bath removed. After 3 h, the reaction mixture

was transferred by cannula to a LDA solution [prepared from diisopropylamine (4.59 mL, 30 mmol) and *n*BuLi (1.6 M in hexane, 30 mmol, 20.4 mL)] in anhydrous THF (85 mL) at –78 °C. After 1 h, DMF (2.19 g, 30 mmol, 2.3 mL) was added and the mixture was allowed to come to room temp. After 1 h, the mixture was poured into a mixture of an ice cold solution of aqueous KH_2PO_4 and diethyl ether, and stirred for another 10 min. The layers were separated and the organic phase washed with brine and dried with Na_2SO_4. The solvents were removed and the crude product was purified by column chromatography on silica gel with pentane to yield **46** (50 mg, 0.25 mmol, 6 %, lit.[39] yield: 67 %).

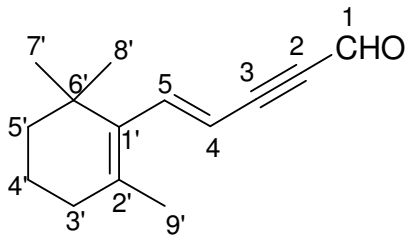

46

^{1}H NMR (200 MHz, $CDCl_3$): δ = 9.35 (s, 1H, 1-H), 7.05 (dd, $^3J_{5,4}$ = 16.1, $^5J_{5,9'}$ = 0.7 Hz, 1H, 5-H), 5.68 (d, $^3J_{4,5}$ = 16.1 Hz, 1H, 4-H), 2.07 (t, $^3J_{3',4'}$ = 5.9 Hz, 2H, 3-H'), 1.77 (d, $^5J_{9',5}$ = 0.7 Hz, 3H, 9-H'), 1.70-1.41 (m, 4H, 4-H', 5-H'), 1.06 (s, 6H, 7-H', 8-H').

^{13}C NMR (50 MHz, $CDCl_3$): δ = 176.6 (d, C-1), 149.4 (d, C-5), 136.8 (s, C-1'), 136.3 (s, C-2'), 108.3 (d, C-4), 96.0 (s, C-2), 89.6 (s, C-3), 39.7 (t, C-5'), 34.0 (s, C-6'), 33.6 (t, C-3'), 28.7 (q, C-7', C-8'), 21.6 (q, C-9'), 18.8 (t, C-4').

MS [GC-MS]: *m/z* (%) = 202 (60) [M^+], 187 (100) [M^+-CH_3], 173 (20) [M^+-CHO], 159 (70), 145 (50), 131 (80), 117 (63), 105 (58), 91 (75), 77 (60), 69 (38), 53 (30).

IR (ATR): $\tilde{\nu}$ = 2929 cm^{-1} (m), 2865 (m), 2170 (s, C≡C), 1714 (w), 1654 (s, C=O), 1589 (m), 1456 (m), 1382 (w), 1362 (w), 1294 (w), 1174 (m), 1128 (m), 959 (m), 905 (w), 860 (m), 829 (m).

13-*d*$_3$-β-Ionone (**84**):

To a solution of β-ionone (**22**, 9 g, 46.88 mmol) in D_2O (28 g) and pyridine (50 mL) was added 0.1 % NaOD in D_2O (3 mL). After stirring for 1 h at room temp. the product was extracted with ether and washed with water. The organic phase was dried with

Na_2SO_4, and the solvent was evaporated. The product **84** (9.34 g, 46.8 mmol, 100 %, lit.[42] yield: 98 %) was obtained as a colorless oil with d_3:d_2:d_1:d_0 ratio of 79:18:2:1 determined by mass spectrometry.

All spectroscopic data correspond to the literature.[42]

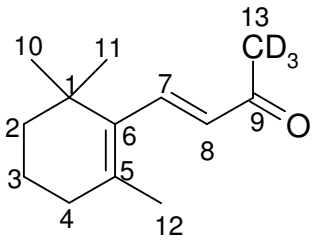

84

4-Oxo-β-ionone (**23**):

In a three-necked flask equipped with reflux condenser and two funnels, DMSO (10 mL) was heated to 100 °C. Simultaneously were added during 3 h, **22** (19.2 g, 100 mmol, 20.3 mL) and a solution of PCC (64.7 g, 0.3 mol) in DMSO (110 mL). After additional heating for 2 h, the mixture was cooled to room temp. and poured into diethyl ether (200 mL). After decantation, the black slurry was washed 3 times with ether. The combined organic phases were added to a solution of brine (100 mL), 2 N HCl (50 mL) and ice and extracted twice with diethyl ether. Washing of the organic phase with brine, drying with Na_2SO_4 and solvent removal followed by recrystallization from hexane gave yellow crystals of **23** (15.46 g, 75 mmol, 49 %, m.p. 53 °C, lit.[27] yield: 52 %, m.p. 51-52 °C). NMR spectra correspond to the literature.[27]

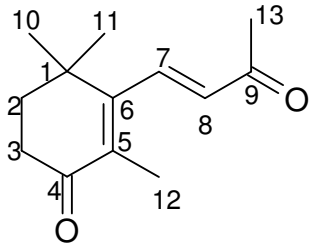

23

MS (**EI, 70 eV**)**:** *m/z* (%) = 206 (50) [M^+], 191 (10) [M^+-CH_3], 163 (100) [M^+-CH_3CO], 150 (15) [M^+-CH_3COCH_2], 149 (20) [M^+-CH_3CO, -CH_3] , 135 (24) [M^+-CH_3COCH_2, -CH_3], 43 (73) [CH_3CO^+].

IR (KBr): $\tilde{\nu}$ = 2956 – 2870 cm^{-1} (m, CH_3, CH_2, CH), 1660 (s, C=O).

UV ($CHCl_3$): λ_{max} (lg ε) = 230 nm (3.73), 242 (2.92), 280 (4.05).

13-d_3-4-Oxo-β-ionone (**91**):

13-d_3-β-Ionone (**84**, 6.35 g, 32.5 mmol) was oxidized with PCC (21.02 g, 97.5 mmol), in dry DMSO (50 mL) as described for **23**, to give **91** (2.85 g, 13.6 mmol, 53 %) with d_3:d_2:d_1:d_0 ratio of 9:41:29:9 determined by mass spectrometry.

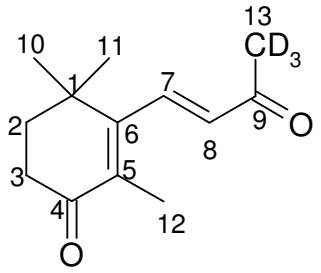

91

^{1}H NMR ($CDCl_3$): δ = 7.25 (br d, $^3J_{7,8}$ = 16.5 Hz, 1H, 7-H), 6.19 (d, $^3J_{8,7}$ = 16.5 Hz, 1H, 8-H), 2.54 (t, $^3J_{3,2}$ = 6.9 Hz, 2H, 3-H), 2.35 (s, undeuterated CH_3, 13-H), 2.34-2.31 (m, partially deuterated CH_2D and CHD_2, 13-H), 1.90 (t, $^3J_{2,3}$ = 6.9 Hz, 2H, 2-H), 1.80 (d, $^5J_{12,7}$ = 1.0 Hz, 3H, 12-H), 1.2 (s, 6H, 10-H, 11-H).

^{13}C NMR ($CDCl_3$): δ = 198.4 (s, C-4), 197.3 (s, C-9), 157.6 (s, C-6), 140.2 (d, C-7), 133,5 (d, C-8), 131.3 (s, C-5), 37.2 (t, C-2), 35.4 (s, C-1), 34.1 (t, C-3), 27.8 (q, C-13), 27.2 (q, C-10, C-11), 13.3 (q, C-12).

MS [GC-MS]: *m/z* (%) = 209 [M^+ , 9 % d_3], 208 [M^+ , 29 % d_2], 207 [M^+ , 41 % d_1], 206 [M^+, 21 % d_0], 194/193/192/191, 166/165/,164/163, 150 (14), 136 (17), 121 (37), 107 (12), 91 (12), 77 (10), 55 (12).

IR (ATR): $\tilde{\nu}$ = 2957-2870 cm^{-1} (m), 1660 (s), 1601 (w), 1450 (m), 1416 (m), 1369 (m), 1351 (m), 1335 (m), 1296 (m), 1252 (m), 1206 (m), 1178 (m), 1143 (m), 1094 (m), 1031 (m), 1011 (m), 978 (s), 882 (m), 686 (w), 569 (m).

UV ($CHCl_3$): λ_{max} (lg ε) = 240 nm (3.90), 280 (4.01).

β-Ionylidene-acetaldehyde (**47**):

General procedure 1 with **52** (13.37 g, 31.3 mmol) in anhydrous THF (60 mL), KO*t*Bu (3.5 g, 31.3 mmol), **22** (3 g, 15.6 mmol) in anhydrous THF (30 mL), oxalic acid

solution (13.78 g, 109.3 mmol, in 110 mL water). Column chromatography with pentane/diethyl ether 10:1 on Alox (activity III, 8 % water w/w) gave 9-*cis*- (R_f = 0.55) and all-*trans*-**47** (R_f = 0.42) in 1.0:1.5 ratio (2.83 g, 13 mmol, 83 %).

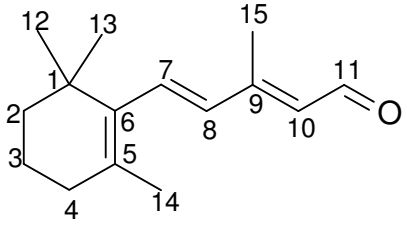

all-*trans*-**47**

^{1}H NMR (400 MHz, $CDCl_3$): δ = 10.13 (d, $^3J_{11,10}$ = 8.1 Hz, 1H, 11-H), 6.74 (dt, $^3J_{7,8}$ = 16.2, $^5J_{7,4}$ = $^5J_{7,14}$ = 0.8 Hz, 1H, 7-H), 6.21 (d, $^3J_{8,7}$ = 16.2 Hz, 1H, 8-H), 5.93 (br d, $^3J_{10,11}$ = 8.1 Hz, 1H, 10-H), 2.31 (d, $^4J_{15,10}$ = 1.1 Hz, 3H, 15-H), 2.04 (br t, $^3J_{4,3}$ = 6.0 Hz, 2H, 4-H), 1.72 (d, $^5J_{14,7}$ = 0.8 Hz, 3H, 14-H), 1.62 (m, 2H, 3-H), 1.47 (m, 2H, 2-H), 1.05 (s, 6H, 12-H, 13-H).

^{13}C NMR (100 MHz, $CDCl_3$): δ = 191.2 (d, C-11), 154.8 (s, C-9), 137 (s, C-6), 135.6 (d, C-8), 135.5 (d, C-7), 132.6 (s, C-5), 128.7 (d, C-10), 39.5 (t, C-2), 34.2 (s, C-1), 33.1 (t, C-4), 28.8 (q, C-12/C-13), 21.6 (q, C-14), 19 (t, C-3), 12.9 (q, C-15).

UV ($CHCl_3$): λ_{max} (lg ε) = 252 nm (4.04), 304 (4.23).

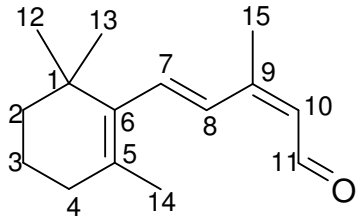

9-*cis*-**47**

^{1}H NMR ($CDCl_3$): δ = 10.16 (d, $^3J_{11,10}$ = 8.1 Hz, 1H, 11-H), 7.09 (d, $^3J_{8,7}$ = 16.0 Hz, 1H, 8-H), 6.63 (dt, $^3J_{7,8}$ = 16.0, $^5J_{7,4}$ = $^5J_{7,14}$ = 0.8 Hz, 1H, 7-H), 5.86 (dd, $^3J_{10,11}$ = 8.1, $^4J_{10,15}$ = 0.9 Hz, 1H, 10-H), 2.1 (d, $^4J_{15,10}$ = 1.1 Hz, 3H, 15-H), 2.06 (m, 2H, 4-H), 1.75 (d, $^5J_{14,7}$ = 1.1 Hz, 3H, 14-H), 1.65-1.60 (m, 2H, 3-H), 1.50-1.47 (m, 2H, 2-H), 1.06 (s, 6H, 12-H, 13-H).

^{13}C NMR (100 MHz, $CDCl_3$): δ = 190.1 (d, C-11), 155 (s, C-9), 137.2 (s, C-6), 136.5 (d, C-7), 132.5 (s, C-5), 127.8, 127.73 (d, C-10, C-8), 39.5 (t, C-2), 34.2 (s, C-1), 33.1 (t, C-4), 28.9 (q, C-12, C-13), 21.7 (q, C-14), 21.1 (q, C-15), 19 (t, C-3).

UV ($CHCl_3$): λ_{max} (lg ε) = 248 nm (3.86), 286 (3.85).

isomeric mixture:

MS [GC-MS]: *m/z* (%) = 218 (40) [M^+], 203 (15) [M^+-CH_3], 189 (20), 175 (20), 161 (20), 147 (45), 133 (35), 119 (100), 107 (40), 95 (40), 91 (30), 77 (30), 69 (15), 55 (15).

IR (ATR): $\tilde{\nu}$ = 2959 cm^{-1} (m), 2924 (m), 2864 (m), 2825 (w),2764 (w), 2723 (w), 1664 (C=O, s), 1608 (m), 1448 (m), 1378 (m), 1359 (m), 1206 (m), 1114 (m), 967 (m).

15-d_3-β-Ionylidene-acetaldehyde (**85**):

General procedure 1 with **52** (13.19 g, 30.7 mmol) in anhydrous THF (60 mL), KO*t*Bu (3.44 g, 30.7 mmol), **84** (3.0 g, 15.36 mmol) in anhydrous THF (40 mL), aqueous oxalic acid (13.5 g, 107.5 mmol, 110 mL water). Column chromatography on Alox (activity III, 8 % water w/w) with pentane/diethyl ether 10:1, gave a mixture of 9-*cis*- (R_f = 0.54) and all-*trans*-**85** (R_f = 0.43) as a yellow oil (1.18 g, 5.3 mmol, 35 %).

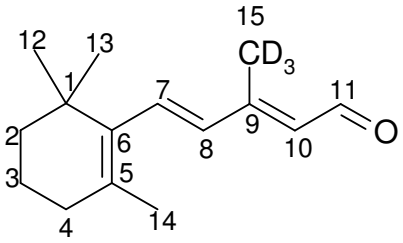

all-*trans*-**85**

^{1}H NMR (400 MHz, $CDCl_3$): δ = 10.17 (d, $^3J_{11,10}$ = 8.0 Hz, 1H, 11-H), 6.74 (d, $^3J_{7,8}$ = 16.2 Hz, 1H, 7-H), 6.22 (d, $^3J_{8,7}$ = 16.2 Hz, 1H, 8-H), 5.93 (d, $^3J_{10,11}$ = 8.0 Hz, 1H, 10-H), 2.31 (s, undeuterated CH_3, 15-H), 2.28-2.27 (m, partially deuterated CH_2D and CHD_2, 15-H), 2.05 (t, $^3J_{4,3}$ = 5.8 Hz, 2H, 4-H), 1.73 (s, 3H, 14-H), 1.67-1.57 (m, 2H, 3-H), 1.51-1.47 (m, 2H, 2-H), 1.05 (s, 6H, 12-H, 13-H).

^{13}C NMR (100 MHz, $CDCl_3$): δ = 191.1 (d, C-11), 154.8 (s, C-9), 136.9 (s, C-6), 135.6 (d, C-8), 135.4 (d, C-7), 132.5 (s, C-5), 128.6 (d, C-10), 39.6 (t, C-2), 34.1 (s, C-1), 33.1 (t, C-4), 28.8 (q, C-12, C-13), 21.6 (q, C-14), 19 (t, C-3).

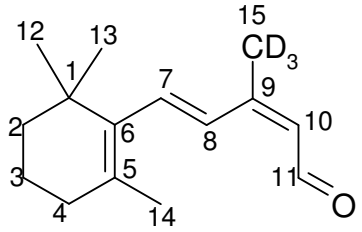

9-*cis*-**85**

^{1}H NMR (400 MHz, $CDCl_3$): δ = 10.13 (d, $^3J_{11,10}$ = 8.0 Hz, 1H, 11-H), 7.10 (d, $^3J_{8,7}$ = 16.0 Hz, 1H, 8-H), 6.63 (d, $^3J_{7,8}$ = 16.0 Hz, 1H, 7-H), 5.86 (d, $^3J_{10,11}$ = 8.0 Hz, 1H, 10-H), 2.30 (s, undeuterated CH_3, 15-H), 2.28-2.27 (m, partially deuterated CH_2D and CHD_2, 15-H), 2.13-2.11 (m, 2H, 4-H), 1.75 (s, 3H, 14-H), 1.67-1.57 (m, 2H, 3-H), 1.51-1.47 (m, 2H, 2-H), 1.04 (s, 6H, 12-H, 13-H).

^{13}C NMR (100 MHz, $CDCl_3$): δ = 189.9 (d, C-11), 155.0 (s, C-9), 137.1 (s, C-6), 136.4 (d, C-8), 132.4 (s, C-5), 128.6, 127.7 (d, C-10, C-7), 39.4 (t, C-2), 34.1 (s, C-1), 33.1 (t, C-4), 28.8 (q, C-12, C-13), 21.7 (q, C-14), 18.9 (t, C-3).

isomeric mixture:

MS [EI, 70 eV]: *m/z* (%) = 221 [M^+, 16 % d_3], 220 [M^+, 29 % d_2], 210 [M^+, 40 % d_1], 218 [M^+, 12 % d_0], 204 (18) [M^+-CH_3], 190 (22), 176 (23), 149 (60), 133 (40), 123 (60), 120 (100), 107 (98), 97 (40), 91 (37), 79 (28), 69 (20), 67 (15), 55 (28).

IR (ATR): $\tilde{\nu}$ = 2957-2744 cm^{-1} (m), 1659 (s), 1606 (m), 1450 (s), 1378 (s), 1300 (s), 1198 (m), 1147 (m), 1103 (m,), 967 (m).

UV ($CHCl_3$): λ_{max} (lg ε) = 233 nm (3.83), 283 (4.01).

4-Oxo-β-ionylidene-acetaldehyde (**53**):

General procedure 1 with **52** (12.46 g, 29.13 mmol) in anhydrous THF (200 mL), KO*t*Bu (3.26 g, 29.13 mmol), **23** (3.0 g, 14.56 mmol) in anhydrous THF (50 mL), aqueous oxalic acid (12.85 g, 101.92 mmol, 100 mL water). Column chromatography on Alox (activity III, 8 % water w/w, pentane/diethyl ether 3:2, gave a mixture of 9-*cis*-(R_f = 0.42) and all-*trans*-**53** (R_f = 0.34) as a yellow oil (1.0:1.5 ratio, 2.15 g, 9.3 mmol, 63 %).

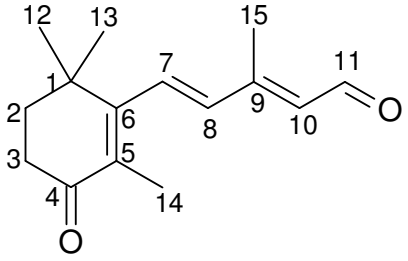

all-*trans*-**53**

^{1}H NMR (400 MHz, $CDCl_3$): δ = 10.17 (d, $^3J_{11,10}$ = 7.9 Hz, 1H, 11-H), 6.76 (br. d, $^3J_{7,8}$ = 16.4 Hz, 1H, 7-H), 6.33 (dd, $^3J_{8,7}$ = 16.4, $^4J_{8,10}$ = 0.7 Hz, 1H, 8-H), 6.02 (br. d, $^3J_{10,11}$ = 7.9 Hz, 1H, 10-H), 2.54 (m, 2H, 3-H), 2.36 (d, $^4J_{15,10}$ = 1.2 Hz, 3H, 15-H), 1.89 (m, 2H, 2-H), 1.82 (d, $^5J_{14,7}$ = 1.1 Hz, 3H, 14-H), 1.2 (s, 6H, 12-H, 13-H).

^{13}C NMR (100 MHz, $CDCl_3$): δ = 198.8 (s, C-4), 191.1 (d, C-11), 159.2 (s, C-6), 152.7 (s, C-9), 138.3 (d, C-8), 132.5 (d, C-7), 131.0 (s, C-5), 130.7 (d, C-10), 37.2 (t, C-2), 35.6 (s, C-1), 34.1 (t, C-3), 27.4 (q, C-12, C-13), 13.5 (q, C-14), 12.8 (q, C-15).

IR (KBr): $\tilde{\nu}$ = 2962 cm^{-1} (m), 2927 (m), 2858 (m), 2774 (w), 2729 (w), 1667 (C=O, s), 1616 (m), 1595 (m), 1447 (m), 1387 (w), 1376 (w), 1351 (m), 1333 (m), 1203 (m), 1148 (m), 1092 (m).

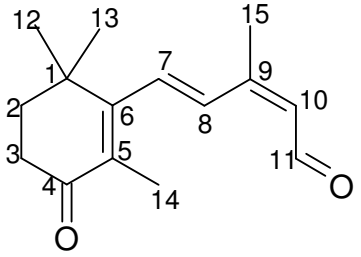

9-*cis*-**53**

^{1}H NMR (400 MHz, $CDCl_3$): δ = 10.14 (d, $^3J_{11,10}$ = 7.7 Hz, 1H, 11-H), 7.22 (d, $^3J_{8,7}$ = 16.2 Hz, 1H, 8-H), 6.65 (dd, $^3J_{7,8}$ = 16, $^5J_{7,14}$ = 1.1 Hz, 1H, 7-H), 6.00 (dd, $^3J_{10,11}$ = 7.7, $^4J_{10,15}$ = 1.1 Hz, 1H, 10-H), 2.54 (m, 2H, 3-H), 2.13 (d, $^4J_{15,10}$ = 1.1 Hz, 3H, 15-H), 1.9 (m, 2H, 2-H), 1.85 (d, $^5J_{14,7}$ = 1.1 Hz, 14-H), 1.2 (s, 6H, 12-H, 13-H).

^{13}C NMR (100 MHz, $CDCl_3$): δ = 198.8 (s, C-4), 189.7 (d, C-11), 159.2 (s, C-6), 152.8 (s, C-9), 133.7 (d, C-7), 131.1 (s, C-5), 130.6 (d , C-8), 129.7 (d, C-10), 37.3 (t, C-2), 35.7 (s, C-1), 34.2 (t, C-3), 27.5 (q, C-12, C-13), 20.9 (q, C-15), 13.6 (q, C-14).

isomeric mixture:

MS [GC-MS]: *m/z* (%) = 232 (18) [M^+], 217 (10) [M^+-CH_3], 203 (20) [M^+-COH], 189 (11) [M^+-COH, -CH_3], 161 (12), 148 (15), 133 (22), 119 (14), 105 (14), 95 (100) [CH^+=CHCH(CH_3)=CHCH=O].

UV ($CHCl_3$): λ_{max} (lg ε) = 276 nm (4.02), 336 (4.13).

IR (KBr): $\tilde{\nu}$ = 2962 cm^{-1} (m), 2924 (m), 2869 (w), 1663 (C=O, s), 1619 (m), 1447 (m), 1334 (m), 1202 (m), 1117 (m), 1031 (m), 970 (m).

15-*d*$_3$-4-Oxo-β-ionylidene-acetaldehyde (**86**):

General procedure 1 with **52** (11.67 g, 27.26 mmol) in anhydrous THF (60 mL), KO*t*Bu (3.05 g, 27.26 mmol), **91** (2.85 g, 13.63 mmol) in anhydrous THF (40 mL), aqueous oxalic acid (12.02 g, 95.41 mmol, 100 mL water). Column chromatography on Alox (activity III, 8 % water w/w), pentane/diethyl ether 3:2, gave a mixture of 9-*cis*- (R_f = 0.42) and all-*trans*-**86** (R_f = 0.34) as a yellow oil (1.95 g, 8.3 mmol, 61 %).

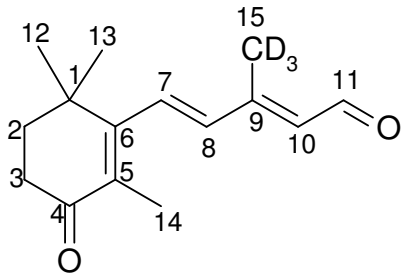

all-*trans*-**86**

^{1}H NMR (400 MHz, $CDCl_3$): δ = 10.17 (d, $^3J_{11,10}$ = 7.8 Hz, 1H, 11-H), 6.76 (d, $^3J_{7,8}$ = 16.3 Hz, 1H, 7-H), 6.33 (d, $^3J_{8,7}$ = 16.3 Hz, 1H, 8-H), 6.02 (d, $^3J_{10,11}$ = 7.8 Hz, 1H, 10-H), 2.56-2.51 (m, 2H, 3-H), 2.37-2.34 (m, partially deuterated CDH_2, 15-H), 2.18-2.17 (m, partially deuterated CD_2H, 15-H), 1.88-1.92 (m, 2H, 2-H), 1.82 (s, 3H, 14-H), 1.20 (s, 6H, 12-H, 13-H).

^{13}C NMR (100 MHz, $CDCl_3$): δ = 198.6 (s, C-4), 191.0 (d, C-11), 159.1 (s, C-6), 152.6 (s, C-9), 138.2 (d, C-8), 132.4 (d, C-7), 130.9 (s, C-5), 130.6 (d, C-10), 37.2 (t, C-2), 35.6 (s, C-1), 34.1 (t, C-3), 27.3 (q, C-12/C-13), 13.4 (q, C-14), 12.8 (q, partially deuterated C-15).

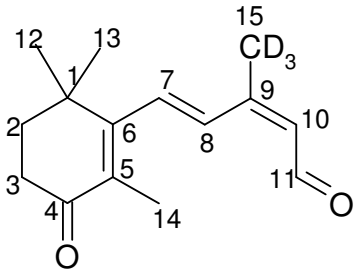

9-*cis*-**86**

^{1}H NMR (400 MHz, $CDCl_3$): δ = 10.14 (d, $^3J_{11,10}$ = 7.8 Hz, 1H, 11-H), 7.24 (d, $^3J_{8,7}$ = 16.2 Hz, 1H, 8-H), 6.65 (d, $^3J_{7,8}$ = 16.2 Hz, 1H, 7-H), 6.00 (d, $^3J_{10,11}$ = 7.8 Hz, 1H, 10-H), 2.56-2.51 (m, 2H, 3-H), 2.37-2.34 (m, partially deuterated CDH_2, 15-H), 2.18-2.17 (m, partially deuterated CD_2H, 15-H), 1.92-1.88 (m, 2H, 2-H), 1.85 (s,3H, 14-H), 1.22 (s, 6H, 12-H, 13-H).

^{13}C NMR (100 MHz, $CDCl_3$): δ = 198.6 (s, C-4), 189.5 (d, C-11), 159.2 (s, C-6), 152.7 (s, C-9), 133.6 (d, C-7), 130.9 (s, C-5), 130.4 (d , C-8), 129.5 (d, C-10), 37.1 (t, C-2), 35.5 (s, C-1), 34.1 (t, C-3), 27.4 (q, C-12, C-13), 20.8 (q, partially deuterated C-15), 13.5 (q, C-14).

MS [GC-MS]: *m/z* (%) = 235 [M^+, 4 % d_3], 234 [M^+, 18 % d_2], 233 [M^+, 40 % d_1], 232 [M^+, 38 % d_0], 217 (15), 204 (20), 189 (20), 163 (15), 148 (20), 133 (20), 119 (20), 105 (20), 95 (100), 77 (20), 69 (20), 55 (18), 41 (22).

IR (ATR): $\tilde{\nu}$ = 2961-2738 cm^{-1} (w), 1657 (s), 1614 (m), 1445 (w), 1351 (m), 1333 (m), 1311 (w), 1199 (m), 1146 (m), 1117 (m), 1091 (m), 1030 (m), 969 (m).

UV ($CHCl_3$): λ_{max} (lg ε) = 250 nm (4.08), 302 (4.25).

13,14-Dihydro-retinoic acid methyl ester (**74**):

General procedure 2 with LiHMDS [prepared from *n*BuLi (1.78 mL, 2.84 mmol) and HMDS (0.458 g, 0.59 mL, 2.84 mmol) in anhydrous THF (20 mL)], **66** (1.43 g, 2.84 mmol), **47** (0.5 g, 2.27 mmol) in anhydrous THF (10 mL). Column chromatography on Alox (activity III) with pentane/diethyl ether 5:1 gave all-*trans*-, 9-*cis*-, 11-*cis*-, 9,11-di-*cis*-**74** (0.58 g, 1.77 mmol, 78 %) in 1.75:1.0:3.0:1.0 ratio by NMR analysis, as yellow oil. When all-*trans*-**47** was reacted with **66**, all-*trans*- and 11-*cis*-**74** were obtained in 1.0:1.5 ratio, while 9-*cis*-**47** gave 9-*cis*- and 9,11-di-*cis*-**74** in 1:1 ratio.

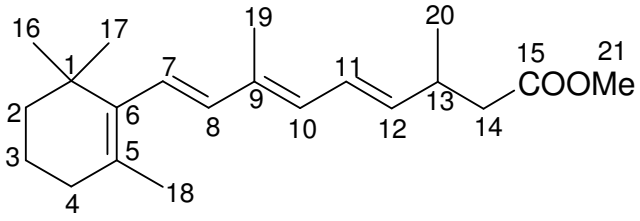

all-*trans*-**74**

^{1}H NMR (400 MHz, $CDCl_3$): δ = 6.42 (ddd, $^{3}J_{11,12}$ = 15.0, $^{3}J_{11,10}$ = 11.1, $^{5}J_{11,19}$ = 0.8 Hz, 1H, 11-H), 6.09 (d, $^{3}J_{7,8}$ = 16.4 Hz, 1H, 7-H), 6.04 (d, $^{3}J_{8,7}$ = 16.4 Hz, 1H, 8-H), 5.98 (d, $^{3}J_{10,11}$ = 11.1 Hz, 1H, 10-H), 5.62 (dd, $^{3}J_{12,11}$ = 15.0, $^{3}J_{12,13}$ = 7.7 Hz, 1H, 12-H), 2.80-2.75 (m, 1H, 13-H), 2.41-2.36 (m, 2H, 14-H), 2.02-1.98 (m, 2H, 4-H), 1.90 (s, 3H, 18-H), 1.71 (d, $^{5}J_{19,11}$ = 0.8 Hz, 3H, 19-H), 1.65-1.59 (m, 2H, 3-H), 1.48-1.45 (m, 2H, 2-H), 1.09 (d, $^{3}J_{20,13}$ = 6.8 Hz, 3H, 20-H), 1.01 (s, 6H, 16-H, 17-H).

^{13}C NMR (100 MHz, $CDCl_3$): δ = 172.8 (s, C-15), 137.9 (d, C-12), 137.8 (s, C-6), 137.7 (d, C-8), 134.7 (s, C-5), 129.4 (d, C-10), 128.9 (s, C-9), 126.3 (d, C-7), 125.8 (d, C-11), 41.6 (t, C-14), 39.6 (t, C-2), 34.2 (s, C-1), 34.1 (d, C-13), 33.0 (t, C-4), 28.9 (q, C-16, C-17), 21.6 (q, C-19), 20.3 (q, C-20), 19.3 (t, C-3), 12.5 (q, C-18).

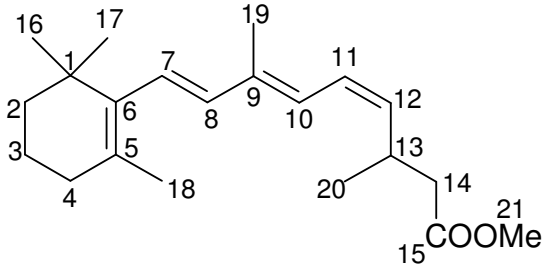

11-*cis*-**74**

^{1}H NMR (400 MHz, $CDCl_3$): δ = 6.31 (br t, $^{3}J_{11,12}$ = $^{3}J_{11,10}$ = 11.8 Hz, 1H, 11-H), 6.30 (d, $^{3}J_{10,11}$ = 10.7 Hz, 1H, 10-H), 6.15-6.14 (m, 2H, 7-H, 8-H), 5.26 (t, $^{3}J_{12,11}$ = $^{3}J_{12,13}$ = 9.2 Hz, 1H, 12-H), 3.24-3.16 (m, 1H, 13-H), 2.36-2.28 (m, 2H, 14-H), 2.01 (t, $^{3}J_{4,3}$ = 6.2 Hz, 2H, 4-H), 1.90 (s, 3H, 18-H), 1.68 (d, $^{5}J_{19,11}$ = 0.7 Hz, 3H, 19-H), 1.65-1.59 (m, 2H, 3-H), 1.48-1.45 (m, 2H, 2-H), 1.06 (d, $^{3}J_{20,13}$ = 6.7 Hz, 3H, 20-H), 1.02 (s, 6H, 16-H, 17-H).

^{13}C NMR (100 MHz, $CDCl_3$): δ = 172.8 (s, C-15), 137.9 (d, C-8), 137.8 (s, C-6), 136.3 (s, C-5), 135.4 (d, C-12), 129.1 (s, C-9), 126.8 (d, C-7), 124.5 (d, C-11), 124.3 (d, C-10), 41.9 (t, C-14), 39.6 (t, C-2), 34.2 (s, C-1), 33 (t, C-4), 29.4 (d, C-13), 28.9 (q, C-16, C-17), 21.7 (q, C-19), 20.9 (q, C-20), 19.3 (t, C-3), 12.3 (q, C-18).

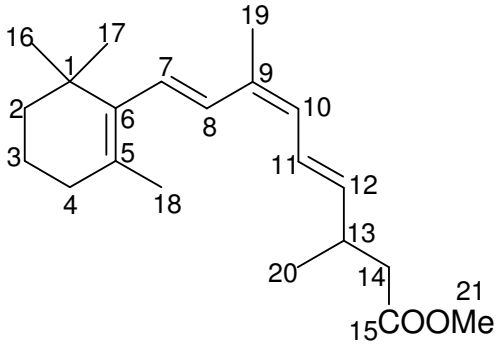

9-*cis*-**74**

^{1}H NMR (400 MHz, $CDCl_3$): δ = 6.57 (d, $^{3}J_{8,7}$ = 16.1 Hz, 1H, 8-H), 6.50 (dd, $^{3}J_{11,12}$ = 15.0, $^{3}J_{11,10}$ = 11.1 Hz, 1H, 11-H), 6.13 (d, $^{3}J_{7,8}$ = 16.1 Hz, 1H, 7-H), 5.88 (d, $^{3}J_{10,11}$ = 11.1 Hz, 1H, 10-H), 5.55 (dd, $^{3}J_{12,11}$ = 15.0, $^{3}J_{12,13}$ = 7.6 Hz, 1H, 12-H), 2.80-2.72 (m, 1H, 13-H), 2.26-2.4 (m, 2H, 14-H), 2.01 (t, $^{3}J_{4,3}$ = 6.0 Hz, 2H, 4-H), 1.91 (s, 3H, 19-H), 1.72 (s, 3H, 18-H), 1.66-1.58 (m, 2H, 3-H), 1.53-1.45 (m, 2H, 2-H), 1.05 (d, $^{3}J_{20,13}$ = 6.7 Hz, 3H, 20-H), 1.02 (s, 6H, 16-H, 17-H).

^{13}C NMR (100 MHz, $CDCl_3$): δ = 172.5 (s, C-15), 138.04 (s, C-6), 137 (d, C-12), 134.8 (s, C-5), 129.9 (d, C-8), 129.1 (s, C-9), 128.02 (d, C-10), 128 (d, C-7), 124.6 (d, C-11), 41.8 (t, C-14), 39.5 (t, C-2), 34.15 (s, C-1), 33.9 (d, C-13), 33 (t, C-4), 28.9 (q, C-16, C-17), 21.7 (q, C-18), 20.8 (q, C-20), 20.4 (q, C-19), 19.2 (t, C-3).

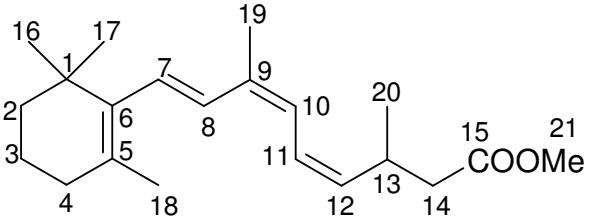

9,11-di-*cis*-**74**

^{1}H NMR (400 MHz, $CDCl_3$): δ = 6.60 (d, $^{3}J_{8,7}$ = 15.9 Hz, 1H, 8-H), 6.41 (t, $^{3}J_{11,10}$ = $^{3}J_{11,12}$ = 11.2 Hz, 1H, 11-H), 6.21 (d, $^{3}J_{10,11}$ = 11.2 Hz, 1H, 10-H), 6.17 (d, $^{3}J_{7,8}$ = 15.9 Hz, 1H, 7-H), 5.19 (t, $^{3}J_{12,11}$ = $^{3}J_{12,13}$ = 10.3 Hz, 1H, 12-H), 3.25-3.17 (m, 1H, 13-H), 2.40-2.26 (m, 2H, 14-H), 2.03 (t, $^{3}J_{4,3}$ = 6.0 Hz, 2H, 4-H), 1.97 (s, 3H, 19-H), 1.73 (s, 3H, 18-H), 1.66-1.58 (m, 2H, 3-H), 1.53-1.45 (m, 2H, 2-H), 1.08 (d, $^{3}J_{20,13}$ = 6.8 Hz, 3H, 20-H), 1.03 (s, 6H, 16-H, 17-H).

^{13}C NMR (100 MHz, $CDCl_3$): δ = 172.8 (s, C-15), 138.1 (s, C-6), 135.5 (d, C-12), 133.3 (s, C-5), 129.7 (d, C-8), 129.3 (s, C-9), 128.6 (d, C-7), 123.2 (d, C-11), 122.8 (d,

C-10), 41.5 (t, C-14), 39.5 (t, C-2), 34.1 (s, C-1), 32.96 (t, C-4), 29.1 (d, C-13), 28.9 (q, C-16, C-17), 21.72 (q, C-18), 20.8 (q, C-19), 20.2 (q, C-20),19.2 (t, C-3).

isomeric mixture:

MS [EI, 70 eV]: *m/z* (%) = 316 (18) [M^+], 301 (9) [M^+-CH_3], 260 [M^+-C_3H_4O], 243, 227 (10) [M^+-CH_3-$C_3H_6O_2$], 215 (10), 206 (5), 193 (8), 180 (10), 177 (30), 159 (17), 149 (17), 135 (20), 123 (98), 109 (57), 95 (45), 87 (40), 74 (100) [$C_3H_6O_2^+$], 69 (58), 55 (42) [$C_3H_3O^+$].

IR (ATR): $\tilde{\nu}$ = 2957 cm^{-1} (m), 2928 (m), 2867 (m), 1781 (C=O, s), 1682 (w), 1454 (m), 1437 (m), 1360 (m), 1252 (m), 1167 (s), 1008 (m), 968 (s).

UV (EtOH): λ_{max} (lg ε) = 227 nm (3.90), 290 (4.45).

HRMS: $C_{21}H_{32}O_2$ (316.48) calcd. 316.24023; found 316.20350 ± 2.27 ppm.

19-*d*$_3$-13,14-Dihydro-retinoic acid methyl ester (**87**):

General procedure 2 with LiHMDS [prepared from *n*BuLi (3.53 mL, 5.65 mmol) and HMDS (0.91 g, 1.18 mL, 5.65 mmol) in anhydrous THF (50 mL) at –78 °C], **66** (2.85 g, 5.65 mmol), **85** (1.0 g, 4.52 mmol) in anhydrous THF (10 mL). Column chromatography with pentane/diethyl ether 1:1 on Alox (activity III, 8 % water w/w) gave **87** (0.65 g, 2.04 mmol, 45 %) as a yellow oil.

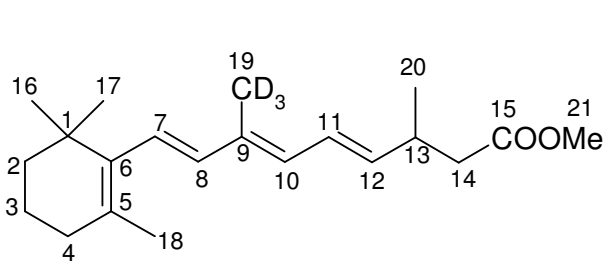

all-*trans*-**87**

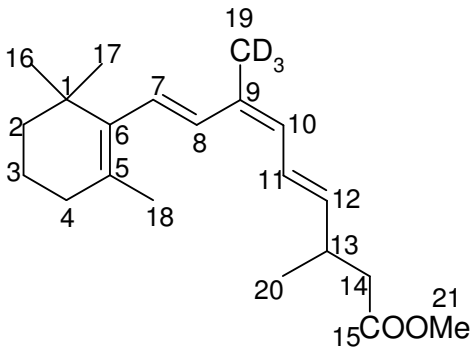

9-*cis*-**87**

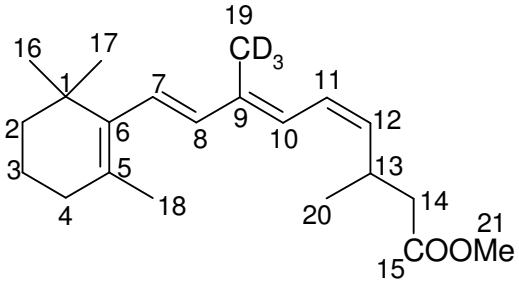

11-*cis*-**87**

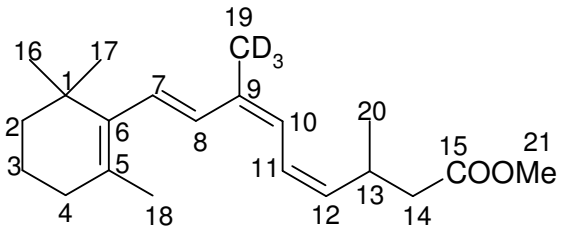

9,11-di-*cis*-**87**

^{1}H NMR ($CDCl_3$): δ = 1.73, 1.71, 1.69 (s, partially deuterated CHD_2, CH_2D and undeuterated CH_3, 19-H), all other signals correspond to **74**.

^{13}C NMR ($CDCl_3$): δ = 21.71, 21.69, 21.65, 21,59 (q, partially deuterated CHD_2, CH_2D and undeuterated CH_3, C-19), all other signals correspond to **74**.

MS [EI, 70 eV]: *m/z* (%) = 319 (60) [M^+, 15 % d_3], 318 (100) [M^+, 31 % d_2], 317 (90) [M^+, 35 % d_1], 316 (40) [M^+, 17 % d_0], 302 (30), 287 (5), 270 (5), 244 (25), 228 (26), 216 (30), 201 (20), 188 (42), 174 (50), 160 (80), 159 (74), 146 (60), 133 (70), 121 (90), 120 (80), 107 (65), 95 (60), 91 (55), 81 (70), 69 (78), 55 (63), 43 (25), 41 (80).

IR and **UV** spectra were identical with those of **74**.

13,14-Dihydro-retinoic acid (**10**):

General procedure 3 with **74** (0.56 g, 1.77 mmol), KOH (1.0 g, 17.7 mmol) in ethanol (20 mL) and water (10 mL) gave the four isomers all-*trans*-, 9-*cis*-, 11-*cis*-, 9,11-di-*cis*-**10** (0.55 mg, 1.73 mmol, 98 %) in 1.65:1.0:3.0:1.2 ratio, as a yellow oil.

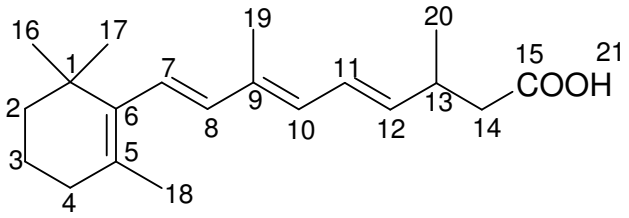

all-*trans*-**10**

^{1}H NMR (400 MHz, MeOH-d_4): δ = 6.45 (ddd, $^3J_{11,12}$ = 15.0, $^3J_{11,10}$ = 11.0, $^5J_{11,19}$ = 1.0 Hz, 1H, 11-H), 6.05 (d, $^3J_{7,8}$ = 16.5 Hz, 1H, 7-H), 6.02 (d, $^3J_{8,7}$ = 16.5 Hz, 1H, 8-H), 5.96 (d, $^3J_{10,11}$ = 11.0 Hz, 1H, 10-H), 5.65 (dd, $^3J_{12,13}$ = 15.0, $^3J_{12,13}$ = 7.6 Hz, 1H, 12-H), 2.79-2.66 (m, 1H, 13-H), 2.37-2.25 (m, 2H, 14-H), 2.01 (t, $^3J_{4,3}$ = 5.9 Hz, 2H, 4-H), 1.87

(d, $^{5}J_{19,11}$ = 1.0 Hz, 3H, 19-H), 1.67 (s, 3H, 18-H), 1.72-1.55 (m, 2H, 3-H), 1.53-1.40 (m, 2H, 2-H), 1.09 (d, $^{3}J_{20,13}$ = 6.8 Hz, 3H, 20-H), 1.01 (s, 6H, 16-H, 17-H).

^{13}C NMR (100 MHz, MeOH-d_4): δ = 176.23 (s, C-15), 139.4 (d, C-12), 139.2 (s, C-6), 139.3 (d, C-8), 130.0 (s, C-5), 131.1 (d, C-10), 129.7 (s, C-9), 127.0 (d, C-7), 126.9 (d, C-11), 42.6 (t, C-14), 40.8 (t, C-2), 35.2 (s, C-1), 35.3 (d, C-13), 33.9 (t, C-4), 29.5 (q, C-16, C-17), 22.0 (q, C-18), 20.7 (q, C-20), 20.4 (t, C-3), 12.7 (q, C-19).

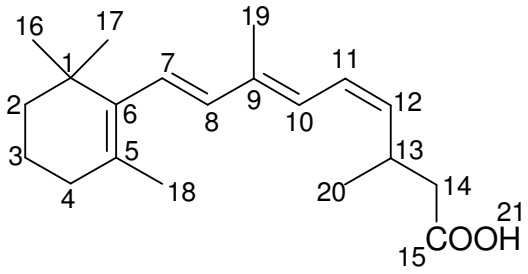

11-*cis*-**10**

^{1}H NMR (400 MHz, MeOH-d_4): δ = 6.32-6.31 (m, 2H, 10-H, 11-H), 6.13 (d, $^{3}J_{8,7} \approx$ 16 Hz, 1H, 8-H), 6.15 (d, $^{3}J_{7,8} \approx$ 16 Hz, 1H, 7-H), 5.29 (t, $^{3}J_{12,11} = {}^{3}J_{12,13} \approx$ 10 Hz, 1H, 12-H), 3.26-3.10 (m, 1H, 13-H), 2.33-2.20 (m, 2H, 14-H), 2.01 (t, $^{3}J_{4,3}$ = 5.9 Hz, 2H, 4-H), 1.88 (s, 3H, 19-H), 1.69 (s, 3H, 18-H), 1.72-1.55 (m, 2H, 3-H), 1.53-1.40 (m, 2H, 2-H), 1.05 (d, $^{3}J_{20,13}$ = 6.7 Hz, 3H, 20-H), 1.01 (s, 6H, 16-H, 17-H).

^{13}C NMR (100 MHz, MeOH-d_4): δ = 176.26 (s, C-15), 139.5 (d, C-8), 139.1 (s, C-6), 135.2 (s, C-5), 136.95 (d, C-12), 129.9 (s, C-9), 127.6 (d, C-7), 125.9 (d, C-10), 125.3 (d, C-11), 42.8 (t, C-14), 40.8 (t, C-2), 35.2 (s, C-1), 33.9 (t, C-4), 30.5 (d, C-13), 29.5 (q, C-16, C-17), 22.0 (q, C-18), 21.2 (q, C-20), 20.4 (t, C-3), 12.5 (q, C-19).

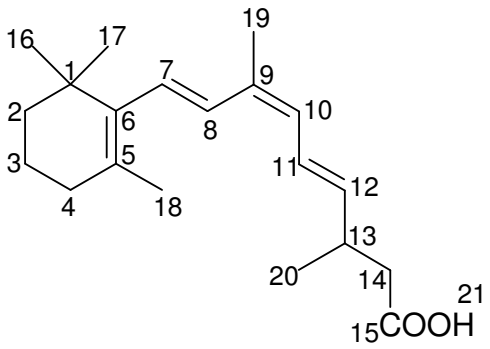

9-*cis*-**10**

^{1}H NMR (400 MHz, MeOH-d_4): δ = 6.60 (d, $^3J_{8,7}$ = 16.0 Hz, 1H, 8-H), 6.51 (dd, $^3J_{11,12}$ = 15.0, $^3J_{11,10}$ = 11.1 Hz, 1H, 11-H), 6.20 (d, $^3J_{7,8}$ = 16.0 Hz, 1H, 7-H), 5.89 (d, $^3J_{10,11}$ = 11.1 Hz, 1H, 10-H), 5.58 (dd, $^3J_{12,11}$ = 15.0, $^3J_{12,13}$ = 7.6 Hz, 1H, 12-H), 2.76-2.65 (m, 1H, 13-H), 2.31-2.24 (m, 2H, 14-H), 2.04 (t, $^3J_{4,3}$ = 6.1 Hz, 2H, 4-H), 1.95 (s, 3H, 19-H), 1.72 (s, 3H, 18-H), 1.68-1.61 (m, 2H, 3-H), 1.51-1.47 (m, 2H, 2-H), 1.07 (d, $^3J_{20,13}$ = 6.7 Hz, 3H, 20-H), 1.03 (s, 6H, 16-H, 17-H).

^{13}C NMR (100 MHz, MeOH-d_4): δ = 176.3 (s, C-15), 139.3 (s, C-6), 138.6 (d, C-12), 135.5 (s, C-5), 131.2 (d, C-8), 130.1 (s, C-9), 129.6 (d, C-10), 129.57 (d, C-7), 125.7 (d, C-11), 42.6 (t, C-14), 40.8 (t, C-2), 35.2 (s, C-1), 35.2 (d, C-13), 33.9 (t, C-4), 29.5 (q, C-16, C-17), 22.05 (q, C-18), 21.02 (q, C-19), 20.7 (q, C-20), 20.4 (t, C-3).

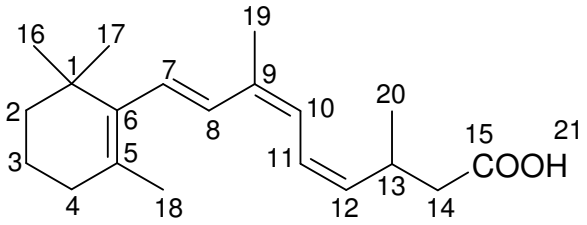

9,11-di-*cis*-**10**

^{1}H NMR (400 MHz, MeOH-d_4): δ = 6.58 (d, $^3J_{8,7}$ = 16.4 Hz, 1H, 8-H), 6.38 (t, $^3J_{11,10}$ = $^3J_{11,12}$ = 11.5 Hz, 1H, 11-H), 6.25 (d, $^3J_{10,11}$ = 11.5 Hz, 1H, 10-H), 6.14 (d, $^3J_{7,8}$ = 16.4 Hz, 1H, 7-H), 5.22 (t, $^3J_{12,11}$ = $^3J_{12,13}$ = 10.5 Hz, 1H, 12-H), 3.24-3.12 (m, 1H, 13-H), 2.31-2.24 (m, 2H, 14-H), 2.04 (t, $^3J_{4,3}$ = 6.1 Hz, 2H, 4-H), 1.89 (s, 3H, 19-H), 1.70 (s, 3H, 18-H), 1.68-1.61 (m, 2H, 3-H), 1.51-1.47 (m, 2H, 2-H), 1.05 (d, $^3J_{20,13}$ = 6.8 Hz, 3H, 20-H), 1.02 (s, 6H, 16-H, 17-H).

^{13}C NMR (100 MHz, MeOH-d_4): δ = 176.3 (s, C-15), 139.3 (s, C-6), 136.1 (d, C-12), 133.8 (s, C-5), 131.5 (d, C-8), 130.3 (s, C-9), 128.8 (d, C-7), 124.04 (d, C-11), 124.3 (d, C-10), 42.9 (t, C-14), 40.8 (t, C-2), 35.2 (s, C-1), 33.9 (t, C-4), 30.35 (d, C-13), 29.5 (q, C-16, C-17), 22.02 (q, C-18), 21.2 (q, C-20), 20.7 (q, C-19), 20.4 (t, C-3).

isomeric mixture:

MS [EI, 70 eV]: *m/z* (%) = 302 (18) [M^+], 287 (10) [M^+-CH_3], 243 (10) [M^+-CH_2COOH], 227 (5), 215 (10), 205 (5), 187 (9), 173 (10), 159 (18), 145 (20), 133 (15), 119 (27), 105 (23), 91 (36), 77 (30), 69 (30), 55 (30), 43 (100).

IR (ATR): $\tilde{\nu}$ = 3402 cm^{-1} (br. COOH), 2961 (m), 2929 (m), 2868 (m), 1706 (s) (C=O), 1454 (m), 1381 (m), 1172 (m), 1126 (m), 1083 (m), 1045 (m), 968 (m), 880 (w), 762 (w), 613 (m).

UV (EtOH): λ_{max} (lg ε) = 233 nm (3.83), 289 (4.14) .

HRMS: $C_{20}H_{30}O_2$ (302.46) calcd. 302.22458; found 302.22425 ± 1.092 ppm.

19-*d*$_3$-13,14-Dihydro-retinoic acid (**88**):

General procedure 3 with **87** (0.65 g, 2.04 mmol), KOH (1.14 g, 20.4 mmol) in ethanol (10 mL) and water (5 mL) gave **88** (0.41 g, 1.34 mmol, 66 %).

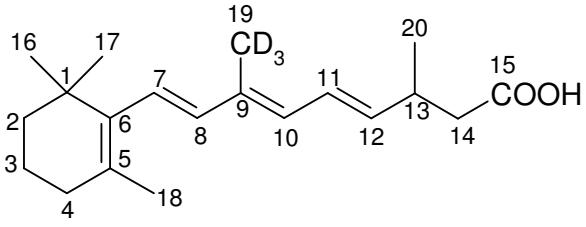

all-*trans*-**88**

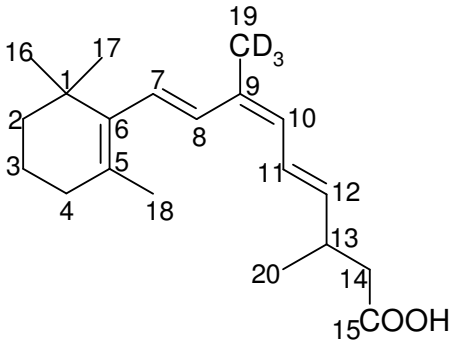

9-*cis*-**88**

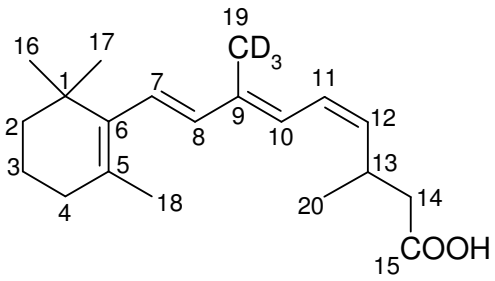

11-*cis*-**88**

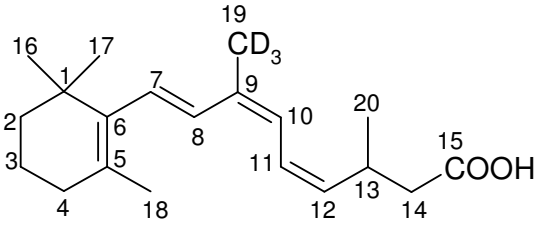

9,11-di-*cis*-**88**

^{1}H NMR (MeOH-*d*$_4$): δ = 1.73, 1.71, 1.69 (s, partially deuterated CHD_2, CH_2D and undeuterated CH_3, 19-H), all other signals correspond to **10**.

^{13}C NMR (MeOH-*d*$_4$): δ = 21.71, 21.69, 21.65, 21,59 (q, partially deuterated CHD_2, CH_2D and undeuterated CH_3, C-19), all other signals correspond to **10**.

MS [EI, 70 eV]: *m/z* (%) = 305 (50) [M^+, 15 % d_3], 304 (90) [M^+, 32 % d_2], 303 (87) [M^+, 35 % d_1], 302 (36) [M^+, 16 % d_0], 288 (30), 262 (5), 244 (20), 219 (20), 216 (30), 202 (20), 189 (40), 188 (43), 173 (57), 160 (95), 147 (77), 133 (80), 121 (90), 107 (83), 91 (100), 81 (80), 69 (100), 55 (90), 51 (40).

IR and **UV** spectra were identical with those of **10**.

4-Oxo-13,14-dihydro-retinoic acid methyl ester (**75**):

General procedure 2 with LiHMDS [prepared from *n*BuLi (3.34 mL, 5.34 mmol) and HMDS (0.862 g, 1.11 mL, 5.34 mmol) in anhydrous THF (50 mL) at –78 °C], **66** (2.69 g, 5.34 mmol), **53** (1.0 g, 4.27 mmol) in anhydrous THF (10 mL). Column chromatography with pentane/diethyl ether 3:1 on Alox (activity III, 8 % water w/w, R_f = 0.27-0.23) gave **75** (0.87 g, 2.64 mmol, 62 %) as a yellow oil. Isomer ratio all-*trans*-, 9-*cis*-, 11-*cis*-, 9,11-di-*cis*-**75**: 2.0:1.0:3.4:1.0 by NMR analysis. When all-*trans*-**53** was used, all-*trans*- and 11-*cis*-**75** were obtained in 1.0:1.5 ratio, while 9-*cis*-**53** gave 9-*cis*- and 9,11-di-*cis*-**75** in 1.0:1.3 ratio.

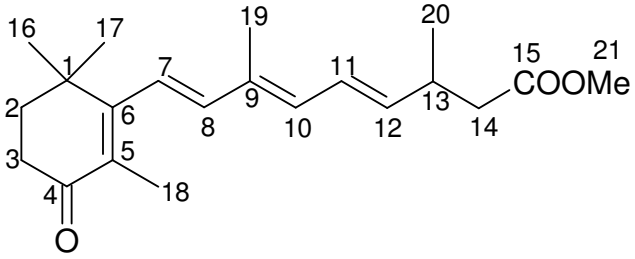

all-*trans*-**75**

^{1}H NMR (400 MHz, $CDCl_3$): δ = 6.44 (dd, $^3J_{11,12}$ = 15.0, $^3J_{11,10}$ = 11.0 Hz, 1H, 11-H), 6.31 (d, $^3J_{8,7}$ = 16.2 Hz, 1H, 8-H), 6.23 (d, $^3J_{7,8}$ = 16.2 Hz, 1H, 7-H), 6.10 (d, $^3J_{10,11}$ = 11.0 Hz, 1H, 10-H), 5.74 (dd, $^3J_{12,11}$ = 15.0, $^3J_{12,13}$ = 7.7 Hz, 1H, 12-H), 2.86-2.76 (m, 1H, 13-H), 2.49 (t, $^3J_{3,2}$ = 6.8 Hz, 2H, 3-H), 2.34 (m, 2H, 14-H), 1.93 (s, 3H, 19-H), 1.85 (t, $^3J_{2,3}$ = 6.8 Hz, 2H, 2-H), 1.84 (s, 3H, 18-H), 1.18 (s, 6H, 16-H, 17-H), 1.10 (d, $^3J_{20,13}$ = 6.8 Hz, 3H, 20-H).

^{13}C NMR (100 MHz, $CDCl_3$): δ = 199.5 (s, C-4), 172.9 (s, C-15), 161.6 (s, C-6), 141.3 (d, C-8), 140.6 (d, C-12), 135.4 (s, C-5), 133.7 (d, C-10), 130 (s, C-9), 125.8 (d, C-11), 124.1 (d, C-7), 41.7 (t, C-14), 37.6 (t, C-2), 36.0 (s, C-1), 34.5 (d, C-13), 34.4 (t, C-3), 27.9 (q, C-16, C-17), 20.4 (q, C-20), 14.0 (q, C-18), 12.7 (q, C-19).

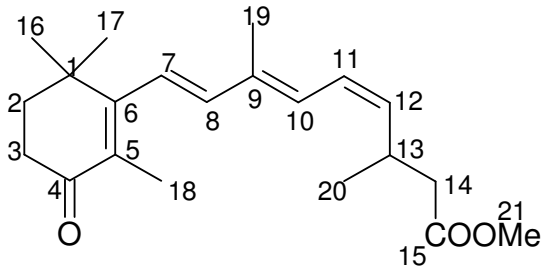

11-*cis*-**75**

^{1}H NMR (400 MHz, $CDCl_3$): δ = 6.43 (d, $^{3}J_{10,11}$ = 11.7 Hz, 1H, 10-H), 6.35 (d, $^{3}J_{8,7}$ = 16.2 Hz, 1H, 8-H), 6.33 (t, $^{3}J_{11,10}$ = $^{3}J_{11,12}$ = 11.2 Hz, 1H, 11-H), 6.27 (d, $^{3}J_{7,8}$ = 16.2 Hz, 1H, 7-H), 5.38 (t, $^{3}J_{12,11}$ = $^{3}J_{12,13}$ = 10.4 Hz, 1H, 12-H), 3.27-3.16 (m, 1H, 13-H), 2.52 (m, 2H, 3-H), 2.33 (m, 2H, 14-H), 1.93 (s, 3H, 19-H), 1.83 (m, 2H, 2-H), 1.86 (s, 3H, 18-H), 1.19 (s, 6H, 16-H, 17-H), 1.07 (d, $^{3}J_{20,13}$ = 6.7 Hz, 3H, 20-H).

^{13}C NMR (100 MHz, $CDCl_3$): δ = 199.5 (s, C-4), 172.9 (s, C-15), 161.5 (s, C-6), 141.4 (d, C-8), 140.6 (d, C-12), 137.9 (s, C-5), 130.1 (s, C-9), 128.2 (d, C-10), 124.7 (d, C-7), 124.2 (d, C-11), 41.96 (t, C-14), 37.7 (t, C-2), 36.0 (s, C-1), 34.5 (t, C-3), 29.8 (d, C-13), 27.9 (q, C-16, C-17), 21.1 (q, C-20), 14.0 (q, C-18), 12.5 (q, C-19).

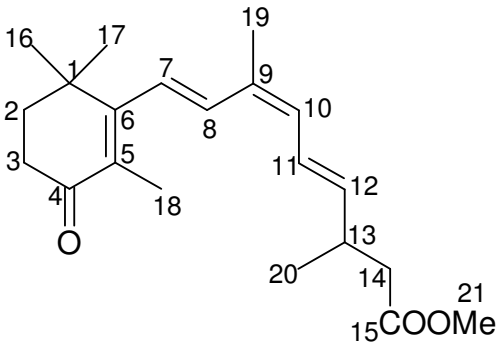

9-*cis*-**75**

^{1}H NMR (400 MHz, $CDCl_3$): δ = 6.79 (d, $^{3}J_{8,7}$ = 16.2 Hz, 1H, 8-H), 6.47 (dd, $^{3}J_{11,12}$ = 14.9, $^{3}J_{11,10}$ = 11.2 Hz, 1H, 11-H), 6.25 (d, $^{3}J_{7,8}$ = 16.2 Hz, 1H, 7-H), 6.04 (d, $^{3}J_{10,11}$ = 11.2 Hz, 1H, 10-H), 5.66 (dd, $^{3}J_{12,11}$ = 14.9, $^{3}J_{12,13}$ = 7.6 Hz, 1H, 12-H), 2.82-2.72 (m, 1H, 13-H), 2.54-2.49 (m, 2H, 3-H), 2.36-2.25 (m, 2H, 14-H), 1.94 (s, 3H, 19-H), 1.88 (s, 3H, 18-H), 1.87-1.84 (m, 2H, 2-H),1.19 (s, 6H, 16-H, 17-H), 1.09 (d, $^{3}J_{20,13}$ = 6.8 Hz, 3H, 20-H).

^{13}C NMR (100 MHz, $CDCl_3$): δ = 199.3 (s, C-4), 172.7 (s, C-15), 161.3 (s, C-6), 139.2 (d, C-12), 133.6 (s, C-5), 132.9 (d, C-8), 132.7 (d, C-10), 130.0 (s, C-9), 126.32 (d, C-7), 125.2 (d, C-11), 41.4 (t, C-14), 37.3 (t, C-2), 35.7 (t, C-3), 34.3 (d, C-13), 34.1 (s, C-1), 27.6 (q, C-16, C-17), 25.3 (q, C-20), 20.1 (q, C-19), 13.8 (q, C-18).

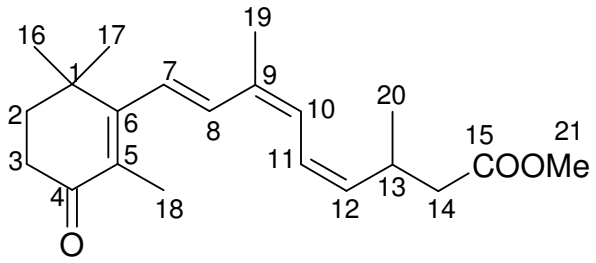

9,11-di-*cis*-**75**

^{1}H NMR (400 MHz, $CDCl_3$): δ = 6.82 (d, $^{3}J_{8,7}$ = 16.2 Hz, 1H, 8-H), 6.38 (d, $^{3}J_{10,11}$ = 11.5 Hz, 1H, 10-H), 6.37 (t, $^{3}J_{11,10}$ = $^{3}J_{11,12}$ = 10.6 Hz, 1H, 11-H), 6.21 (d, $^{3}J_{7,8}$ = 16.2 Hz, 1H, 7-H), 5.30 (t, $^{3}J_{12,11}$ = $^{3}J_{12,13}$ = 9.7 Hz, 1H, 12-H), 3.16-3.28 (m, 1H, 13-H), 2.54-2.49 (m, 2H, 3-H), 2.25-2.36 (m, 2H, 14-H), 2.05 (s, 3H, 19-H), 1.84-1.87 (m, 2H, 2-H), 1.86 (s, 3H, 18-H), 1.18 (s, 6H, 16-H, 17-H), 1.06 (d, $^{3}J_{20,13}$ = 6.7 Hz, 3H, 20-H).

^{13}C NMR (100 MHz, $CDCl_3$): δ = 199.3 (s, C-4), 172.7 (s, C-15), 161.4 (s, C-6), 136.6 (d, C-12), 134.22 (d, C-8), 133.8 (s, C-5), 129.9 (s, C-9), 127.7 (d, C-10), 127.2 (d, C-7), 123 (d, C-11), 41.7 (t, C-14), 37.3 (t, C-2), 34.1 (s, C-1), 35.7 (t, C-3), 29.2 (d, C-13), 27.6 (q, C-16, C-17), 20.8 (q, C-20), 20.1 (q, C-19), 13.8 (q, C-18).

isomeric mixture:

MS [EI, 70 eV]: *m/z* (%) = 330 (30) [M^+], 315 (90) [M^+-CH_3], 299 (10), 283 (18), 265 (17), 257 (15), 241 (27), 229 (20), 206 (40), 187 (20), 173 (30), 163 (100), 145 (30), 137 (35), 133 (50), 121 (57), 199 (60), 109 (50), 95 (50), 91 (70), 77 (50), 67 (42), 55 (45).

IR (ATR): $\tilde{\nu}$ = 2958 cm^{-1} (m), 2924 (m), 2869 (s), 1736 (C=O, s), 1659 (C=O, s), 1582 (w), 1437 (m), 1351 (m), 1279 (m), 1197 (s), 969 (s).

UV (EtOH): λ_{max} (lg ε) = 255 nm (4.16), 314 (4.08).

HRMS: $C_{21}H_{30}O_3$ (330.47) calcd. 330.21948; found 330.21939 ± 1,1 ppm.

19-d_3-4-Oxo-13,14-dihydro-retinoic acid methyl ester (**89**):

General procedure 2 with LiHMDS [prepared from *n*BuLi (3.32 mL, 5.31 mmol) and HMDS (0.86 g, 1.11 mL, 5.31 mmol) in anhydrous THF (50 mL) at –78 °C], **66** (2.7 g, 5.31 mmol), **86** (1.0 g, 4.25 mmol) in anhydrous THF (10 mL). Column chromatography with pentane/diethyl ether 5:1 on Alox (activity III, 8 % water w/w) gave **89** (0.45 g, 1.35 mmol, 32 %) as a yellow oil.

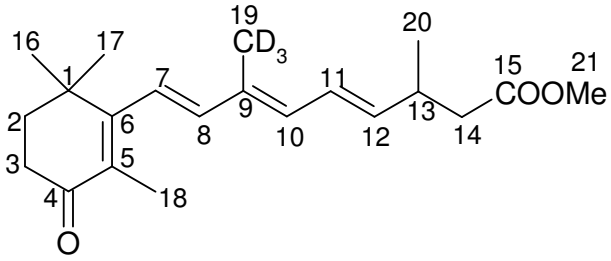

all-*trans*-**89**

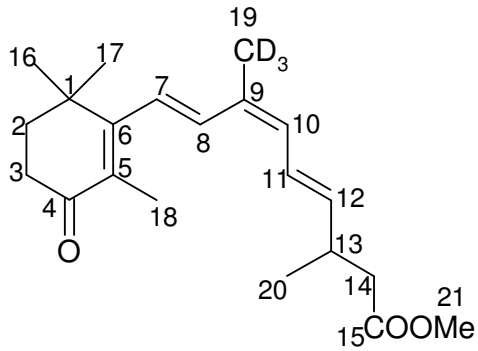

9-*cis*-**89**

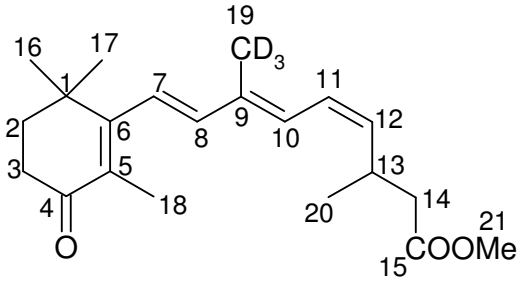

11-*cis*-**89**

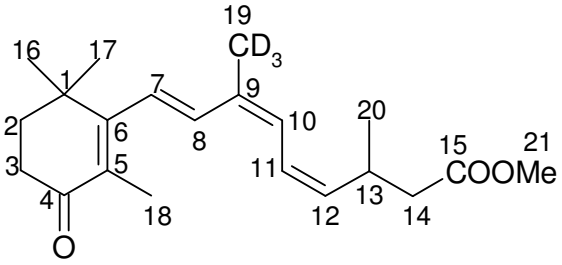

9,11-di-*cis*-**89**

^{1}H NMR (CDCl$_3$): δ = 1.95-1.91 (s, partially deuterated CHD_2, CH_2D and undeuterated CH_3, 19-H), all other signals correspond to **75**.

^{13}C NMR (CDCl$_3$): δ = 20.1 and 19.0 (q, 9-*cis*- and 9,11-di-*cis*-**89** partially deuterated C-19), 11.8 and 11.7 (q, all-*trans*- and 11-*cis*-**89** partially deuterated C-19), all other signals correspond to **75**.

MS [EI, 70 eV]: *m/z* (%) = 333 (8) [M^+, 4 % d_3], 332 (20) [M^+, 14 % d_2], 331 (40) [M^+, 38 % d_1], 330 (38) [M^+, 44 % d_0], 315 (100), 299 (15), 283 (20), 265 (20), 257 (18), 241 (37), 229 (23), 215 (25), 203 (30), 201 (30), 187 (30), 173 (40), 157 (43), 145 (43), 134 (50), 129 (62), 119 (55), 105 (43), 95 (50), 91 (78), 77 (50), 69 (62), 55 (50), 43 (70).

IR and **UV** spectra were identical with those of **75**.

4-Oxo-13,14-dihydro-retinoic acid (**11**):

Method A:

General procedure 3 with KOH (747 mg, 13.3 mmol), **75** (440 mg, 1.33 mmol) in ethanol (10 mL) and water (5 mL) gave **11** (0.38 g, 1.2 mmol, 91 %) as a yellow oil. Ratio all-*trans*-, 11-*cis*-**11**: 1.25:1.0; 9-*cis*-, 9,11-di-*cis*-**11**: 1.0:1.2 or as all four isomers all-*trans*-, 11-*cis*-, 9-*cis*-, 9,11-di-*cis*-**11** in 2.2:1.0:3.1:1.2 ratio.

Method B:

In a Schlenk tube, phosphonium salt **38** (1.75g, 3.16 mmol) was stirred under argon with KO*t*Bu (0.44 g, 3.95 mmol) in anhydrous THF (45 mL) for 30 min, followed by addition of **43** (0.5 g, 3.16 mmol) in anhydrous THF (30 mL) and stirring of the reaction mixture overnight. After extraction with diethyl ether/water, the organic phase was dried with Na_2SO_4, and the solvents were evaporated. The product was purified by column chromatography on Alox with pentane/diethyl ether 4:1 (R_f = 0.28) and further saponified with KOH in ethanol/water at 70 °C for 3 h to give **11** (70 mg, 0.22 mmol, 7 %) in all-*trans*-, 9-*cis*-, 11-*cis*-, 9,11-di-*cis*-ratio = 8.0:1.5:2.0:1.0, determined by ^{1}H NMR analysis.

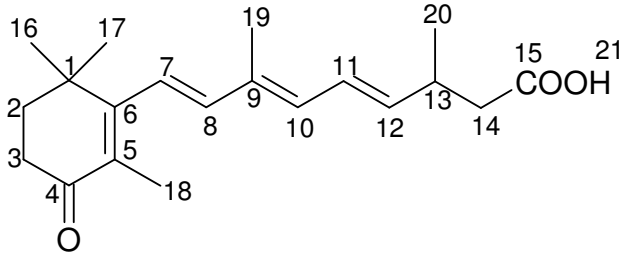

all-*trans*-**11**

^{1}H NMR (MeOH-d_4): δ = 6.49 (dd, $^3J_{11,12}$ = 15.0 Hz, $^3J_{11,10}$ = 11.0 Hz, 1H, 11-H), 6.34 (d, $^3J_{8,7}$ = 16.2 Hz, 1H, 8-H), 6.27 (d, $^3J_{7,8}$ = 16.2 Hz, 1H, 7-H), 6.15 (d, $^3J_{10,11}$ = 11.0 Hz, 1H, 10-H), 5.78 (dd, $^3J_{12,11}$ = 15.0, $^3J_{12,13}$ = 7.7 Hz, 1H, 12-H), 2.76 (m, 1H, 13-H), 2.49 (t, $^3J_{3,2}$ = 6.9 Hz, 2H, 3-H), 2.35 (dd, $^2J_{14,14}$ = 14.9, $^3J_{14,13}$ = 7.4 Hz, 1H, 14-H), 2.31 (dd, $^2J_{14,14}$ = 14.9, $^3J_{14,13}$ = 7.1 Hz, 1H, 14-H), 1.94 (s, 3H, 19-H), 1.86 (t, $^3J_{2,3}$ = 6.9 Hz, 2H, 2-H), 1.81 (s, 3H, 18-H), 1.20 (s, 6H, 16-H, 17-H), 1.11 (d, $^3J_{20,13}$ = 6.9 Hz, 3H, 20-H).

^{13}C NMR (MeOH-d_4): δ = 201.5 (s, C-4), 175.9 (s, C-15), 164.3 (s, C-6), 142.7 (d, C-8), 141.8 (d, C-12), 134.7 (d, C-10), 134.3 (s, C-5), 130.22 (s, C-9), 126.6 (d, C-11),

124.6 (d, C-7), 42.4 (t, C-14), 38.3 (t, C-2), 36.9 (s, C-1), 35.4 (d, C-13), 35.1 (t, C-3), 27.9 (q, C-16, C-17), 20.6 (q,C-20), 14.0 (q, C-18), 12.3 (q, C-19).

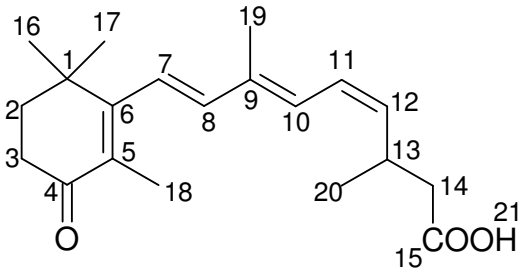

11-*cis*-**11**

^{1}H NMR (MeOH-d$_4$): δ = 6.52 (d, $^3J_{10,11}$ = 11.4 Hz, 1H, 10-H), 6.41 (d, $^3J_{8,7}$ = 16.2 Hz, 1H, 8-H), 6.37 (t, $^3J_{11,10}$ = $^3J_{11,12}$ = 11.5 Hz, 1H, 11-H), 6.32 (d, $^3J_{7,8}$ = 16.2 Hz, 1H, 7-H), 5.42 (t, $^3J_{12,11}$ = 10.5 Hz, 1H, 12-H), 3.18-3.23 (m, 1H, 13-H), 2.50 (t, $^3J_{3,2}$ = 7.0 Hz, 2H, 3-H), 2.34 (dd, $^2J_{14,14}$ = 15.7, $^3J_{14,13}$ = 7.2 Hz, 1H, 14-H), 2.30 (dd, $^2J_{14,14}$ = 15.7, $^3J_{14,13}$ = 6.3 Hz, 1H, 14-H), 1.94 (s, 3H, 19-H), 1.87 (t, $^3J_{2,3}$ = 7.0 Hz, 2H, 2-H), 1.82 (s, 3H, 18-H), 1.21 (s, 6H, 16-H, 17-H), 1.14 (d, $^3J_{20,13}$ = 6.2 Hz, 3H, 20-H).

^{13}C NMR (MeOH-d$_4$): δ = 201.4 (s, C-4), 175.9 (s, C-15), 164.2 (s, C-6), 142.7 (d, C-8), 139.1 (d, C-12), 136.0 (s, C-5), 130.3 (s, C-9), 129.4 (d, C-10), 125.2 (d, C-7), 124.8 (d, C-11), 42.7 (t, C-14), 38.3 (t, C-2), 36.9 (s, C-1), 35.1 (t, C-3), 30.7 (d, C-13), 27.9 (q, C-16, C-17), 21.2 (q, C-20), 14.0 (q, C-18), 12.25 (q, C-19).

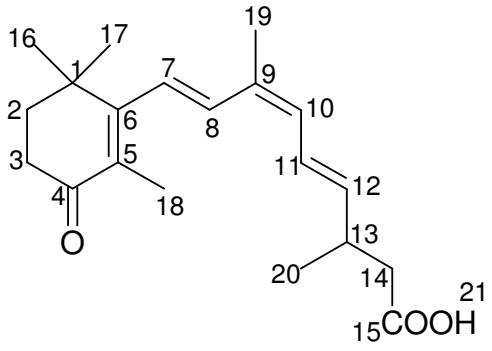

9-*cis*-**11**

^{1}H NMR (MeOH-*d*$_4$): δ = 6.82 (d, $^3J_{8,7}$ = 16.2 Hz, 1H, 8-H), 6.52 (dd, $^3J_{11,12}$ = 14.9, $^3J_{11,10}$ = 11.2 Hz, 1H, 11-H), 6.24 (d, $^3J_{7,8}$ = 16.2 Hz, 1H, 7-H), 6.09 (d, $^3J_{10,11}$ = 11.2 Hz, 1H, 10-H), 5.68 (dd, $^3J_{12,11}$ = 14.9, $^3J_{12,13}$ = 7.6 Hz, 1H, 12-H), 2.72 (m, 1H, 13-H), 2.51 (t, $^3J_{3,2}$ = 6.9 Hz, 2H, 3-H), 2.32 (dd, $^2J_{14,14}$ = 15.0, $^3J_{14,13}$ = 7.4 Hz, 1H, 14-H), 2.30

(dd, $^{2}J_{14,14}$ = 15.0, $^{3}J_{14,13}$ = 7.1 Hz, 1H, 14-H), 1.95 (s, 3H, 19-H), 1.88 (t, $^{3}J_{2,3}$ = 6.9 Hz, 2H, 2-H), 1.85 (s, 3H, 18-H), 1.21 (s, 6H, 16-H, 17-H), 1.14 (d, $^{3}J_{20,13}$ = 6.2 Hz, 3H, 20-H).

^{13}C NMR (MeOH-d_4): δ = 201.5 (s, C-4), 176.0 (s, C-15), 164.3 (s, C-6), 140.4 (d, C-12), 134.4 (d, C-8), 133.0 (s, C-5), 132.6 (d, C-10), 130.5 (s, C-9), 126.3 (d, C-7), 125.2 (d, C-11), 42.2 (t, C-14), 38.2 (t, C-2), 36.8 (s, C-1), 35.2 (d, C-13), 35.0 (t, C-3), 27.9 (q, C-16, C-17), 25.3 (q, C-20), 20.3 (q, C-19), 14.5 (q, C-18).

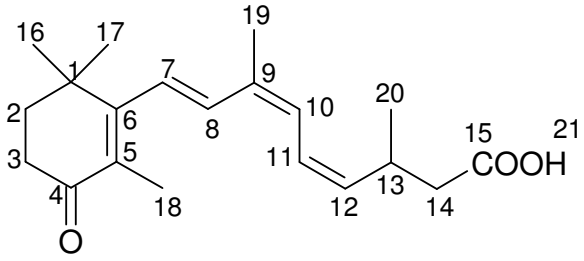

9,11-di-*cis*-**11**

^{1}H NMR (MeOH-d_4): δ = 6.86 (d, $^{3}J_{8,7}$ = 16.2 Hz, 1H, 8-H), 6.57 (d, $^{3}J_{10,11}$ = 11.5 Hz, 1H, 10-H), 6.37 (t, $^{3}J_{11,10}$ = $^{3}J_{11,12}$ = 11.5 Hz, 1H, 11-H), 6.32 (d, $^{3}J_{7,8}$ = 16.2 Hz, 1H, 7-H), 5.25 (t, $^{3}J_{12,11}$ = $^{3}J_{12,13}$ = 10.8 Hz, 1H, 12-H), 3.1 (m, 1H, 13-H), 2.41 (t, $^{3}J_{3,2}$ = 6.9 Hz, 2H, 3-H), 2.21 (dd, $^{2}J_{14,14}$ = 14.7, $^{3}J_{14,13}$ = 6.9 Hz, 1H, 14-H), 2.16 (dd, $^{2}J_{14,14}$ = 14.7, $^{3}J_{14,13}$ = 7.3 Hz, 1H, 14-H), 2.01 (s, 3H, 19-H), 1.89 (t, $^{3}J_{2,3}$ = 6.9 Hz, 2H, 2-H), 1.84 (s, 3H, 18-H), 1.21 (s, 6H, 16-H, 17-H), 1.03 (d, $^{3}J_{20,13}$ = 6.7 Hz, 3H, 20-H).

^{13}C NMR (MeOH-d_4): δ = 201.7 (s, C-4), 175.9 (s, C-15), 164.3 (s, C-6), 138.1 (d, C-12), 134.5 (s, C-5), 134.2 (d, C-8), 130.7 (s, C-9), 127.7 (d, C-10), 127.2 (d, C-7), 123.5 (d, C-11), 42.7 (t, C-14), 38.3 (t, C-2), 36.8 (s, C-1), 35.1 (t, C-3), 30.7 (d, C-13), 27.9 (q, C-16, C-17), 21.1 (q, C-20), 20.3 (q, C-19), 14.0 (q, C-18).

isomeric mixture:

MS [EI, 70 eV]: *m/z* (%) = 316 [M^+] (65), 301 (100), 283 (40), 265 (27), 261 (30), 247 (33), 241 (45), 229 (30), 215 (40), 201 (30), 187 (37), 173 (55), 159 (45), 145 (45), 133 (40), 119 (43), 105 (39), 91 (58), 77 (38), 69 (47), 55 (40).

IR (ATR): $\tilde{\nu}$ = 3431 cm^{-1} (br, OH), 2965 (m), 2930 (m), 2873 (w), 1779 (m), 1731 (s, C=O), 1661 (s, C=O), 1456 (w), 1375 (m), 1333 (m), 1199 (m), 1144 (m), 1089 (m), 973 (m).

UV (EtOH): λ_{max} (lg ε) = 256 nm (4.32), 332 (4.28).

HRMS: $C_{20}H_{28}O_3$ (316.44) calc: 316.20345; found: 316.20366 ± 1.45 ppm.

19-*d*$_3$-4-Oxo-13,14-dihydro-retinoic acid (**90**):

General procedure 3 with **89** (450 mg, 1.35 mmol), KOH (0.76 g, 13.5 mmol) in ethanol (10 mL) and water (5 mL) gave **90** in 75 % yield (0.32 g, 1 mmol).

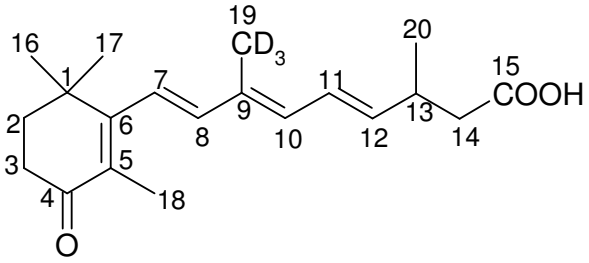

all-*trans*-**90**

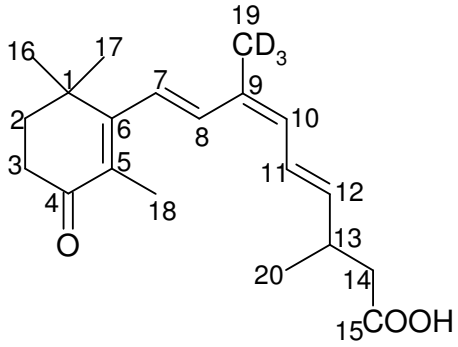

9-*cis*-**90**

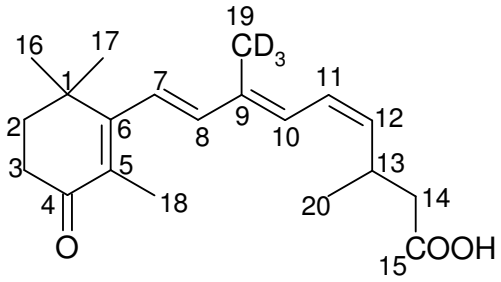

11-*cis*-**90**

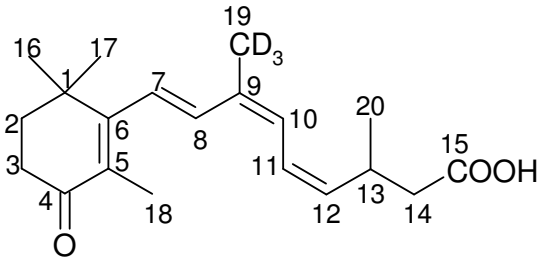

9,11-di-*cis*-**90**

^{1}H NMR (MeOH-*d*$_4$): δ = 1.95-1.92 (partially deuterated CHD_2, CH_2D and undeuterated CH_3, 19-H), all other signals correspond to **11**.

^{13}C NMR (MeOH-*d*$_4$): δ = 20.6, 20.2 (q, 9-*cis*- and 9,11-di-*cis*-**90** partially deuterated CHD_2, CH_2D and undeuterated CH_3, C-19), 12.4, 12.2 (q, all-*trans*- and 11-*cis*-**90** partially deuterated CHD_2, CH_2D and undeuterated CH_3, C-19), all other signals correspond to **11**.

MS [EI, 70 eV]: *m/z* (%) = 319 (8) [M^+, 4 % d_3], 318 (15) [M^+, 13 % d_2], 317 (40) [M^+, 37 % d_1], 316 (36) [M^+, 46 % d_0], 301 (78), 283 (38), 265 (20), 257 (10), 241 (40), 231 (25), 215 (20), 201 (30), 187 (30), 173 (42), 159 (40), 145 (44), 129 (50), 119 (50), 105 (47), 91 (72), 77 (57), 69 (58), 55 (50), 43 (75), 41 (100).

IR and **UV** spectra were identical with those of **11**.

13-Phenyl-13,14-dihydro-retinoic acid methyl ester (**78**):

General procedure 2 with LiHMDS [prepared from *n*BuLi (1.78 mL, 2.84 mmol) and HMDS (0.46 g, 0.59 mL, 2.84 mmol)], **73** (1.61 g, 2.84 mmol) in anhydrous THF (20 mL), **47** (0.5 g, 2.27 mmol) in anhydrous THF (10 mL). Column chromatography on Alox (8 % water w/w, activity III) with pentane (R_f = 0.65) gave **78** in 85 % yield (0.73 g, 1.93 mmol). Isomer ratio: all-*trans*-, 9-*cis*-, 11-*cis*-, 9,11-di-*cis*-**78** = 2.15:1.0:3.7:1.1 (by ^{1}H NMR analysis).

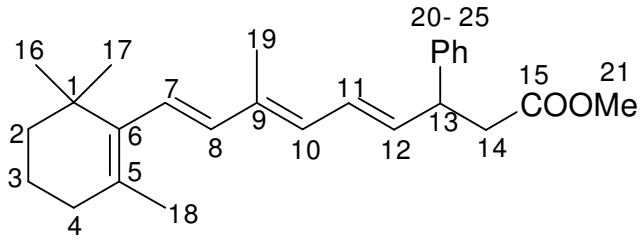

all-*trans*-**78**

^{1}H NMR ($CDCl_3$): δ = 7.40-7.16 (m, Ar), 6.45 (dd, $^3J_{11,12}$ = 15.0 , $^3J_{11,10}$ = 12.0 Hz, 1H, 11-H), 6.14 (d, $^3J_{8,7}$ = 16.1 Hz, 1H, 8-H), 6.12 (d, $^3J_{7,8}$ = 16.1 Hz, 1H, 7-H), 5.99 (d, $^3J_{10,11}$ = 12.0 Hz, 1H, 10-H), 5.83 (dd, $^3J_{12,11}$ = 15.0, $^3J_{12,13}$ = 7.8 Hz, 1H, 12-H), 3.96 (dd, $^3J_{13,12}$ = 7.8, $^3J_{13,14}$ = 6.9 Hz, 1H, 13-H), 3.62 (s, 3H, COO**CH$_3$**), 2.77 (d, $^3J_{14,13}$ = 6.9 Hz, 2H, 14-H), 2.02 (t, $^3J_{3,4}$ = 6.0 Hz, 2H, 4-H), 1.87 (s, 3H, 19-H), 1.67 (s, 3H, 18-H), 1.65-1.56 (m, 2H, 3-H), 1.50-1.43 (m, 2H, 2-H), 1.03 (s, 6H, 16-H, 17-H).

^{13}C NMR ($CDCl_3$): δ = 172.2 (s, C-15), 137.8 (s, C-6), 137.6 (d, C-5), 135.3 (d, C-12), 130.0 (d, C-8), 129.3 (s, C-9), 129.1 (d, C-10), 129.0-126.0 (Ar), 126.5 (d, C-7), 125.0 (d, C-11), 51.6 (q, COO**CH$_3$**), 45.1 (d, C-13), 41.3 (t, C-14), 39.5 (t, C-2), 34.2 (s, C-1), 33.0 (t, C-4), 28.9 (q, C-16, C-17), 21.7 (q, C-18), 19.3 (t, C-3), 12.6 (q, C-19).

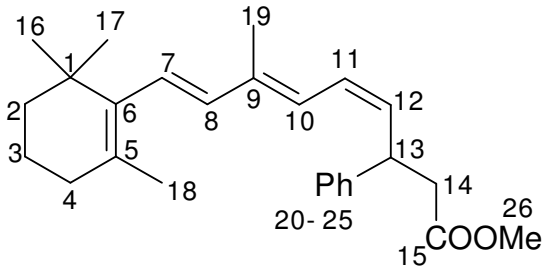

11-*cis*-**78**

^{1}H NMR ($CDCl_3$): δ = 7.40-7.16 (m, Ar), 6.48 (d, $^{3}J_{10,11}$ = 11.0 Hz, 1H, 10-H), 6.40 (t, $^{3}J_{11,10}$ = $^{3}J_{11,12}$ = 11.5 Hz, 1H, 11-H), 6.16 (d, $^{3}J_{8,7}$ = 16.2 Hz, 1H, 8-H), 6.02 (d, $^{3}J_{7,8}$ = 16.2 Hz, 1H, 7-H), 5.56 (t, $^{3}J_{12,11}$ = $^{3}J_{12,13}$ = 9.8 Hz, 1H, 12-H), 4.40-4.34 (m, 1H, 13-H), 3.59 (s, 3H, COO**C**$\mathbf{H_3}$), 2.71-2.65 (m, 2H, 14-H), 2.02 (t, $^{3}J_{4,3}$ = 6.0 Hz, 2H, 4-H), 1.90 (s, 3H, 19-H), 1.72 (s, 3H, 18-H), 1.62-1.56 (m, 2H, 3-H), 1.50-1.43 (m, 2H, 2-H), 1.03 (s, 6H, 16-H, 17-H).

^{13}C NMR ($CDCl_3$): δ = 172.1 (s, C-15), 137.8 (s, C-6), 137.2 (d, C-5), 132.5 (d, C-12), 129.3 (s, C-9), 129.0-126.0 (Ar), 127.7 (d, C-8), 127.0 (d, C-10), 126.6 (d, C-7), 125.0 (d, C-11), 51.6 (q, COO**C**$\mathbf{H_3}$), 41.3 (t, C-14), 40.1 (d, C-13), 39.5 (t, C-2), 34.2 (s, C-1), 33.0 (t, C-4), 28.9 (q, C-16, C-17), 21.7 (q, C-18), 19.3 (t, C-3), 12.4 (q, C-19).

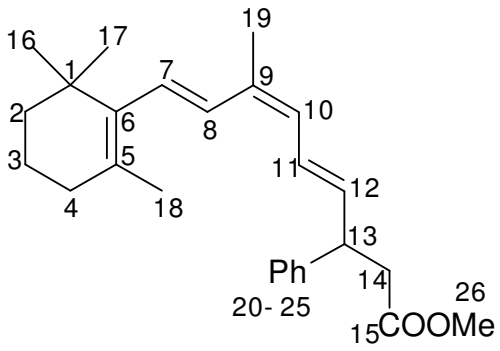

9-*cis*-**78**

^{1}H NMR ($CDCl_3$): δ = 7.40-7.16 (m, Ar), 6.59 (d, $^{3}J_{8,7}$ = 15.9 Hz, 1H, 8-H), 6.55 (dd, $^{3}J_{11,12}$ = 15.0, $^{3}J_{11,10}$ = 11.4 Hz, 1H, 11-H), 6.21 (d, $^{3}J_{7,8}$ = 16.0 Hz, 1H, 7-H), 5.89 (d, $^{3}J_{10,11}$ = 11.4 Hz, 1H, 10-H), 5.76 (dd, $^{3}J_{12,11}$ = 15.0, $^{3}J_{12,13}$ = 7.7 Hz, 1H, 12-H), 3.98-3.91 (m, 1H, 13-H), 3.62 (s, 3H, COO**C**$\mathbf{H_3}$), 2.74-2.72 (m, 2H, 14-H), 2.02 (t, $^{3}J_{4,3}$ = 6.0

Hz, 2H, 4-H), 1.90 (s, 3H, 19-H), 1.70 (s, 3H, 18-H), 1.65-1.56 (m, 2H, 3-H), 1.50-1.43 (m, 2H, 2-H), 1.03 (s, 6H, 16-H, 17-H).

^{13}C NMR ($CDCl_3$): δ = 172.2 (s, C-15), 137.8 (s, C-6), 135.7 (d, C-5), 134.4 (d, C-12), 129.4 (s, C-9), 129.0-126.0 (Ar), 127.5 (d, C-10), 126.7 (d, C-7), 126.0 (d, C-8), 125.9 (d, C-11), 51.6 (q, COO**C**H_3), 45.1 (d, C-13), 41.3 (t, C-14), 39.5 (t, C-2), 34.2 (s, C-1), 33.0 (t, C-4), 28.9 (q, C-16, C-17), 21.7 (q, C-18), 20.9 (q, C-19), 19.3 (t, C-3).

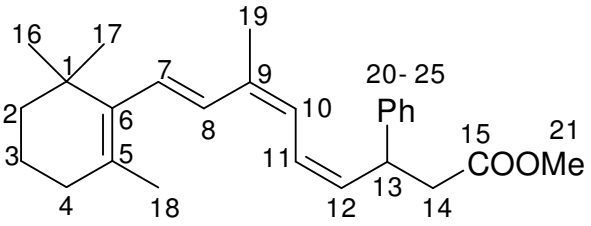

9,11-di-*cis*-**78**

^{1}H NMR ($CDCl_3$): δ = 7.40-7.16 (m, Ar), 6.54 (d, $^{3}J_{8,7}$ = 16.1 Hz, 1H, 8-H), 6.51 (t, $^{3}J_{11,10}$ = $^{3}J_{11,12}$ = 11.3 Hz, 1H, 11-H), 6.32 (d, $^{3}J_{10,11}$ = 12.1 Hz, 1H, 10-H), 6.14 (d, $^{3}J_{7,8}$ = 16.1 Hz, 1H, 7-H), 5.49 (t, $^{3}J_{12,11}$ = 10.5 Hz, 1H, 12-H), 4.40-4.34 (m, 1H, 13-H), 3.62 (s, 3H, COO**C**H_3), 2.82-2.79 (m, 2H, 14-H), 2.02 (t, $^{3}J_{4,3}$ = 6.0 Hz, 2H, 4-H), 1.90 (s, 3H, 19-H), 1.72 (s, 3H, 18-H), 1.65-1.56 (m, 2H, 3-H), 1.50-1.43 (m, 2H, 2-H), 1.03 (s, 6H, 16-H, 17-H).

^{13}C NMR ($CDCl_3$): δ = 172.1 (s, C-15), 137.8 (s, C-6), 132.5 (d, C-12), 134.0 (d, C-5), 130.0 (d, C-8), 129.4 (s, C-9), 129.0-126.0 (Ar), 127.0 (d, C-7), 126.0 (d, C-11), 122.5 (d, C-10), 51.6 (q, COO**C**H_3), 41.3 (t, C-14), 40.1 (d, C-13), 39.5 (t, C-2), 34.2 (s, C-1), 33.0 (t, C-4), 28.9 (q, C-16, C-17), 21.7 (q, C-18), 20.9 (q, C-19), 19.3 (t, C-3).

isomeric mixture:

MS [EI, 70 eV]: *m/z* (%) = 378 (15) [M^+], 363, 338, 305 (10), 277, 219 (10), 192 (14), 177 (85), 162 (32), 149 (23), 131 (70), 123 (100), 121 (80), 104 (70), 91 (72), 77 (83), 51 (38).

UV (HPLC, MeOH/H_2O 90:10): λ_{max} = 295 nm.

IR (ATR): $\tilde{\nu}$ = 3061 cm^{-1} (w), 3029 (m), 2953 (m), 2928 (m), 2864 (m), 2827 (w), 1740 (s, C=O), 1494 (m), 1451 (m), 1437 (m), 1359 (w), 1253 (m), 1204 (m), 1161 (m), 1027 (w), 968 (m), 752 (m), 699 (m).

HRMS: $C_{26}H_{34}O_2$ (378.55) calcd. 378.25589; found 378.25615 ± 1.58 ppm.

13-Phenyl-13,14-dihydro-retinoic acid (**82**):

General procedure 3 with **78** (0.4 g, 1.02 mmol), KOH (0.57 g, 10.2 mmol) in ethanol (10 mL) and water (5 mL) gave **82** as a yellow oil in 97 % yield (0.37 mg, 0.98 mmol). The NMR spectra show no or minimal chemical shift differences between ester **78** and acid **82**, for this reason a detailed assignement of each isomer is not given, the structure was assigned by MS-, IR- and UV analysis.

MS [EI, 70 eV]: *m/z* (%) = 364 (85) [M^+], 349 (15), 321 (10), 305 (30), 279 (10), 231 (20), 215 (60), 187 (20), 173 (20), 165 (30), 159 (57), 145 (50), 129 (50), 119 (52), 107 (76), 91 (100), 77 (58), 69 (42), 55 (37), 45 (25).

UV (HPLC, CH_3CN/H_2O 80:20): λ_{max} = 348 nm.

IR (ATR): $\tilde{\nu}$ = 3401 cm^{-1} (br. COOH, w), 3062 (w), 3031 (w), 2961 (m), 2931 (m), 2869 (m), 1708 (C=O, s), 1635 (m), 1495 (w), 1452 (m), 1375 (m), 1256 (m), 1201 (s), 1161 (s), 1079 (m), 1030 (m), 968 (m), 760 (m), 701 (s).

HRMS: $C_{25}H_{32}O_2$ (364.53) calcd. 364.24023; found 364.23968 ± 1.86 ppm.

4-Oxo-13-phenyl-13,14-dihydro-retinoic acid methyl ester (**79**):

General procedure 2 with LiHMDS [prepared from *n*BuLi (1.67 mL, 2.67 mmol) and HMDS (0.43 g, 0.56 mL, 2.67 mmol)], **73** (1.512 g, 2.67 mmol) in anhydrous THF (20 mL), **53** (0.5 g, 2.137 mmol) in anhydrous THF (10 mL). Column chromatography on Alox (8 % water w/w, activity III) with pentane/diethyl ether 3:1 (R_f = 0.24) gave **79** as a yellow oil in 82 % yield (0.161 g, 0.41 mmol).

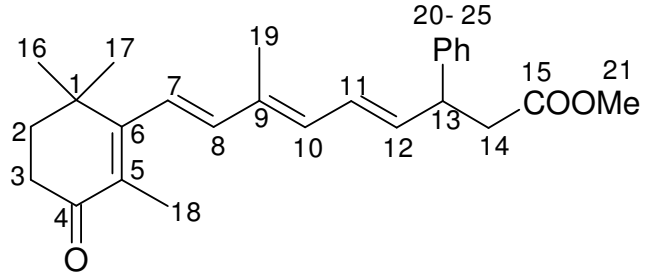

all-*trans*-**79**

^{1}H NMR ($CDCl_3$): δ = 7.35-7.18 (m, Ar), 6.46 (dd, $^3J_{11,12} \approx 15$, $^3J_{11,10} \approx 11$ Hz, 1H, 11-H), 6.23 (s, 2H, 7-H, 8-H), 6.14 (d, $^3J_{10,11} \approx 11$ Hz, 1H, 10-H), 5.93 (dd, $^3J_{12,11} \approx 15$, $^3J_{12,13} = 7.7$ Hz, 1H, 12-H), 4.01-3.94 (m, 1H, 13-H), 3.63 (s, 3H, COO**C**$\mathbf{H_3}$), 2.79-2.77 (m, 2H, 14-H), 2.49 (t, $^3J_{3,2} \approx 7$ Hz, 2H, 3-H), 1.90 (s, 3H, 19-H), 1.87 (t, $^3J_{2,3} \approx 7$ Hz, 2H, 2-H), 1.82 (s, 3H, 18-H), 1.16 (s, 6H, 16-H, 17-H).

^{13}C NMR ($CDCl_3$): δ = 199.3 (s, C-4), 172.0 (s, C-15), 161.3 (s, C-6), 141.0 (d, C-8), 137.7 (d, C-12), 136.0 (d, C-5), 134.1 (d, C-10), 129.8 (s, C-9), 128.7-126.7 (Ar), 126.8 (d, C-11), 124.8 (d, C-7), 51.5 (q, COO**C**$\mathbf{H_3}$), 40.5 (t, C-14), 39.8 (d, C-13), 37.4 (t, C-2), 35.7 (s, C-1), 34.3 (t, C-3), 27.6 (q, C-16, C-17), 13.8 (q, C-18), 12.4 (q, C-19).

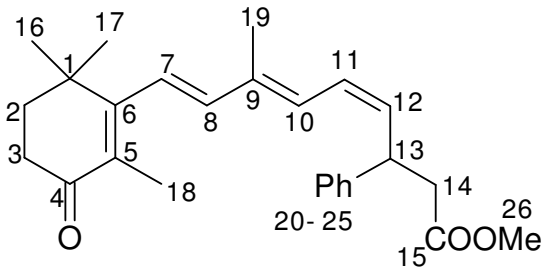

11-*cis*-**79**

^{1}H NMR ($CDCl_3$): δ = 7.35-7.18 (m, Ar), 6.53 (d, $^3J_{10,11} \approx 11$ Hz, 1H, 10-H), 6.43 (d, $^3J_{8,7} \approx 16$ Hz, 1H, 8-H), 6.38 (t, $^3J_{11,10} \approx {}^3J_{11,12} \approx 11$ Hz, 1H, 11-H), 6.36 (d, $^3J_{7,8} \approx 16$ Hz, 1H, 7-H), 5.68 (t, $^3J_{12,11} = {}^3J_{12,13} = 10.5$ Hz, 1H, 12-H), 4.41-4.35 (m, 1H, 13-H), 3.60 (s, 3H, COO**C**$\mathbf{H_3}$), 2.79-2.77 (m, 2H, 14-H), 2.53 (t, $^3J_{3,2} \approx 7$ Hz, 2H, 3-H), 1.91 (s, 3H, 19-H), 1.87 (t, $^3J_{2,3} \approx 7$ Hz, 2H, 2-H), 1.84 (s, 3H, 18-H), 1.16 (s, 6H, 16-H, 17-H).

^{13}C NMR ($CDCl_3$): δ = 199.34 (s, C-4), 172.1 (s, C-15), 161.2 (s, C-6), 140.9 (d, C-8), 136.0 (s, C-5), 134.5 (d, C-12), 129.8 (s, C-9), 128.7 (d, C-10), 128.7-126.7 (Ar), 125.4 (d, C-7), 124.8 (d, C-11), 51.6 (q, COO**C**$\mathbf{H_3}$), 41.1 (t, C-14), 39.8 (d, C-13), 37.3 (t, C-2), 35.7 (s, C-1), 34.3 (t, C-3), 27.6 (q, C-16, C-17), 13.8 (q, C-18), 12.3 (q, C-19).

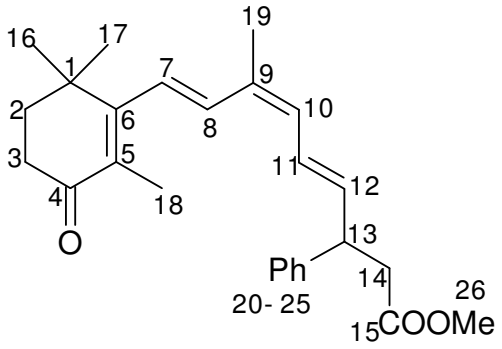

9-*cis*-**79**

^{1}H NMR ($CDCl_3$): δ = 7.35-7.18 (m, Ar), 6.75 (d, $^{3}J_{8,7} \approx 16$ Hz, 1H, 8-H), 6.47 (dd, $^{3}J_{11,12} \approx 15$, $^{3}J_{11,10} \approx 11$ Hz, 1H, 11-H), 6.19 (d, $^{3}J_{7,8} \approx 16$ Hz, 1H, 7-H), 6.08 (d, $^{3}J_{10,11} \approx$ 11 Hz, 1H, 10-H), 5.87 (dd, $^{3}J_{12,11} \approx 15$, $^{3}J_{12,13} \approx 7$ Hz, 1H, 12-H), 4.01-3.97 (m, 1H, 13-H), 3.61 (s, COO**CH_3**), 2.79-2.77 (m, 2H, 14-H), 2.50 (t, $^{3}J_{3,2} \approx 7$ Hz, 2H, 3-H), 1.91 (s, 3H, 19-H), 1.85 (t, $^{3}J_{2,3} \approx 7$ Hz, 2H, 2-H), 1.84 (s, 3H, 18-H), 1.16 (s, 6H, 16-H, 17-H).

^{13}C NMR ($CDCl_3$): δ = 199.4 (s, C-4), 172.1 (s, C-15), 161.2 (s, C-6), 137.7 (d, C-12), 134.1 (d, C-8), 133.6 (s, C-5), 132.8 (d, C-10), 129.9 (s, C-9), 128.7-126.7 (Ar), 126.7 (d, C-7), 125.8 (d, C-11), 51.6 (q, COO**CH_3**), 40.5 (t, C-14), 39.8 (d, C-13), 37.3 (t, C-3), 35.7 (s, C-1), 34.3 (t, C-2), 27.6 (q, C-16, C-17), 20.1 (q, C-19), 15.3 (q, C-18).

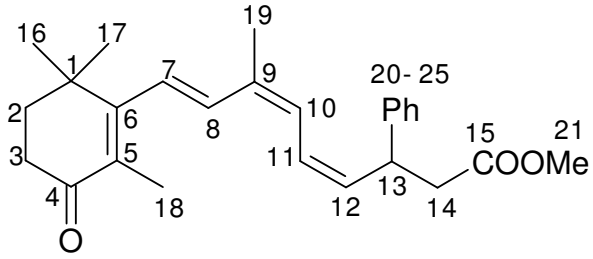

9,11-di-*cis*-**79**

^{1}H NMR ($CDCl_3$): δ = 7.35-7.18 (m, 5H, Ar), 6.80 (d, $^{3}J_{8,7} = 16.3$ Hz, 1H, 8-H), 6.53 (d, $^{3}J_{10,11} = 11.5$ Hz, 1H, 10-H), 6.35 (t, $^{3}J_{11,10} = {}^{3}J_{11,12} = 11.5$ Hz, 1H, 11-H), 6.27 (d, $^{3}J_{7,8} = 16.3$ Hz, 1H, 7-H), 5.59 (t, $^{3}J_{12,11} \approx {}^{3}J_{12,13} \approx 11$ Hz, 1H, 12-H), 4.41-4.35 (m, 1H, 13-H), 3.61 (s, 3H, COO**CH_3**), 2.51 (t, $^{3}J_{3,2} \approx 7$ Hz, 2H, 3-H), 2.74-2.71 (m, 2H, 14-H), 2.01 (s, 3H, 19-H), 1.85 (t, $^{3}J_{2,3} \approx 7$ Hz, 2H, 2-H), 1.84 (s, 3H, 18-H), 1.16 (s, 6H, 16-H, 17-H).

^{13}C NMR ($CDCl_3$): δ = 199.4 (s, C-4), 172.1 (s, C-15), 161.4 (s, C-6), 136.7 (d, C-12), 133.6 (s, C-5), 132.8 (d, C-8), 129.9 (s, C-9), 128.7 (d, C-10), 127.5 (d, C-7), 124.2 (d, C-11), 51.6 (q, COO**C**H_3), 41.2 (t, C-14), 39.8 (d, C-13), 37.3 (t, C-2), 35.7 (s, C-1), 34.3 (t, C-3), 27.6 (q, C-16, C-17), 20.7 (q, C-19), 13.7 (q, C-18).

isomeric mixture:

MS [EI, 70 eV]: *m/z* (%) = 392 (60) [M^+], 377 (90) [M^+-CH_3], 352 (10), 327 (10), 319 (20), 303 (22), 285 (30), 245 (15), 229 (45), 215 (20), 203 (70), 173 (33), 145 (30), 133 (90), 121 (70), 105 (50), 91 (100), 77 (54), 69 (30), 51 (30)

UV (HPLC, hex/*i*PrOH 90:10): λ_{max} = 246, 317 nm.

IR (ATR): $\tilde{\nu}$ = 3029 cm^{-1} (w), 2957 (m), 2925 (m), 2866 (w), 1736 (C=O, s), 1658 (C=O, s), 1582 (m), 1494 (w), 1437 (m), 1352 (m), 1310 (m), 1279 (m), 1197 (m), 1092 (m), 968 (s), 755 (m), 699 (s).

HRMS: $C_{26}H_{32}O_3$ (392.54) calcd. 392.2351; found 392.23404 ± 1.27 ppm.

4-Oxo-13-phenyl-13,14-dihydro-retinoic acid (**83**):
General procedure 3 with **79** (0.25 g, 0.66 mmol), KOH (0.37 g, 6.6 mmol) in ethanol (5 mL) and water (3 mL) gave **83** in 92 % yield (0.23 g, 0.61 mmol). The NMR spectra show no or minimal chemical shift difference between ester **79** and acid **83**, for this reason a detailed assignment of each isomer is not given, the structure was assigned by low and high resolution MS spectrometry, and IR- and UV-analysis.

MS [EI, 70 eV]: *m/z* (%) = 378 (50) [M^+], 363 (80) [M^+-CH_3], 345 (10), 319 (12), 303 (30), 285 (25), 261 (53), 247 (15), 229 (47), 215 (40), 201 (30), 173 (42), 133 (50), 115 (57), 91 (100), 77 (50), 69 (48), 51 (30), 43 (60).

UV (HPLC, CH_3CH/H_2O 80:20): λ_{max} = 260, 326 nm.

IR (ATR): $\tilde{\nu}$ = 3400 cm^{-1} (br, COOH), 3030 (m), 2965 (s), 2930 (s), 2870 (m), 1711 (s, C=O), 1658 (s, C=O), 1494 (m), 1356 (m), 1336 (m), 1201 (m), 1094 (m), 1033 (m), 971 (m), 760 (m), 701 (m).

HRMS: $C_{25}H_{30}O_3$ (378.51) calcd. 378.21949; found 378.21946 ± 2.43 ppm.

13-Isopropyl-13,14-dihydro-retinoic acid methyl ester (**31**):

General procedure 2 with LiHMDS prepared from *n*BuLi (1.77 mL, 2.83 mmol) and HMDS (0.46 g, 0.59 mL, 2.83 mmol)], **72** (1.51 g, 2.83 mmol) in anhydrous THF (30 mL), **47** (0.5 g, 2.26 mmol) in anhydrous THF (20 mL). Column chromatography on Alox (8 % water w/w, activity III) with pentane/diethyl ether 10:1 (R_f = 0.63) gave **31** (25 mg, 0.07 mmol, 3 %). This RA derivative was much more labile than the others synthesized in this study. During spectroscopic analysis it underwent decomposition. Assignement of the ^{1}H and ^{13}C chemical shifts to each isomer was not possible from the NMR sprectra of the isomeric mixture.

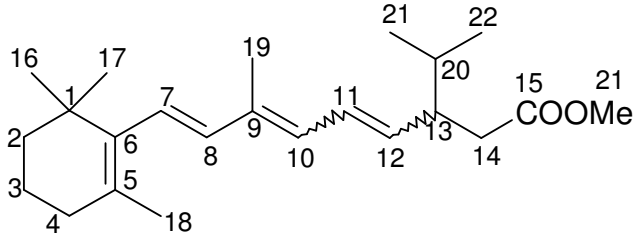

31

MS [GC-MS]: *m/z* (%) = 344 (100) [M^+], 329 (20), 301 (73), 271 (17), 255 (10), 245 (10), 227 (37), 215 (20), 187 (28), 171 (25), 157 (38), 145 (40), 119 (45), 105 (35), 93 (25), 69 (55), 55 (35).

GC-HRMS: $C_{23}H_{36}O_2$ (344.54) calcd. 344.2715; found 344.2740

4-Oxo-13-isopropyl-13,14-dihydro-retinoic acid methyl ester (**76**):

General procedure 2 with LiHMDS [prepared from *n*BuLi (1.69 mL, 2.7 mmol) and HMDS (0.44 g, 0.56 mL, 2.7 mmol)], **72** (1.44 g, 2.7 mmol) in anhydrous THF (30 mL), **53** (0.5 g, 2.16 mmol) in anhydrous THF (10 mL). Column chromatography on Alox (8 % water w/w, activity III) with pentane/diethyl ether (R_f = 0.17) gave **76** (22.3 mg, 0.07 mmol, 3 %). This RA derivative was much more labile than the others synthesized in this work. During spectroscopic analysis it underwent decomposition and for this reason detailed spectroscopic investigations were impossible.

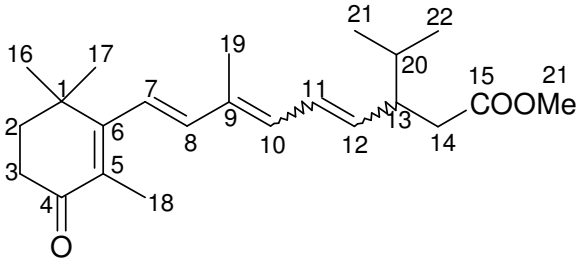

31

MS [GC-MS]: *m/z* (%) = 358 (50) [M^+], 343 (100), 311 (20), 283 (45), 255 (30), 241 (55), 229 (30), 215 (90), 203 (75), 171 (55), 157 (70), 145 (50), 133 (70), 105 (50), 91 (40), 69 (80), 55 (50).

IR (ATR): $\tilde{\nu}$ = 2960-2871 cm^{-1} (w), 1739 (s), 1664 (s), 1584 (w), 1438 (m), 1334 (m), 1141 (m), 971 (m), 884 (w).

Vinyl-β-ionol (**35**):

In a three-necked flask was dissolved **22** (20 g, 104 mmol, 21.2 mL), in anhydrous THF (350 mL). After cooling to 0 °C, vinylmagnesium bromide (15.66 g, 180 mmol, 180 mL 1M solution in THF) was added dropwise during 1 h. Stirring was continued at room temp. overnight. The solution was poured into ice-cold aqueous NH_4Cl and extracted with diethyl ether. The combined organic extracts were washed with saturated $NaHCO_3$ and brine solution and then dried with Na_2SO_4. Concentration under reduced pressure and bulb to bulb distillation at 89 °C/0.35 mmHg afforded **35** as a colorless oil (19.5 g, 88 mmol, 80 %, lit.[76] yield: 94 %, b.p. 110 °C/1.4 mmHg). R_f (pentane/diethyl ether 6:1) = 0.49.

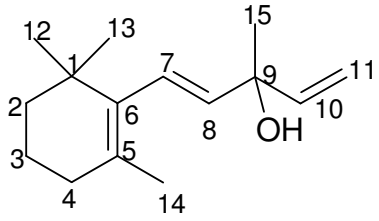

35

^{1}H NMR ($CDCl_3$): δ = 6.08 (d, $^3J_{7,8}$ = 16.2 Hz, 1H, 7-H), 6.01 (dd, $^3J_{10,11}$ = 17.3, $^3J_{10,11}$= 10.6 Hz, 1H, 10-H), 5.54 (d, $^3J_{8,7}$ = 16.2 Hz, 1H, 8-H), 5.26 (d, $^3J_{11,10}$ = 17.3 Hz, 1H, 11-H), 5.07 (d, $^3J_{11,10}$ = 10.6 Hz, 1H, 11-H), 1.97 (t, $^3J_{4,3}$ = 6.0 Hz, 2H, 4-H), 1.65

(s, 3H, 14-H), 1.56-1.63 (m, 2H, 3-H), 1.42 (s, 3H, 15-H), 1.40-1.47 (m, 2H, 2-H), 0.98 (s, 6H, 12-H, 13-H).

^{13}C NMR ($CDCl_3$): δ = 144.3 (d, C-10), 141.9 (s, C-6), 138.9 (d, C-8), 136.8 (s, C-5), 125.7 (d, C-7), 112.0 (t, C-11), 73.5 (s, C-9), 39.2 (t, C-2), 34.0 (s, C-1), 32.6 (t, C-4), 28.7 (q, C-12, C-13), 28.0 (q, C-15), 21.3 (q, C-14), 19.2 (t, C-3).

MS [GC-MS]: *m/z* (%) = 220 (20) [M^+], 202 (80) [M^+-H_2O], 187 (60) [M^+-H_2O-CH_3], 177 (10), 159 (40), 146 (60), 131 (100), 117 (68), 105 (60), 91 (65), 81 (55), 69 (37), 55 (40), 41 (34).

IR (ATR): $\tilde{\nu}$ = 3379 cm^{-1} (br, OH), 2962 (m), 2926 (m), 2864 (m), 2827 (w), 1454 (m), 1409 (w), 1360 (m), 1099 (w), 993 (s), 974 (s), 917 (s), 678 (m).

UV ($CHCl_3$): λ_{max} (lg ε) = 241 nm (3.70), 318 (3.98), 332 (3.87).

β-Ionylidene-ethyl-triphenylphosphonium bromide (**37**):

In a Schlenk flask was suspended PPh_3HBr (24.47 g, 71.31 mmol) in anhydrous methanol (200 mL). A solution of **35** (15.91 g, 71.31 mmol) in anhydrous methanol (200 mL) was added dropwise during 30 min. Stirring was continued at room temp. for 75 h and the solution was concentrated under reduced pressure and high vacuum to give a viscous oil. Crystallization from acetone/hexane and further washing with pentane afforded **37** (38.33 g, 70.1 mmol, 98 %, lit.[74] yield: 64 %) as a yellow solid. (m.p. 135-137 °C, lit.[74] m.p.:135-137 °C).

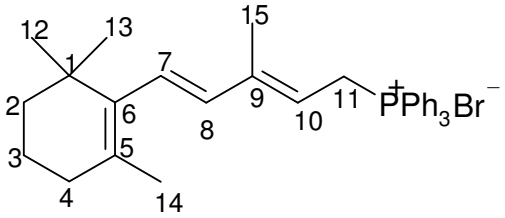

37

^{1}H NMR ($CDCl_3$): δ = 7.89-7.66 (m, 15H, Ar), 6.02 (d, $^3J_{7,8}$ = 16.6 Hz, 1H, 7-H), 5.92 (d, $^3J_{8,7}$ = 16.6 Hz, 1H, 8-H), 5.32 (q, $^3J_{10,11}$ = $^3J_{10,P}$ = 7.6 Hz, 1H, 10-H), 4.85 (dd, $^2J_{11,P}$ = 15.5, $^3J_{11,10}$ = 7.6 Hz, 2H, 11-H), 2.17 (s, 3H, 15-H), 1.97 (t, $^3J_{4,3}$ = 6.0 Hz, 2H, 4-H), 1.61 (s, 3H, 14-H), 1.60-1.55 (m, 2H, 3-H), 1.44-1.39 (m, 2H, 2-H), 0.94 (s, 6H, 11-H, 13-H).

^{13}C NMR ($CDCl_3$): δ = 143.9 (s, $J_{C,P}$ = 6 Hz, C-6), 137.1 (s, $J_{C,P}$ = 2 Hz, C-5), 135.5 (d, $J_{C,P}$ = 6 Hz, C-8), 134.9 (d, $J_{C,P}$ = 3 Hz, C-19), 133.9 (d, $J_{C,P}$ = 10 Hz, C-18), 130.3 (d, $J_{C,P}$ = 12.4 Hz, C-17), 129.6 (s, $J_{C,P}$ = 2 Hz, C-9), 128.7 (d, $J_{C,P}$ = 5 Hz, C-7), 118.2 (d, $J_{C,P}$ = 85 Hz, C-16), 112.5 (d, $J_{C,P}$ = 11.5 Hz, C-10), 39.3 (t, C-2), 34 (s, C-1), 32.7 (t, C-4), 30.8 (q, C-15), 28.8 (q, C-12, C-13), 25.1 (t, $J_{C,P}$ = 49 Hz, C-11), 21.5 (q, C-14), 19.1 (t, C-3).

MS [ESI, 70 eV]: *m/z* (%) = 465 [M^+-Br].

IR (ATR): $\tilde{\nu}$ = 3057-2790 cm^{-1} (m), 1705 (m), 1587 (s), 1485 (s), 1437 (s), 1361 (m), 1223 (s), 1162 (s), 1111 (s), 1066 (s), 995 (m), 966 (m), 748 (s), 721 (s), 689 (s).

UV ($CHCl_3$): λ_{max} (lg ε) = 240 nm (4.30), 276 (4.15).

4-Oxo-vinyl-β-ionol (**36**):

In a three-necked flask equipped with dropping funnel was dissolved **22** (10 g, 48.5 mmol,) in anhydrous THF (60 mL). After cooling to 0 °C, vinylmagnesium bromide (6.77 g, 77.6 mmol, 78 mL of 1M solution in THF) was added dropwise during 1 h. Stirring was continued at room temp. overnight. The reaction mixture was poured into ice-cold saturated NH_4Cl solution and extracted several times with diethyl ether. The combined organic extracts were washed with saturated $NaHCO_3$, brine solution, and dried with Na_2SO_4. Concentration under reduced pressure afforded **36** (6.7 g, 28.6 mmol, 59 %) as a light yellow oil. The NMR spectra correspond to those given in the literature.[30c]

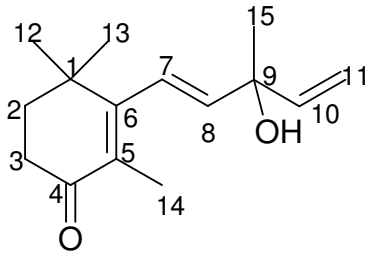

36

MS [GC-MS]: *m/z* (%) = 234 (3) [M^+], 219 (7) [M^+-CH_3], 201 (3) [M^+-CH_3-H_2O], 191 (100) [M^+-CH_3CO^+], 179 (10), 163 (20), 149 (15), 135 (20), 121 (20), 107 (16), 91 (15), 81 (10), 69 (15), 55 (22), 43 (30).

IR (ATR): $\tilde{\nu}$ = 3422 cm^{-1} (br, OH), 2966 (m), 2928 (m), 2868 (w), 1646 (s, C=O), 1594 (m), 1452 (m), 1415 (m), 1355 (m), 1335 (m), 1312 (m), 1199 (w), 1123 (m), 1094 (m), 1030 (m), 973 (m), 919 (s), 689 (m).

UV ($CHCl_3$): λ_{max} (lg ε) = 236 nm (3.80), 263 (4.00).

4–Oxo-β-ionylidene-ethyl-triphenylphosphonium bromide (**38**):

To a solution of PPh_3HBr (10.3 g, 28.6 mmol) in anhydrous methanol (100 mL) was added **36** (6.7 g, 28.6 mmol) in methanol (100 mL). After stirring for 75 h at room temp., the solvent was evaporated and **38** (10.57 g, 18.9 mmol, 66 %, lit.[30c] yield: 84 %) was obtained as a yellow solid. (m.p. 50 °C). The NMR spectra correspond to the literature.[30c]

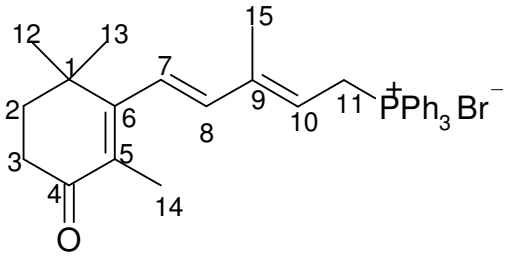

38

MS [ESI]: *m/z* (%) = 479 [M^+-Br].

IR (ATR): $\tilde{\nu}$ = 2960-2861 cm^{-1} (w), 1655 (s, C=O), 1588 (w),1480 (s), 1107 (s), 756 (s), 721 (s), 690 (s).

UV ($CHCl_3$): λ_{max} (lg ε) = 240 nm (4.30).

Retinoic acid ethyl ester (**40**):

A solution of β-formyl ethyl crotonate (2.5 g, 1.751 mL 12.86 mmol) in ethanol (5 mL) was cooled to -30 °C. To the reaction mixture was added dropwise during 30 min a solution of phosphonium salt **37** (4 g, 7.35 mmol) in ethanol (10 mL) and 0.41 g (17.70 mmol) Na in ethanol (7.5 mL). After 10 min at -10 °C, the cooling bath was removed and the reaction left for 2 h to come to room temp. The pH was adjusted to neutral by adding a diluted solution of acetic acid. Extraction with diethyl ether and drying the organic phase with Na_2SO_4 followed by solvent evaporation and column chromatography on Alox with pentane/diethyl ether 20:1 gave **40** (1.74 g, 8.55 mmol, 72 %) as a yellow oil. R_f (pentane/diethyl ether 20:1) = 0.36.

Spectroscopic data are in accordance with the literature.[75]

Retinoic acid (**3**):

To ester **40** (1.74 g, 8.55 mmol), dissolved in ethanol (15 mL), was added a solution of KOH (4.8 g, 85.5 mmol) in ethanol/water. The mixture was heated to 70 °C for 3 h. After cooling to room temp., the mixture was extracted with ether. The aqueous phase was acidified to pH 5.5 with dilute acetic acid, and extracted with diethyl ether. This organic phase was dried with Na_2SO_4 and evaporated to give acid **3** (2.5 g, 8.38 mmol, 98 %). The spectroscopic data were in accordance with literature.[76,77]

4-Oxo-retinoic acid (**42**):

Ester **41** was obtained as described for **40**, with β-formyl ethyl crotonate (1.27 mL, 9.36 mmol) in ethanol (3.1 mL), **38** (3 g, 5.35 mmol) in ethanol (6.3 mL) and Na (0.3 g, 12.9 mmol) in ethanol (5.5 mL). Purification by column chromatography on silica gel with pentane/diethyl ether 3:1 gave **41** (1.34 g, 3.9 mmol, 73 %). R_f (pentane/diethyl ether 3:1) = 0.18. This product was dissolved in ethanol, and a solution of KOH in ethanol/water was added. Heating to 70 °C for 3 h followed by workup gave **42** (1.66 g, 5.3 mmol, 99 %). The spectroscopic data were in accordance with the literature.[30b]

4,5-Epoxy-4,5-dihydro-α-ionone (**93**):

To *meta*-chloroperbenzoic acid (20.05 g, 0.07 mol) in dichloromethane (200 mL) was added dropwise during 30 min a solution of α–ionone (**92**, 10 g, 0.056 mol, 11.11 mL) in dichloromethane (25 mL). After 3 h stirring, the organic phase was extracted with saturated Na_2SO_3 solution, followed by extraction with Na_2CO_3 solution, washing with brine, and drying with Na_2SO_4. Column chromatography on silica gel with pentane/diethyl ether 1:1 gave **93** (11.3 g, 54.3 mmol, 96 %) as a colorless oil. R_f (pentane/diethyl ether 1:1) = 0.54.

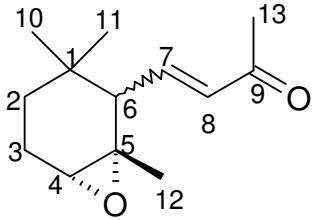

93

^{1}H (400 MHz, $CDCl_3$): δ = 6.72 (dd, $^3J_{7,8}$ = 16.0, $^3J_{7,6}$ = 10.2 Hz, 1H, 7-H), 6.10 (d, $^3J_{8,7}$ = 16.0 Hz, 1H, 8-H), 3.10 (t, $^3J_{4,3}$ = 1.9 Hz, 1H, 4-H), 2.30 (s, 3H, 10-H), 2.09 (d, $^3J_{6,7}$ = 10.2 Hz, 1H, 6-H), 1.98-1.91 (m, 4H, 3-H), 1.46-1.38 (m, 2H, 2-H), 1.25 (s, 3H, 13-H), 0.93, 0.75 (s, 6H, 11-H, 12-H).

^{13}C (100 MHz, $CDCl_3$): δ = 198.7 (s, C-9), 146.3 (d, C-7), 134.0 (d, C-8), 59.4 (d, C-6), 58.7 (s, C-5), 53 (d, C-4), 31.1 (s, C-1), 28.4 (t, C-2), 27.8 (q, C-11 or C-12), 27.4 (q, C-11 or C-12), 26.4 (q, C-10), 24.0 (q, C-13), 21.7 (t, C-3).

MS [GC-MS]: *m/z* (%) = 208.1 (25), [M^+], 193.1 (4) [M^+-CH_3], 179.1 (45), 165.1 (28), 151.1 (26), 147.1 (14), 137.1 (10), 123.1 (22), 111.1 (40), 109.1 (81), 107.1 (18), 95.1 (53), 81.1 (13), 69.1 (16), 55.1 (19).

IR (ATR): $\tilde{\nu}$ = 2958 cm^{-1} (m), 2925 (m), 2869 (s), 1698 (s), 1672 (s), 1622 (s), 1450 (s), 1361 (s), 1251 (s), 1178 (s), 988 (s), 962 (s), 901 (s), 885 (s), 857 (s), 790 (s), 706 (s), 652 (s), 603 (s), 576 (s), 545 (s).

UV ($CHCl_3$): λ_{max} (lg ε) = 244 nm (3.58), 318 (1.95).

4-Hydroxy-β-ionone (**94**):

A solution of 1.7M NaOMe (0.197 g, 8.56 mmol Na in 5 mL methanol) was added dropwise to **93** (11.3 g, 54.3 mmol) in methanol (80 mL). After stirring for 1 d, the reaction was quenched with 2 M HCl solution and extracted with diethyl ether. The product was purified by silica gel column chromatography with pentane/diethyl ether 1:1 to give **94** (9.44 g, 45.4 mmol, 84 %, lit.[26] yield: 65 %). R_f (pentane/diethyl ether 1:1) = 0.19.

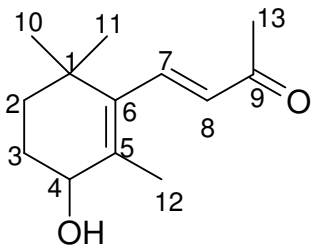

94

^{1}H (400 MHz, $CDCl_3$): δ = 7.20 (br d, $^3J_{8,7}$ = 16.5 Hz, 1H, 8-H), 6.12 (dd, $^3J_{7,8}$ = 16.5, $^5J_{7,12}$ = 2.0 Hz, 1H, 7-H), 4.01 (br s, 1H, 4-H), 2.38 (br s, 1H, OH), 2.36 (d, $^5J_{13,8}$ = 2.2

Hz, 3H, 13-H), 1.95-1.67 (m, 2H, 3-H), 1.85 (br s, 3H, 12-H), 1.71-1.42 (m, 2H, 2-H), 1.07, 1.04 (s, 6H, 10-H, 11-H).

^{13}C (100 MHz, $CDCl_3$): δ = 198.5 (s, C-9), 142.8 (d, C-8), 139.0 (s, C-6), 134.3 (s, C-5), 132.8 (d, C-7), 69.6 (d, C-4), 34.6 (t, C-2), 34.5 (s, C-1), 28.7 (q, C-10 or C-11), 28.2 (t, C-3), 27.4 (C-10 or C-11), 27.2 (q, C-13), 18.3 (q, C-12).

MS [EI, 70 eV]: *m/z* (%) = 208.1 (64), [M^+], 193.1 (18) [M^+-CH_3], 175.1 (13), 165.1 (14), 151.1 (18), 137.1 (24), 134.1 (13), 123.1 (38), 109.1 (100), 91.1 (16), 79.1 (10), 55.1 (9).

IR (ATR): $\tilde{\nu}$ = 3403 cm^{-1} (m), 2960 (m), 2934 (s), 2866 (s), 1661 (s), 1606 (s), 1449 (m), 1360 (s), 1253 (s), 1174 (s), 1145 (s), 1077 (s), 1023 (s), 998 (s), 978 (s), 962 (s), 921 (s), 903 (s), 877 (s), 731 (s).

UV ($CHCl_3$): λ_{max} (lg ε) = 240 nm (3.51), 286 (3.87).

4-Triethylsilyloxy-β-ionone (**115**):

A solution of **94** (9.44 g, 45.4 mmol), triethylamine (5.16 g, 51.1 mmol, 5 mL) and DMAP (0.34 g, 2.8 mmol) in dichloromethane (40 mL) was cooled to 0 °C, and TESCl (5.17 g, 51.1 mmol, 7.2 mL) was added dropwise. After stirring for 1 d at room temp., the reaction mixture was washed with brine, the organic phase was dried with Na_2SO_4, and the solvent evaporated. Column chromatography on silica gel gave **115** (10.8 g, 33.4 mmol, 74 %) as a colorless oil. R_f (pentane/diethyl ether 5:1) = 0.16.

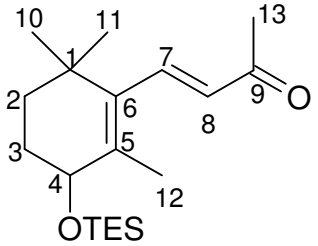

115

^{1}H (400 MHz, $CDCl_3$): δ = 7.20 (d, $^3J_{8,7}$ = 16.5 Hz, 1H, 8-H), 6.12 (d, $^3J_{7,8}$ = 16.5 Hz, 1H, 7-H), 4.05 (t, $^3J_{4,3}$ = 5.7 Hz, 1H, 4-H), 2.29 (s, 3H, 13-H), 1.88-1.63 (m, 2H, 3-H), 1.78 (s, 3H, 12-H), 1.45-1.38 (m, 2H, 2-H), 1.08, 1.02 (s, 6H, 10-H, 11-H), 0.98 (t, *J* = 8.0 Hz, 9H, $Si(CH_2C\mathbf{H}_3)_3$), 0.65 (q, *J* = 7.6 Hz, 6H, $Si(C\mathbf{H}_2CH_3)_3$).

^{13}C (100 MHz, $CDCl_3$): δ = 198.4 (s, C-9), 143.1 (d, C-8), 138.1 (s, C-6), 135.5 (s, C-5), 132.8 (d, C-7), 70.8 (d, C-4), 35.4 (t, C-2), 34.5 (s, C-1), 29.0 (t, C-3), 28.2 (q, C-10, 11), 27.2 (q, C-13), 18.2 (q, C-12), 6.9 (q, $Si(CH_2\mathbf{C}H_3)_3$), 5.0 (t, $Si(\mathbf{C}H_2CH_3)_3$).

MS [EI, 70 eV]: *m/z* (%) = 322.3 (100), [M^+], 307.2 (12) [M^+- CH_3], 293.2 (9), 279.3 (17), 266.2 (15), 251.2 (24), 237.2 (12), 223.2 (56), 193.1 (8), 173.2 (8), 147.1 (11), 134.1 (12), 115.1 (24), 103.1 (38), 87.1 (40), 75.0 (49), 43.1 (29).

IR (ATR): $\tilde{\nu}$ = 2955 cm^{-1} (m), 2912 (s), 2877 (s),1695 (s), 1674 (s),1610cm^{-1}(s), 1459 (s), 1415 (m), 1357 (s), 1249 (s), 1174 (s), 1148 (s), 1084 (s), 1051 (s), 1004 (s), 978 (s), 934 (s), 883 (s), 821 (s), 796 (s), 724 (m), 688 (s), 576 (s).

UV ($CHCl_3$): λ_{max} (lg ε) = 238 nm (3.52), 289 (3.87).

HRMS: $C_{19}H_{34}O_2Si$ (322.56) calcd. 322.23282; found 322.23307 ± 1.98 ppm.

4-Acetoxy-β-ionone (**95**):

A solution of **94** (3.85 g, 18.48 mmol), Ac_2O (2.26 g, 2.09 mL, 22.2 mmol) and pyridine (2.92 g, 2.98 mL, 36.96 mmol) in dichloromethane (75 mL) was stirred at room temp. for 4 h. The reaction mixture was washed with aqueous $NaHCO_3$ solution and a cold solution of 2 M HCl. The organic phase was dried with Na_2SO_4 and the solvent was removed. Column chromatography on silica gel with pentane/diethyl ether 10:1 gave **95** (1.95 g, 7.79 mmol, 42 %, lit.[26] yield: 89 %) as a colorless oil. Spectroscopic data correspond to the literature.[26]

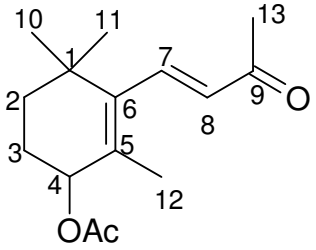

95

4-Acetoxy-β-ionylidene-acetaldehyde (**96**):

General procedure 1 with **52** (6.62 g, 15.44 mmol) in anhydrous THF (70 mL), KO*t*Bu (1.73 g, 15.44 mmol), **95** (1.93 g, 7.72 mmol) in anhydrous THF (30 mL), oxalic acid solution (6.81 g, 54.04 mmol, in 60 mL water). Column chromatography with

pentane/diethyl ether 2:1 on Alox (activity III, 8 % water w/w) gave 9-*cis*- and all-*trans*-**96** (1:1 ratio) in 41 % yield (0.87 g, 3.17 mmol). R_f(9-*cis)* = 0.49, R_f(all-*trans*) = 0.41.

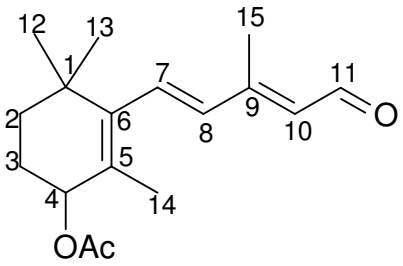

all-*trans*-**96**

^{1}H NMR (400 MHz, $CDCl_3$): δ = 10.17 (d, $^3J_{11,10}$ = 8.1 Hz, 1H, 11-H), 6.69 (d, $^3J_{7,8}$ = 16.1 Hz, 1H, 7-H), 6.25 (d, $^3J_{8,7}$ = 16.1 Hz, 1H, 8-H), 5.96 (br d, $^3J_{10,11}$ = 8.1 Hz, 1H, 10-H), 5.27-5.24 (m, 1H, 4-H), 2.33 (d, $^4J_{15,10}$ = 1.1 Hz, 3H, 15-H), 2.08 (s, 3H, COC**H$_3$**), 1.98-1.62 (m, 2H, 3-H), 1.70 (s, 3H, 14-H), 1.50-1.20 (m, 2H, 2-H), 1.06, 1.05 (s, 6H, 12-H, 13-H).

^{13}C NMR (100 MHz, $CDCl_3$): δ = 191.3 (d, C-11), 171 (s, O**C**OCH_3), 154.0 (s, C-9), 143 (s, C-6), 137.4 (d, C-8), 134.3 (d, C-7), 142 (s, C-5), 129.7 (d, C-10), 72.2 (d, C-4), 34.8 (t, C-2), 34.6 (s, C-1), 29.0 (q, C-12, C-13), 25.3 (t, C-3), 21.4 (q, OCO**C**H_3), 18.5 (q, C-14), 13.1 (q, C-15).

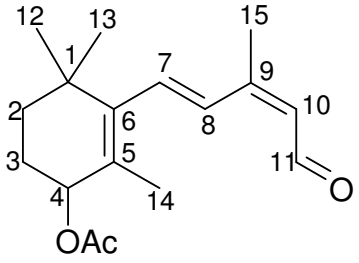

9-*cis*-**96**

^{1}H NMR ($CDCl_3$): δ = 10.15 (d, $^3J_{11,10}$ = 8.1 Hz, 1H, 11-H), 7.13 (d, $^3J_{7,8}$ = 16.1 Hz, 1H, 7-H), 6.58 (d, $^3J_{8,7}$ = 16.1 Hz, 1H, 8-H), 5.91 (br d, $^3J_{10,11}$ = 8.1, Hz, 1H, 10-H), 5.27-5.24 (m, 1H, 4-H), 2.14 (d, $^4J_{15,10}$ = 1.1 Hz, 3H, 15-H), 2.09 (s, 3H, OCOC**H$_3$**), 1.98-1.62 (m, 2H, 3-H), 1.73 (s, 3H, 14-H), 1.50-1.20 (m, 2H, 2-H), 1.10, 1.09 (s, 6H, 12-H, 13-H).

^{13}C NMR (100 MHz, $CDCl_3$): δ = 190.1 (d, C-11), 171 (s, O**C**OCH_3), 154.2 (s, C-9), 143 (s, C-6), 135.3 (d, C-8), 142 (s, C-5), 129.5 (d, C-7), 128.7 (d, C-10), 72.2 (s, C-4),

34.8 (t, C-2), 34.3 (s, C-1), 29.0 (q, C-12, C-13), 25.3 (t, C-3), 21.4 (q, OCO**C**H_3),18.4 (q, C-14), 21.2 (q, C-15).

isomeric mixture:

MS [EI, 70 eV]: *m/z* (%) = 276 (37) [M^+], 234 (60) [M^+-$COCH_3$], 216 (38), 201 (40), 187 (20), 173 (20), 152 (100), 145 (20), 119 (35), 105 (35), 95 (57), 77 (20), 55 (20), 43 (60).

IR (ATR): $\tilde{\nu}$ = 2959-2864 cm^{-1} (w), 1730 (s, CO), 1663 (s, CO), 1614 (m), 1447 (w), 1369 (m), 1232 (s), 1207 (s), 1176 (w), 1152 (w), 1110 (m), 1017 (m), 993 (m), 962 (m), 915 (m), 865 (m), 731 (s), 648 (w).

4-Acetoxy-13,14-dihydro-retinoic acid methyl ester (**97**):
General procedure 2 with LiHMDS [prepared from *n*BuLi (2.09 mL, 3.61 mmol) and HMDS (0.58 g, 0.75 mL, 3.61 mmol)], **66** (1.82 g, 3.61 mmol) in anhydrous THF (30 mL), **96** (0.8 g, 2.89 mmol) in anhydrous THF (20 mL). Column chromatography on Alox (8 % water w/w, activity III) with pentane/diethyl ether 5:1 (R_f = 0.37) gave **97** (0.14 g, 0.37 mmol, 13 %) as a yellow oil.

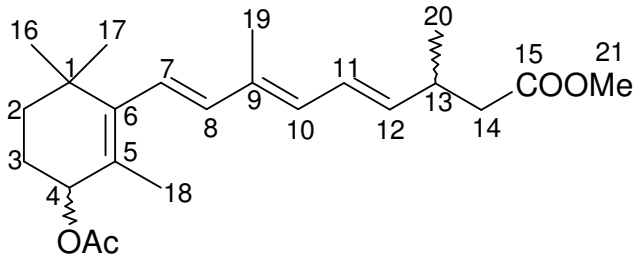

all-*trans*-**97**

^{1}H NMR (400 MHz, $CDCl_3$): δ = 6.43 (dd, $^3J_{11,12}$ = 15.0, $^3J_{11,10}$ = 11.0 Hz, 1H, 11-H), 6.10 (d, $^3J_{7,8}$ = 15.7 Hz, 1H, 7-H), 6.05 (d, $^3J_{8,7}$ = 15.7 Hz, 1H, 8-H), 6.01 (d, $^3J_{10,11}$ = 11.0 Hz, 1H, 10-H), 5.67 (dd, $^3J_{12,11}$ = 15.0, $^3J_{12,13}$ = 7.7 Hz, 1H, 12-H), 5.27-5.21 (m, 1H, 4-H), 3.7 (s, 3H, 21-H), 2.83-2.73 (m, 1H, 13-H), 2.41-2.27 (m, 2H, 14-H), 2.07 (s, 3H, OCOC**H$_3$**), 1.90 (s, 3H, 18-H), 1.79-1.58 (m, 2H, 3-H), 1.70 (s, 3H, 19-H), 1.47-1.39 (m, 2H, 2-H), 1.1 (d, $^3J_{20,13}$ = 6.8 Hz, 3H, 20-H), 1.03 (s, 6H, 16-H, 17-H).

^{13}C NMR (100 MHz, $CDCl_3$): δ = 172.7 (s, C-15), 171.0 (s, O**C**OCH_3), 138.9 (d, C-8), 138.7 (d, C-12), 136.2 (s, C-6), 135.7 (s, C-5), 132.6 (s, C-9), 130.6 (d, C-10), 126.7 (d, C-11), 126.1 (d, C-7), 72.5 (d, C-4), 51.4 (q, C-21), 41.2 (t, C-14), 34.6 (s, C-1), 34.3 (t,

C-2), 33.7 (d, C-13), 28.9 (q, C-16, C-17), 25.0 (t, C-3), 21.5 (q, OCO**C**H$_3$), 20.5 (q, C-20), 18.1 (q, C-18), 12.5 (q, C-19).

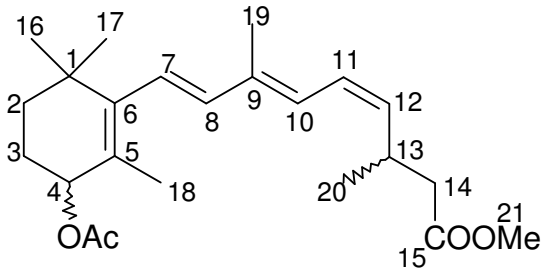

11-*cis*-**97**

^{1}H NMR (400 MHz, CDCl$_3$): δ = 6.34 (t, $^3J_{11,10}$ = $^3J_{11,12}$ = 11.5 Hz, 1H, 11-H), 6.31 (d, $^3J_{10,11}$ = 11.5 Hz, 1H, 10-H), 6.13 (m, 2H, 7-H, 8-H), 5.31 (t, $^3J_{12,11}$ = $^3J_{12,13}$ = 9.7 Hz, 1H, 12-H), 5.27-5.21 (m, 1H, 4-H), 3.64 (s, 3H, 21-H), 3.25-3.15 (m, 1H, 13-H), 2.41-2.27 (m, 2H, 14-H), 2.07 (s, 3H, OCOC**H$_3$**), 1.90 (s, 3H, 18-H), 1.79-1.58 (m, 2H, 3-H), 1.70 (s, 3H, 19-H), 1.47-1.39 (m, 2H, 2-H), 1.09 (d, $^3J_{20,13}$ = 6.8 Hz, 3H, 20-H), 1.03 (s, 6H, 16-H, 17-H).

^{13}C NMR (100 MHz, CDCl$_3$): δ = 172.7 (s, C-15), 171.0 (s, O**C**OCH$_3$), 139.2 (d, C-8), 136.2 (s, C-6), 136.2 (d, C-12), 135.7 (s, C-5), 132.6 (s, C-9), 126.7 (d, C-7), 124.1 (d, C-11), 124.0 (d, C-10), 72.5 (d, C-4), 51.4 (q, C-21), 41.4 (t, C-14), 34.6 (s, C-1), 34.3 (t, C-2), 28.9 (q, C-16, C-17), 28.5 (d, C-13), 25.0 (t, C-3), 21.5 (q, OCO**C**H$_3$), 20.5 (q, C-20), 18.1 (q, C-18), 12.3 (q, C-19).

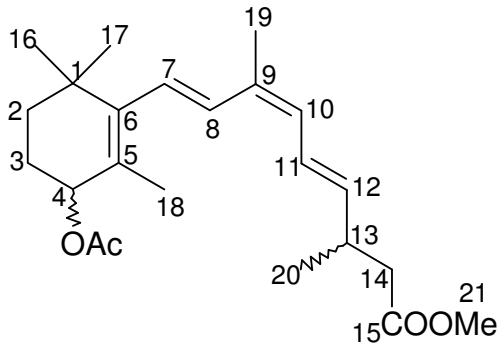

9-*cis*-**97**

^{1}H NMR (400 MHz, CDCl$_3$): δ = 6.61 (d, $^3J_{8,7}$ = 14.0 Hz, 1H, 8-H), 6.50 (dd, $^3J_{11,12}$ = 14.7, $^3J_{11,10}$ = 11.5 Hz, 1H, 11-H), 6.15 (d, $^3J_{7,8}$ = 14.0 Hz, 1H, 7-H), 5.93 (d, $^3J_{10,11}$ = 11.1 Hz, 1H, 10-H), 5.59 (dd, $^3J_{12,11}$ = 15.0, $^3J_{12,13}$ = 7.7 Hz, 1H, 12-H), 5.27-5.21 (m,

1H, 4-H), 3.65 (s, 3H, 21-H), 2.83-2.73 (m, 1H, 13-H), 2.41-2.27 (m, 2H, 14-H), 2.07 (s, 3H, OCOC**H$_3$**), 1.90 (s, 3H, 19-H), 1.70 (s, 3H, 18-H), 1.79-1.58 (m, 2H, 3-H), 1.47-1.39 (m, 2H, 2-H), 1.09 (d, $^3J_{20,13}$ = 6.8 Hz, 3H, 20-H), 1.03 (s, 6H, 16-H, 17-H).

^{13}C NMR (100 MHz, CDCl$_3$): δ = 172.7 (s, C-15), 171.0 (s, O**C**OCH$_3$), 137.8 (d, C-12), 136.2 (s, C-6), 135.2 (s, C-5), 132.6 (s, C-9), 131.1 (d, C-8), 129.2 (d, C-10), 126.0 (d, C-7), 124.8 (d, C-11), 72.5 (d, C-4), 51.4 (q, C-21), 41.2 (t, C-14), 34.6 (s, C-1), 34.3 (t, C-2), 33.7 (d, C-13), 29 (q, C-16, C-17), 25 (t, C-3), 21.5 (q, OCO**C**H$_3$), 21 (q, C-20), 20.5 (q, C-19), 18.1(q, C-18).

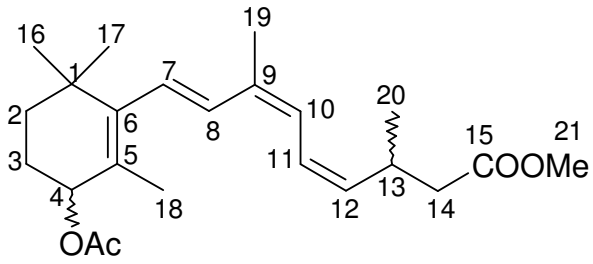

9,11-di-*cis*-**97**

^{1}H NMR (400 MHz, CDCl$_3$): δ = 6.65 (d, $^3J_{8,7}$ = 16.0 Hz, 1H, 8-H), 6.43 (dd, $^3J_{11,12}$ = 15.1, $^3J_{11,10}$ = 11.1 Hz, 1H, 11-H), 6.29 (d, $^3J_{10,11}$ = 11.1 Hz, 1H, 10-H), 6.19 (d, $^3J_{7,8}$ = 16.0 Hz, 1H, 7-H), 5.27-5.21 (m, 2H, 4-H, 12-H), 3.65 (s, 3H, C-21), 3.25-3.15 (m, 1H, 13-H), 2.41-2.27 (m, 2H, 14-H), 2.07 (s, 3H, OCOC**H$_3$**), 1.90 (s, 3H, 19-H), 1.70 (s, 3H, 18-H), 1.79-1.58 (m, 2H, 3-H), 1.47-1.39 (m, 2H, 2-H), 1.08 (d, $^3J_{20,13}$ = 6.8 Hz, 3H, 20-H), 1.03 (s, 6H, 16-H, 17-H).

^{13}C NMR (100 MHz, CDCl$_3$): δ = 172.7 (s, C-15), 171.0 (s, O**C**OCH$_3$), 136.2 (s, C-6), 135.2 (d, C-12), 135.2 (s, C-5), 132.6 (s, C-9), 130.9 (d, C-8), 127.0 (d, C-7), 124.0 (d, C-10), 123.1 (d, C-11), 72.5 (d, C-4), 51.4 (q, C-21), 41.2 (t, C-14), 34.6 (s, C-1), 34.3 (t, C-2), 28.9 (q, C-16, C-17), 28.5 (d, C-13), 25.0 (t, C-3), 21.5 (q, OCO**C**H$_3$), 21.0 (q, C-20), 20.5 (q, C-19), 18.1 (q, C-18).

isomeric mixture:

MS [EI, 70 eV]: *m/z* (%) = 374 (45) [M$^+$], 332 (57), 314 (100), 299 (40), 292 (10), 283 (10), 276 (20), 274 (22), 267 (20), 259 (20), 241 (30), 234 (35), 225 (63), 218 (30), 185 (10), 157 (20), 119 (30), 105 (30), 91 (37), 77 (28), 55 (20), 43 (100).

IR (ATR): $\tilde{\nu}$ = 2959-2867 cm^{-1} (w), 1731 (s), 1438 (m), 1369 (m), 1236 (s), 1169 (m), 1016 (m), 963 (m), 911 (m), 864 (m), 731 (s), 648 (w).

UV ($CHCl_3$): λ_{max} (lg ε) = 229 nm (3.91), 289 (4.35).

HRMS: $C_{23}H_{34}O_4$ (374.52) calcd. 374.24573; found 374.24470 ± 1.15 ppm.

12 Abbreviations

DMSO	Dimethylsolfoxide
RA	Retinoic Acid
LiHMDS	Lithiumhexamethyldisilazide
KO*t*Bu	Potassium tert-butoxide
PCC	Pyridiniumchlorochromat
RA	Retinoic acid
ROH	Retinol
CSP	Chiral stationary phase
CTA	Cellulose triacetate
CTB	Cellulose tribenzoate
MCPB	*meta*-Chloroperbenzoic acid
TESCl	Triethylsilyl chloride
HWE	Horner-Wadsworth-Emmons
dh-RA	Dihydro-retinoic acid

13 References

1 M. Howe-Grant, *Encyclopedia of Chemical Technology*, vol *25*, Wiley 4th ed New York **1998**.

2 C. Funk, *J. State Med.* **1912**, *20*, 341-368.

3 E. V. McCollum, C. Kennedy, *J. Biol. Chem.* **1916**, *24*, 491-502.

4 J. C. Drummond, *J. Biochem.* **1920**, *14*, 660.

5 G. Wald, *Nature* **1934**, *134*, 65.

6 R. A. Morton, *Nature* **1944,** *153*,69-7l.

7 R. A. Morton, T. W. Goodwin, *Nature* **1944***, 153*, 405-406.

8 P. Karrer, R. Morf, K. Schoepp, *HeIv. Chim. Acta* **1931**,*14*, 1431-1436.

9 V. Euler, P. Karrer, U. Solmssen, *Helv. Chim. Acta* **1938**, *21*, 211-222.

10 J. R. Edisbury, R. A. Morton, G. W. Simkins, *Nature* **1937***, 140*, 234.

11 IUPAC Commission on the Nomenclature of Biological Chemistry, Definitive rules for the nomenclature of vitamins, *J. Am. Chem. Soc*. **1960**, *80*, 5581-5581.

12 M. B. Sporn, A. B. Roberts, D. S. Goodman (Ed.) *The Retinoids: Biology, Chemistry and Medicine*, 2nd Ed., Raven Press, Ltd., New York, **1994**: a). D. J. Mangelsdorf, K. 120 Umesono, R. M. Evans, *The Retinoid Receptors*; b). W. S. Blaner, J. A. Olson, *Retinol and Retinoic Acid Metabolism*; c). J. C. Saari, *Retinoids in Photosensitive Systems*; d).R. B. Armstrong, K. O. Ashenfelter, C. Eckhoff, A. A. Levin, S. S. Shapiro, *General and Reproductive Toxicology of Retinoids*; e). M. I. Dawson, P. D. Hobbs, *The Synthetic Chemistry of Retinoids*.

13 T. Arnhold, Ph. d. thesis, Tierärztliche Hochschule Hannover **1999**.

14 N. I. Krinsky, S. T. Mayne, *Vitamin A and retinoids: an update of biological aspects and clinical applications*, M. A. Livrea (Ed.), Birkhäuser Verlag Basel **2000**, 45-57.

15 W. S. Blaner, R. Piantedosi, A. Sykes, S. Vogel, *Retinoic Acid Synthesis and Metabolism*, in H.Nau, W. S. Blazer, *Retinoids: The Biochemical and Molecular Basis of Vitamin A and Retinoid Action*, Sprinter Verlag, Berlin, **1999**, 117-149.

16 M. Shirley, Y. L. Bennani, M. F. Boehm, A. P. Breau, C. Pathirana, E. Ulm, *Drug Metab. Dispos.* **1996***, 24*, 293-302.

17 C. K. Schmidt, Ph. d. thesis, Tierärztliche Hochschule Hannover, **2002**.

18 C. K Schmidt, J. Volland, G. Hamscher, H. Nau, *Biochim. Biophys. Acta* **2002**, *1583*, 237-251.

19 a). A. R. Moise, V. Kuska, Y. Imanishi, K. Palczewshi, *J. Biol. Chem*, **2004**, *279*, 50230-50242 b) A. R. Moise, V. Kuska, W. S. Blaner, W. Baehr, K. Palczewshi, *J. Biol. Chem.* **2005**, 280, 27815-27825.

20 A. Orita, Y. Yamashita, A. Toh, J. Otera, *Angew. Chem.* **1997**, *109*, 804-805; *Angew. Chem Int. Ed.* **1997**, *36*, 779-780.

21 G. Wittig, *Angew. Chem.* **1980**, *9*, 671-675.

22 R. Kaiser, O. Lamparsky, *Helv. Chim. Acta* **1978**, *61*, 373-382.

23 E. Demole, P. Enggist, M. Winter, A. Furrer, K. H. Schulte-Elte, B. Egger, G. Ohloff, *Helv. Chim. Acta* **1979**, *62*, 67-75.

24 K. Ina, H. Eto, *Agric. Biol. Chem.* **1971**, *35*, 962-965.

25 D. L. Davis, K. L. Stevens, L. Jurd, *Agric. Food Chem.* **1976**, *24*, 187-189.

26 A. Haag, W. Eschenmoser, C. H. Eugster, *Helv. Chim. Acta* **1980**, *63*, 10-15.

27 E. Becher, R. Albrecht, K. Bernhard, H. G. W. Leuenberger, H. Mayer, R. K. Müller, W. Schüep, H. P. Wagner, *Helv. Chim. Acta* **1981,** *64*, 2419-2435.

28 L. K. P. Lam, R. A. H. F. Hui, J. B. Jones, *J. Org. Chem* **1986**, *51*, 2047-2050.

29 E. P. Grimsrud, J. W. Taylor, *J. Am. Chem. Soc.* **1970**, *92*, 741-742.

30 a) M. Rosenberger, C. Neukom, *J. Org. Chem* **1982**, *47*, 1779-1782; b) M. Rosenberger, *J. Org. Chem.* **1982**, *47*, 1698-1701; c) M. Rosenberger, P. McDougal, J. Bahr, *J. Org. Chem* **1982**, *47*, 2130-2134.

31 U. Schwieter, C. v. Planta, R. Rüegg, O. Isler, *Helv. Chim, Acta* **1962**, *64*, 541-548.

32 K. Bernhard, F. Kienzle, H. Mayer, R. K. Müller, *Helv. Chem Acta* **1980**, *63*, 1473-1490.

33 O. Isler, G. Brubacher, *Vitamine I: Fettlösliche Vitamine*, Georg Thieme Verlag, Stuttgart-New York **1982**.

34 E. Negishi, A. O. King, W. L. Klima, *J. Org. Chem* **1980**, *45*, 2526-2528.

35 V. Vuligonda, S. M. Thacher, R. A. S. Chandraratna, *J. Med. Chem.* **2001**, *44*, 2298-2303.

36 Y. Bennani, *J. Org. Chem* **1996**, *61*, 3542-3544.

37 Y. Katsuta, M. Ito, *J. Org. Chem*, **1994**, *59*, 6917-6921.

38 A. Haag, C. H. Eugster, *Helv. Chim. Acta*, **1982**, *65*, 1795-1803.

39 Y. Wang, J. Lugtenburg, *Eur. J. Org. Chem*, **2004**, 3497-3510.

40 a). R. Brückner, *Reaktionsmechanismen: Organische Reaktionen, Stereochemie, moderne Synthesemethoden* **2003**, 2 Aufl., Spektrum, Akademischer Verlag, Heidelberg-Berlin; b). J. March, *Advanced Organic Chemistry: Reactions, Mechanisms, and Structure* **1992**, 4th Ed., John Wiley & Sons Inc., pages 176, 214

41 A. J. Irwin, J. B. Jones, *J. Am. Chem. Soc* **1977**, *99*, 556-561.

42 J. E. Johansen, S. Liaaen-Jensen, *Acta Chem. Scand B* **1974**, *28*, 349-356.

43 U. Skogsberg, D. Zeeb, K. Albert, *Chromatographia* **2004**, *59*, 153-160.

44 H. C. Furr, A. B. Barua, J. A. Olson, *Analytical Methods*, M. B. Sporn, A. B. Roberts, D. S. Goodman (eds), *The Retinoids: Biology, Chemistry and Medicine*, 2nd Ed., Raven Press, Ltd., New York, **1994**.

45 L. Pasteur, *Ann. Chim. Phys.* **1848**, *24*, 442.

46 C. Wolf, W. H. Pirkle, C. J. Welch, D. H. Hochmuth, W. A. König, G. L. Chee, J. L. Charlton, *J. Org. Chem* **1997**, *62*, 5208-5210.

47 W. H. Pirkle, P. G. Murray, S. R. Wilson, *J. Org. Chem*. **1996**, *61*, 4775-4777.

48 G.Hesse, R. Hagel, *Chromatographia* **1973**, *6*, 227-228.

49 G.Hesse, R. Hagel, *Liebigs Ann. Chem.* **1976**, 996-1008.

50 C. Yamamoto, Y. Okamoto, *Bull. Chem. Soc. Japan* **2004**, *77*, 227-257.

51 T. Shibata, I. Okamoto, K. Ishii, *J. Liq. Chromatogr.* **1986**, *9*, 313-316.

52 T. Kubota, C. Yamamoto, Y. Okamoto, *J. Polym. Sci. Part A: Polym. Chem.* **2004**, *42*, 4704-4710.

53 C. Yamamoto, Y. Okamoto, *Methods in Molecular Biology*, *Vol. 243*: *Chiral Separations: Methods and Protocols*, G. Gubits and M. G. Schmid (eds), Chapter 5, p.173-181 Ed. Humana Press, Inc. **2004**.

54 N. Fishkin, G. Pescitelli, J. R. Sparrow, K. Nakanishi, N. Berova, *Chirality* **2004**, 16(9), 637-641.

55 Y. Okamoto, E. Yashima, *Angew. Chem.* **1998**, *110*, 1072-1095; *Angew. Chem. Int Ed*. **1998**, *37*, 1020-1043.

56 M. J. Frisch, G. W. Trucks, H. B. Schlegel, G. E. Scuseria, M. A. Robb, J. R. Cheeseman, J. A. Montgomery, Jr., T. Vreven, K. N. Kudin, J. C. Burant, J. M. Millam, S. S. Iyengar, J. Tomasi, V. Barone, B. Mennucci, M. Cossi, G. Scalmani, N. Rega, G. A. Petersson, H. Nakatsuji, M. Hada, M. Ehara, K. Toyota, R. Fukuda, J. Hasegawa, M. Ishida, T. Nakajima, Y. Honda, O. Kitao,

H. Nakai, M. Klene, X. Li, J. E. Knox, H. P. Hratchian, J. B. Cross, V. Bakken, C. Adamo, J. Jaramillo, R. Gomperts, R. E. Stratmann, O. Yazyev, A. J. Austin, R. Cammi, C. Pomelli, J. W. Ochterski, P. Y. Ayala, K. Morokuma, G. A. Voth, P. Salvador, J. J. Dannenberg, V. G. Zakrzewski, S. Dapprich, A. D. Daniels, M. C. Strain, O. Farkas, D. K. Malick, A. D. Rabuck, K. Raghavachari, J. B. Foresman, J. V. Ortiz, Q. Cui, A. G. Baboul, S. Clifford, J. Cioslowski, B. B. Stefanov, G. Liu, A. Liashenko, P. Piskorz, I. Komaromi, R. L. Martin, D. J. Fox, T. Keith, M. A. Al-Laham, C. Y. Peng, A. Nanayakkara, M. Challacombe, P. M. W. Gill, B. Johnson, W. Chen, M. W. Wong, C. Gonzalez, J. A. Pople, Gaussian 03, Revision C.02, Gaussian, Inc., Wallingford CT, 2004.

57 N. L. Rockley, B. A. Halley, M. G. Rockley, E. C. Nelson, *Anal. Biochem.* **1983**, *133*, 314-321.

58 H. H. Jaffe, M. Orchin, *Theory and Applications of Ultraviolet Spectroscopy*, John Wiley & Sons, Inc., New York London **1962**.

59 W. Vetter, G. Englert, N. Rigassi, U. Schwieter, *Spectroscopic Methods* in *Carotenoids*, O. Isler (ed.), Birkhäuser Verlag Basel **1991**.

60 K. Nakanishi, N. Berova, R. W. Woody, *Circular Dichroism: Principles and Applications*, VCH Publishers, Inc. New York **1994**.

61 G. Snatzke, *Angew. Chem.* **1979**, *91*, 380-393; *Angew. Chem. Int. Ed.* **1979**, 18, 363-376.

62 G. Bringmann, S. Busemann, K. Krohn, K. Beckmann, *Tetrahedron* **1997**, *53*, 1655-1664.

63 S. R. Wilson, W. Cui, *J. Org. Chem.* **1989**, *54*, 6047-6055.

64 W. S. Blaner, R. Piantedosi, A. Sykes, S. Vogel, "*Retinoic Acid Synthesis and Metabolism*", Chapt. 4 in "*Retinoids: The Biochemical and Molecular Basis of Vitamina A and Retinoid Action*", H. Nau, W. S. Blaner (eds.), Springer-Verlag Berlin Heidelberg **1999**.

65 a) P. F. Egea, N. Rochel, C. Birck, P. Vachette, P. A. Timmins, D. Moras, *J. Mol. Biol.* **2001**, *307*, 557-576, b) P. F. Egea, A. Mitschler, N. Rochel, M. Ruff, P. Chambon, D. Moras, *Eur. Mol. Biol. Org. J.* **2000**, *11*, 2592-2601, c) P. F. Egea, B. P. Klaholz, D. Moras, *FEBS Letters* **2000**, *476*, 62-67.

66 a) G. Snatzke, *Chem. uns. Zeit* **1981**, *15*, 78-87; b) G. Snatzke, *Chem. uns. Zeit* **1982**, *16*, 160-168; c) G. Snatzke, *Pure Appl. Chem.* **1979**, *51*, 769-785.

67 J. Retey, W. E. Hull, *Tetrahedron* **1979**, *35*, 1845-1849.

68 P. Herold, P. Mohr, C. Tamm, *Helv. Chim. Acta.* **1983**, *66*, 745-754

69 L. K. P. Lamm, R. A. F. Hui, J. B. Jones, *J. Org. Chem.* **1986**, *51*, 2047-2050.

70 C. B. Chapleo, P. Hallett, B. Lythgoe, I. Waterhouse, P. W. Wright, *J. Chem. Soc. Perkin 1*, **1977**, 1211-1217.

71 C. D. Buttery, A. G. Cameron, C. P. Dell, D. W. Knight, *J. Chem. Soc. Perkin 1*, **1990**, 1601-1610.

72 C. Wawrzenczyk, J. Zon, E. Leja, *Phosphorus, Sulfur and Silicon* **1992**, *71*, 179-184.

73 M. Yamaguchi, Y. Tsukamoto, A. Hayashi, T. Minami, *Tetrahedron Lett.* **1990**, *31*, 2423-2424.

74 R. W. Curley, H. F. DeLuca, *J. Org. Chem* **1984**, *49*, 1941-1944.

75 B. A. Halley, E. C. Nelson, *J. Chromatogr. A* **1979**, *175*, 113-123.

76 G. Englert, *Helv. Chim. Acta* **1975**, *58*, 2367-2390.

77 M. G. Motto, K. L. Facchine, P. H. Hamburg, D. J. Burinski, R. Dunphy, A. R. Oiler, M. L. Cotter, *J. Chromatogr. A* **1989**, *481*, 255-262.